THE ADENOVIRUS TYPE 2 PROTEASE : GENERATION AND CHARACTERISATION OF MONOCLONAL ANTIBODIES AND THEIR USE IN DETERMINING THE SUBCELLULAR DISTRIBUTION OF THE PROTEASE WITHIN LYTICALLY INFECTED CELLS

Owen Anthony Vaughan

A Thesis Submitted for the Degree of PhD
at the
University of St Andrews

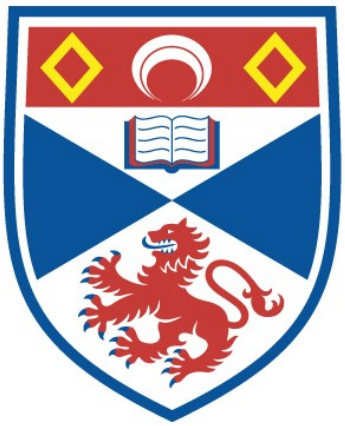

1997

THE ADENOVIRUS TYPE 2 PROTEASE:

GENERATION AND CHARACTERISATION OF MONOCLONAL ANTIBODIES AND THEIR USE IN DETERMINING THE SUBCELLULAR DISTRIBUTION OF THE PROTEASE WITHIN LYTICALLY INFECTED CELLS.

Owen Anthony Vaughan

Division of Cell and Molecular Biology

School of Biological and Medical Sciences

University of St.Andrews.

A thesis presented for the degree of Doctor of Philosophy at the University of St.Andrews, September 1997.

ProQuest LLC.
789 East Eisenhower Parkway
P.O. Box 1346
Ann Arbor, MI 48106 – 1346

DECLARATION

I, Owen Vaughan, hereby certify that this thesis, which is approximately 70,000 words in length, has been composed by myself, that it is a record of my own work, and that it has not been accepted in partial or complete fulfilment of any other degree or professional qualification.

Signed ..... Date 17 Sept 1997

I was admitted as a research student in October 1993 and as a candidate for the degree of Doctor of Philosophy in October 1993; the higher study for which this is a record was carried out in the Faculty of Science of the University of St.Andrews between 1993 and 1997.

Signed ..... Date 17 Sept 1997

I hereby certify that the candidate has fulfilled the conditions of the Resolution and Regulations appropriate to the Degree of Doctor of Philosophy in the University of St.Andrews and that the candidate is qualified to submit this thesis in application for that degree.

Signed ..... Date 17 Sep 97

In submitting this thesis to the University of St.Andrews, I understand that I am giving permission for it to be made available for use in accordance with the regulations of the University Library for the time being in force, subject to any copyright vested in the work not being affected thereby. I also understand that the title and the Abstract will be published and that a copy of the work may be made and supplied to any *bona fide* library or research worker.

Acknowledgements

I would like to thank my supervisor Graham Kemp for his help during this work and also for his unlimited patience (and faith!) during the writing of this thesis. I would also like to thank Paul Szawlowski whose advice and assistance during the first year of this work was invaluable and Willie Russell, Ailsa Webster and Ron Hay for useful discussions on various aspects of adenovirus infection.

Many thanks go to Gonzo Cabrita, Martin Ryan and Edwin for their help when I got myself into problems with computers. I am also indepted to John Mackie, Bill Blythe and Ian Armitt for their technical assistance and Sarah Jones, Stuart Annan, Lewis Murray, Munir Iqbal, and many others who have come and gone throughout my time in Lab 6M.

Finally, a special thanks to everyone who has made my stay in St.Andrews an enjoyable one especially Chris Strong, Paul Marsh and Jane.

This work was supported by a grant from the Medical Research Council.

List of abbreviations.

A	Adenine
Abs	Absorbance
Ad	Adenovirus
amp	ampicillin
ATP	Adenosine triphosphate
bp	base pairs
ß-MeSH	ß-mercaptoethanol
BSA	Bovine serum albumin
C	Cytosine
C- (also ct).	Carboxy- (terminus)
cDNA	complementary DNA
CE	Capillary Electrophoresis
CM	Carboxymethyl
CMV	Cytomegalovirus
DAPI	4, 6 diamidino-2-phenylindole
DBP	DNA binding protein
dCMP	deoxycytosine monophosphate
dd.	deionised distilled
DEAE	Diethyl-aminoethyl
DMF	Dimethyl formamide
DMSO	Dimethyl sulphoxide
DNA	Deoxyribonucleic acid
dNTP	deoxynucleotide triphosphates
dsDNA	double stranded DNA
EBNA	Epstein-Barr virus nuclear factor
EBV	Epstein-Barr virus
ECL	Enhanced chemiluminesence
E.coli.	*Eschericia coli*
EDTA	Ethylenediaminetetracetic acid
E1-E4	Early genes (or proteins) 1 to 4
eIF	eukaryotic initiation factor
ELISA	Enzyme-linked immunosorbent assay

EM	Electron microscopy
FCS	Foetal calf serum
FDNB	Dinitrofluorobenzene
FITC	Fluorescein isothiocyanate
FMDV	Foot and mouth disease virus
FPLC	Fast Protein Liquid Chromatography
G	Guanine
G-MEM	Glasgow's modified essential medium
Gp	Glycoprotein
GST	Glutathione S-transferase
GTP	Guanosine triphosphate
HA	Haemagglutinin
HAT	Hypoxanthine-Aminopterin-Thymidine
HCV	Hepatitis C virus
HIV	Human immunodeficiency virus
hnRNA	heterogenous nuclear RNA
hnRNP	heterogenous nulear ribonuclearprotein
h.p.i	hours post infection
HPLC	High performance liquid chromatography
HRP	Horseradish peroxidase
HSA	Human serum albumin
HSV	Herpes simplex virus
HT	Hypoxanthine-Thymidine
Ig	Immunoglobulin
IPTG	Isopropyl-ß-D-thiogalactopyranoside
kb	Kilobases
kbp	Kilobase pairs
kd	Kilodaltons
L1-L5	Late genes (or proteins) 1 to 5
LB	Luria broth
Mab	Monoclonal antibody
MLP	Major late promoter

MLTU	Major late transcription unit
moi	mutiplicity of infection
mRNA	messenger ribonucleic acid
MW	Molecular weight
Mtr	4-methoxy 2, 3, 6 trimethylbenzene sulphonyl
N-	Amino-
NEM	N-ethyl maleimide
NF	Nuclear factor
NLS	Nuclear localisation signal
NP-40	Nonidet P-40
ORF	Open reading frame
PAGE	Polyacrylamide gel electrophoresis
PBS	Phosphate buffered saline
PCR	Polymerase chain reaction
PEG	Polyethylene glycol
PfG	Paraformaldehyde and Glutaraldehyde
p.f.u.	plaque forming units
pH	pondus hydrogen ($-\log_{10}[H^+]$)
PML	Promyelocytic protein
PMSF	Phenylmethylsulphonylfluoride
pol	Adenovirus DNA polymerase
pRB	Retinoblastoma susceptibility gene product
pTP	Pre-terminal protein
PVDF	Polyvinylidene difluoride
RGD (motif)	Arginine-Glycine-Aspartic acid
RNA	Ribonucleic acid
rpm	revolutions per minute
RSV	Rous sarcoma virus
SBTI	Soya bean trypsin inhibtor
SDS	Sodium dodecyl sulphate
Sf	*Spodoptera frugiperda*
ssDNA	single stranded dNA
S-MEM	Earle's minimal essential medium for suspension culture
snRNP	small nuclear ribonuclearprotein

SPDP	N-succinimidyl 3, 2(piridyl-dithio)propionate
SV40	Simian virus 40
T	Thymine
TAE	Tris-acetate-EDTA buffer
TBS	Tris buffered saline
TEMED	N, N, N', N' tetramethylethylenediamine
TF	Transcription factor
TFA	Trifluoracetic acid
TLCK	Tosyl-lysine-chloromethyl ketone
TP	Terminal protein
TPCK	Tosyl-phenylalanine-chloromethyl ketone
Tris	2-amino-2-(hydroxymethyl)propane-1, 3-diol
tRNA	transfer RNA
ts	temperature sensitive
T-TBS	Tris buffered saline containing Tween 20
uv	ultta-violet
VA RNA	Viral associated ribonucleic acid
V/V	volume per volume ratio
wt	wild type
W/V	Weight per volume ratio

Single letter code and abbreviations for amino acids:

A	Alanine	Ala	**P**	Proline	Pro
C	Cysteine	Cys	**Q**	Glutamine	Gln
D	Aspartic acid	Asp	**R**	Arginine	Arg
E	Glutamic acid	Glu	**S**	Serine	Ser
G	Glycine	Gly	**T**	Threonine	Thr
H	Histidine	His	**V**	Valine	Val
I	Isoleucine	Ile	**W**	Tryptophan	Trp
K	Lysine	Lys	**Y**	Tyrosine	Tyr
L	Leucine	Leu			
M	Methionine	Met			
N	Asparagine	Asp			

Genetic Code

TTT	phe	F	**TCT**	ser	S	**TAT**	tyr	Y	**TGT**	cys	C
TTC	phe	F	**TCC**	ser	S	**TAC**	tyr	Y	**TGC**	cys	C
TTA	leu	L	**TCA**	ser	S	**TAA**	och	Z	**TGA**	opa	Z
TTG	leu	L	**TCG**	ser	S	**TAG**	amb	Z	**TGG**	trp	W
CTT	leu	L	**CCT**	pro	P	**CAT**	his		**CGT**	arg	R
CTC	leu	L	**CCC**	pro	P	**CAC**	his	H	**AGC**	arg	R
CTA	leu	L	**CCA**	pro	P	**CAA**	gln	Q	**AGA**	arg	R
CTG	leu	L	**CCG**	pro	P	**CAG**	gln	Q	**AGG**	arg	R
ATT	ile	I	**ACT**	thr	T	**AAT**	asn	N	**AGT**	ser	S
ATC	ile	I	**ACC**	thr	T	**AAC**	asn	N	**AGC**	ser	S
ATA	ile	I	**ACA**	thr	T	**AAA**	lys	K	**AGA**	arg	R
ATG	met	M	**ACG**	thr	T	**AAG**	lys	K	**AGG**	arg	R
GTT	val	V	**GCT**	ala	A	**GAT**	asp	D	**GGT**	gly	G
GTC	val	V	**GCC**	ala	A	**GAC**	asp	D	**GGC**	gly	G
GTA	val	V	**GCA**	ala	A	**GAA**	glu	E	**GGA**	gly	G
GTG	val	V	**GCG**	ala	A	**GAG**	glu	E	**GGG**	gly	G

Physical Units

°C	Temperature in degrees celsius.
g	gram.
s	second.
mol	mole.
m	metre.
Da	Dalton (Relative molecular mass).
g	gravitational accelaration (9.81 ms^{-2}).
hr(s)	hour(s).
l	litre (volume; $10^{-3}m^3$).
min	minute (time).
Ci	Curie [radioactivity; $3.7x10^{10}s^{-1}$ (disintegrations per second)].
M	molar concentration ($mol.l^{-1}$).
U	units of enzymatic activity.
S	Svedberg (sedimentation).
V	volts.
A	amperes

Ordered Prefixes

d	deci	10^{-1}	**k**	kilo	10^3
c	centi	10^{-2}	**M**	mega	10^6
m	milli	10^{-3}	**G**	giga	10^9
μ	micro	10^{-6}	**T**	tera	10^{12}
n	nano	10^{-9}			
p	pico	10^{-12}			
f	femto	10^{-15}			
a	atto	10^{-18}			

Contents

Abstract.

Production of mature infectious adenovirus type 2 depends on the action of the L3 coded 23kd protease which is known to cleave 7 virus proteins and the host cell proteins cytokeratin K7 and K18. Previous studies have shown the enzyme to be a cysteine proteinase with a novel mechanism of activation requiring the presence of an 11 residue peptide derived from the C-terminus of virus structural protein pVI. It has been proposed that the protease is activated within the assembled virion, although other evidence suggests that the protease is active outwith the virus particle, and is partly responsible for the degradation of the intermediate filament system prior to virion release from the infected cell.

The subcellular localisation of the 23kd protease during productive adenovirus infection was investigated using a panel of monoclonal antibodies generated during the course of this study. The monoclonal antibodies were partially characterised and those of interest were epitope mapped using a combination of techniques which included limited and chemical proteolysis, and deletion mutagenesis of the recombinant protein, and screening against overlapping peptides corresponding to specific regions within the 23kd protease.

The viral 23kd protease, capsid protein pVIII, and the L1-52kd probable scaffold protein were shown to colocalise within virus-induced intranuclear clear amorphous inclusions late in infection (24 h.p.i onwards). These inclusions were typically associated with crystalline arrays of assembled virions and are believed to be the same sites which contain relocated PML during the earlier stages of infection. The structural appearance of these inclusions varied depending on the fixation method used. The distribution of the viral protease, PML and another cellular protein P80-coilin during the late-phase of nuclear transformation was investigated with possible cleavage of both cellular proteins also partially determined.

The viral protease and protein pVIII were also shown to colocalise within cytoplasmic structures but were not found to be associated with cytokeratin K18. The degradation of cytokeratin K18 occurred as early as 20 to 22 h.p.i although the intranuclear distribution of pVI at this stage of infection suggested that the viral protease may be regulated by an as yet unknown mechanism. Isoforms of recombinant wild type 23kd protease (but not Ad2ts1) were detected *in vitro* which suggested that dimerisation may be an *in vivo* regulatory mechanism, possibly involving intranuclear trafficking.

List of Tables:

List of Figures:

1 Introduction

1.1 Adenoviruses

1.1.1 Epidemiology and classification.

First isolated from adenoidal tissue of chidren, Adenoviruses were reported as being distinct etiological agents in 1953 by Rowe *et al.* Since then, over 100 serotypes have been identified which infect different animal species. Human adenoviruses (Ad) are members of the genus Mastadenovirus, which together with Aviadenovirus make up the Adenoviridae family (Horwitz 1990b). Although the 15 serotypes of aviadenoviruses identified to date have economic implications within the poultry industry (Isibashi and Yasue,1984), most studies have concentrated on the mastadenoviruses which infect a broad range of mammalian species. These viruses share a common antigenic determinant which is located on the major viral coat protein, the Hexon (Norrby *et al.*, 1977).

To date, 47 serotypes have been found to infect humans, however despite the large number and world-wide distribution, their clinical importance is largely restricted to epidemics of acute respiratory disease (ARD), an influenza like illness in military recruits, and to limited outbreaks among children (reviewed by Horwitz,1990a). Types 7, 4 and 3 (in order of decreasing importance) are the viruses most frequently responsible for epidemics of acute respiratory, and ocular diseases, although types 11, 14, 21, 40 and 41 have increasingly been implicated. Peculiarly, Ad4 commonly causes ARD in military recruits but rarely in civilians. There is as yet no explanation for this epidemiological behaviour.

Epidemiological studies indicate that adenoviruses annually cause at most 4 to 5% of viral respiratory illnesses in civilians. Person to person spread in respiratory and ocular secretions is the most common mode of viral transmission implicated in epidemics of pharyngoconjuctival fever and conjunctivitis. The spread of epidemic keratoconjunctivitis caused by types 8, 19 and 37 adenoviruses appears to be associated with conjunctival trauma produced by dust found in many working environments. Adenoviruses are commonly present in the faeces of infected persons, even those with ocular and respiratory infections, yet only types 40 and 41 (the agents of infantile gastro-enteritis most evident in developing countries) appears to be transmitted by the faecal-oral route.

In 1962, Trentin *et al.* discovered that adenovirus serotype 12 could induce tumours in rodents. This discovery led to an intense period of research on adenoviruses. Although no adenovirus serotype has been associated with human malignancy, the ability to transform rodent cells has served as a useful model to study the molecular basis of cell transformation (Graham,1984).

The 47 human serotypes are arranged together into six subgroups (A to F) on the basis of several criteria (table 1.1) that include haemagglutination, morphology (for instance, length of fibre protein), %G+C content of the genomes, DNA sequence homologies, and the ability to induce tumours in laboratory rodents (Horwitz,1990a). DNA sequence homologies between members of the same group are usually very high (48-85%) with most significant differences occurring in the coding regions for the major coat proteins. In contrast, less than 20% DNA sequence homology has been shown between viruses from different groups (Garon *et al.* , 1973). Despite their differences, all the adenoviruses have the same basic organisation, with sequences of many functional proteins being highly conserved between viruses from different subgroups (Horwitz,1990a).

Subgroup	Serotypes	Oncogenic	% GC in DNA
A	12, 18, 31	High	48-49
B	3, 7, 11, 14, 16, 21, 34, 35	Moderate	50-52
C	1, 2, 5, 6	Low or none	57-59
D	8, 9, 19, 37, 10, 13, 15, 17, 19, 20, 22-30, 32, 33, 36, 37, 38, 39, 42-47	Low or none	57-61
E	4	Low or none	57-59
F	40, 41	Unknown	-

Table 1.1: Classification of the human adenoviruses. Classification based on DNA homologies and the ability to induce tumours in animals. Modified from Horwitz (1990a).

1.1.2 Virion structure.

Adenovirus virions are non-enveloped and icosahedral in structure containing a double stranded genome of approximately 34 to 36kb (Akusjärvi *et al.*, 1984). In the 40 years since the discovery of this virus, a wide range of biophysical and biochemical techniques have been

applied to understanding the structure of the virion. For instance, analysis of purified virions by SDS- Polyacrylamide gel electrophoresis revealed 12 distinct polypeptides which were termed II to XII according to their relative mobilities (Maizel *et al.*, 1968a). Seven of these, namely II, III, IIIa, IV, VI, and IX have been shown to be associated with the viral coat, which can be removed from the viral cores by treatment with 0.5% deoxycholate or 5M urea (Russell *et al.*, 1968). The cores are made up of the viral DNA, and a number of proteins including V, VII, mu (X), and the DNA linked terminal protein (Chatterjee *et al.*, 1986). In addition, enzyme activity associated with the viral encoded 23kd protease has also been recovered from disrupted particles (Trembley *et al.*, 1983; Anderson, 1990).

i) Structural proteins:

The capsid shell is composed of 252 capsomeres which comprise of 240 hexon capsomeres (protein II), and 12 penton capsomeres, which are in turn composed of 5 penton molecules (protein III) and three fibre proteins (protein IV). The hexon capsomeres assemble to form the 20 sides of the virion particle, while the penton capsomeres are isolated to the 12 vertices of the virion (Stewart and Burnett, 1995). The 3-dimensional structure of the entire particle has been determined by cryo-electron microscopy together with 3-dimensional image reconstruction (Stewart *et al.*, 1991). A schematic illustration outlining the relative positions of the known virion components is shown in figure 1.1.

To date, the atomic structure of only one of the capsid components, the hexon derived from Ad2, has been determined (Roberts *et al.*, 1986; Athapilly,1994). The hexon monomer has 967 amino-acid residues with a predicted molecular weight of 109kd. In the virion coat, 3 hexon monomers come together to form each of the 240 hexon capsomeres (Grutter and Franklin, 1974), a process facilitated by the virus encoded L4 100kd protein (Cepko and Sharp, 1983). Each monomer has two eight-stranded ß-barrels and three extended loops, of which the latter intertwine in the trimer and are exposed on the surface of the virus. In the trimer, six ß-barrels, two from each monomer, sit at the corners of a hexagon to generate a pseudohexagonal base. This shape is convenient for close packing of the hexon capsomers on the surface of the virion. It has been proposed that the N-terminal region of hexon interacts with the viral core DNA and protein (Stewart and Burnett,1995). The hexon surface loops display the greatest variability between adenovirus serotypes and contain many of the

The Adenovirus Virion

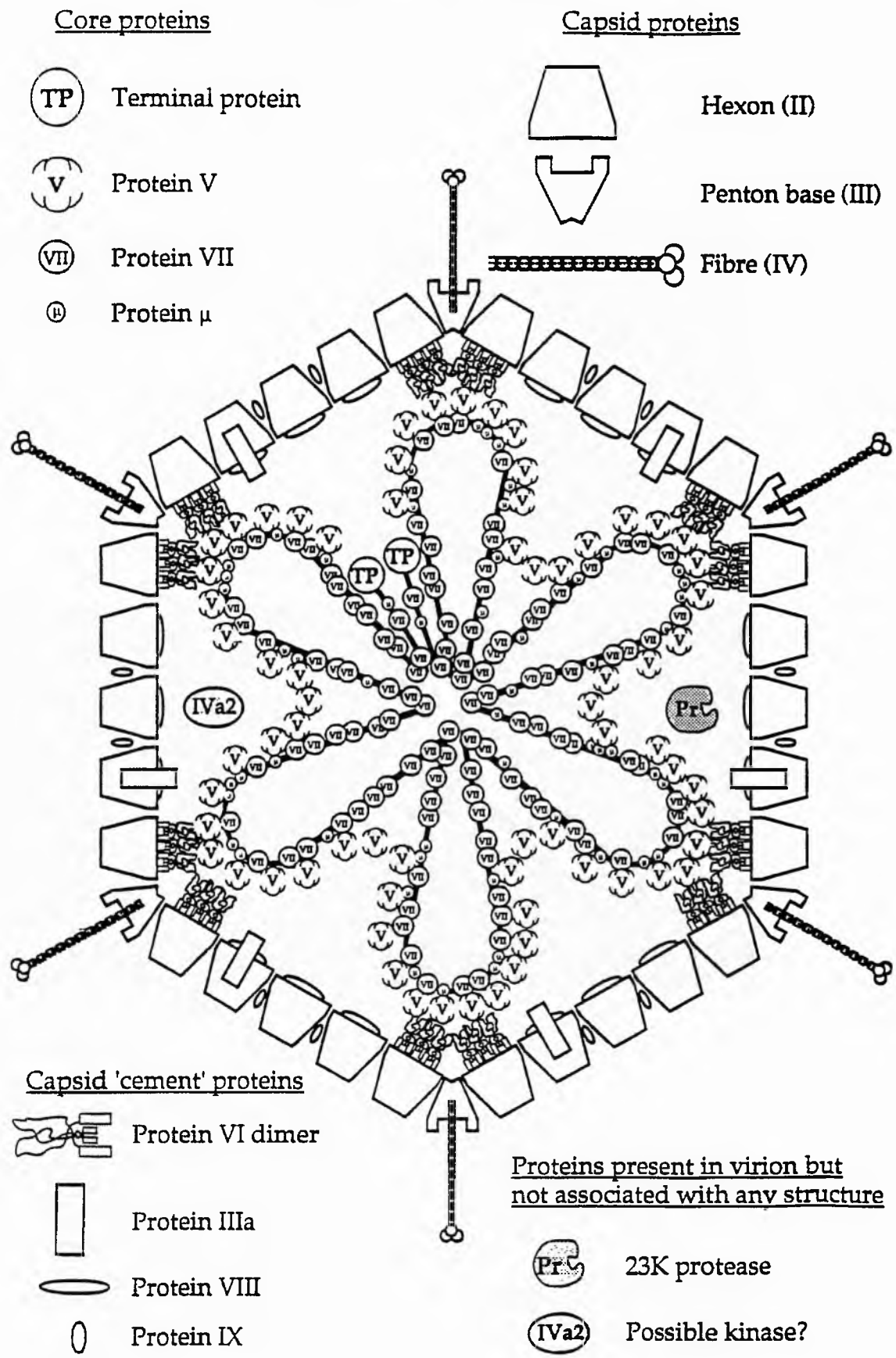

type specific epitopes (Toogood *et al.*, 1989). Five hexons, known as peripentonal hexons have been shown in atomic detail to be closely associated with the penton base at the particle vertices. One of the two hexon ß-barrels fits nicely into a groove on the side of the penton base.

Each penton capsomer is composed of five copies of penton base, and three identical copies of fibre protein (Van Oostrum *et al.*, 1987). The penton base contains 571 amino-acid residues, with an apparent molecular weight of 63kd (Stewart and Burnett,1995). The five penton base monomers are non-covalently associated to give a ring like pentamer (Stewart *et al.*, 1991) which has a 30Å diameter central core, in which the N-terminal region of the fibre protein is linked (Devaux et al., 1987; Stewart and Burnett, 1995). This polypeptide is 582 amino acid residues in length with a predicted molecular mass of 62kd in Ad2 (Hérisse *et al.*, 1981). The fibre in this serotype is 37nm in length, however, the length of the 'shaft' varies between serotypes (Signas *et al.*, 1985; Kidd *et al.*, 1993), and within those which contain two types of fibre proteins (Ad40). In either case the length of the fibre depends on the amount of repeating units (15 amino acid residues in length) in the main body of the polypeptide, for instance, Ad2 has 22 repeated units, Ad3 has 6, and the two fibre Ad40 has 21 and 12 repeated units (Green *et al.*, 1983). At the C-terminal region of the fibre protein, a globular ß-barrel domain exists which is thought to confer receptor recognition.

Figure 1.1: Schematic illustration of the adenovirion. The currently predicted positions for both core and capsid proteins are outlined (provided by Dr. D. Mathews, University of St.Andrews).

Hexons have been shown to interact with another capsid protein, IIIa, which has 585 amino acid residues and a predicted molecular mass of 65kd (Roberts*et al.*, 1984). Three-dimensional difference mapping has revealed 60 copies of this elongated component (5 to 6 copies per vertex) that appear to span the hexon capsid (Stewart and Burnett, 1995), an observation supported by the fact that recombinant IIIa polypeptide in 1M urea is long enough (200Å) for this to be possible (Cuillel *et al.*, 1990). It has been proposed that IIIa polypeptide interacts with two ß-barrel strands of hexon, with the C-terminal region, which is known to be cleaved by the L3 23kd protease (Anderson,1990) possibly associating with core proteins V and VII (Boudin *et al.*, 1980). Protein IIIa is phosphorylated early in infection, although the significance of this is not yet known (Tsuzuki and Luftig, 1983).

Protein VI is derived by proteolysis from a 250 amino acid precursor (pVI) with a predicted molecular weight of 27kd. The precursor protein is processed by the viral 23kd protease which removes the N-terminal 33 amino acids (Akusjärvi and Persson, 1981; Anderson, 1990). The mature VI is thought to have a role in linking the core complex to the capsid (Russell and Precious, 1982), and recent work (Mathews and Russell, 1994; Stewart and Burnett, 1995) has provided evidence that there is a strong interaction between the peripentonal hexons and mature VI. This interaction appears to be 300 times stronger than the interaction between hexon and pVI, suggesting that proteolytic maturation alters the conformation of mature VI, thereby facilitating tighter binding. Stewart and Burnett (1995) have suggested that VI exists as disordered dimers within the capsid. Interestingly, the 11 amino acid C-terminus of pVI, functions as a cofactor which enhances proteolytic activity (Webster *et al.*, 1993; Mangel *et al.*, 1993).

Protein VIII, with a molecular mass of 15kd, is derived from a precursor protein of approximately 25kd (pVIII) which comprises of 227 amino acid residues (Pieniazek *et al.*, 1989). pVIII contains three potential processing sites (Webster *et al.*, 1989a and b), however, the derivation of protein VIII from pVIII is still not completely understood. Initially it was thought that protein VIII was inside the capsid and associated with hexons (Everitt *et*

al., 1975; Pettersson, 1984), however, recent evidence suggests that VIII is closely associated with the penton base and fibre at the vertices of the virion (Hong and Boulanger, 1995). A temperature sensitive mutant of adenovirus which is defective for protein VIII, and termed H5sub304 (Lui *et al.*, 1985), has a marked thermolability which indicates, like protein IX, that this protein could serve as a scaffolding protein and/or be involved in stabilising the final virion structure.

Protein IX has 139 amino acid residues with a predicted molecular weight of 15kd (Alestrom *et al.*, 1980). Biochemical analysis (Furcinitti *et al.*, 1989) has shown that 12 copies of polypeptide IX and 9 copies of hexon associate to form the group of nine hexon (GON) structure. These were confirmed by combined X-ray crystallography and scanning transmission electron microscopy studies (Stewart *et al.*, 1993). Trimers of protein IX are shown to bind on the outer surface of closely packed hexon bases, with four trimers being associated with each of the 20 facets (Boulanger *et al.*, 1979; Van Oostrum and Burnett, 1985; Stewart *et al.*, 1991). Mutant viruses lacking this protein can form intact virions (Colby and Shenk, 1981), but these are less stable than wild type virions.

ii) Core components:

At least four proteins, polypeptides V and VII (Philipson, 1983), polypeptide mu (Hosokawa and Sung, 1976), and the DNA binding terminal protein (Rekosh *et al.*, 1977), are complexed with the DNA in the core of the virion. In addition, it has also been estimated that approximately half of the capsid component protein VI is disordered and interacting with the internal DNA (Stewart and Burnett, 1995). The 10 copies of the 23kd protease (Anderson, 1990) have not been assigned to any particular location within the virion, although it seems possible like protein VI, that an interaction with the viral genome may exist (Mangel *et al.*, 1993). The Ad2 23kd protease is discussed in detail in section 1.1.5.

The exact structure of the adenovirus core within the virus particle is somewhat controversial, although it appears that the core DNA-protein complex is positioned in 12 globular domains with the outside loop of each domain in close proximity with each penton vertex (Brown *et al.*, 1975; Newcomb *et al.*, 1984). This may correlate well with the suggestion that disordered dimers of protein VI can interact with viral DNA.

Protein VII is the major component of the viral core, with an estimated 833 copies per virion (Hosokawa and Sung, 1976; Stewart and Burnett, 1995). The protein initially exists as a precursor of 197 amino acid residues in length, and a molecular mass of 21.8kd, which is cleaved by the 23kd protease to mature VII, with a predicted mass of 19.4kd and 174 amino acid residues in length (Anderson *et al.*, 1973; Sung *et al.*, 1983; Aleström *et al.*, 1984). Protein VII has a high content of both arginine (23%) and alanine (18.9%), and binds tightly to DNA, with 3M NaCl being required to dissociate the complex (Cupo *et al.*, 1987).

The minor core protein, V, is 368 amino acid residues in length, with a predicted molecular mass of 41.6kd (Aleström *et al.*, 1984). This protein can be removed from viral DNA by relatively mild treatments leading to the suggestion that it forms a protein shell around the DNA-protein VII complex, perhaps forming the link between the core and the capsid (Nermut, 1979; Chatterjee *et al.*, 1985). Chemical cross-linking studies have indicated that VII, mu, and V interact, although the only core protein to interact with capsid component protein VI is V. Protein V is moderately basic with 20% of residues being arginine or lysine. These residues are clustered to give a lysine rich N-terminus, and arginine rich C-terminus. Stoichiometric estimates range from 120 to 160 copies of protein V per virion (Hosokawa and Sung, 1976; Van Oostrum and Burnett, 1985). During virion assembly, protein V is highly phosphorylated, however, within the maturing virion the protein is dephosphorylated, a step which is blocked by the Ad2ts1 mutation (section 1.1.5). This is suggestive that cleavage of precursor proteins and dephosphorylation of V are linked events which require functional viral protease (Weber and Khitoo, 1983).

Associated with protein V is the protein derived from a 79 amino acid precursor, pmu, which has a predicted molecular mass of 11kd. mu has 19 amino acid residues, including 9 arginines and 3 histidines and is known to bind tightly to DNA. There is an estimated 180 to 340 copies per virion (Weber and Anderson, 1988). The viral protease is thought to cleave pmu at two sites releasing a 31 amino acid long N-terminus fragment and a 29 amino acid C-terminal region. Proteins XI and XII are believed to be products of viral protease processing. The above authors reported that XII may be derived from the N-terminal region of pVII and XI from pmu, although this has yet to be confirmed.

In addition to V,VII and mu, at least two other proteins are present in the viral cores at very low copy numbers. One of these, the terminal protein (TP), is made as a precursor (pTP)

which is proteolytically processed by the viral protease via an intermediate, iTP (Trembley *et al.*, 1983, Webster *et al.*, 1994). Terminal protein has a molecular mass of 55kd, and is covalently linked to the dCMP residue at the 5' end of each DNA strand (Rekosh *et al.*, 1977; Smart and Stillman, 1982). pTP and TP are discussed in more detail in section 1.1.3iii.

Very little is known about the second low copy protein, IVa2, which is composed of 448 amino acid residues, and has a molecular mass of 51kd (Russell and Precious, 1982; Russell and Kemp, 1995). IVa2 may be associated with the core (Weber *et al.*, 1983), possibly being encapsidated with the viral genome, as it is known to specifically bind to viral DNA. The virus encoded L1 52kd and 55kd scaffold proteins have been shown to interact with IVa2 in immature virions (Lutz *et al.*, 1996; Gustin *et al.*, 1996). These authors suggest IVa2 may be involved in removing the scaffold proteins during virion assembly. Although IVa2 is present in immature virions it has only been detected in a phosphorylated state within mature virions (Weber and Khitoo, 1983). Interestingly, IVa2 has a motif for ATP/GTP binding (Russell and Kemp, 1995) and may facilitate phosphorylation events in virion maturation. Protein kinase activity has been associated with human adenoviruses (Blair and Russell, 1978), although it is unknown whether it is virus encoded or of cellular origin.

1.1.3 Infectious life cycle.

Adenovirus infection can persist for long periods in human lymphoid tissues. In normal circumstances, recurrent illness has not been shown to arise from these latent infections, although activation can occur in patients with immunosupression. It appears that latent persistent infections are readily established because infected cells are not lysed, and viral particles remain protected within nuclei. In nature this is confined to relatively few cells.

In contrast, cultured cells infected with human adenovirus can either be transformed by the integration of part or all of the viral DNA into their genome (Sharp, 1984; Boulanger and Blair, 1991) or play host to a full lytic infection, which can spread to uninfected cells and produce detectable cytopathic effects. Transformation takes place in semi- or non-permissive cells, and depends on virus serotype and the nature of the host cell. All of the human adenoviruses are able to transform new born rodent cells, but only serotypes from groups A and B are known to be oncogenic. Full lytic infections are best observed using cultured human epithelial cell lines such as HeLa or KB, where the human adenovirus types 2 and 5

have been shown to replicate very efficiently. Adenovirus infection in permissive cells can be divided into distinct stages which are outlined in this section.

i) Receptor recognition and cellular uptake:

Adenovirus attaches with high affinity to as yet unidentified cellular receptors via the fibre protein head domain (Philipson *et al.*, 1968; Louis *et al.*, 1994; Xia *et al.*, 1995). Fibre length, which varies among serotypes, may have a role in facilitating the attachment of virus to more than one receptor if necessary (Kidd *et al.*, 1993). The number of receptors available for virus binding has been determined for a range of cells (Defer *et al.*, 1990; Belin and Boulanger, 1993) and varies from 3x to 6x 10^3. The vitronectin and fibronectin binding integrins have recently been identified as the secondary receptors (Wickham *et al.*, 1993), interacting with the conserved RGD motif of penton base proteins. Adsorption appears to be followed by an energy-dependent clustering of virus particles at the cell surface (Patterson and Russell, 1983), with internalisation occurring via clathrin-coated vesicles into endosomes (Greber *et al.*, 1993).

During the course of receptor-mediated endocytosis, adenoviruses undergo multiple sequential uncoating steps as they move from the cell surface to the nuclear membrane (Svensson and Persson, 1984; Greber *et al.*, 1993). Within 20 minutes, 80% of receptor bound virus is located in early endosomes, where the fibre, VIII and IIIa proteins are dissociated, thereby weakening the virion structure (figure 1.2). The acidification of the endosome may facilitate penetration of the virus into the cytoplasm (Bai *et al.*, 1993; Ródriguez and Everitt, 1996). The first proteins to be eliminated at this stage are those located at the 12 vertices of the viral particle, including penton base, protein IX, and subpopulations of hexons. Fibre release may have a specific role at this stage in promoting virus escape from endosomes. Additionally, a cytopathic effect has been associated with the penton base protein (Valentine and Periera, 1965).

The degradation of protein VI at this stage of protein elimination has been attributed to the activity of the viral 23kd protease (Cotten and Weber, 1995; Greber *et al.*, 1996). It has been suggested that the RGD-dependant interaction of the penton base with integrin receptors induces a conformational change in the vertex region of the capsid which exposes hidden protease cleavage sites in VI. The role of the viral protease in disassembly is best illustrated

with studies incorporating the temperature sensitive mutant, Ad2ts1, which is protease deficient (Weber, 1976; Rancourt *et al.*, 1995) and fails to uncoat (Mirza and Weber, 1979). With wild type Ad2 infection, between 40 and 60% of virus can be seen inside cells, with 20 to 35% located in the cytoplasm 30 minutes after uptake. After Ad2ts1 infection, although 80% of virus has been endocytosed, only 0.4% can be visualised in the cytoplasm (Russell and Kemp, 1995), the majority being retained in endosomes which are then recycled in the cytoplasm (Greber *et al.*, 1996).

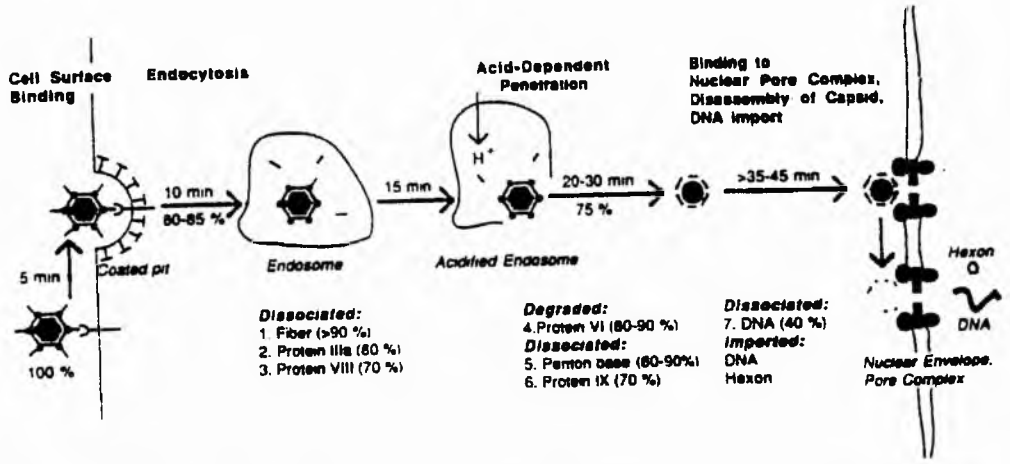

Figure 1.2: Steps involved in the uncoating process. The adenovirus binds to a high-affinity fibre receptor and endocytosis occurs after a lag period of 5 minutes. Efficient penetration from endosomes occurs after 15 minutes and after 45 minutes 50% of the cell-bound viruses have been completely disassembled and have released their DNA inside the nucleus (reproduced from Greber, 1993).

Following uncoating, the virus particle resembles adenovirus cores with some of the hexons from the capsid shell still associated. The DNA genome is delivered to the cell nucleus, possibly directed by viral core proteins V and/or TP, both of which have nuclear localisation sequences (Russell and Kemp, 1995). The sequence within TP is highly conserved among all the serotypes in which the sequence is known. Protein V may dissociate at the nuclear membrane (Greber *et al.*, 1993), with the viral genome complexed with TP, VII and mu being localised to the nuclear matrix. Nuclear localisation signals (NLS) could mediate transport of disassembled complexes in other viral systems. For instance, the structural Vp2/3 proteins of SV40 (Clever and Kasamatsu, 1991) and the nucleoprotein component of the viral RNA-protein complex of influenza virus contain nuclear localisation sequences which mediate events after release from endosomes (Davey *et al.*, 1985). The gag matrix

also contains an NLS which may be involved in the active transport of the pre-integration complex following infection (Bukrinsky *et al.*, 1993).

ii) Early events in gene expression:

The first transcription units to be activated shortly after infection are classed as the immediate early (E1A), delayed early (E1B,E2A,E2B,E3 and E4), and intermediate genes (IVa2 and IX), with maximum levels of transcription from the late genes (L1 to L5) occurring at 18 hours post infection onwards (Lucas and Ginsberg, 1971). Figure 1.3 shows the transcriptional organisation of the Ad2 genome, which has been divided into 100 map units to readily identify individual genes (Akusjärvi *et al.*, 1986).

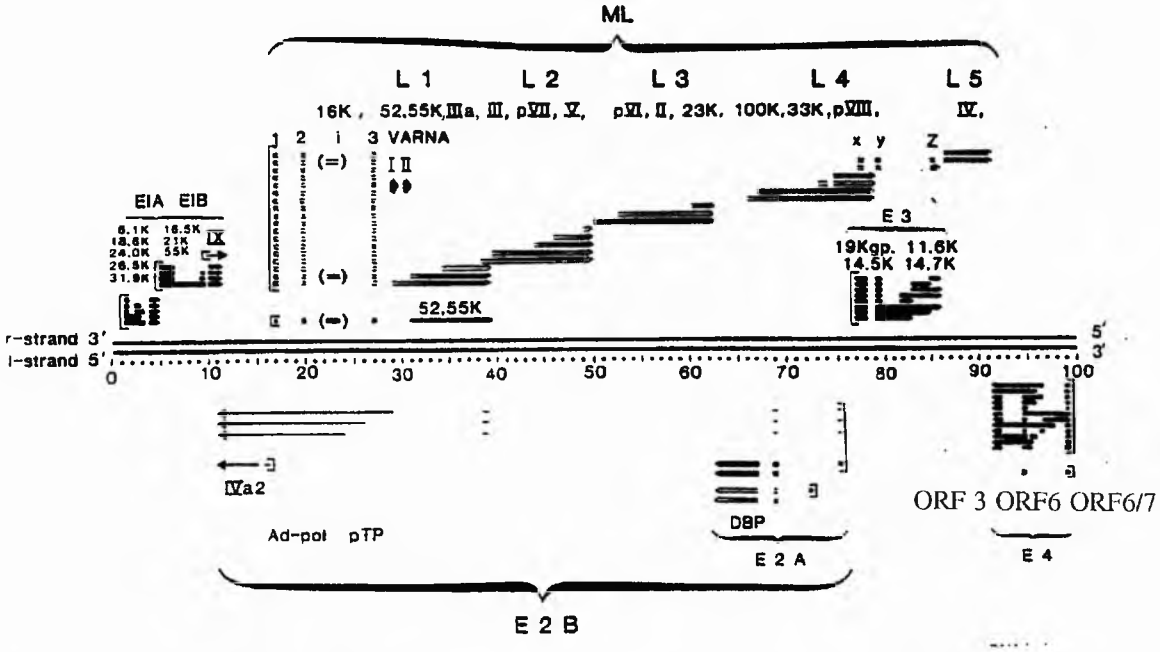

Figure 1.3: Schematic map of genes and transcription units encoded by the Ad2/5 genomes. The linear dsDNA is depicted in the centre of the figure with r and l referring to rightward and leftward transcription. Thick lines indicate early mRNA's and thin lines indicate mRNA's expressed at intermediate times of infection. Open arrows show mRNA's expressed late after infection. Gaps in arrows denote the positions of introns. Arrowheads show the positions of 3'ends of the mRNA's and the promoter sites are indicated by brackets (reproduced from Akusjärvi *et al.*, 1986).

The immediate early genes (E1A) are switched on within one hour post infection, encoding proteins involved in cellular transformation and trans-activation of viral and cellular transcription units (Flint and Shenk, 1989). Although five mRNA transcripts are generated

through alternative splicing from the E1A region, only two major mRNA's, which encode the E1A13s and E1A12s proteins (289 and 243 amino acid residues respectively) are generated early in infection (Moran and Mathews, 1987). The proteins share N-terminal sequences, and differ only in a 46 residue internal exon segment unique to the E1A13s protein. This region (CR3) appears to stimulate transcription from several adenovirus promoters, including those requiring RNA polymerase II and III (Green *et al.*, 1988). E1A13s protein switches on the transcription of all viral early genes (E1B, E2A, E2B, E3 and E4) and also activates the major late promoter (MLP), probably functioning through various cis-acting elements such as the TATA-binding protein (which is shared by RNA polymerase II and III transcription systems), E2F (see below), ATF, AP-1, and the YY1 transcription factor (Lewis *et al.*, 1994). Such trans-activation is widespread among viral systems, for instance, the Herpes α-trans-activation factor (Michael *et al.*, 1988), and the pseudorabies immediate early protein do not bind DNA directly, whereas the SV40 large T-antigen, and the papilloma E2 protein do (Philipson, 1995).

In adenovirus transformed cells, constitutively expressed E1a12s protein can interact with unphosphorylated pRb, a cellular transcriptional regulation protein, and other pRb-like proteins (Whyte *et al.*, 1988; Zamanian and La Thangue, 1992). Since phosphorylation of pRb is required for the normal cellular growth cycle, the elimination of pRb in a complex with E1A12s protein can lead to constitutive growth potential. Unphosphorylated pRb also binds to E2F, a transcriptional factor required for several genes involved in growth control, thereby inhibiting cell cycle progression (Helin *et al.*, 1993). This association is disrupted by the E1A protein, liberating E2F from pRb thereby promoting expression of E2F dependent genes, leading to unrestricted growth.

These interactions would result in apoptosis in infected cells, however, the E1A and E1B products work in synchrony to sustain productive infection in human cells, or in transforming of rodent cells. E1A proteins initiate cellular proliferation which causes p53 (a tumour suppresser protein) accumulation and apoptosis (White *et al.*, 1995). The E1B 55kd protein appears to protect against apoptosis by binding to, and inactivating p53, probably by suppressing p53-mediated trans-activation of death genes such as bax (Teodoro *et al.*, 1995; White *et al.*, 1995). The cellular mechanism of p53 control is through bcl-2 protein, which has an adenovirus homolog, the E1B 19kd protein. It is thought that the E1B 19kd protein

may act similarly to bcl-2 by binding to the same antagonist, bax, to prevent induction of apoptosis.

In addition to its role in transformation, the E1B 55kd protein is important in exerting post-transcriptional control, late in infection, of differentially spliced mRNA's derived from the IX, IVa2 and major late promoters (Pilder *et al.*, 1986; Ornelles and Shenk, 1991; Leppard, 1993). The stability and accumulation of viral mRNA's in the cytoplasm has been attributed to the E1B 55kd protein, complexed with the E4 34kd protein, located at specific nuclear inclusions that are believed to be sites of DNA replication and transcription. A number of different proteins are encoded by the E4 region, corresponding to seven different translational open reading frames (ORF's). Mutation in either ORF3 (E4 11kd protein), or ORF6 (E4 34kd protein) results in productive infection, however, a double mutation results in defects for DNA replication, late viral mRNA cytoplasmic accumulation, viral protein synthesis, and a failure in shutoff of host protein synthesis (Smiley *et al.*, 1990 and 1994; Doucas *et al.*; 1996). Little is known about the biological activities of these proteins, although they do exhibit functions characteristic of RNA splicing factors (Nordqvist *et al.*, 1994).

The E4 19kd hybrid protein (E4 ORF6/7) transcriptionally activates the E2A gene by binding to the cellular factor E2F and consequently increasing its affinity for the E2A promoter (Neill *et al.*, 1990). The binding of E4 19kd to E2F is enhanced in the presence of E1A12s protein, probably releasing the cellular factor from interactions with other proteins. Transcription from the E2A and E2B promoter generates mRNA encoding the 59kd DNA binding protein (DBP), and the E2B 80kd preterminal protein (pTP), and 140kd Ad-polymerase, all of which are required for DNA replication (reviewed by Van Der Vleit, 1995). The mRNA's are transcribed early in infection from a single promoter at genome co-ordinate 75, however, late in infection, DBP transcription is initiated from a promoter at map position 72, and is independent of E1A13s protein activity.

DBP is a multi functional protein which has been implicated in a number of viral functions, including multiple roles in viral DNA replication (section 1.1.3iii), and early (Ricigliano *et al.*, 1994) and late (Silverman and Klessig, 1989) gene expression. For each of these processes DBP appears to have several roles, for instance, in early gene expression DBP has been reported to alter transcription from E2 and E4 promoters, and to destabilise E1

mRNA's. It appears that the diverse nature of the processes in which DBP functions are, in part, due to interactions with as yet unidentified cellular proteins.

The E3 region of adenovirus, like that of E2, is served by a single promoter early in infection, which is trans-activated by E1A13s protein. However, the promoter is unique in that it contains recognition sequences for NFkB transcription factor, that can lead to independent transcription in lymphoid cells (Wold and Gooding, 1991), which may explain why adenoviruses can persist in lymphoid tissue. During the early stages of infection, the E3 promoter drives expression of about nine alternatively spliced mRNA, that are polyadenylated at either the E3A or E3B sites (figure 1.4), generating proteins that are not required for virus replication, but which counteract the host cell defences (Wold and Gooding, 1991; Tollefson *et al.*, 1996a). Five of the E3 proteins are integral membrane proteins, the most abundant of which (Gp 19kd) prevents lysis of infected cells by cytotoxic T-lymphocytes (CTL) through binding to the major histocompatibility class-1 antigen (MHC-1) heavy chain, and blocking its transport to the cell surface. After E1A proteins have increased the infected cells susceptibility to tumour necrosis factor (TNF), expression of the E3 14.7kd and 10.5kd proteins, and the E3 19kd protein confer resistance to cytolysis. The E3 11.6kd protein is of particular interest as it is not expressed until late stages of infection, and may be involved in promoting cell lysis and virion release (Tollefson *et al.*, 1996a and b).

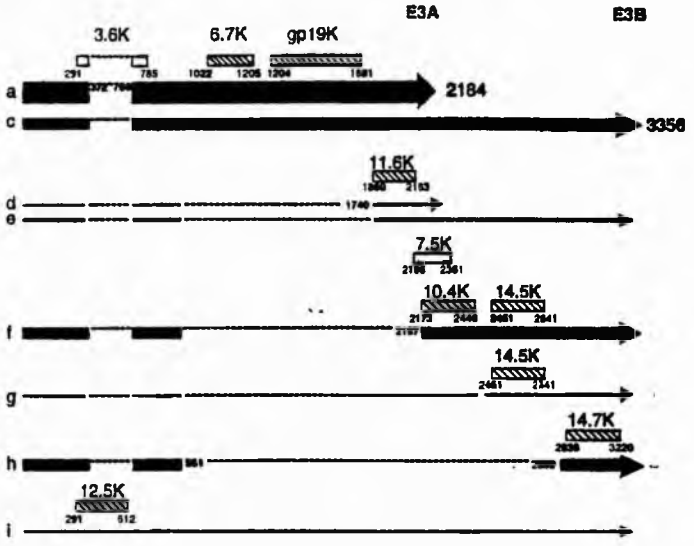

Figure 1.4: E3 transcription unit of Ad2. The split arrows depict the spliced structures of the mRNA; exons are solid, and the thickness implies the relative abundance. E3A and E3B are polyadenylation sites. The 3'end of mRNA i may be at the E3A or E3B site (reproduced from Wold *et al.*, 1995).

Transcription of the intermediate IX and IVa2 genes occurs at 6 to 8 hours post infection. The mRNA generated from the IX transcript is unique as it is the only adenovirus mRNA transcript not to be differentially spliced (Alestrom *et al.*, 1980). If RNA splicing is a prerequisite for the generation, transport, and cytoplasmic stability of Ad2 mRNA then the IX transcript must be subject to different rules. The IX protein is also unique as it is synthesised before the other structural proteins, and augmented late in infection (Boulanger *et al.*, 1979; Alestrom *et al.*, 1980). This may signify that protein IX has alternative functions in the replicative cycle.

The IVa2 protein has been shown to be a late stage specific transcriptional activator of the major late transcription unit (MLTU) promoter after the onset of DNA synthesis (Lutz and Kedinger, 1995; Lutz *et al.*, 1996). The IVa2 protein is a component of two complexes, DEF-A and DEF-B, that bind to sequence elements (DE) located downstream of the MLP start site. DEF-B consists of a IVa2 homodimer, and DEF-A of a IVa2 monomer complexed with a 40kd polypeptide thought to be the cleavage product of the L1 52kd/55kd scaffold proteins (Gustin *et al.*, 1996). An interaction between IVa2 and the L1 52kd/55kd proteins has been demonstrated, and possible cleavage of the L1 52kd/55kd proteins has been additionally proposed (Hasson *et al.*, 1992; Diouri *et al.*, 1996; Rancourt *et al.*, 1996). The early appearance of the L1 52kd/55kd proteins is unique among the gene products transcribed from the MLP and is suggestive that the proteins may have functions in addition to those involved in assembly.

iii) DNA replication:

Replication of the adenovirus 36kbp genome begins with the formation of a preinitiation complex at the origins of replication located within the 100bp inverted terminal repeat regions. The preinitiation complex consists of 3 viral proteins encoded by the E2 transcription unit, namely, the precursor terminal protein (pTP), DNA polymerase (Pol), and the DNA binding protein (DBP). The first two are present in infected cells as a heterodimer (pTP-Pol), and together with DBP can sustain a low level of replication from the core region (Smart and Stillman, 1982; Van der Vleit, 1995). The terminal protein (TP) which is bound to the parental DNA via a phosphodiester bond can enhance initiation, possibly by conferring subtle changes on the conformation of the core structure.

DBP, which is known to destabilise the DNA helical structure (Hay *et al.*, 1995), forms a multimeric protein-DNA complex which enhances the association of host protein nuclear factor 1 (NF1) with its own recognition site. In turn, NF1 interacts with Pol (Bosher *et al.*, 1992), thereby orientating pTP-Pol to the core region. The preinitiation complex is further stabilised by another host nuclear factor, NFIII/oct-1, which is capable of DNA bending, and may also bind to pTP-Pol.

The initial reactions of replication involve the distortion of the origin to permit the template strand to enter the Pol active site and coupling of dCMP to pTP. Once elongation has started, NF1 and NFIII/oct-1 dissociate (figure 1.5), and daughter molecules are synthesised as long as DBP and host protein NFII are present to remove topological stress. Initiation and elongation are ATP independent. The replication fork proceeds to the 3' inverted terminal repeat where the polymerase may dissociate having generated a daughter duplex and a ssDNA-DBP complex. In the second stage of DNA replication, displaced ssDNA-DBP complexes can be used for the same protein-primed initiation process if the template forms a panhandle structure. Alternatively, displaced strands with opposite polarity might renature to form a dsDNA daughter molecule.

Viral genome replication occurs in defined subnuclear structures (Hozak *et al.*, 1993; Pombo *et al.*, 1994; Besse and Puvion-Dutilleul, 1994) which develop from early replicative sites containing a mixture of ssDNA and dsDNA complexes, to distinct compartments which contain either ssDNA-DBP (viral ssDNA accumulation sites) or dsDNA complexes located to the fibrillogranular network. DNA replication occurs at the borders of the fibrillogranular network contiguous with the viral ssDNA accumulation sites. Besse and Puvion-Dutilleul (1994) suggest that replicating ssDNA genomes migrate to the nearest fibrillogranular site as soon as a portion of the genome becomes double stranded. Conversely, a non-replicating strand separated from dsDNA migrates to the viral ssDNA accumulation site. The mechanism by which viral DNA migrates is unknown, although there is evidence that pTP-DNA and TP-DNA can interact with nuclear matrix components at replication and transcription sites (Schaak *et al.*, 1990; Fredman and Engler, 1993).

Within two hours of synthesis, viral genomes can be located in capsids (Besse and Puvion-Dutilleul, 1994). Fredman and Engler (1993) suggest that processing of pTP-DNA to TP-DNA by the viral 23kd protease is required to release TP-DNA for encapsidation. However,

pTP-DNA is packaged within virus particles in Ad2ts1 infected cells, which can replicate efficiently at the non-permissive temperature (Webster *et al.*, 1994; Rancourt *et al.*, 1995).

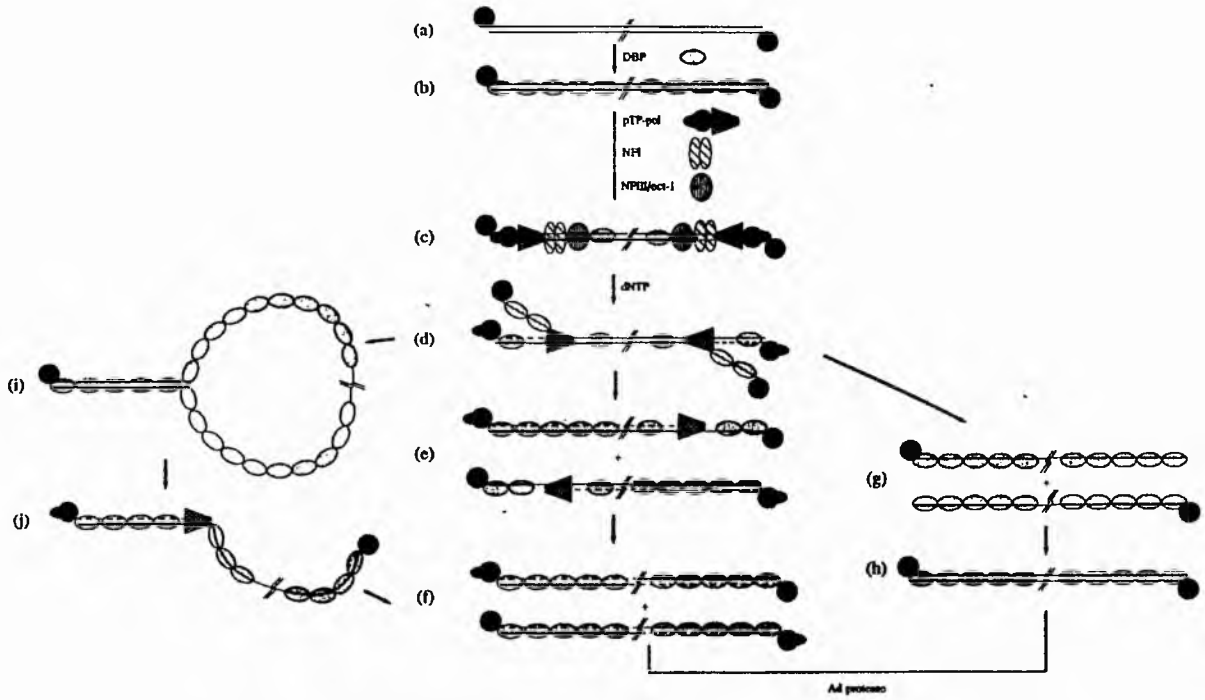

Figure 1.5: General outline of the first round of Ad DNA replication. The parental TP containing template DNA (a) forms a multi-protein-DNA complex with DBP (b). A preinitiation complex (c) is assembled with the various replication proteins and initiation occurs by covalent coupling of a dCMP residue to pTP. In the presence of dNTP elongation starts by a displacement mechanism, requiring minimally pol and DBP. Replication can proceed from both sides of the molecule (d and e), and finally duplex daughter strands containing TP at one end and pTP at the other. Alternatively, if displaced strands of different polarity are formed (g), these can renature, to form a duplex with two TP molecules (h). In addition, if intrastrand renaturation of the ITR occurs, this can lead to a panhandle structure (i). The regenerated double stranded origin can be used again for protein primed initiation, leading to a partially duplex intermediate (j) and finally a daughter molecule (f). reproduced from Van Der Vleit (1995).

Webster *et al.* provide evidence that TP, processed from pTP, cannot interact with Pol to form the heterodimer required for DNA replication initiation. It seems likely that pTP-Pol, pTP-DNA, and TP-DNA have distinct nuclear matrix binding properties which have a direct bearing on viral replication and transcription site localisation during the course of infection. Recent evidence (Angeletti and Engler, 1996) suggests that pTP attachment to the nuclear matrix can be regulated by one or more tyrosine kinase mediated phosphorylation events. The implications are that such events may facilitate pTP-DNA encapsidation and have a functional role in pTP-DNA localisation at DNA replication sites. Similarly, phosphorylation and

dephosphorylation events ascribed to DBP during DNA replication (Russell *et al.*, 1989) may facilitate ssDNA-DBP complex localisation to viral ssDNA accumulation sites.

iv) Late gene transcription and translation:

After the onset of DNA synthesis, most late proteins are translated from mRNA's originating from the major late transcription unit (MLTU) which extends from the major late promoter (MLP) at map co-ordinate 16.8 (figure 1.6a) to a termination signal close to the right end of the genome. Although during the early phase of infection the MLP is active at a level comparable to other transcription units, transcription is subject to control at the level of transcriptional termination and does not extend beyond map co-ordinate 75. At late times post infection, the transcription termination block is alleviated (Larsson *et al.*, 1992) and the primary transcript generated can be processed into a minimum of 20 mRNA's that are grouped into five families (L1 to L5) according to their different polyadenylation sites (poly (A) sites).

An important event governing the transition from early to late gene expression is viral DNA replication. The intermediate gene product, protein IVa2, gains efficient access to viral templates during replication and contributes to the late phase dependant MLP activation. In this respect, IVa2 is a temporal regulator, promoting late MLP activity and the generation of late (L1 to L5) mRNA transcripts (Tribouley *et al.*, 1994; Lutz and Kedinger, 1995). Accumulation of late mRNA's is also regulated at the level of poly (A) site selection. Prior to the onset of DNA synthesis, only L1 mRNA's encoding the 52kd and 55kd phosphoproteins accumulate in the cytoplasm. L1 pre-mRNA poly (A) sites have additional *cis*-acting elements that are required for recruiting cellular 3' end processing factors utilised for addition of the 200 residue poly (A) tail (Dezazzo *et al.*, 1991; Imperiale *et al.*, 1995). Late in infection, the situation is reversed and the L2 and L3 poly (A) sites are used 2-3x more frequently than the L1 poly(A) site because of a higher affinity for 3' processing factors. Additionally, Larsson *et al.* (1992) have shown that by blocking translation late in infection, only L1 and L4 mRNA's accumulate in the cytoplasm, implying that the use of the L2, L3, and L5 poly (A) sites require one or more late viral factors.

A further layer of regulation of gene expression is the temporal control of alternative splicing of mRNA transcripts. Most viral mRNA's are matured by removal of one to three introns, the

extreme examples being mRNA for protein IX, which contains no introns, and mRNA encoding the fibre protein, which contains auxiliary x, y and z leaders and requires the removal of six introns (Alestrom *et al.*, 1980). Most often the introns are positioned in the 5' or 3' non-coding portion of the pre-mRNA. For instance, expression of the L1 mRNA family represents an example of alternative splicing in which the last intron is spliced using a common 5' splice site and two alternative 3' splice sites, generating mRNA's for the 52kd/55kd (proximal 3' splice site) and IIIa (distal 3' splice site) proteins. The IIIa distal 3' splice site is relatively weak and does not bind cellular splicing factors as effectively as the proximal site. Efficient IIIa splicing requires late viral protein synthesis, possibly virus encoded splicing factors, or virus induced/modified cellular splicing factors (Imperiale *et al.*, 1995).

Regulation of the E3 splicing system is perhaps the best studied (Scaria and Wold, 1994; reviewed by Wold *et al.*, 1995). The E3 region is embedded within the MLTU which allows for both transcriptional and post-transcriptional control of E3 mRNA. Approximately nine alternatively spliced mRNA are polyadenylated at one of two sites generating two families of mRNA's. Transcription occurs from the E3 promoter early in infection, but is reduced at late stages, with E3 mRNA arising from MLP activity. These new mRNA contain the tripartite

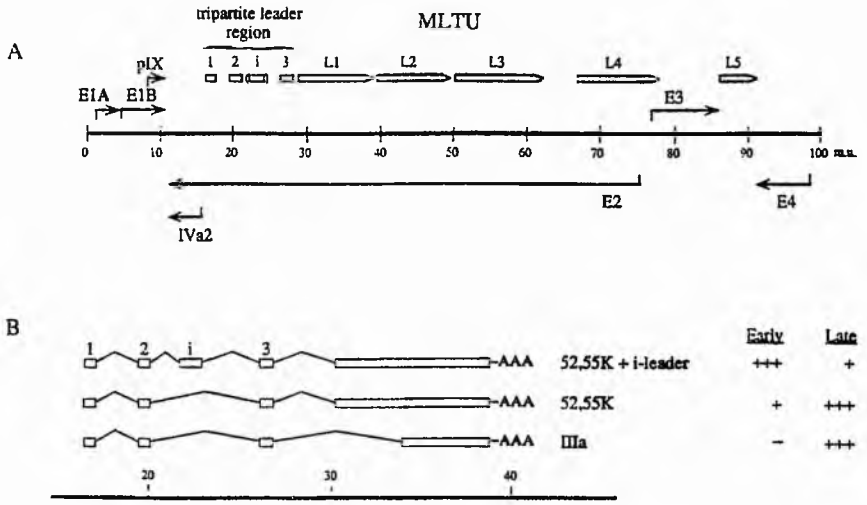

Figure 1.6: Organisation of the Ad2 genome. (A) schematic representation of the MLTU which encodes 5 families of mRNA's (L1 to L5). All mRNA's from this unit receive a common set of 5' leaders through splicing the tripartite leader region. (B) spliced structures of the major mRNA's expressed from the L1 region and their relative expression during infection (reproduced from Nordqvist et al., 1994).

leader sequence and are as abundant as the L4 family of mRNA, thus, the E3 11.6kd protein is a major late protein being detected approximately 24 hours post infection.

All the late mRNA's from the MLTU have a common 201-nucleotide tripartite leader sequence at their 5' end, which is important for cytoplasmic stability and for selective transport late in infection (figure 1.6b). A variant form of this leader contains a 440-nucleotide i-leader exon, the splicing of which is temporally regulated during infection by the E4 ORF3 and E4 ORF6 proteins (Nordqvist *et al.*, 1994; Ohman *et al.*, 1993). E4 ORF3 facilitated splicing of major late mRNA at early times of infection usually leads to the inclusion of the i-leader exon (1,2,i,3), however, the majority of mRNA's expressed late in infection contain the common tripartite leader (1,2,3), which is dependant on the exon skipping functions of E4 ORF6. Interestingly, the functions of E4 ORF3 and ORF6 are dependant on late viral protein synthesis, which if defective, results in late mRNA's retaining the i-leader exon. In addition, The E4 ORF4 inhibition of E1A trans-activation of early gene expression, may autoregulate E4 ORF3 and ORF6 splicing events (Bondesson *et al.*, 1996).

Viral protein synthesis dominates synthetic activity during the late stages of infection, and cellular protein synthesis ceases. The events involved have been attributed to a variety of processes, for instance, the accumulation of viral mRNA in the cytoplasm is facilitated by the combined functions of the E1B 55kd and E4 ORF6 proteins which do not assist the transport of cellular mRNA's (Babiss *et al.*, 1985; Pilder *et al.*, 1986; Ornelles and Shenk, 1991), although recent evidence indicates that some translocation of small cellular mRNA's via nuclear pore complexes can occur (Smiley *et al.*, 1994). Furthermore, the expression of the 160 nucleotide viral associated mRNA's (VA RNA I and II) blocks the anti-viral activities induced by interferon (Zhang and Schneider, 1993). Interferon activates a double stranded RNA dependant kinase (DAI), which inactivates the essential translation factor elf2-a (O'Malley *et al.*, 1988). This has the effect of blocking the initiation of protein synthesis during viral infection. The VA RNA's are able to prevent this process by binding to the kinase, blocking its activation by interferon, and so allowing the initiation of protein synthesis to proceed. The dephosphorylation of CAP binding protein (elf-4f), another essential translation factor, has been shown to correlate with shutoff of host cell protein synthesis (Yang *et al.*, 1996). Synthesis of viral proteins continues because the common tripartite leader sequence of all viral mRNA's can promote ribosome binding late in infection.

The virus-encoded L4 100kd protein is also required for efficient late viral protein synthesis (Riley and Flint, 1993). The protein appears to enhance late translation by binding with mRNA, possibly via the tripartite leader sequence, and may be involved in the selective export of late mRNA's to the cytoplasm.

v) Virion assembly and maturation:

Late in the infectious cycle, structural proteins are preferentially translated and rapidly transported to the nucleus, with a lag period of 3 to 6 minutes after release from the polyribosomes (D'Halluin, 1995). The uptake of proteins by the nucleus is extremely selective, often requiring nuclear localisation signals (reviewed by Garcia-Bustos *et al.*, 1991). Several adenovirus proteins, namely, fibre (Shing Hong and Engler, 1991), E1A13s (Lyons *et al.*, 1987), DBP (Morin *et al.*, 1989), pTP (Zhao and Padmanabhan, 1988) and V (Russell and Kemp, 1995), contain arginine and lysine rich sequences that constitute these signals. The nuclear transport of viral proteins lacking NLS sequences may be facilitated by an association with proteins that do, as is the case with Ad-Pol which is chaperoned with pTP.

The first step in adenovirus assembly is the formation of hexon capsomers, which requires the L3 encoded protein II (hexon) and the L4 100kd protein. The L4 100kd protein binds to hexon in stoichiometric amounts while the latter is still attached to polyribosomes. The L4 100kd protein facilitates trimerisation of hexon monomers shortly after translation, then dissociates from the complex. Although the L4 100kd protein may be involved in transporting the hexon to the nucleus (Cepko and Sharp, 1983), there is evidence that the L3 encoded protein, pVI, is required for this function (Morin and Boulanger, 1984). On reaching the nucleus, hexon capsomers appear to be able to self assemble to form groups of nine (GON) hexon molecules which assemble to form the 20 sides of the virion molecule, while penton capsomers will assemble to form the 12 vertices. There is evidence that hexon capsomeres can assemble to form virus-like particles, and that formation of penton base may be a rate limiting step in the assembly process (Boudin *et al.*, 1979). In contrast to hexon, the L2 encoded penton, and L5 encoded fibre proteins oligomerise in the absence of other viral proteins (Karayan *et al.*, 1994).

After the construction of hexon shells, the assembly of virus particles proceeds through an ordered series of events (figure 1.7) which have been studied thoroughly using viral temperature sensitive mutants (blocked at different stages of assembly at the restrictive temperature), and by pulse-chase kinetic studies (Edvardsson *et al.*, 1976; D'Halluin *et al.*,1978 and reviewed by D'Halluin, 1995). Initially, the first recognisable viral assembly intermediate is a light intermediate particle (buoyant density of 1.315g/cc in a CsCl equilibrium gradient), that contains the capsid structural components pVI, pVIII, pIIIa, and possibly IX, which confer stability to the virion structure. Although thermolabile mutants of pVIII (H5sub304; Liu *et al.*, 1985), and protein IX (H5dl313; Colby and Shenk, 1981), have been identified, it is as yet unclear if both have any additional functional roles during the assembly process. Also associated with light intermediate particles are the 50kd and 39kd probable scaffold proteins and the L4 100kd protein. The light intermediate particles mature into heavy intermediate particles (buoyant density of 1.37g/cc) with the insertion of viral DNA and the removal of the 50kd and 39kd proteins.

The left end of the viral genome including the E1A region has been shown to be inserted into the virion first, with nucleotide sequences at 200 to 400bp appearing to be essential for the encapsidation of the genome (Hammerskjold and Winberg, 1980). The factors involved in binding to the *cis*-acting elements have not been identified, although the IVa2 protein, which is present in light intermediate particles (Edvardsson *et al.*, 1976; D'Halluin *et al.*, 1978) possibly in association with the L1 52kd/55kd proteins have been implicated (Gustin *et al.*, 1996), as they are both known to bind DNA. The possible role of the L1 52kd/55kd proteins in packaging was suggested by the analysis of a temperature sensitive mutant (ts369), which accumulates incomplete particles at the restrictive temperature that carry only small segments of the left end of the genome (Hasson *et al.*, 1989 and 1992). Similarly, possible roles for DBP and pIIIa in DNA packaging have been suggested by the analysis of mutants, ts19 (Roovers *et al.*, 1990), and H2ts112 (D'Halluin *et al.*, 1982), both of which accumulate light intermediate particles at the restrictive temperature.

The viral DNA is condensed into a core structure by the viral proteins V, pVII and possibly pmu (Vayda and Flint, 1987). It is unclear whether the core proteins are encapsidated with the viral genome, as they are not detected in either light or heavy intermediate particles (D'Halluin 1995; Schmid and Hearing, 1995).

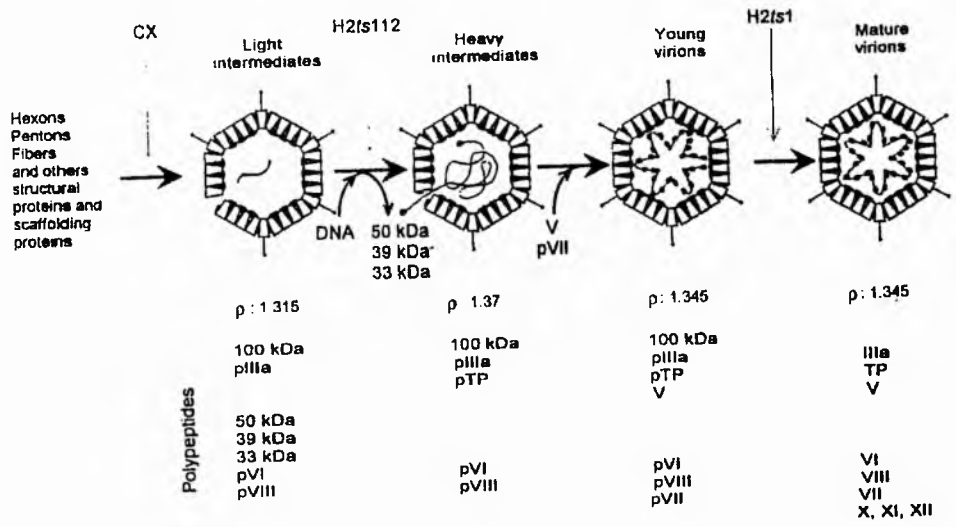

Figure 1.7: Assembly pathway for Ad2/5. The different stages of virus assembly have been indicated at the top and the polypeptides only present in some structures are indicated below. Defective mutants in the assembly pathway are indicated at the top of the arrow at the right side. CX; cyclohexamide (reproduced from D'Halluin, 1995).

After DNA packaging, young virions are matured into infectious particles by the cleavage of structural proteins pVI, pVIII, pIIIa, and the core proteins pVII, pTP, and pmu (Trembley *et al.*, 1983; reviewed by Weber, 1995). There is evidence that the L1 52kd/55kd scaffold proteins are also cleaved during virus assembly, as probable cleavage products have been identified in mature virions (Hasson *et al.*, 1992). None of these cleavages takes place in cells infected with the Ad2ts1 temperature sensitive mutant at the non-permissive temperature. The mutation has been mapped to the L3 region encoding the viral 23kd protease, with a proline substituted for lysine at residue position 137 (Yeh-Kai *et al.*, 1983). Viral 23kd protease activity has been detected in nuclei of infected cells, and inside mature virions, but not in Ad2ts1 young virions accumulated at the non-permissive temperature (Bhatti and Weber, 1979). The temperature sensitive protease is synthesised and transported to the nucleus to become associated with incomplete particles in a manner similar to the wild type protease (Anderson, 1990; Rancourt *et al.*, 1995). The defect apparently resides in a failure of the enzyme to be activated and encapsidated. The failure to dephosphorylate protein V is another interesting consequence of Ad2ts1 infection (Weber and Khitoo, 1983), the significance of which is still unclear.

1.1.4 Progressive reorganisation of host cell structure.

The cytoskeletal and nuclear morphological changes associated with adenovirus infections of cultured cells are a result of complex interactions between host and viral components which allows for efficient production of virus particles. The cytopathic effects that are observable by light microscopy, culminate in cell death and release of progeny virions. In recent years, information provided by electron microscopy techniques such as immunocytochemistry, autoradiography,*insitu*-hybridisation and selective staining have been complementary in determining the structure-function relationships of cellular domains at the ultrastructural level, and are reviewed in this section.

i) Nuclear organisation of replication and transcription:

The nucleus is organised into a series of structural domains which includes the nucleolus, chromatin (in various degrees of condensation), and interchromatin regions which contain several characteristic structures, including perichromatin fibrils and granules, and other nuclear bodies including coiled bodies (Brasch and Ochs, 1992; Puvion-Dutilleul *et al.*, 1995a; Hassan, 1995). In uninfected cells, active DNA synthesis occurs at ovoid bodies adjacent to chromatin (Hozak *et al.*, 1993; Hassan, 1995). However, nuclei of infected cells progressively accumulate new induced structures as a consequence of viral replication (Puvion-Dutilleul and Puvion, 1995; Puvion-Dutilleul *et al.*, 1995b; Besse and Puvion-Dutilleul, 1994; Pombo and Carmo-Fonseca, 1995). The earliest ultrastructural changes, detected at 6 to 8 h.p.i, are small irregularly shaped masses of thin fibrils that rapidly increase in size and become pleomorphic, appearing as crescents, rings, and spheres by 16 to 20 h.p.i (figure 1.8). These structures contain DBP, and are contiguous for DNA synthesis at the early stage. However, late in infection, at the pleomorphic stage, these structures contain the majority of viral ssDNA-DBP and continuous replication is displaced from these sites to the surrounding fibrillogranular network (peripheral replicative zone), which contains viral dsDNA (figure 1.9). Still later, the ssDNA-DBP accumulation sites become smaller and more homogenous in shape appearing as globular inclusions rather than crescents and rings (Chaly and Chen, 1993). These centres are eventually located at the outer edge of the viral genome storage site which is detected in cells after 18 to 20 h.p.i. The genome storage site is frequently associated with crystalline arrays of virus, and it has been suggested that DNA

from this compartment may be incorporated into virions (Puvion-Dutilleul and Puvion, 1990).

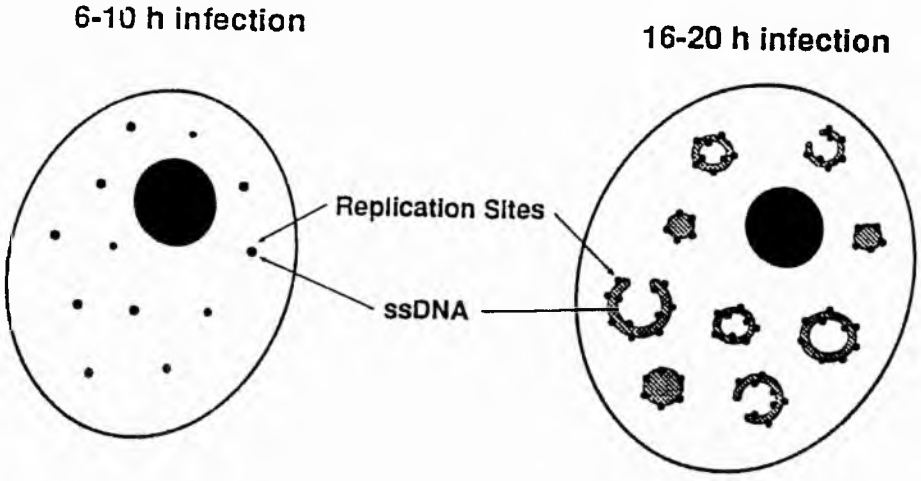

Figure 1.8: Intranuclear organisation of Ad2/5 replication. Shortly after the onset of viral replication, Ad DNA synthesis occurs at focal centres that are scattered in the nucleoplasm and excluded from the nucleolus. Later, at 16-20 h.p.i, ssDNA and DBP accumulate next to the replication sites, giving rise to goblet-shaped structures (reproduced from Pombo and Carmo-Fonseca, 1995).

Infected cells subjected to a pulse of ^{3}H-uridine (Puvion-Dutilleul *et al.*, 1992) have been examined by electron microscopy to locate viral transcription sites. At early stages of infection, transcription is present at the early replicative sites, and at intermediate stages, is detected at peripheral replicative zones. From 17 h.p.i onwards, labelled RNA is present in peripheral replicative zones, interchromatin granules, virus induced compact ring structures, and ribosome containing areas of the cytoplasm. Pombo *et al.* (1994) suggest that replication and transcription occur together in the early replicative sites, and peripheral replicative zones, and that interchromatin granules and compact rings may be involved in post-transcriptional processing and intranuclear trafficking of viral RNA as it moves through the nucleus into the cytoplasmic compartment.

ii) Post-transcriptional processing and assembly centres:

In non-infected cells, splicing factors have been shown to accumulate in several distinct nuclear structures, including interchromatin granules, perichromatin fibrils, coiled bodies (Bridge *et al.*, 1993; Bridge and Pettersson, 1995; Rebelo *et al.*, 1996) and interchromatin granule-associated zones (Puvion-Dutilleul *et al.*, 1994 and 1995a). Although the

concentrations of splicing components in discrete nuclear compartments raises the possibility that they are involved in splicing, Bridge *et al.* (1995) suggest that some compartments may be important in aspects of spliceosome assembly, including recycling and storage of splicing factors. For instance, the clusters of interchromatin granules and their associated zones, as well as coiled bodies, may be involved in pre- and/or post-splicing events such as spliceosome assembly and/or sorting of spliced molecules and intron degradation (Ferreira *et al.*, 1994; Puvion-Dutilleul *et al.*, 1995a).

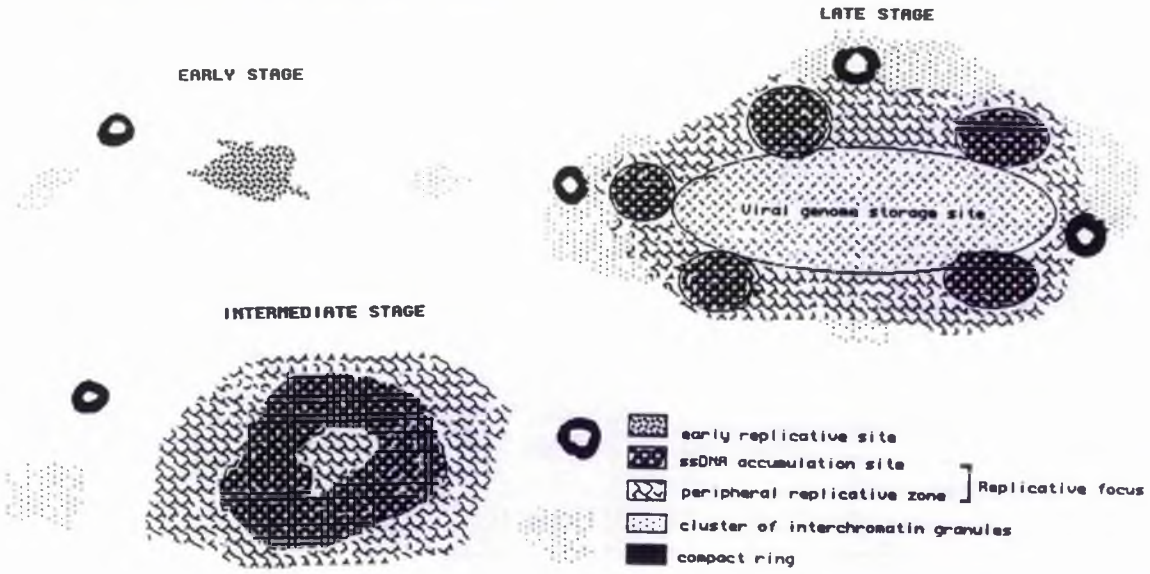

Figure 1.9: Schematic drawing summarising the three distinct phases of ultrastructural modifications observed in Ad5 infected cell nuclei. At the earliest stage of nuclear transformation, replicative foci consist of small areas of densely packed fibrils. In the intermediate stage, the replicative foci are enlarged and give rise to multiple copies of two contiguous structures, the pleomorphic ssDNA accumulation sites and the surrounding peripheral replicative zone. In the late stage of nuclear transformation, the two compartments of the replicative foci decrease in size, whereas the new centrally located viral genome storage site appears. At this stage, clusters of interchromatin granules, which are also present in uninfected nuclei, are enlarged, and virus induced compact rings of unknown significance are numerous. Both structures are located at the periphery of the large viral inclusion body (reproduced from Puvion-Dutilleul *et al.*, 1992).

Following adenovirus infection, the initial distribution of splicing components remains unchanged (Besse and Puvion-Dutilleul, 1995; Bridge *et al.*, 1993 and 1995), however, after the onset of DNA synthesis small nuclear ribonuclear particles (snRNP's) are associated with the early replicative sites (figure 1.10) that contain DNA, RNA and ssDNA-DBP. As infection progresses and the ssDNA-DBP accumulation sites become pleomorphic, snRNP distribution appears to be confined to the peripheral replicative zones and interchromatin

granules. Therefore, at late stages of nuclear changes, splicing components are no longer in the centre of the nucleus, which is occupied by the viral genome storage site (figure 1.10), but are localised at the border of this large inclusion body, where they form a spherical shell consisting of enlarged clusters of interchromatin granules and fibrillogranular networks. The compact ring structures, which do not contain snRNP's, are also embedded in this shell at the nuclear periphery.

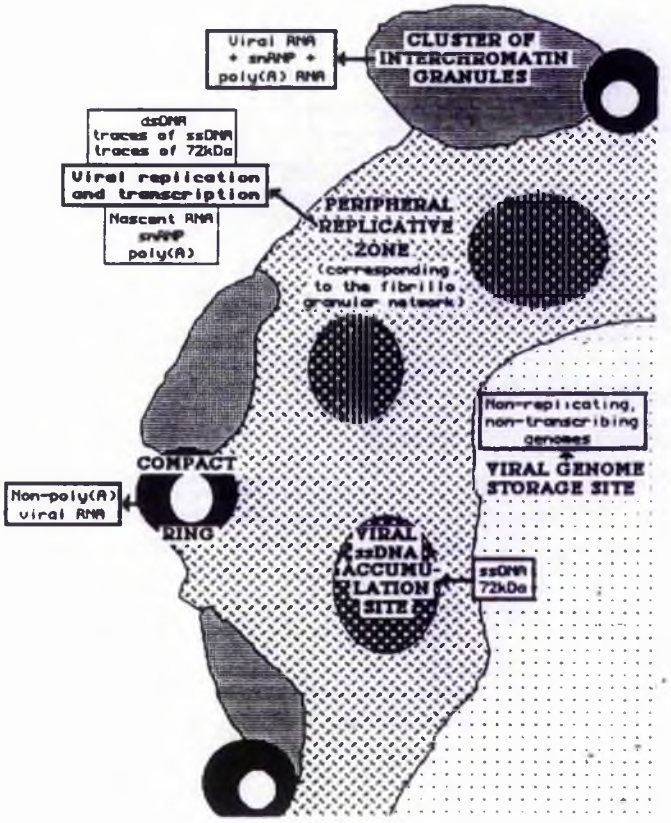

Figure 1.10: Schematic model of a quarter nucleus at the late stage of nuclear transformation. The large viral genome storage site, which is not involved in the transcription and RNA processing steps, is surrounded by a shell consisting of four structures, three of which contain viral RNA. Both the peripheral replicative zone, which is also a transcription site for viral genomes, and the clusters of interchromatin granules, in which viral RNA is present, contain spliceosome components and poly(A)+ RNA. The virus induced compact rings contain non-polyadenylated viral RNA, which could correspond to unused portions of the viral transcripts. The viral ssDNA accumulation sites, which are devoid of RNA, are not involved in the synthesis and processing of viral transcripts.

Through the specific detection of viral RNA transcripts and poly(A) RNA molecules (viral and cellular), Puvion-Dutilleul *et al.* (1994) have proposed that the peripheral replicative zone

is the precise site of viral genome transcription and the main site of viral RNA splicing. Additionally, the interchromatin granules participate in post-splicing events, and may contribute to the regulation of the amount of individual mRNA in the cytoplasm at defined periods of time. The virus induced compact ring structures containing viral RNA (but not poly(A) RNA) are probably not involved in splicing events, but contain non-used portions of primary late transcripts resulting from differential poly(A) site selection at the post-transcriptional level.

These authors also observed the disappearance of coiled bodies and interchromatin granule-associated zones at intermediate stages of nuclear transformation. These sites are likely to be concerned with spliceosome maturation and/or storage/recycling of snRNP's, but additionally are highly enriched in p80-coilin, an 80kd phosphoprotein of unknown function (Puvion-Dutilleul *et al.*, 1995a; Rebelo *et al.*, 1996). The finding that coiled bodies are very labile structures that require ongoing protein synthesis is suggestive that adenovirus induced inhibition of cellular protein synthesis may, in part, cause the disassembly of these sites, and consequently affect splicing events late in infection.

Coiled bodies are known to be associated with other structural domains, the most prominent being the nucleolus which is actively involved in the biogenesis of pre-ribosome's and the transport of poly(A) RNA from the nucleus to the cytoplasm (Carmo-Fonseca *et al.*, 1993; Bridge and Pettersson, 1995; Schneiter *et al.*, 1995). The inhibition of cellular protein synthesis by adenovirus infection has been shown to result in the inhibition of ribosomal RNA production and cause the redistribution of nucleolar antigens (Castiglia and Flint, 1983; Bridge *et al.*, 1995). Additionally, fibrillarin, a structural component of coiled bodies and nucleoli, has also been shown to be redistributed to the proximity of ssDNA-DBP accumulation sites and latterly to the peripheral replicative zones late in infection (Puvion-Dutilleul and Christensen, 1993). Studies utilising deletion mutants of p80-coilin (Bohmann *et al.*, 1995) have demonstrated that these effects may be specifically related to p80-coilin which appears to have a role in maintaining nucleolar structure and function. Recent studies (Schul *et al.*, 1996) have also shown coiled bodies to be intimately associated with cleavage bodies and PML (promyelocytic leukaemia) bodies within uninfected cells (figure 1.11). These authors suggest that 3' cleavage factors, required for 3' processing and polyadenylation of pre-mRNA, undergo transcriptional dependent recycling in cleavage

bodies, and that components required for splicing factor recycling may be involved in this process. Their findings have also led them to propose that cleavage bodies are closely associated with sites of RNA synthesis, and although coiled bodies and PML bodies are outside these sites, they may be involved in processing of specific RNA's.

The PML protein was first identified as part of a fusion protein with retinoic acid receptor-α (RARα), which results from a chromosomal translocation associated with acute promyelocytic leukaemia (APL). The PML protein contains a cysteine-rich motif, known as the RING finger, that is commonly found in a family of proteins involved in RNA transcriptional control and processing (Koken *et al.*, 1994; Borden *et al.*, 1995; Puvion-Dutilleul *et al.*, 1995b). The latter authors have shown PML to concentrate in PML bodies and interchromatin granule-associated zones in uninfected cells, however during adenovirus infection, the protein is located in virus-induced clear amorphous inclusions (figure 1.12). These structures are initially small, and irregularly shaped, but as infection progresses they become larger, more spherical, and abundant, usually surrounded by virus particles.

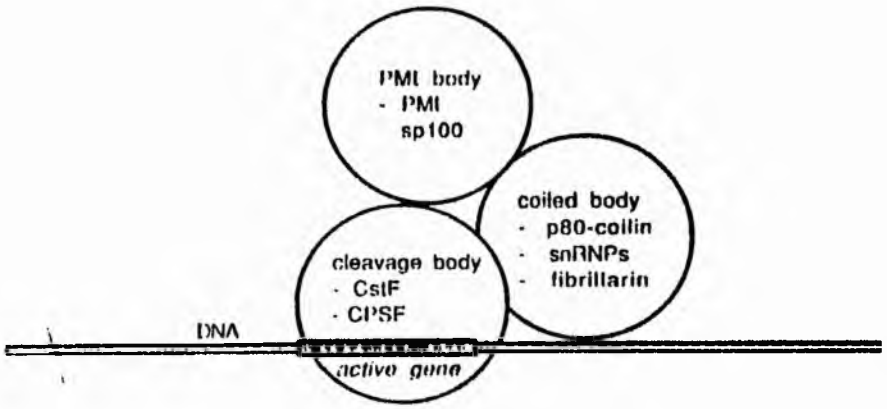

Figure 1.11: Schematic representation of the proposed organisation of a trio of cleavage body, coiled body and PML body on an active gene. The cleavage body is in contact with the entire gene or just with the downstream part containing the cleavage site. The other two bodies do not contain DNA or newly transcribed RNA, yet are associated with the specific locus (reproduced from Schul *et al.*, 1996).

In addition to its presence in inclusions, PML is also detected within virus-induced protein crystals that are known to contain at least one viral structural protein, namely, the hexon. The origin of clear amorphous inclusions and protein crystals is unclear, although recent studies

have indicated that the E1B 55kd and E4 ORF3/ORF6 proteins are responsible for the redistribution of PML protein and PML body components during the course of infection (Carvalho *et al.*, 1995; Doucas *et al.*, 1996). Doucas *et al.* (1996) have shown the E1B 55kd protein to localise transiently with PML bodies early in infection (5 to 8 h.p.i) and complex with the E4 ORF6 protein. The E4 ORF3/ORF6 proteins appear to induce the morphological changes that culminate in the formation of the PML containing fibrillar tract, although evidence suggests that the E4 ORF3 protein, by itself, is able to promote this reorganisation, and remains localised to the tracts throughout the later stages of infection. The E1B 55kd/E4 ORF6 protein complexes have a more diffuse nucleoplasmic distribution, which probably correlates to viral replicative zones (Ornelles and Shenk, 1991). Doucas *et al.* have proposed that the morphological changes associated with the E4 ORF3/ORF6 proteins may facilitate the movement of regulated host factors from PML bodies to viral replication and transcription sites. The sequestration of PML protein into virus-induced clear amorphous inclusions (fibrillar tracts) may be required for its inactivation, as recent evidence demonstrates a direct involvement of PML in interferon anti-viral effects (Puvion-Dutilleul *et al.*, 1995b; Grotzinger *et al.*, 1996).

Nuclear reorganisation is considered to have reached the late phase when crystalline arrays of virus particles are distributed in the electron-translucent regions of the nucleoplasm (Chaly and Chen, 1993; Lutz *et al.*, 1996). Associated with virion containing centres are the viral genome storage sites, clear amorphous inclusions, and protein crystals (figure 1.12). The L1 52kd/55kd proteins have been shown to be associated with virion particles in assembly centres and to two other domains, termed, loading centres, and densely stained structures (Hasson *et al.*, 1992). These domains may correlate to the electron-dense amorphous inclusions described by Lutz *et al.*, which have been shown to contain protein IVa2 (figure 1.12). These electron-dense structures have the appearance of altered nucleoli (Zhongue *et al.*, 1986) and are anchored to the nuclear lamina by matrix filaments. Using embedment free electron microscopy, these authors have shown that by 28 h.p.i the filaments connecting amorphous and granular virus centres are decorated with capsids and mature virions, which suggests that they may be involved in transport of capsid intermediates, and mature virions. The granulated regions contain capsids and may be the sites of capsid assembly and storage, whilst the electron-dense amorphous inclusions may be the sites of DNA packaging into

immature virions. After 48 h.p.i, lysed nuclei still contain remnants of the nuclear-virus related structures, and many virions are still attached to the nuclear matrix filaments. In addition, virions are also attached to intermediate filaments of the host cell cytoplasm.

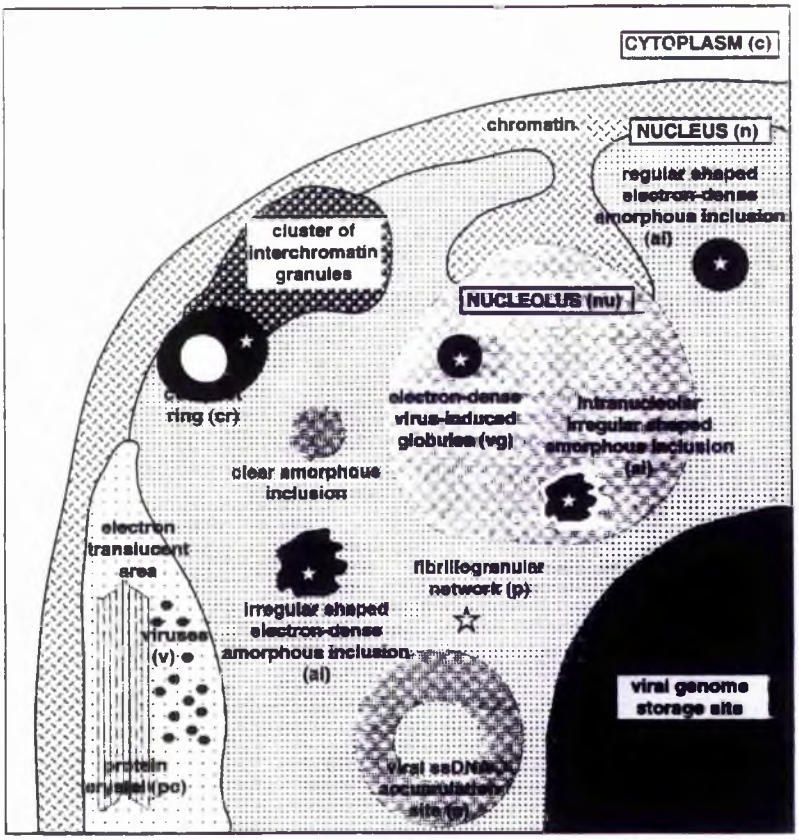

Figure 1.12: Ad-induced alterations of cell nuclei during infection. The main structural alterations appearing during infection are schematically represented and named. Protein IVa2 was shown to localise to structures indicated with stars (reproduced from Lutz *et al.*, 1996).

iii) Disruption of intermediate filaments:

The cytoskeleton is composed of microtubules, microfilaments, and intermediate filaments which form an interconnected network of fibrils that altogether, impart structural integrity to the cell. The intermediate filament (IF) family of proteins includes vimentin, and the cytokeratins (reviewed by Goldman *et al.*, 1986). In addition, the nuclear lamins, the main components of the peripheral nuclear lamina (Georgatos *et al.*, 1994), are also members of the IF family, and have a regulatory role in determining the morphology of the nuclear envelope.

Disruption of the vimentin system occurs within 30 minutes of virus uptake (Belin and Boulanger, 1987), and depends on the adenovirus induced activation of a cellular protease,

the activity of which is required for efficient transcytoplasmic migration of virion components to the nuclear envelope. Later in infection, from 14 h.p.i onwards, adenovirus induces a distinct sequence of cytoskeletal rearrangements that occur continuously during the course of infection (Staufenbiel *et al.*, 1986). For instance, the extended vimentin system has been shown to collapse into the perinuclear region of infected cells. A similar pattern of disruption is also observed in E1B 19kd transfected cells (White and Cipriani, 1989). Of interest is the disassembly of cytokeratin 18 (K18) late in infection (20 h.p.i onwards), to form spheroid globules and cytoplasmic clumps (Chen *et al.*, 1993). This alteration is due, at least in part, to the activity of the L3 23kd protease which cleaves the cytokeratin 18 protein, removing its N-terminal head domain, and thereby blocking its ability to form fibres. The disruption of the IF system, and the nuclear matrix (Zhongue *et al.*, 1986), might make the cell more susceptible to rupture, and facilitate the release of progeny virions. The inhibition of cellular protein synthesis prevents restoration of the cytoskeletal structure (Zhang and Schneider, 1994) and therefore may promote these events.

1.1.5 The L3 23kd protease:

Adenoviruses, like many viruses, encode an endoproteinase that is essential for virus maturation and infectivity. The enzyme is synthesised late in infection and is required for the proteolytic cleavage of at least six viral proteins, namely, pVI, pVII, pVIII, pIIIa, pTP, pmu, and possibly the L1 52kd scaffold protein (reviewed by Weber, 1995; Russell and Kemp, 1995). Synthetic peptides have been used *in vitro* to determine the consensus cleavage site as being (M,L,I)XGG'X and (M,L,I)XGX'G (Webster *et al.*, 1989; Anderson, 1990). The GENBANK/EMBL nucleotide databanks have been screened for adenovirus protease substrate proteins (reviewed by Weber, 1995) and putative cleavage sites in homologous regions compiled (Table 1.2). None of these cleavages occur in cells infected with the Ad2ts1 mutant, at the non-permissive temperature, resulting in the production of non-infectious virus particles devoid of protease activity (Weber, 1976; Rancourt *et al.*, 1995).

Inhibitory profiles (Webster *et al.*, 1989; Anderson, 1990; Tihanyi *et al.*, 1993; McGrath *et al.*, 1996) and mutagenesis studies (Grierson *et al.*, 1994; Rancourt *et al.*, 1994) have classified the enzyme as a cysteine protease that is active as a monomer and which does not require proteolytic activation. However, the Ad2 and Ad2ts1 recombinant enzymes have little

Virus	Protein[a]	Cleavage site		P1	Peptide cleaved[b]	
					in vitro	in vivo
H2[c]	pVII (197)	MFGG	AKKR	24	Yes	Yes
	pVIII (227)	IGGA	GRSS	157	–	Yes
	pVIII (227)	LAGG	FRHR	111	Yes	–
	pVI (250)	MSGG	AFSW	33	Yes	Yes
	pVI (250)	IVGL	GVQS	239	–	Yes
	11-kDa (79)	MAGH	GLTG	26	–	–
		LTGG	MRRA	31	–	Yes
		MRGG	ILPL	50	–	Yes
	pTP (668)	MRGF	GVTR	172	Yes	–
		MGGR	GRHL	180	Yes	–
		LGGG	VPTQ	314	No	–
		MTGG	VFQL	346	No	–
	pIIIa (585)	LGGS	GNPF	570	–	–
	L1 52-kDa (415)	LAGT	GSGD	351	–	–
H12	pVI (265)[d]	LNGG	AFNW	33	–	Yes
	pVI (265)[d]	IVGL	GVKS	254	–	Yes
	11-kDa (72)[d]	LTGN	GRFR	27	–	Yes
	11-kDa (72)[d]	MKGG	VLPF	42	–	Yes
	pVII (188)[d]	MYGG	AKTR	23	–	Yes
	pIIIa (582)[d]	LGGS	GNPF	565	–	Yes
	pTP (606)[e]	LQGY	GSTH	140	–	–
		LRGG	VFEL	289	–	–
	pVIII (233)[d]	IRGK	GIQL	138	–	Yes
		LGGS	GRSS	163	–	Yes
	L1 52-kDa (373)[e]	LTGA	GTED	328	–	–
H40[f]	pVI (267)	LNGG	AFSW	33	–	–
	pVI (267)	IVGL	GVKS	256	–	–
	pVIII (233)	LAGG	ARHV	111	–	–
	pVII (185)	MYGG	AKRR	23	–	–
	pTP (643)	LRGF	GSTR	172	–	–
	pTP (643)	LSGS	GMQG	318	–	–
	pTP(643)	MQGG	VFEL	323	–	–
	L1 52-kDa (380)	LTGT	GTDA	336	–	–
	11-kDa (70)	MAGS	GRRR	27	–	–
	11-kDa (70)	IKGG	FLPA	40	–	–
	IIIa (576)	LGGT	GAAS	556	–	–
H41	pVIII (233)[g]	LAGG	SRHV	111	–	–
	pVI[h]	IVGL	GVKS	–	–	–
CAN1	pVII (132)[i]	LFGG	AKQK	23	–	–
MAVI	pVI[j]	IMGL	GLQP	–	–	–

Table 1.2: Adenovirus substrate proteins and putative cleavage sites.

activity compared with that in disrupted wild type virions (Webster *et al*, 1993; McGrath *et al.*, 1996), and requires activation through the addition of an 11 residue peptide, GVQSLKRRRCF, that is the C-terminal cleavage product of pVI (Webster and Kemp, 1993; Mangel *et al.*, 1993; Rancourt *et al.*, 1995). The activating peptide (pVI-ct) is highly conserved among other serotypes (Weber, 1995) and a similar peptide derived from Ad12 pVI, GVKSLKRRRCY, has also been shown to activate the Ad2 enzyme (Friemuth and Anderson, 1993). Additionally, protease's from a wide range of serotypes have been shown to cleave Ad2 precursor proteins when incubated with Ad2ts1 virions (Houde and Weber, 1990). Recently, Rancourt *et al.* (1995) determined that full infectivity is restored in Ad2ts1 infected cells after the addition of activating peptide late in infection. The authors suggest that

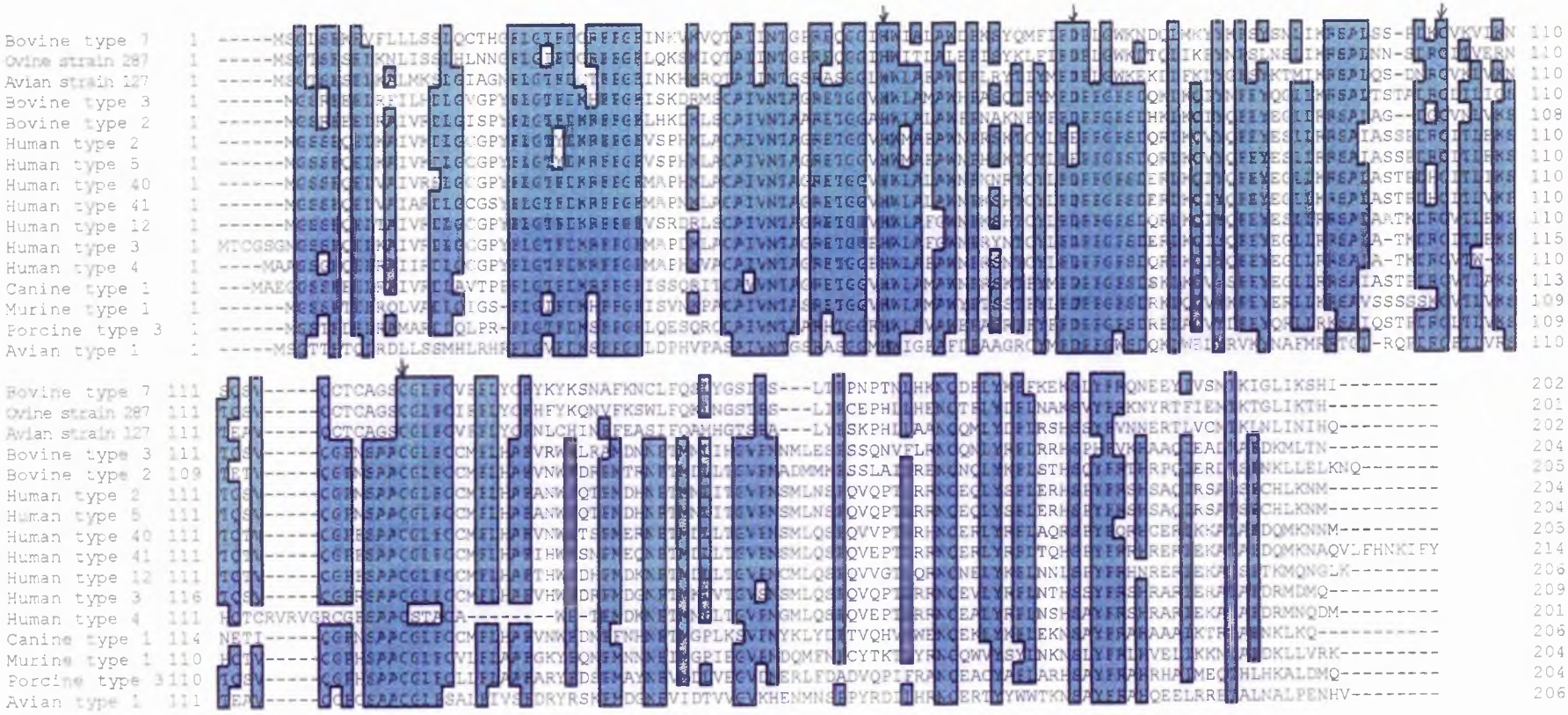

Figure 1.13: Alignment of protease sequences from 16 Adenovirus serotypes. Increased gap length penalty and manual adjustments based on DNA sequence alignment. Alignments created using the pileup program of the University of Wisconsin GCG package. The single conserved Histidine and the two conserved cysteines (arrows) and conserved residues (green) are highlighted. Sequences taken from N.C.B.I Entrez Browser, except for Avian strain 127 which was kindly provided by Lewis Murray (University of St.Andrews).

the protease defective phenotype is, at least in part, due to specific interactions involving pVI that are required for protease packaging *in vivo*.

Webster *et al.* (1993) proposed that activation of the enzyme occurs via a disulphide bond interchange between the oxidised (dimeric) form of pVI-ct and a conserved cysteine residue of the viral protease. Mutagenesis studies (Grierson *et al.*, 1994; Jones *et al.*, 1996; Rancourt *et al.*, 1996) have indicated that an interaction between the highly conserved Cys104 residue of the 23kd protease (figure 1.13) and pVI-ct can occur, and have identified the active site triad to be composed of the highly conserved His54, Glu71, and Cys122. Jones *et al.* (1996) have indicated that a conformational change induced by pVI-ct binding can enhance the availability of the Cys122 nucleophile for catalysis.

Recently, confirmation of the proposed mechanism of activation has come from the atomic structure of the Ad2 23kd protease co-crystallised with pVI-ct (Ding *et al.*, 1996). The active site triad appears to have a 3-dimensional arrangement similar to that of papain (figure 1.14), although the order of active site residues on the linear polypeptide differs between both enzymes. In addition, the activating peptide has been shown to interact with two non-contiguous regions of the protease, with the N-terminal 3 residues of pVI-ct interacting with ß-strand S7 and residues 4 to 10 interacting with S5 residues 104 to 109. The authors suggest that a peptide corresponding to residues 4 to 11 of pVI-ct could be an enzyme inhibitor, and therefore a potential anti-viral agent. Cabrita *et al.* (1997) have also indicated that the N- and C-terminal regions of pVI-ct are essential for productive interaction, indicating that the removal of the N-terminal glycine and valine residues does not affect peptide binding but does abolish activation.

Redox modulation has a profound effect on recombinant Ad2 and Ad2ts1 enzyme activity, with several isoforms resulting from intra- and inter-chain disulphide bridge formation being detected (Keyvani-Amineh *et al.*, 1996). Of interest is the observation that recombinant Ad2ts1, but not Ad2, enzyme activity is stimulated by low concentrations of oxidising agent. The Ad2ts1 proline to leucine substitution (P137L) has been shown to induce a slight structural change in an externally disposed loop of the recombinant protease that may offset the geometry of cysteine residues involved in disulphide bond formation (Keyvani-Amineh *et al.*, 1995). The addition of oxidising agent may overcome this defect and promote pVI-ct binding. Isoforms of 23kd protease have been isolated from infected cells late in infection,

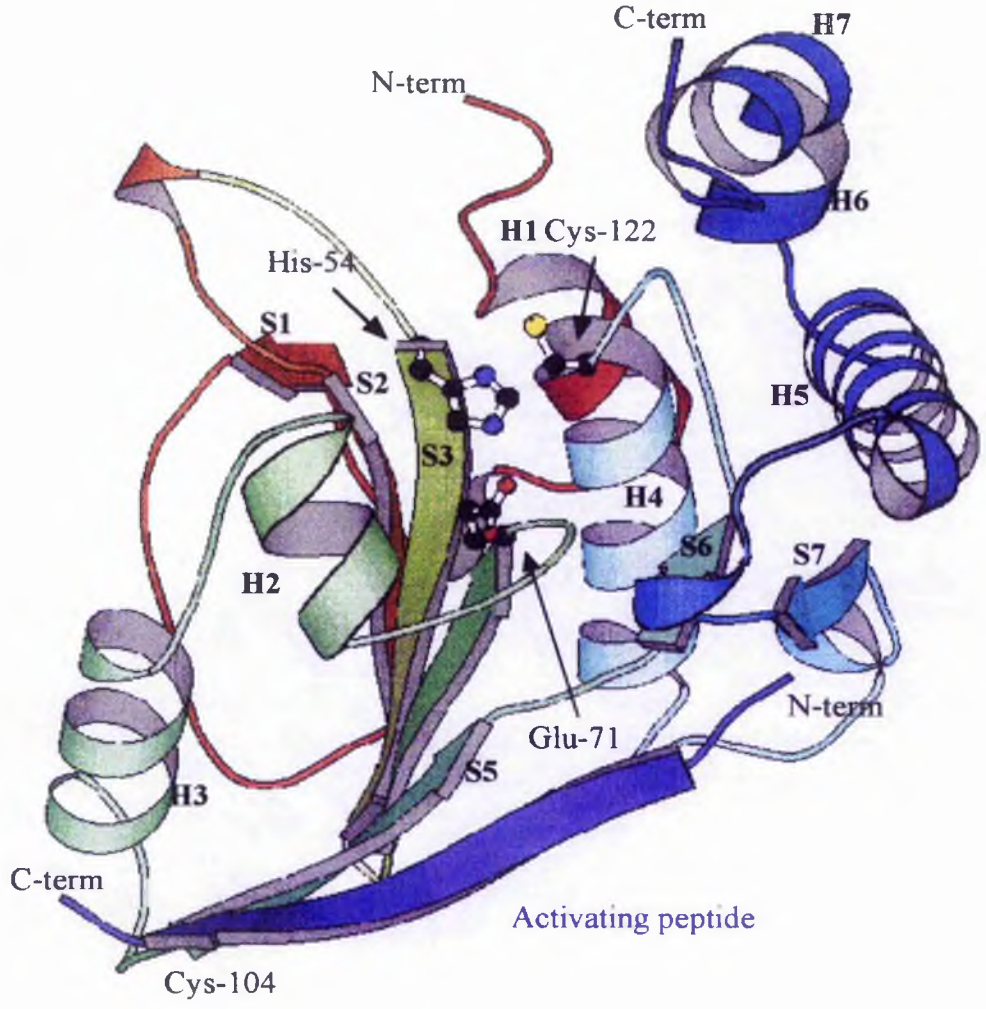

Figure 1.14: Atomic structure of the Ad2 23kd protease co-crystalised with pVI-ct. The complex is ovoid with α-helices labelled H1 through to H7 and ß-strands S1 through to S7 from the N-terminus to C-terminus. pVI-ct is the nearest ß-strand in the figure. The heterodimer is ovoid with three α-helices forming the blunt end. In the central region are three α-helices which interact with a single ß-sheet. A seventh helix is at the pointed end. The cofactor becomes the sixth ß-strand in the central ß-sheet, forming a disulphide bond and several hydrogen bonds. Two small ß-strands cross near the bottom of the central helix. Side chains are shown only for the active site residues Cys-122, His-54, and Glu-71. Reproduced from Ding *et al.* (1996).

and from wild type virus particles (Keyvani-Amineh *et al.*, 1996; Greber *et al.*, 1996). Native enzyme isolated from cytoplasmic extracts of cells, and virus particles, have been shown to be oxidised, while nuclear isoforms, which are presumed to be active, are reduced. Greber *et al.* (1996) have proposed that when newly assembled viruses are released from the lysing cell, the viral protease encounters the oxidising extracellular environment and is inactivated by intra-chain disulphide bond formation. Conversely, when the virus enters the more reducing environment of the endosome, early in infection, the inactivating disulphide bond is reduced, and the protease is reactivated.

It is still unclear whether activation is an absolute requirement for enzyme activity when the substrate is a protein instead of a peptide. The purified enzyme alone has been shown to cleave actin, ovalbumin, and fibrin *in vitro* (Tihanyi *et al.*, 1993). Additionally, Webster *et al.* (1993) have shown that co-infection of insect cells with recombinant baculovirus expressing pTP and 23kd protease results in processing of pTP to an intermediate, iTP, but not to mature TP. The authors speculated that other mechanisms of activation may occur, and additional evidence also supports this. Several reports have proposed that viral DNA may be involved in the catalytic mechanism (Mangel *et al.*, 1993 and 1996), although Webster *et al.* (1994) have suggested that viral DNA may only serve to stabilise the protease *in vitro*, and possibly enhance the interaction of protease and substrates *in vivo.* Recently, the peptide VEGGS, has been shown to mimic the activity of pVI-ct by inducing a similar conformational change (Diouri *et al.*, 1996). The sequence of the peptide resembles the conserved cleavage site (M,L,I)XGG'X, although the authors noted that the serine residue was not cleaved. Surprisingly, although no adenovirus proteins contain the VEGGS motif, like pVI-ct, VEGGS incorporation into Ad2ts1 infected cells results in the recovery of infectious particles.

1.2 General themes in virus assembly and maturation.

1.2.1 Herpesviruses.

i) Herpes simplex virus (HSV) assembly:

The herpesvirus family is composed of Herpes simplex (fever blister), Herpes zoster (Chickenpox and shingles), Cytomegalovirus (salivary gland virus) and Epstein-Barr virus which, like adenoviruses, are dsDNA (130kbp) viruses that replicate in the cell nucleus. The DNA genome is contained inside an icosahedral capsid (125nm in diameter) that is separated from the virion envelope by an amorphous complex of virus-encoded proteins called the tegument (reviewed by Roizman and Sears, 1990) The envelope contains a number of glycoproteins which facilitate the attachment of virions to susceptible cells. After attachment, the viral envelope glycoprotein B induces its fusion with the cellular plasma membrane, permitting the nucleocapsid to enter directly into the cytoplasm. In the cytoplasm the capsid migrates to a nuclear pore, where the viral DNA is released into the nucleus and initiates viral multiplication. Like polyomavirus/SV40 and adenoviruses, there is a programme of early transcription which produces proteins required for the replication of the viral genome and subsequent late gene expression.

Assembly of virions also takes place in the nucleus and three types of capsid, designated A, B and C (in order of increasing sedimentation distance in sucrose gradients) can be isolated from HSV-1 infected cells (Gao *et al.*, 1994; Robertson *et al.*, 1996). Type C capsids contain the viral genome and are able to mature into infectious virions when associated with tegument proteins arranged at the inner nuclear membrane. Types A and B capsids lack DNA, although type A capsids are very similar to type C capsids in protein composition. Type B capsids differ in that they contain an additional polypeptide termed VP22a. In addition to VP22a, which is believed to be a scaffold protein that is removed after DNA encapsidation, B capsids are also composed of at least seven other proteins, namely, VP5, VP19c, VP21, VP23, VP24, VP26 and the recently reported UL26 gene product (Patel *et al.*, 1995). The 162 capsomers that make up the outer shell are composed of 150 hexons and 12 pentons which are predominantly composed of VP5 protein. The three other proteins that make up the outer shell are VP19c, VP23, which together form triplexes which connect capsomers in groups of

three (Zhou *et al.*, 1994) and VP26, which is found at the distal tips of the hexons only (Booy *et al.*, 1994).

The core of the B capsid is composed of three proteins, VP21, VP24 (products of the UL26 gene) and VP22a (product of the UL26.5 gene). The UL26 transcript encodes the 635 residue serine protease which undergoes autoproteolytic processing at two sites to generate VP21, VP24 and the 25 amino-acid C-terminal peptide (Preston *et al.*, 1994; Matusick-Kumar *et al.*, 1995; Thomsen *et al.*, 1995). VP24 comprises the first 247 amino acids of the UL26 protein and is the region of the protein that contains proteolytic activity. The protease also cleaves the product of the UL26.5 gene (Which shares the same C-terminal cleavage site as the UL26 gene product) to generate VP22a and the 25 residue C-terminal peptide. Although capsid structures are observed in the absence of functional protease (Gao *et al.*, 1995) the major capsid protein VP5 does not adopt the correct conformation and viral DNA is not encapsidated. It has been proposed that the 25 residue C-terminal peptide is involved in the formation of sealed capsids and may directly interact with VP5 (Robertson *et al.*, 1996).

ii) The human cytomegalovirus (hCMV) protease:

The hCMV UL80 gene encodes the full length 80kd protease and its substrate which, like the HSV-1 UL26 protein and BVRF2 protein of Epstein-Barr virus (Donaghy and Jupp, 1994), is autocatalytically cleaved at two internal sites generating a fully active 28kd serine protease. In addition, the 28kd CMV protease can proteolytically cleave itself at two internal sites located within its own catalytic domain (Baum *et al.*, 1996a; Margosiak *et al.*, 1996). The CMV 28kd protease is inhibited by serine-specific reagents and also by cysteine-specific compounds (Baum *et al.*, 1996a and b) the latter of which induce the formation of specific intramolecular disulphides by a thiol-disulphide exchange reaction. It has been proposed that conserved cysteines have potential roles in the formation of homodimers which are believed to be the active form of the enzyme (Margosiak *et al.*, 1996; Baum *et al.*, 1996b). Recently the atomic structure of both the monomeric and dimeric forms of the protease have been determined (Tong *et al.*, 1996; Qui *et al.*, 1996; Shiek *et al.*, 1996), and although the dimer interface is not in the immediate vicinity of the active site, dimerisation may have a profound effect on the conformation of the active site region.

It has been suggested that during viral infection, the regulation of protease activity by intra-molecular disulphide bond formation may maintain the enzyme in an inactive state until required. Although the CMV protease is a serine protease which does not require a cofactor, its mechanism of activation is very similar to the Ad2 L3 23kd protease in that the enzyme is redox-regulated. It is possible that the UL80 precursor is stable only in the cytoplasm of infected cells, and once exposed to the reducing environment of the developing viral capsid, the protease is activated. Like the hCMV and HSV-1 protease's, the retrovirus HIV-1, HIV-2, and RSV protease's (section 1.2.3iii) dimerise to form a catalytically active species with one active site per dimer. This dimerisation plays an important role in the regulation of viral replication (Kräusslich, 1995) and is achieved by high concentrations of protease in the capsid.

iii) Reorganisation of nuclear bodies:

The HSV-1 immediate early protein, VMW110, is a general trans-activator which is required for fully efficient viral gene expression and reactivation from latency (Everett and Maul, 1994; Maul *et al.*, 1995). At early times of infection, VMW110 localises to PML bodies and, like the adenovirus E4 ORF3 protein causes redistribution of PML. Both PML and VMW110 have the RING finger motif, and initially it was thought that both proteins had similar functions *in vivo* (Everett *et al.*, 1995a). However, it appears that the motif is required for modification of the PML containing nuclear bodies, suggesting, that the RING finger has a functional role in complex interactions between the components of the nuclear domain (Everett *et al.*, 1995b). Although the mechanism of VMW110 action is unknown, the protein has been shown to complex with a 135kd ubiquitin-specific protease, which may facilitate the release of PML body components (Everett *et al*, 1997). Interestingly, the CMV IE1 major protein (Kelly *et al.*, 1995), the EBNA-5 nuclear antigen of Epstein-Barr virus (Szekely *et al.*, 1996) and the SV40 large T-antigen (Carvalho *et al.*, 1995) are also localised to PML bodies early in infection, but the PML protein is only redistributed during CMV infection.

Puvion-Dutilleul *et al.* (1995c) have shown that HSV-1 infection, like adenovirus infection (section 1.1.4ii), induces the formation of translucent structures composed of finally granular material (which may be analogous to clear amorphous inclusions) which are located at the nuclear border and contain the redistributed PML, SP100, and p80-coilin antigens.

These structures appear late in infection, are localised with viral capsids, and contain high concentrations of capsid proteins. The authors suggest that these structures may have a potential role in virus assembly, possibly as storage sites of over-synthesised viral capsid proteins and that sequestration of cellular proteins into these virus induced structures may be required for the shutoff of host cell metabolism which occurs in HSV-1 infected cells.

1.2.2 Polyomavirus/SV40 assembly.

The structurally similar polyomavirus and SV40 are members of the Parvovirus family of dsDNA viruses. These viruses have a 5kbp genome which is complexed with cellular histones (often referred to as the minichromosome) inside a non-enveloped icosahedral capsid of 50nm in diameter (reviewed by Echhart, 1990). The small genome of SV40 codes for only a limited number of nonstructural proteins (reviewed by Deppert and Schirmbeck, 1995), and with the exception of the helicase activity of the large T-antigen, all the functions of these proteins are regulatory, serving to modulate cellular functions for the needs of viral replication and assembly. For small genomes, most functions regulating assembly must involve cellular pathways recruited by the virus, which are facilitated by various activities of proteins made early in infection. For instance, the large T-antigen of SV40/polyomavirus, like the E1A protein of adenovirus, interacts with the cellular Rb protein, serving to enhance DNA replication (Hendrix and Garcea, 1994).

DNA replication has been shown to be subcompartmentalised with cellular chromatin being involved in initiation processes and elongation/termination of SV40 replication occurring at the nuclear matrix (reviewed by Deppert and Schirmbeck, 1995). This subnuclear partitioning also occurs during virion assembly, with capsid proteins assembling around minichromosomes associated with cellular chromatin. The capsid proteins, termed, VP1, VP2, and VP3, are all derived from an alternatively spliced single transcript and are post-translationally modified (Salunke *et al.*, 1986). All the late proteins contain nuclear targeting signals (Garcia-Bustos et al., 1991), however, VP1 protein has been shown to promote the nuclear accumulation of VP2 and VP3. Protein VP1 is the major component of the virus, and spontaneously assembles into pentomers, 72 of which form the icosahedral capsid. Although VP2 and VP3 proteins are not required for assembly, they associate with the minichromosome and interact with the capsid shell, and have therefore been implicated in

genome packaging. VP1 has been expressed in E.coli, and has been shown to assemble into capsids *in vitro* (Liddington *et al.*, 1991). Unlike the late stage of adenovirus capsid assembly, SV40 virion assembly does not involve proteolytic processing of capsid components, but instead, VP1 appears to pass through a series of conformational states. Bond switching between penta- and hexa-valent positions in the icosahedral lattice is an inherent property of VP1. Liddington *et al.* (1991) have identified 3 types of intercapsomeric bonds and suggest that bonding contacts probably act as control mechanisms for assembly.

1.2.3 Proteinases of RNA viruses.

The replication of many animal and plant viruses is dependant on the action of specific protease's which serve a variety of functions including the separation of structural and nonstructural proteins, generation of specific enzymes (RNA polymerases), and the co-ordinated assembly, and maturation of the virion. Proteolytic processing is common in the positive strand RNA viruses and retroviruses (reviewed by Kräuslich and Wimmer, 1988; Hellen *et al.*, 1989), and usually involves the cleavage of large polyproteins into functional units. Proteolysis of viral proteins also occurs during the replication of negative strand RNA viruses (such as Ortho- and Paramyxoviruses), although these cleavages are catalysed by cellular protease's and are confined to viral glycoprotein precursors (Kawakara *et al.*, 1992). Some of the well characterised positive strand RNA viruses and retrovirus systems are reviewed in this section.

i) Picornaviruses:

Picornaviridae are a family of small icosahedral viruses that cause a number of important disease syndromes. The family is currently divided into four genera: Rhinoviruses (the common cold), Enteroviruses (poliovirus), Cardioviruses (encephalomyocarditis) and Aphtoviruses (foot and mouth disease). All have a positive sense single-stranded monopartite genome which contains a single long open reading frame that is translated to yield a large polyprotein of 200 to 300kd (Kay and Dunn, 1990). The processing of the polyprotein occurs in three stages and involves the separation of the capsid precursor from the growing chain (primary cleavage), then processing of the structural and nonstructural precursor

proteins (secondary cleavage) and finally the maturation cleavage of the capsid components (Kräuslich and Wimmer, 1988).

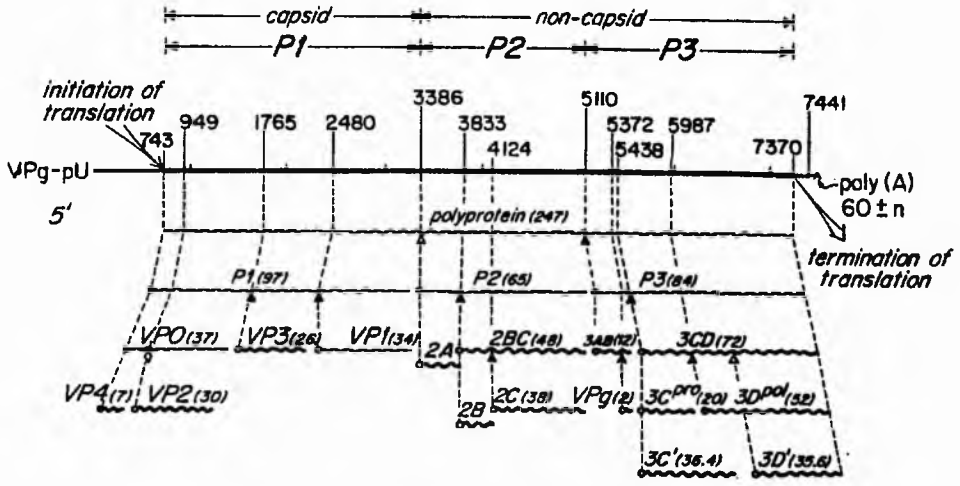

Figure 1.15: Gene organisation and polyprotein processing of poliovirus. The coding region has been divided into three regions (P1, P2 and P3), corresponding to major cleavage products of the polyprotein. Polypeptides are presented as wavy lines. Open circles indicate glycine residues except for VP2, where it is a serine, and filled circles denote blocked N-termini (reproduced from Kräusslich and Wimmer, 1988).

The first cleavage within the poliovirus polyprotein (figure 1.15) occurs while it is still nascent on the ribosome, and is an autocatalytic process mediated by the 2A component of the polyprotein. Its cleavage results in the separation of the structural region (P1) that consists only of capsid proteins. Most of the cleavages which subsequently take place within the respective capsid and nonstructural protein precursors are catalysed by the viral 3C protease. Of the two poliovirus protease's, the 3C enzyme has been investigated in more detail than the 2A protease. However, the 2A protease is known to cleave the Tyr-Gly bond linking P1 and P2 *in vitro*, and is therefore active as a mature protein as well as an intrinsic component of the polyprotein itself. The polyprotein contains a further nine Tyr-Gly bonds, yet only one of these (in the 3D polymerase region) appears to be cleaved by the enzyme, which suggests that additional determinants can influence whether cleavage occurs. The second 2A protease cleavage is not essential for virus replication, but is thought to provide a means of regulating the activities of the 3C protease and the 3D polymerase (Skern and Liebig, 1994).

Eight of the 11 cleavages of the poliovirus polyprotein are catalysed by the 3C protease, either alone or in association with the 3D polymerase. Although all the cleavage sites are Gln-Gly bonds, the separation of the capsid proteins VP0, VP1, and VP3 are carried out by 3CD and not 3C alone. It has been proposed that elements in 3D are required to bind to the capsid protein precursor and so increase the affinity of 3C for its structural substrates. The 6 remaining Gln-Gly sites that link the nonstructural proteins are readily cleaved by the 3C protease, and Hellen *et al.* (1988) have suggested that the different affinities of the 3C protease for its various substrates may be important in the regulation of the lytic cycle. The final processing event in poliovirus replication is the cleavage of the structural protein VP0 (for which no protease has been identified) to generate VP4 and VP2, which takes place after the assembly of virus particles.

Proteolytic events catalysed by the 2A and 3C enzymes also leads to changes in cell structure and function. For instance, poliovirus 2A protease activity has been shown to facilitate the reduction in cellular DNA synthesis, transcription, and translation when expressed in COS-1 cells (Skern and Liebig, 1994). The reduction in translation appears to be due to the limited specific proteolysis of eukaryotic translation initiation factor elf4. In addition, foot and mouth disease virus (FMDV) has been shown to cleave histone H3 in Baby Hamster Kidney cells, and the poliovirus 3C enzyme to cleave the activated form of transcription factor TFIIIC in HeLa cells, thus inactivating the protein and consequently facilitating the shutoff of host cell transcription. Poliovirus 3C also mediates the cleavage of microtubule associated protein 4 which leads to a collapse of microtubules late in infection (Joachim *et al.*, 1995).

All picornaviruses encode active and closely related 3C protease's, but there is little similarity between the sequences of enzymatically active 2A protease's of rhino- and enteroviruses and their counterparts in cardioviruses. The 2A protease's of cardioviruses and apthoviruses consist of 135 to 145 and 16 amino acids respectively and are considered to be unrelated, although they have evolved different mechanisms for primary cleavage. Inhibitor studies (reviewed by Kräuslich and Wimmer,1988; Nicklin, 1988) indicate that picornaviral 3C and 2A protease's constitute a class of cysteine protease's distinct from the papain superfamily. It appears that the 3C enzyme is structurally similar to the chymotrypsin like serine protease's, whereas the 2A protease resembles the smaller bacterial serine protease's.

There is a surprising degree of similarity between 3C and other nonstructural proteins of picornaviruses and proteins encoded by cowpea mosaic virus and tobacco etch virus, which are members of the comovirus, and potyvirus groups of plant viruses respectively (Verchat and Carrington, 1995). Comoviruses have a genome consisting of two positive sense RNA strands which separately encode polyproteins for capsid and nonstructural proteins which eliminates the requirement for a 2A-like protease. However, the 24kd 3C-like protease can cleave all the sites within both polyproteins in vitro, and interestingly requires a cofactor for processing of the capsid precursor, although it is not a viral polymerase as is the case for poliovirus. The 48kd 3C-like protease of tobacco etch virus mediates its own autocatalytic cleavage from a single large polyprotein at Gln-Gly bonds. This cysteine protease, termed NIA, cleaves the viral polyprotein at 5 other sites, whereas the two other protease's (one of which is a cysteine protease termed HCpro) mediate the remaining cleavage events.

ii) Hepatitis C virus.

Hepatitis C virus (HCV) is the major etiological agent of human parentally transmitted non-A, non-B hepatitis where chronic infection may lead to the development of liver cirrhosis, and hepatocellular carcinoma (reviewed by Houghton, 1996). The HCV virion contains a positive-strand RNA genome (9.4kbp) that has a single large open reading frame encoding a polyprotein of 3010 to 3033 amino acid residues. The genetic organisation of HCV is similar to that of Flavi- and Pestivruses and has been classified as a separate genus of the Flaviviridae family (reviewed by Van Doorn, 1994).

At least 10 cleavage products are generated from the polyprotein precursor and they are arranged in the order: NH_2-CORE-E1-E2-p7-NS2-NS3-NS4a-NS4b-NS5a-NS5b-COOH (Bartenschlager *et al.*, 1995). Core, a basic RNA-binding protein, is assumed to be the major constituent of the viral nucleocapsid, E1 and E2 are most likely virion envelope glycoproteins, and NS2 and NS5b are nonstructural proteins (probably involved in RNA replication). Although host cell signal peptidases located in the lumen of the endoplasmic reticulum are responsible for maturation of the structural proteins (Butkiewicz *et al.*, 1996), at least two virus encoded protease's are involved in processing of the nonstructural (NS) proteins. A zinc-dependant metalloprotease encompassing the NS2 region and the N-terminal one-third of NS3 (the NS2-3 protease) is required for cleavage between NS2 and NS3.

Processing of NS3/4a, NS4a/4b, NS4b/5a, and NS5a/5b sites is mediated by a trypsin-like serine protease which is also encoded by the N-terminal one-third of NS3, but functioning independantly of NS2-3 (Bartenschlager *et al.*, 1995; Koch *et al.*, 1996). It has been shown that NS4a enhances the cleavage at the NS5a/5b site, and is absolutely required for cleavage at the NS4b/5a site. NS4a is cleaved off from NS3 by intramolecular cleavage at the NS3/4a site and has been shown to enhance NS3 activity in *cis* and in *trans* (Koch *et al.*, 1996). The central 12 amino acid residues, CVVIVGRIVLSK, of the 54 residue polypeptide are important for cofactor activity (Butkiewicz *et al.*, 1996; Love *et al.*, 1996), although sequences at the NS4a N-terminus improve the activation function, possibly by stabilising the NS3/4a interaction.

How NS4a exerts the activation function is unknown, although one possibility is that binding of NS4a changes the conformation within NS3, making the structure more ideal for substrate binding and/or catalysis. Koch *et al.* (1996) have suggested that the hydrophobic NS4a may also be required for localisation of NS3 to membranes of the endoplasmic reticulum, thereby increasing the local concentration of the protease in close proximity to the membrane associated polyprotein substrate. Closely related flaviviruses such as yellow fever virus and dengue virus also have a requirement for a protease cofactor, although processing of their NS proteins are mediated by a NS3/NS2b heterodimer (Amberg *et al.*, 1994).

iii) Retroviruses.

Retroviridae are a large family of enveloped viruses that contain a single stranded genome that replicates via an obligatory DNA intermediate. After the initial events which leads to virus uncoating, the retroviral genomic RNA is reverse transcribed by the virion associated, virus encoded RNA-dependant DNA polymerase (reverse transcriptase). This process results in the synthesis of virus-specific dsDNA intermediates that integrate into the host chromosomal DNA to form a provirus (reviewed by Kräusslich and Wimmer, 1988). The proviral DNA is then transcribed by cellular RNA polymerase II into the genomic 35S mRNA which can be spliced to yield subgenomic mRNA's.

The retrovirus genome consists of three major genetic elements referred to as gag, pol, and env. The gag (group-specific antigen) region encodes the capsid (CA), matrix (MA), and nucleocapsid (NC) proteins, and is translated as a precursor from 35S mRNA. Current

evidence indicates that gag plays a fundamental role in the assembly of virions, and even in the absence of other viral proteins can assemble to form virus like particles (Kräusslich *et al.*, 1995). The pol region encodes the viral replicative enzymes, namely, reverse transcriptase, integrase, and in most instances, the viral protease, which are also translated from 35S mRNA as part of a gag-pol fusion protein. Synthesis of the gag-pol polyprotein in human immunodeficiency virus type 1 (HIV-1), and rous sarcoma virus (RSV) infection, is achieved by ribosomal frame-shifting at one or two sites at the end of, or within, the gag gene (Yu *et al.*, 1995). The infrequency of frame-shifting leads to an overproduction of structural proteins compared to replicative enzymes. The env gene encodes a polyprotein that is cleaved by cellular protease's in transport vesicles to yield glycoproteins of the viral envelope.

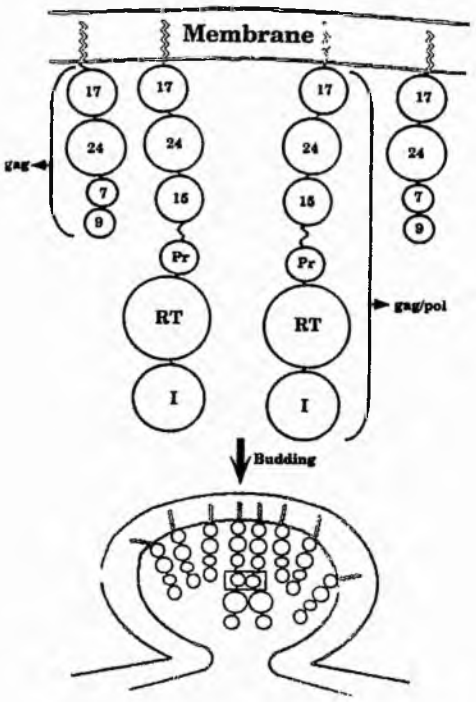

Figure 1.16: Schematic representation of HIV-1 protease activation. Polyprotein concentration-facilitated dimerisation during HIV-1 budding (reproduced from Tomasseli and Heinrikson, 1994).

The gag and gag-pol polyproteins are not cleaved immediately after synthesis but instead are transported to the plasma membrane, a process facilitated by the cotranslational probably concentrates and aligns the polypeptides (figure 1.16), thereby promoting inter-molecular

interactions that may result in some self-assembly of gag molecules and dimerisation of protease domains (Tomasselli and Heinrikson, 1994; Davis *et al.*, 1995).

Cleavage of polyproteins occurs largely after the release of virions from cells and may require an intra-molecular event in which two gag-pol polyproteins dimerise to cleave at their N- and C-termini, or as an inter-molecular event, in which two such dimers cleave each other. HIV protease activity is dependent on dimerisation of monomeric subunits present in gag-pol polyproteins, thereby preventing premature activation prior to virus budding. When the protease is inactivated, or in the presence of HIV protease inhibitors, non-infectious viral particles are produced which display a distended spherical capsid structure, identical to that resulting from expression of gag alone, rather than the condensed cone shaped electron-dense core that is typical of mature particles (Quillent *et al.*, 1996). Additionally, gag processing is reduced if gag-pol is truncated in distal regions of pol. This suggests that regions within the reverse transcriptase and integrase domains are essential in determining the overall conformation of the gag-pol precursor, which in effect modifies the ability of the protease domains to dimerise or cleave itself out of the polyprotein. Once released, the viral protease is confined to the budding particle, and thus initiates a cascade of proteolytic events resulting in maturation of virus particles.

The gag precursor (55kd) in HIV-1 is cleaved into smaller products that include the matrix protein (17kd), capsid protein (24kd), nucleocapsid protein (9kd), and a 6kd proline rich protein (P6) derived from the C-terminus of gag (Dorfman *et al.*, 1994; Huang *et al.*, 1995). The P6 domain appears to be required for the incorporation of the HIV-1 vpr accessory protein into virus particles (Wu *et al.*, 1994), but has also been reported to have a functional role in virus particle production at late stages in the budding process (Huang *et al.*, 1995). These authors have suggested that P6 can directly enhance or suppress protease activity, possibly by altering the conformation of the gag precursor, thereby altering protease mediated gag processing. Besides polyprotein precursors and mature end products, intermediate processing products are transiently present in the maturation process because of sequential cleavage of polyproteins. CA and NC, and also NC and P6, are separated by short spacer peptides of 14 and 10 amino acid residues, termed, SP1 and SP2 respectively (Kräusslich *et al.*, 1995). The latter authors have suggested that initial cleavage of the gag precursor occurs at the C-terminus of SP1 to yield an MA-CA-SP1 intermediate, which is subsequently

processed to CA-SP1. The presence of SP1 on cleavage intermediates infers that an ordered regulation of polyprotein processing occurs.

Activity of the HIV protease is not restricted to proteolytic processing of gag and gag-pol. The enzyme has been reported to specifically cleave the HIV-1 nef accessory protein within maturing virion particles (Welker *et al.*, 1996). In addition, a number of studies of HIV protease cleavage of non-viral proteins suggest that the enzyme could have devastating effects on infected cells if it were activated outwith the virion particle. Several studies have shown that the intermediate filaments (IF's) vimentin, desmosin, and glial fibrillary acidic proteins are cleaved in vitro by purified HIV-1 protease, and also that microinjection of the enzyme into human stem fibroblasts results in the collapse of the vimentin network (reviewed by Tomasselli and Heinrikson, 1994). The HIV-1 protease is also able to cleave microtubule associated proteins 1 and 2 *in vitro* and that the cleavage interferes with microtubule assembly. Several groups have speculated that HIV-1 protease may have a functional role in the pathogenesis associated with retroviral infection, which is in part supported by the finding that the protease is active in infected host cells. It remains to be determined how the enzyme is activated in infected cells as homodimer formation is facilitated by the increase in concentration of gag-pol polyproteins during the budding process.

Retroviral protease's have been classified as aspartyl type protease's due to the presence of the active site triad Asp-Thr-Gly, inhibition by pepstatin A, and sequence homologies with other enzymes of this class (reviewed by Kräusslich and Wimmer, 1988; Tomasselli and Heinrikson, 1994). Although the retroviral enzymes are related to pepsin, renin, and other members of the aspartyl protease family, the requirement to form homodimers is unique to them. Whereas pepsin and renin are composed of approximately 350 amino acid residues, the retroviral protease monomer varies from 99 to 123 residues, giving a dimer of 198 to 246 residues in total, with a triad from each monomer contributing to the active site.

1.3 Subcellular localisation of viral antigens.

As mentioned previously, the aims of this project involve the further examination of virus-encoded proteins at the ultrastructural level. To obtain meaningful results from immunocytochemical studies, the production and use of well characterised antibodies of defined specificities is required. The methods most commonly used are reviewed in this section. For a more complete discussion on aspects of the immune system and immunocytochemistry, the following reviews and texts are recommended: Harlow and Lane (1988), and Griffiths (1993).

1.3.1 Monoclonal antibody production and characterisation.

Because of the polyclonal nature of the immune response, immunisation of an animal with a single protein antigen will give rise to an antiserum containing a mixture of antibodies with varying affinities that are directed against a variety of epitopes. Therefore, ideally it would be advantageous to select a single B lymphocyte, secreting an antibody of interest, and allow it to grow up as a clone of cells in culture, from which antibodies can be selected as required. As B cells have only a limited life span in culture, continuous production of monoclonal antibodies requires a means of immortalising these cells. The methodology for doing this was provided in 1975 by Köhler and Milstein. They showed that B lymphocytes, if induced to fuse with a continuously growing myeloma cell (lymphoid tumour cell), acquired the ability to grow indefinitely in culture, whilst continuing to secrete antibody.

The cells used for producing hybridoma cell lines are usually of mouse origin, with B cells being most commonly obtained from the spleen of the donor mouse. In order to maximise the chances of obtaining antibodies of the desired specificity, the spleen cell population of the donor mouse is enriched for B cells specific for the antigen during the weeks prior to collection of spleen cells. Alternatively, *in vitro* immunisation is also possible. In this case spleen cells are collected from an non-immunised mouse and cultured (under defined conditions) in the presence of antigen. This results in the proliferation of antigen specific B cells which negates some of the problems of immunological tolerance or suppression. However, a disadvantage is that this method gives rise to predominantly IgM antibodies which are generally less desirable than IgG's derived from *in vivo* immunisation.

Several mouse myeloma cell lines have been employed for monoclonal antibody production, most being derived from MOPC 21 plasmacytoma's of the Balb/c mouse strain. These myelomas have been chosen because of their inability to grow in selective medium containing Hypoxanthine, Aminopterin, and Thymidine (HAT) medium. The myelomas are deficient in the enzyme hypoxanthine guanine phosphoribosyl transferase (HGPRT) and consequently are resistant to the drug 8 azaguanine. HGPRT is a key enzyme in the salvage of purines and will utilise exogenously supplied hypoxanthine to produce inosinic acid, the common purine nucleotide precursor. Thus a cell blocked in purine biosynthesis will nevertheless be able to survive if supplied with hypoxanthine, provided that the HGPRT is functional. Inhibition of de novo purine biosynthesis may be achieved with the drug aminopterin. Aminopterin is a potent inhibitor of the enzyme dihydrofolate reductase (DHFR) which catalyses the reduction of dihydrofolate to tetrahydrofolate (FH_4). FH_4, in turn, is an essential cofactor in the biosynthesis of both purines and thymidine. To survive in the presence of aminopterin, a normal cell needs to be provided with a source of purines (in the form of hypoxanthine) and with thymidine, which can be utilised via the enzyme thymidine kinase (TK). Therefore, a normal cell will survive in HAT medium, while a cell deficient in HGPRT or TK will not.

Fusion of spleen cells with myelomas is most frequently achieved using polyethylene glycol as the fusogen. Following fusion, the cells are transferred into HAT medium which selects for the hybridoma cells. The unfused myelomas are killed by HAT medium, while the spleen cells have only a very limited growth potential in culture. Identification of hybridomas secreting the desired antibody is achieved by plating the cells in limited dilution's and allowing the cells to grow to near confluence. The testing procedure depends on the nature of the antigen, although typically some form of radioimmunoassay, immunoblotting, or immunofluorescence microscopy is used. Cells secreting the antibody of interest are separated from other non-secreting cells (or cells secreting irrelevant antibodies) in culture, by limited dilution cloning, or plating at low density in agarose. If necessary, monoclonal antibodies of interest can be epitope mapped using a variety of techniques that can include limited proteolysis, and deletion mutagenesis of protein antigens, although methods selected are primarily determined by the nature of the antigen.

It is noteworthy that a recent innovation in antibody production has come from the ability to clone and express immunoglobulin genes in non-lymphoid eukaryotic cells and prokaryotic

systems (Rosa *et al.*, 1989). Perhaps the simplest method of producing antibodies by expression in these systems is to micro-inject mRNA isolated from the parent hybridoma into target cells of interest. However, a major obstacle to efficient production of recombinant immunoglobulins is that they are constructed from two chains encoded by separate genes.

1.3.2 Immunocytochemistry

Immunofluorescence microscopy can provide important information regarding the subcellular localisation of antigens of interest. However, the various electron microscopy techniques now commonly used can provide additional information, at the ultrastructural level, which is often required. For instance, the high resolution localisation of viral DNA replication in Ad infected cells to border domains between ssDNA-DBP accumulation sites and the peripheral replicative zone (Besse and Puvion-Dutilleul, 1994), would be less apparent using immunofluorescence microscopy (Pombo *et al.*, 1994). To obtain high resolution data, the structural organisation of cells must be preserved without introducing artefacts which may interfere with interpretation of results.

The first part of fine structure preservation is the fixation step, which is critical in determining how closely the image in the electron microscope resembles the *in vivo* structure. The aim of fixation is to 'freeze' cell organisation in a particular time frame, so that every molecule remains in its original location during visualisation. The only fixative procedure which can achieve this is cryo-fixation (followed by cryo-sectioning), although for immunolabelling procedures this technique is not applicable. An exception is the freeze-substitution approach in which cells must be exposed to chemical solvents to protect the structural integrity of the cell throughout immunolabelling procedures. Hence, for immunocytochemistry, and enzyme cytochemistry, chemical fixation is the only method available. However, chemical fixation can lead to the loss of epitopes (such as occurs with osmium tetroxide), and volume and shape changes which lead to structural distortions within the cell. In addition, steric hindrance, and chemical alteration of epitopes can also occur through fixative-induced cross-links. Therefore a compromise between preserving the antigens of interest, and organelle structure, with maintaining immunoreactivity is required if meaningful results are to be obtained.

Embedding media also affect the structural organisation of the cell and have a profound effect on immunoreactivity. Resin-free embedding has been used successfully with Ad infected cells (Zhongue *et al.*, 1986) and is probably the most suitable method for immunolabelling studies. However, a major disadvantage with this method is the difficulty in thin-sectioning, which can ultimately affect the structural preservation of the cell. Therefore most immunocytochemical protocols involve embedding in either hydrophilic acrylic resins (Puvion-Dutilleul and Puvion, 1995), or the more hydrophobic epoxy resins (Chaly and Chen, 1993; Greber *et al.*, 1993), both of which are generally considered to result in diminished immunoreactivity. This is a major disadvantage of the epoxy resins especially. Fixed cells must be completely dehydrated in protein denaturing solvents before resin infiltration, and then the resin can only be polymerised by heating above 50°C. Although the acrylic resins are not water-miscible, they are designed so that they combine at least some degree of hydrophilicity with good sectioning properties. Additionally, acrylic resins can be polymerised at low temperatures, and interestingly have been used for immunofluorescence microscopy studies (Jackson and Blythe, 1993).

Immunolabelling reactions can be performed pre- or post-embedding, with each method having distinct advantages and disadvantages. For instance, pre-embedding procedures require permeabilisation of membranes to allow penetration of antibody to cellular compartments. The detergents and solvents used can inevitably destroy some fine structure, and lead to extraction of antigens. After the antibody reactions the cells are treated with fixative (usually osmium tetroxide), dehydrated, and conventionally embedded in epoxy resin. The most widely used pre-embedding procedure is the immunoperoxidase technique using horseradish peroxidase (HRP), conjugated to a secondary antibody. This method is considered attractive because the HRP effectively amplifies the primary immune reaction by catalytically oxidising proportionately large amounts of its substrate. Additionally, a further amplification can be obtained by using antibodies against HRP in the peroxidase anti-peroxidase (PAP) technique (reviewed by Griffiths, 1993).

The use of antibodies on thin sections has a wide field of application, although a disadvantage is that only antigenic sites which are accessible at the surface of thin sections are detected. However, in the absence of permeabilisation steps, and with the use of gold particles as markers, the post-embedding technique allows the precise identification of labelled structures

which are generally well preserved. The post-embedding technique also allows the simultaneous detection of several antigens, provided that the primary antibodies are raised from different animals and that the gold particles bound to the secondary antibodies are of different sizes. In addition, this procedure can also be combined with specific staining of proteins and DNA (Puvion-Dutilleul and Puvion, 1995). For instance, among the protein stains which reveal subsets within the total viral and cellular proteins are the periodic acid-schiff (PAS)-like reaction for glycoproteins, and the silver staining method which reveals acidic proteins. However, the bismuth staining method is of interest due to the exclusive staining of highly phosphorylated proteins and has the advantage of being compatible with the post-embedding technique. Immunodetection, in conjunction with selective staining of proteins and DNA, has been used successfully in studies examining the nature of virus-induced intranuclear structures (Puvion-Dutilleul and Puvion, 1995; Puvion-Dutilleul *et al.*, 1995a and b), however, there are no rules governing which immunocytochemical protocol will provide the most useful information regarding a specific antigen of interest, and often, several parameters mentioned in this section must be altered.

1.4 Aims of the project.

Although the Ad2 23kd protease is believed to be activated within the 'young' virion, several reports have suggested that the viral protease has cleavage activity prior to activation by the pVI-ct peptide, or the pVI protein from which it is derived. For instance, the L1-52kd scaffolding protein is cleaved at an early stage in virus assembly and prior to the cleavage of other viral proteins (Hasson *et al*, 1992), and cytokeratins K7 and K18 are cleaved exterior to the virus (Chen *et al*, 1993), whilst protease activation presumably takes place within the newly assembled virion. This suggested that other mechanisms of regulation might affect viral protease activity within lytically infected cells.

The aim of the project was to generate a panel of monoclonal antibodies specific to the Ad2 23kd protease, which after characterisation, could be used to determine the subcellular distribution of the viral protease within Ad2 and Ad2ts1 infected HeLa cells.

The second objective of this project was to determine the epitopes of monoclonal antibodies which could be used to study the effect of ligand binding on the conformation of the viral enzyme.

2 Methods and Materials

2.1 Expression and Purification of Recombinant Ad2 23kd Protease.

2.1.1 The GST gene fusion system.

The glutathione s-transferase (GST) fusion system introduced by Smith and Johnson (1988) consists of the pGEX series of plasmids that contain the GST gene from *Shistosoma japonicum*. The 26kd GST protein forms an affinity tail on the protein products of genes inserted into the multiple cloning site (MCS). The pGEX plasmids also feature a tac promoter that enables inducible high-level expression of fusion proteins, and the Lac I^q gene which ensures that any *E.coli* strain can be used. Fusion proteins are recovered from bacterial lysates using glutathione-containing affinity matrices, and eluted under mild, non-denaturing conditions (5mM reduced glutathione). Once purified, the protein of interest can be cleaved away from GST using site specific protease's that recognise sequences between GST and the MCS.

The plasmid pGEX23k was previously constructed using the vector pGEX-2T (Webster and Kemp, 1993) and transformed into *Escherichia coli* JM101 cells. A single colony was picked from a selective agar plate and used to inoculate 5ml of Luria Broth (LB) containing 100µg/ml Ampicillin (Amp) and left for six hours at 37°C with shaking. A fraction of the starter culture was added to 250ml of LB-Amp and grown until cells had reached an absorbance of between 0.5 and 0.8 at 600nm. The expression of recombinant fusion protein was induced by the addition of freshly prepared 0.1mM Isopropyl-ß-thiogalactopyranoside (IPTG) from a 0.1M stock. After a period of four to six hours (at 37°C), cells were harvested by centrifugation at 10000 rpm (JA-14 rotor, Beckman centrifuge J2-21) for 5 minutes at 4°C, and the pellet washed with ice-cold STE buffer (1mM EDTA; 150mM NaCl; 10mM Tris/HCl, pH 8.0). After a second centrifugation, the pellet was stored at -20°C.

2.1.2 Purification of fusion proteins from *E.coli.*

Thawed cell pellets were resuspended in 6ml of STE buffer containing 100 μg/ml lysozyme and incubated on ice for 15 minutes at 37°C. Lysis was achieved by the addition of 1.5% Sarkosyl, and after 3x 10 second sonication bursts on ice (Sanyo Soniprep 150), the lysate was clarified by centrifugation at 10000 rpm (JA-14 rotor, Beckman centrifuge J2-21) for 5 minutes at 4°C. Supernatants were adjusted to 2 or 4% Triton X-100 (Frangioni and Neel, 1992), vortexed, and applied to a 1 ml column of pre-equilibrated (PBS) Glutathione Sepharose-4B beads (Sigma), at a flow rate of 0.5ml/min. Unbound protein was washed through the column by applying 10x column volume of wash buffer (150mM NaCl; 75mM Hepes, pH 7.4) or PBS, before addition of elution buffer (10mM reduced glutathione; 150mM NaCl; 75mM HEPES, pH7.4). Collected fractions were examined by SDS-PAGE and/or Western blotting (methods 2.2.2 and 2.2.3) and stored at -20°C.

2.1.3 Expression using the pET11c vector in *E.coli.*

The pET series of vectors are examples of T7 expression systems that take advantage of the highly specific nature of the T7 RNA polymerase. The plasmids used for cloning and expression of cDNA's are based on the multi-copy plasmid pBR322, and carry a T7 promoter followed by a unique cloning site. For efficient expression, vectors must be transformed into an *E.coli* strain that expresses the T7 RNA polymerase, such as DH1 (DE3) and BL21 (DE3). The bacteriophage DE3 present in these strains is a lambda derivative that has been engineered to contain the gene for the T7 polymerase under the control of the Lac UV5 promoter. It also carries the Lac I gene so that the T7 polymerase gene, normally switched off, can be activated by IPTG.

Plasmid pT7AD23K6 (Grierson *et al.*, 1994) was transformed into *E.coli* BL21(DE3) cells. Starter cultures were grown for six hours at 37°C, and 1ml used to inoculate 250ml of M9 medium. The minimal medium was prepared by mixing 12.5ml of 20x M9 (370mM NH_4Cl; 68mM KH_2PO_4; 845mM Na_2HPO_4), 5ml of 20% (w/v) glucose, 0.25ml of 1M $MgSO_4$, 250μl of 100μg/ml Amp and made up to 250ml with ddH_20 (Novagen Technical Bulletin). All components were sterile filtered (Acrodisc 0.2μm). Cultures were grown until an optical density of between 0.5 and 0.8 was observed at 600nm, and expression induced by the addition of IPTG to a final concentration of 0.6mM. After six hours at 37°C, cells were

harvested as described in methods 2.1.1, except that cell pellets were resuspended in Suspension buffer (5mM EDTA; 4% glycerol; 50mM Tris/HCl, pH 8.0). Pellets were stored at -20°C.

2.1.4 Preparation of bacterial lysates for FPLC.

Thawed cell pellets were resuspended in 6ml suspension buffer containing 100µg/ml lysozyme for 15 minutes at 37°C. Cells were freeze/thawed three times in liquid nitrogen before the addition of 100µl of 1M $MgSO_4$ and 100µl of DNAase I (2mg/ml stock). After an incubation of 15 minutes at 37°C, lysates were centrifuged for 5 minutes at 15000rpm (JA-20 rotor, Beckman centrifuge J2-21). Clarified lysates were filtered (Acrodisc 0.2µm) before applying to DEAE-Sepharose column (methods 2.1.7).

2.1.5 Expression of recombinant 23kd protease in Sf9 cells.

i) Insect cell culture:

Spodoptera frugiperda cells (Sf9) were maintained in suspension cultures at 28°C in TC-100 medium (Gibco-BRL) supplemented with 10% Foetal Calf Serum (FCS) and 50µg/ml Gentamycin (Gibco-BRL). For routine maintenance, cells were passaged every 2 to 3 days (at a cell count of $2x10^6$ cells per ml), and 80% of the culture was discarded and replaced with the same volume of TC-100/FCS.

ii) Sf9 infection with recombinant virus:

Recombinant baculovirus containing the plasmid pVL23K (derived from the transfer vector pVL1393) were constructed and purified (Webster, 1992). Suspension cultures (500ml) of Sf9 cells were grown to a density of $8x10^5$ cells per ml. Cells were pelleted by centrifugation at 2500rpm for 5 minutes (IEC-Centra 3), and resuspended in 15ml of a 10^8 p.f.u./ml stock of recombinant virus (kindly donated by Dr.A.Webster, University of St.Andrews). TC-100 medium was added to a volume of 50ml and cells were infected for one to two hours at 28°C, before TC-100/10%FCS was added to give a final volume of 500ml. Infection was allowed to proceed for sixty hours at 28°C. Infected cells were collected by centrifugation at 2500rpm for 15 minutes and washed in PBS. Pellets were stored at -20°C or processed immediately.

2.1.6 Purification of 23kd protease from Sf9 cells.

The washed cell pellet from infected Sf9 cells was suspended in 5ml of ice-cold 50mM Tris/HCL, pH 8.0 and homogenised on ice with twenty strokes of a tight fitting pestle (type B) in a Dounce Homogeniser. The nuclei were sedimented for 5 minutes at low speed in a microfuge and the cytoplasmic extract was clarified by centrifugation for 20 minutes at 30000g (Beckman TL-100 Ultracentrifuge) at 4°C.

2.1.7 Fast Protein Liquid Chromatography (FPLC).

i) Anion exchange (DEAE-Sepharose):

Clarified supernatants (5 to 10ml) were filtered and applied to a DEAE-Sepharose column (Pharmacia), previously equilibrated with vacuum filtered (Anachem 0.2µm) 50mM Tris/HCL, pH 8.0 (buffer A) for one hour (at 1ml/min). After eluting the 23kd protease with buffer A, remaining proteins were eluted with filtered buffer B (1M NaCl; 50mM Tris/HCl, pH 8.0). The elution profile was monitored at 280nm and 1ml fractions collected. Fractions were either stored at -20°C or analysed (methods 2.2) and pooled for further purification. DEAE-Sepharose columns were stored in 0.02% (w/v) sodium azide.

ii) Cation exchange (Mono-S and CM-Sepharose):

Pooled fractions (approximately 20ml) from DEAE-Sepharose separations were applied to a CM-Sepharose and/or Mono-S column (Pharmacia), pre-equilibrated with buffer A (for 30 minutes) at 1ml/min. Retained 23kd protease was eluted by increasing the salt concentration to 150mM with buffer B. The elution profile was monitored at 280nm and 1ml fractions collected. Fractions were stored at -20°C and analysed as described in methods 2.2.

iii) Gel-filtration (Superdex-75):

For the separation of isomeric forms of the 23kd protease, 200µl of concentrated protein (minimum of 1 mg/ml) was applied to a Superdex-75 column (Pharmacia), pre-equilibrated with elution buffer (150mM NaCl; 50mM Tris/HCL, pH 8.0) for two hours at a flow rate of 0.5ml/min. The elution profile was monitored at 280nm and 0.5ml fractions collected. Fractions were stored at -20°C.

2.1.8 Concentration of purified protein (ultrafiltration).

Fractions of purified protein were pooled, and concentrated either at high pressure (10ml Amicon chamber) or by centrifugation (Centricon). In both cases the molecular weight cut off of membranes was 10kd. The amicon chamber was fitted with a filtron disc membrane, which was pre-equilibrated with ddH_2O. Amicon ultrafiltration was performed on ice using a magnetic stirrer, concentrating protein solutions into a final volume of 1ml. Centricon ultrafiltration was achieved by centrifugation at 3000rpm (IEC Centra-R), at 4°C, until protein solutions were of 0.5ml final volume.

2.2 Assessment of protein purification.

2.2.1 Determination of total protein concentration.

Quantification of total protein concentration was done using the microassay procedure as described in the BioRad protein assay manual. A standard curve was prepared with a series of concentrations of Soybean Trypsin Inhibitor (SBTI) ranging from 1.0 to 20μg/ml. Standards of 0.8ml, and samples diluted 1/100 were placed in test tubes, to which a dye reagent concentrate (obtained from BioRad) was added to give a final volume of 10ml. Samples were mixed by gentle inversion, and after 5 minutes the absorbance at 595nm measured against a reagent control. The concentration of protein samples was determined from a calibration curve of SBTI standards.

2.2.2 SDS-Polyacrylamide electrophoresis (SDS-Page).

BioRad mini gel equipment was used in accordance with manufacturers instructions. SDS-PAGE recipes are listed in table 2.1. After the addition of TEMED and freshly prepared ammonium persulphate to the separating gel, the mixture was poured between the assembled glass plates.

The mixture was overlaid with approximately 0.5ml water saturated butanol and allowed to polymerise before the removal of the butanol overlay and washing with 70% ethanol. After the addition of the stacking gel, 10 or 15 well combs were placed between the plates. After polymerisation, these were removed and the wells washed with water.

Table 2.1: SDS-PAGE recipes. volumes in ml.

	Separating gels			Stacking gel
Reagents	10%	15%	20%	3.2%
40% (w/v) Acrylamide	5.625	8.44	11.25	1.275
2% (w/v) N, N' methylenebisacrylamide	1.400	0.975	0.468	0.70
10% (w/v) SDS	0.225	0.225	0.225	0.10
1M Tris/HCL (pH 8.7)	8.40	6.40	-	-
2M Tris/HCL (pH 8.7)	-	-	4.20	-
1M Tris/HCL (pH 6.9)	-	-	-	1.25
Water	4.35	6.46	8.57	6.70
10% (w/v) ammonium persulphate	0.125	0.125	0.125	0.05
TEMED	0.015	0.015	0.015	0.02

Running buffer (Laemmli): 10x Tris/glycine (25mM Tris; 190mM glycine; 0.1% (w/v) SDS; ddH_2O).

Samples were treated with loading buffer (5% (v/v) ß-mercaptoethanol; 2% (w/v) SDS; 2.5% (v/v) glycerol; 0.001% (w/v) Bromophenol blue; 50mM Tris/HCL, pH 7.5), boiled for 2 minutes, and cooled prior to gel loading. Gels were electrophoresed at a constant voltage (100 volts) until the samples reached the separating gel, thereafter, the voltage was increased to 180 volts. After the dye front migrated to within 1cm from the bottom of the plates, the apparatus was disassembled, and gels prepared for Western blotting (methods 2.2.3), or Coomassie blue stained (0.2% (w/v) Coomassie brilliant blue R250; 50% methanol; 10% acetic acid) for 15 minutes, then destained (2% methanol; 10% acetic acid), after which gels were dried onto 3MM Whatman filter paper using a BioRad 583 vacuum gel dryer (heated to 80°C), or sealed in airtight plastic bags. For silver staining of Coomassie stained gels, the gels were first rinsed in 30% ethanol (3x 20min), then washed in water (2x 15min), before being soaked in sodium dithionite (0.25g/l) for 1 minute (with shaking). Gels were then washed (2x 1min), and immersed in 0.2% silver nitrate in 1mM formaldehyde for 30

minutes. Gels were again washed with water (1 minute) then immersed in 6% (w/v) sodium carbonate)/6mM formaldehyde/20μM sodium dithionite until bands developed. Development was stopped by addition of 3.5% acetic acid and gels then rinsed extensively in water (4x 30min). Gels were stored in 20% ethanol.

2.2.3 Western Blotting.

After separation by SDS-PAGE, protein samples were electroblotted to a Hybond PVDF membrane (Amersham,UK) using a semi-dry blotter (Pharmacia LKB Multiphor II). Eight pieces of 3MM Whatman filter paper, and the PVDF membrane, were cut to gel size. PVDF was pre-soaked in methanol for 2 minutes, and all components were equilibrated for 15 minutes in transfer buffer (48mM Tris; 39mM glycine; 20% methanol; 0.00375% SDS). The blotting sandwich was prepared by placing 4 pieces of filter paper on top of the anode plate, then the PVDF membrane, gel, and finally 4 more layers of filter paper (air bubbles removed at each stage). The cathode plate was then placed on top and a constant current of approximately 50mA/gel was applied. After one hour, the PVDF membrane was removed and either stored at -20°C in a sealed plastic bag, or incubated for one hour at room temperature, or overnight at 4°C, in Blocking buffer (5% (w/v) dried milk powder; 0.1% (v/v) Tween-20; PBS). After blocking, the membrane was incubated with primary antibody (either rabbit polyclonal antiserum or cell culture supernatants containing relevant monoclonal antibodies), for 30 minutes in blocking buffer at the required antibody titre and with gentle rocking. After a series of washes in blocking buffer (3x 10 minutes), the membrane was incubated with a 1/5000 dilution of either anti-rabbit Ig, or anti-mouse Ig horseradish peroxidase linked whole antibody (Amersham,UK), for 30 minutes in blocking buffer. The membrane was washed in blocking buffer (3x 10 minutes) and finally in 0.1% Tween-20/PBS for 15 minutes. The blot was immersed in a 1:1 mixture of two ECL reagents (Amersham,UK) for 3 minutes, and placed between two acetate sheets. Finally, the membrane was exposed to an X-ray film (Fuji-RX) for defined periods of time before being processed in a Kodak M35 X-OMAT processor.

2.2.4 Densitometric assay of protein concentration.

An SDS-Page gel containing SBTI standards (ranging from 1.0 to 20µg/ml), and a known dilution of sample protein were stained and destained. The gel image was then digitised using a Mirror 800 Scanner, and using the NIH Image 1.54 Program (for Macintosh) the lanes were marked and plotted. The relevant peaks of each lane were integrated and the areas displayed. With the areas corresponding to the standards, protein concentration of the sample was read directly from the SBTI calibration curve.

2.2.5 Estimation of enzyme activity by capillary electrophoresis.

i) Peptide assay for recombinant protease:

To determine the activity of purified 23kd protease, 10µl of solution containing the enzyme was incubated with 10µl of activating peptide (GVQSLKRRRCF) which was aliquoted from a 1mg/ml stock kept at -20°C, and 25µl of freshly prepared assay buffer (10mM EDTA; 1mM ß-mercaptoethanol; 50mM Tris/HCL, pH 8.0) for 5 minutes at room temperature (in 0.5ml siliconised eppendorf tubes). Synthetic substrate (LSGAGFSW) was added (5µl from a 2mg/ml stock) and the assay was allowed to proceed for one hour at 37°C. At defined time points, 10µl aliquots were transferred to eppendorf tubes containing 10µl CE buffer (BioRad), and 80µl ddH_2O (filtered using 0.2µm Acrodisc) and either analysed immediately by capillary electrophoresis or stored at -20°C. For biological activity assays of monoclonal antibodies (Mabs) against the Ad2 23kd protease, the above synthetic substrate was substituted with the acetylated synthetic substrate (Ac-LRGAGRSR) due to non-specific digestion by cellular aminopeptidases in cell culture supernatants.

ii) Capillary electrophoresis:

All samples were thawed and filtered (Amicon micropure.22) prior to capillary electrophoresis. The BioRad Biofocus 3000 Capillary Electrophoresis System was initiated 15 to 30 minutes before assays were examined. Water (HPLC grade), capillary wash (BioRad) and CE (capillary electrophoresis) buffer were filtered before use, and were replaced regularly.

The Instrument was used in accordance with the manufacturers instructions. In general, when examining digestion of LSGAGFSW, the CZE (capillary zone electrophoresis) method was

used, and runs were typically of 15 minutes duration. For the acetylated substrate, runs were of 5 minutes duration. Using the Biofocus 3000 Integrator program, the area of peaks within spectra were calculated giving relative concentrations of substrate and products.

2.3 Monoclonal Antibody Production.

Some of the methods described in this section are derived from Antibodies: A laboratory manual (Harlow and Lane, 1988).

2.3.1 Immunisations and test bleeds.

For initial immunisations, purified 23kd protease (methods 2.1.3,4,7 and 8) in 100µl PBS, was mixed with an equal volume of Freunds complete adjuvant (Sigma), followed by a series of 15 second sonication bursts, with 2 minute incubations on ice, until droplets of emulsion placed on water did not disperse. Incomplete Freunds adjuvant was used in subsequent immunisations.

Ten male Balb/c strain mice (six weeks old) were injected with 50µg of 23kd protease (in a total volume of 100µl) by the intraperitoneal route, using a 0.5ml syringe with a 23-gauge needle, and marked at the base of the tail with permanent marker for future identification. This procedure was repeated at 14 and 35 days post initial immunisation.

Test bleeds were done 24 and 45 days after the initial immunisation. Isolated mice were heated under an infrared lamp for a few minutes to increase blood flow to the tail, which was then 'nicked' two inches from the base (using a sterile scalpel) across the tail vein. Several drops of blood were collected and incubated for one hour at 37°C, stored overnight at 4°C, then centrifuged at 10000rpm for 10 minutes (MSE microcentaur microfuge). The serum was removed from the cell pellets and centrifuged once more (10000rpm/10min) before being tested (methods 2.2.3 and 2.3.2).

Mice were kept and used in accordance with Home Office guidelines.

2.3.2 Screening for positive antibody response.

Nitrocellulose sheets (Amersham,UK), pre-equilibrated in PBS, were immersed in solutions of 20 to 50µg/ml 23kd protease (purified from Sf9 cells) for two hours with gentle agitation. After washing 3 times in PBS (10 minutes each), the sheets were immersed in blocking buffer (5% (w/v) dried milk powder; 0.1% (v/v) Tween-20; PBS) for two hours, or overnight at 4°C. For long term storage, sheets were covered in plastic wrap and kept at -20°C.

A single nitrocellulose sheet was placed over a Teraski plate (Sterilin) which had 10µl aliquots of cell culture supernatant and/or rabbit polyclonal antiserum per well. Another Teraski plate was placed on top, and the sandwich was clamped with crocodile clips (sides of Teraski plates were cut and smoothed). The sandwich was inverted, tapped lightly to ensure air bubbles were released from the nitrocellulose surface, and placed in a humid chamber. After 30 minutes, the nitrocellulose sheet was released from the plates and rinsed quickly 3 times in PBS, and washed extensively for a further 30 minutes in PBS. Nitrocellulose sheets were incubated with anti-mouse and anti-rabbit Ig horseradish peroxidase whole antibody for 30 minutes in blocking buffer. Dot blots were developed using ECL reagents (methods 2.2.3) after extensive washing in PBS and 0.1% Tween-20/PBS. When screening cell culture supernatants, polyclonal antiserum R11 (raised against the N-terminal region of the Ad2 23kd protease), diluted 1/5000, was aliquoted into specific wells of teraski plates to aid identification of positive responses by correct orientation.

2.3.2 Preparation of tissue culture plates with macrophages.

Balb/c mice were killed by anaesthesia and swabbed with 70% ethanol. Warmed G-MEM (5ml/mouse) was injected into the peritoneal cavity using a 23-gauge needle, and the abdominal region was massaged for 2 to 3 minutes. After re-sterilisation, the peritoneal cavity was pierced on the right side, just below the liver, using a 19-gauge needle, and 4 to 5ml of peritoneal exudate was allowed to drip into a 10ml centrifuge tube. Macrophages were centrifuged at 1200rpm for 10 minutes and resuspended in G-MEM supplemented with Hypoxanthine-Aminopterin-Thymidine (HAT) hybridoma grade (Sigma), and 10% FCS (for cell fusion's only), or G-MEM/10%FCS (for cell resuscitation and maintenance). A single mouse would yield enough macrophages for three 96 well plates (100µl/well), or two 24 well

plates (0.5ml/well), which were placed in an incubator set at 37°C/5% CO_2 and left overnight.

2.3.4 Hybridoma production:

i) Counting myeloma and hybridoma cells:

When an exact cell count was required, a drop of cell suspension was applied to a hemocytometer (Neubauer counting chamber) and examined using an Olympus CK2 phase contrast microscope. Thereafter:

$$\text{number of cells counted}/_{\text{number of squares counted}} \times 10^4 = \text{number of cells/ml.}$$

ii) Preparing myeloma cells for fusion:

Myeloma cells (SP2/0) were resuscitated from liquid nitrogen storage (methods 2.3.5) two weeks before cell fusion and maintained in G-MEM/10%FCS at 37°C/5% CO_2, passing every 3 to 4 days into new 75cm^2 flats (Sterilin, UK). The day before cell fusion, cells were split into fresh G-MEM/10%FCS at a density of 5x10^5 cells/ml in 75cm^2 flats.

iii) Intravenous boost before cell fusion:

Three days before cell fusion's, immunised mice (best responders) were given a final boost of purified 23kd protease (50µg in PBS) without adjuvant. Mice were isolated, warmed using an infrared lamp, and placed into a restraining chamber. After swabbing the tail with 70% ethanol, 0.2ml of solution was injected into the tail vein approximately 2cm from the base using 0.5ml syringe fitted with a 26-gauge needle.

iv) Preparing splenocytes for fusion:

Two mice were killed by anaesthesia. Using sterilised scalpels and forceps the abdominal cavities were cut open and spleens removed. Both were placed in a 100mm tissue culture dish containing 10ml of pre-warmed G-MEM (without FCS), and contaminating tissue removed. Cells were teased through fine wire gauze using forceps and 1ml syringes fitted with 19-gauge needles (cell clumps were disrupted by repeated pipetting). The lysate was transferred

to a centrifuge tube and left for 3 minutes for particulate matter to settle. The supernatant was removed from the cell debris and added to a fresh centrifuge tube (concentration of cells was $8x10^7$ cells/ml).

v) Cell fusion:

Supernatants from splenocyte preparations were centrifuged at 1200rpm for 10 minutes, and pellets were resuspended in 5ml of NH_4Cl to lyse the red blood cells. After 10 minutes, suspensions were centrifuged as before and resuspended in 10ml of pre-warmed G-MEM. Myeloma cells and splenocytes were washed twice (1200rpm/10min) and combined to give a ratio of 5 splenocytes to 1 myeloma cell, then pelleted. During the washing steps, a vial of 0.5g polyethylene glycol (PEG) of hybridoma grade (Sigma) was melted at 50°C and transferred to 37°C after the addition of 0.5ml G-MEM. The PEG solution was added dropwise over a period of a minute to the cell pellet (in a water bath at 37°C) while resuspending the cells by continual mixing with a Pasteur pipette. After mixing for an additional minute, 10ml of G-MEM was added over a period of 3 minutes (1ml in the first minute) to the cell mixture, which was then pelleted (1200rpm/10min), and resuspended in 10ml of G-MEM/10%FCS(HAT). from the 10ml stock, dilution's of 1/5 and 1/10 in G-MEM/10%FCS(HAT) were aliquoted (100µl) into twenty 96 well plates containing macrophages. After one to two weeks, the media was changed to G-MEM/10%FCS(HT) and individual wells screened for positive clones (methods 2.3.2) when cells were approximately 70% confluent.

vi) Single cell cloning:

After a positive well was identified, cells were transferred to a 24 well plate containing macrophages (the original 96 well plate was maintained in the event of contamination). After several days the cells were resuspended when approximately 90% confluent, and 10µl serially diluted in G-MEM/10%FCS(HT) as neat, 1/5, 1/25, and 1/125, before aliquoting (100µl) into two 96 well plates containing macrophages. The plates were left for a further 3 days (undisturbed) and examined using an Olympus CK2 microscope for single cells, or clusters of cells derived from a single clone. If it was unclear that cell clusters were derived from a single clone, then those wells were re-subcloned.

Wells marked as being single cell clone positives, were allowed to grow to 70% confluence before being screened (methods 2.3.2) for antibody production. Positive clones were gradually weaned off HT supplement over a period of two weeks, and were maintained in G-MEM/10%FCS in 24 well plates.

2.3.5 Long term storage of cell lines.

Dimethyl sulphoxide (DMSO) was of hybridoma grade and purchased from Sigma as 5ml ampoules (stored at room temperature).

i) Freezing positive clones:

Cell lines screened positive for antibody production were expanded into 6 well plates. At 90% confluence, cells were resuspended by repeated pipetting and centrifuged (1200rpm/10min). Media was removed by aspiration, and the pellet gently resuspended in pre-chilled freezing mix (10% DMSO; 30% FCS; G-MEM) and quickly placed on ice in screw top vials, then stored at -70°C. After 24 hours, the vials were placed in liquid nitrogen.

ii) Recovering cells from liquid nitrogen storage:

Frozen vials were removed from liquid nitrogen storage and quickly thawed at 37°C. Immediately the vials were sterilised with 70% ethanol and the cell suspension added to 10ml G-MEM. After centrifugation (1200rpm/10min), the cell pellet was resuspended in 0.5ml G-MEM/10%FCS, and dilution's aliquoted (100µl) into 24 well plates containing macrophages.

2.3.6 Cell culture maintenance and supernatant storage.

Monoclonal cell lines were maintained in 24 well plates, and passaged every 2 to 3 days into fresh G-MEM/10%FCS. Those of interest were expanded into 6 well plates and finally into $75cm^2$ flats. In some instances the media was changed to protein free hybridoma media (Gibco-BRL) gradually over a period of two weeks as not to shock the cells. Cell lines were kept at 37°C/5%CO_2.

Cell culture supernatants from $75cm^2$ flats that were 90% confluent were centrifuged for 10 minutes at 3000rpm (IEC Centra-R) and filtered (Acrodisc 0.2µm). The pH was adjusted by

adding 1/20 volume of 1M Tris/HCl (pH 8.0). Sodium azide was added to 0.02%, and supernatants were stored at -20°C.

2.3.7 Isotyping monoclonal antibodies.

The Serotec isotyping kit was used for classing and subclassing monoclonal antibodies from cell culture supernatants. Vials of freeze-dried anti-mouse IgG1, IgG2a, IgG2b, IgG3, IgA and IgM (positive and negative controls were also provided) were reconstituted into 96 well plates containing recommended dilutions (neat, 1/10 and 1/50) of cell culture supernatants. Plates were left for an hour, at room temperature, and agglutination determined as being positive for a particular isotype.

2.3.8 Monoclonal antibody purification.

The choice of purification method depends on a number of variables which include the class and subclass of antibodies, their intended use, and source for purification. During the course of this study it was not deemed necessary to generate ascitic fluids as a source of concentrated antibody for purification. Instead hybridoma cell lines were cultured in either protein free media or 10% NCS/G-MEM, with the method of antibody purification being dependant on the media type used. For instance, 500ml hybridoma cell cultures (maintained in protein free media) were sterile filtered, adjusted to pH 8.8 (using 2M Tris/HCl, pH 8.8) and applied to a pre-equilibrated (50mM Tris/HCl, pH8.8) 5ml Mono-Q column (Pharmacia) at a flow rate of 0.5ml/min (overnight at 4°C). Monoclonal antibodies were eluted by increasing the salt concentration using 1M NaCl/50mM Tris-HCl (pH8.0) and appropriate fractions were assessed by SDS-PAGE and stored at 4°C or 20°C.

Small scale antibody preparations (50ml or less in protein free media) were the primary source of antibodies used in biological assays. These were concentrated by amicon ultrafiltration to a final volume of 2ml then injected into a pre-equilibrated DEAE-sepharose ion exchange column (section 2.1.7). Although a nominal amount of antibody was retained by the matrix (and later eluted with 150mM NaCl/50mM Tris-HCl, pH 8.0), the majority of antibody solution was collected in the flow through fractions. Alternatively, by raising the pH of the antibody solution (pH 8.5), antibodies were retained by the matrix and eluted as described above.

Antibodies were purified from cell cultures maintained in 10% NCS/G-MEM using protein-A/G columns by methods described in Harlow and Lane (1988). Because mouse antibodies of the IgG1 subclass do not have a high affinity for protein-A, the salt concentration of the antibody solution was raised (3m NaCl final concentration) to increase the strength of hydrophobic bonds that are the basis for the interactions. In addition, cell culture supernatants were adjusted to pH 8.9 (through addition of 1/10 volume of 1M Sodium Borate, pH 8.9). Antibody solutions were applied to a 1ml protein-A (or protein-G) Sepharose 4B column (Sigma), then beads were washed with 10 volumes each of 3M NaCl/50mM Sodium Borate (pH8.9), and 3M NaCl/10mM Sodium Borate (pH 8.9) before elution with 100mM glycine (pH 3.0) into eppendorf tubes containing 50µl of 1M Tris/HCl (pH 8.0).

2.4 Epitope Mapping: Limited proteolysis and chemical cleavage.

2.4.1 Proteolytic cleavage of 23kd protease.

Aliquots of purified recombinant 23kd protease (methods 2.1.3/4/7 and 8) at a concentration of 0.8mg/ml, were stored at -20°C in 150mM NaCl/50mM Tris-JCL, pH 8.0. Trypsin, Chymotrypsin, and Endoproteinase Glu-C (*Staphylococcus aureus* V8) were all HPLC pure (Sigma) and stored as freeze-dried powder. Stock solutions of trypsin (10mg/ml in 1mM HCL), chymotrypsin and endoproteinase Glu-C (5mg/ml in ddH_2O), were prepared fresh prior to limited proteolysis experiments (Carrey, 1990). The ratio of proteolytic enzymes to 23kd protease ranged from 1/100 to 1/1000 (w/w), at either 25°C or 37°C. Proteolysis was allowed to proceed for one hour, during which samples were removed at defined time points and stored at -70°C, before being examined by SDS-Page and Western blotting.

2.4.2 Chemical cleavage using Cyanogen Bromide (CNBr).

CNBr (purchased from Sigma) was weighed in a fume hood, and 100 Molar fold excess (in 10M acetonitrile) over methionines was added to purified 23kd protease (0.8mg/ml) pre-treated with 0.1M ß-mercaptoethanol for two hours at 37°C. The mixture was flushed with nitrogen gas, sealed and incubated for 24 hours in the dark (in a fume hood). After chemical cleavage, 10 volumes of ddH_2O was added to remove excess CNBr, frozen at -70°C

overnight and freeze-dried for 24 hours. The lyophilised powder was resuspended in 200µl ddH_2O and aliquots analysed by SDS-Page and Western blotting.

2.4.3 Multiscreen blots of cleavage products.

SDS-Page gels were prepared with a two well comb. Samples to be examined were loaded into the elongated well (200µl), and pre-stained or low molecular weight markers into the first well (20µl). Gels were electroblotted, then blocked for one hour or overnight at 4°C (methods 2.2.3). Blots were placed into a BioRad Protean II Multiscreen apparatus in accordance with the manufacturers recommendations. Cell culture supernatants derived from monoclonal cell lines of interest , were diluted according to titre (1/100 to 1/1000) in 1ml blocking buffer and loaded into the multiscreen (usually lanes 5 to 20). The apparatus was tilted during loading to prevent the accumulation of air bubbles in the lanes. After 30 minutes incubation, lanes were flushed twice with blocking buffer, the blot removed, and washed for 30 minutes (3x 10min) in blocking buffer. Addition of secondary antibody and developing are described in methods 2.2.3.

2.4.4 Protein sequencing.

i) SDS-PAGE:

A 12.5% separating gel was prepared by mixing 1.66ml of 30% acrylamide/0.8% piperazine diacrylamide (PDA) with 1.33ml ddH_2O, and 1ml of 4x gel buffer (0.4% SDS; 1.5M Tris/HCl, pH 8.8), then degassed for 10 minutes. To polymerise the gel, 2µl of TEMED and 15µl of 10% ammonium persulphate were added before pouring between the glass plates in a BioRad minigel apparatus. The gel was overlaid with water saturated butyl-alcohol, which was replaced after one hour with 1x gel buffer, covered with cling film overnight at 4°C. Stacking gel was prepared by mixing 0.99ml of 30% acrylamide/0.8% PDA, 1.5ml of 4x gel buffer, and 3.5ml ddH_2O, degassed, then polymerised by the addition of 2µl TEMED and 15µl of 10% ammonium persulphate. The gel was left for 3 to 4 hours at room temperature after insertion of the comb.

The lower reservoir of the gel apparatus was filled with electrophoresis buffer (75mM Tris; 0.58M Glycine; 0.1% (w/v) SDS), the upper with 1x upper electrode buffer (0.4% (w/v) SDS; 125mM Tris/HCl, pH 6.8) plus 0.75ml of 10mM glutathione per 150ml of upper

buffer. The gel was pre-run with 10µl sample buffer mix (1.25ml upper electrode buffer, 25% glycerol; 0.6mM ß- mercaptoethanol; 0.02% bromophenol blue) for one hour at 15mA/gel. The gel tank was washed out, and the lower reservoir filled with electrophoresis buffer , whilst the upper reservoir was filled with 150ml electrophoresis buffer containing 150µl of 100mM sodium thioglycolate. Samples were loaded with sample buffer and a constant current of 15mA/gel maintained until the dye front was 1cm from the bottom of the gel.

ii) Western blotting:

After protein separation by SDS-Page, proteins were electroblotted onto a problot membrane (Applied Biosystems) using a BioRad mini trans-blot cell. The membrane was cut to gel size and soaked in methanol for 3 minutes. The membrane, two pieces of Whatman 3MM filter paper, gel, and fibre pads were soaked in transfer buffer (10mM CAPS, pH 11.0; 10% methanol) for 10 minutes. This was repeated several times to eliminate glycine from the electrophoresis buffer. A blotting sandwich was prepared by layering the gel on top of filter paper and fibre pad then placing the membrane on top of the gel. Filter paper and fibre pad were placed on top of the membrane, and the sandwich clamped within a holder which was placed into the buffer tank. Transfer buffer and cooling block were inserted into the tank and the apparatus was set at a constant current of 300mA for two hours (cooling block was changed after one hour). The membrane was stained (0.1% amido black; 40% methanol; 1% acetic acid) for 1 minute, then destained with 40% methanol/1% acetic acid overnight.

iii) Sequencer analysis.

Bands of interest were cut out of the membrane and proteins sequenced using a Procise Protein Sequencer coupled with an Applied Biosystems HPLC apparatus. Western blots in parallel with amido black staining aided localisation of protein bands of interest.

2.5 Epitope Mapping: Deletion mutants of the 23kd protease.

Many of the techniques described in this section are based on methods outlined by Sambrook *et al.* (1989).

2.5.1. Vector pGEXcPK and oligonucleotide primer design.

Expression vector pGEXcPK was constructed by Hanke *et al.* (1994) by inserting the PK tag linker into the EcoR1 site of the pGEX-2T polylinker, abolishing the linker 3'- end EcoR1 site, so that genes of interest can be cloned between BamH1 and EcoR1.

Oligonucleotide primers were designed with BamH1 (GGATCC) and EcoR1 (GAATTC) sites in reading frame with the PK tag, Figure 2.1. The numbering of deletion mutants refers to the first and the last amino acids from the 23kd protease that will be expressed as a deletion mutant clone. Oligonucleotide primers are listed below:

1: 5'GCT**GGATCC**ATGGGCTCCAGTGAGCAGGAAC 3'

2: 5' GG**GAATTC**AGTGTACGCCCCCAGTCTC 3'

3: 5' GGGGGAAG**GAATTC**TGGCGCTACGGCGCAGG 3'

4: 5' ATCCATGG**GAATTC**GGGGCCAGTTGGCAAAGGC 3'

5: 5' GTGACAAAAAG**GAATTC**CGCTCCTAATCTGCG 3'

6: 5' CTGCGCCGT**GGATCC**ATTGCTTCTTCCCCCG 3'

7: 5' GCGAGACT**GGATCC**GTACACTGGATGGCC 3'

8: 5' GTACCTGGG**GAATTC**TAAGCATGGAGTTGGG 3'

9: 5' GCGGAAGTAGG**GAATTC**GGCGCTCCAGGAAG 3'

Using the amplifier software package (Macintosh) a simulation of PCR reactions was performed using Ad2 genome as a template. Primers were predicted to bind without mismatches, and were synthesised on a Beckman 1000 DNA Synthesiser. Synthesised primers were resuspended in 200µl HPLC grade water, and concentrations determined by measuring the absorbance at 260nm of a sample diluted 1/100 with water (with one absorbance unit being equivalent top 50µg/ml single stranded DNA, and the average molecular weight of one base being 330 daltons).

1->

1 atg ggc tcc agt gag cag gaa ctg aaa gcc att gtc aaa gat ctt ggt tgt ggg cca tat

1 **Met** gly ser ser glu gln glu leu lys ala ile val lys asp **leu** gly cys gly pro tyr

61 ttt ttg ggc acc tat gac aag cgc ttt cca ggc ttt gtt tct cca cac aag ctc gcc tgc

21 phe leu gly thr tyr asp lys arg phe pro gly phe val ser pro his lys leu ala cys

7->

121 gcc ata gtc aat acg gcc ggt cgc gag act ggg ggc gta cac tgg atg gcc ttt gcc tgg

41 ala ile val asn thr ala gly arg glu thr gly gly **val his** trp met ala phe ala trp

<-2

181 aac ccg cgc tca aaa aca tgc tac ctc ttt gag ccc ttt ggc ttt tct gac caa cga ctc

61 asn pro arg ser lys thr cys tyr leu phe **glu** pro phe gly phe ser asp gln arg leu

6->

241 aag cag gtt tac cag ttt gag tac gag tca ctc ctg cgc cgt agc gcc att gct tct tcc

81 lys gln val tyr gln phe glu tyr glu **ser leu** leu arg arg ser **ala ile** ala ser ser

<-3

301 ccc gac cgc tgt ata acg ctg gaa aag tcc acc caa agc gtg cag ggg ccc aac tcg gcc

101 pro asp arg cys ile thr leu glu lys ser **thr** gln ser val gln gly pro asn ser ala

361 gcc tgt gga cta ttc tgc tgc atg ttt ctc cac gcc ttt gcc aac tgg ccc caa act ccc

121 ala cys gly leu phe cys cys met phe leu his ala phe ala asn tp **pro** gln thr pro

<-4

421 atg gat cac aac ccc acc atg aac ctt att acc ggg gta ccc aac tcc atg ctt aac agt

141 met asp his asn pro thr met asn leu ile thr gly val pro asn ser met **leu** asn ser

<-8

481 ccc cag gta cag ccc acc ctg cgt cgc aac cag gaa cag ctc tac agc ttc ctg gag cgc

161 pro gln val gln pro thr leu arg arg asn gln glu gln leu tyr ser phe leu glu **arg**

<-9

541 cac tcg ccc tac ttc cgc agc cac agt gcg cag att agg agc gcc act tct ttt tgt cac

181 his ser pro tyr phe arg ser his ser ala gln ile arg **ser** ala thr ser phe cys his

<-5

601 ttg aaa aac atg

201 leu lys asn met

Figure 2.1: Oligonucleotide primers used to amplify regions of the Ad2 23kd protease gene. Regions of the 23kd protease gene corresponding to synthesised primers are underlined. The first and last amino acids of expressed deletion mutants are highlighted.

2.5.2 Polymerase chain reaction (PCR).

For deletion mutagenesis, synthetic oligonucleotides were used to amplify regions of the Ad2 23kd protease gene in a polymerase chain reaction (Saiki *et al.*, 1985). The products were amplified using Ad2 DNA (kindly provided by Ian Leith, University of St.Andrews) as a template. The polymerase used was Vent^{tm} (New England Biolabs) together with a 10x concentration reaction buffer. The reactions were carried out in a final volume of 100µl:

1x reaction buffer.
200µM each of dGTP, dATP, dTTP and dCTP (Pharmacia).
1µl of DNA template.
280ng each of 5' (upstream) and 3' (downstream) primers.
1.5 Units Vent^{tm} polymerase.

The reactions were overlaid with 50µl of sterilised white paraffin to prevent evaporation, and placed in a programmable heating block (Techne Dry-Block PHC-1). The conditions used for PCR reactions were:

Cycle 1 (melting) 94°C for 1.5 minutes
Cycle 2 (annealing) 55°C for 1.5 minutes
Cycle 3 (elongation) 72°C for 2 minutes

Repeated 30 times and held at 72°C for 9.9 minutes.

The reaction mixture was removed from under the paraffin overlay to a fresh tube and mixed with 50µl phenol:chloroform:isoamylacohol (Amresco,UK), at a ratio of 25:24:1, pre-mixed and buffered between pH 6.5 and 6.9. The mixture was then vortexed for 20 seconds, and centrifuged at 13000g (bench top microfuge) for 5 minutes. The aqueous top phase was carefully removed to a fresh tube and 3µl of Lithium Chloride (10M stock), and 220µl absolute alcohol was added. The mixture was kept at -20°C for 20 minutes and the precipitated DNA pelleted by centrifugation at 13000g for 10 minutes. After discarding the

supernatant, the pellet was vacuum dried (Howe Gyrovap GT) for 10 minutes and resuspended in 10µl of ddH_2O. DNA was stored at -20°C.

2.5.3 Restriction digests of PCR products and vector DNA.

In a typical reaction, 1µg of vector DNA (pGEXcPK) was added to 1µl of 10x multicore buffer (Promega) and 1µl each of BamH1 and EcoR1 (Promega) and the reaction allowed to proceed for 1.5 hours at 37°C. Usually about 500ng of PCR amplified DNA was obtained, which was mixed with 1µl each of BamH1 and EcoR1 with 5µl multicore buffer in a total volume of 50µl. Digestion occurred over two hours at 37°C.

2.5.4 Agarose gel electrophoresis and purification of restricted DNA.

DNA samples were separated by agarose gel electrophoresis using a Pharmacia DNA 100 gel rig in accordance with manufacturers instructions. Agarose gels of 1 to 2% (restricted DNA of 0.2kb or less were loaded onto 2% gels) were prepared by dissolving 1g of agarose (Sigma) in 70ml ddH_2O, boiled, and added to 10ml of 10x TAE buffer (150mM EDTA; 3M Tris/acetic acid, pH 8.0), 20ml ddH_2O, and 100µl of 0.5mg/ml ethidium bromide. Gels were cooled slightly before pouring, and care taken to ensure that 2% gels did not have trapped air bubbles that would interfere with DNA migration. Appropriate combs were added and the gel allowed to set (usually one hour). DNA samples were mixed with 2.5µl of 5x DNA loading buffer (0.05% bromophenol blue; 40% glycerol; 50mM EDTA; 60mM Tris/acetic acid, pH 8.0) and loaded into the wells. A DNA standard 1kb DNA ladder (Gibco-BRL) was used throughout. Gels were electrophoresed at 100v constant voltage until the dye front had migrated to $^2/_3$ the gel length. The DNA band were examined on a UV (365nm). Vector and amplified restricted DNA of the predicted size, were excised from gels using a sterile scalpel and transferred to a 1.5ml eppendorf tube. Gel slices could be stored at -20°C or DNA extracted using a Qiagen DNA extraction kit in accordance with the manufacturers instructions. Pellets were air dried for 10 minutes and DNA eluted with 20µl ddH_2O. DNA was stored at -20°C.

2.5.5 Ligation of vector and insert DNA.

The ligation of purified insert and vector DNA was achieved using T4 DNA ligase (Promega). The ligation mixtures comprised of 1µl vector DNA and 5µl insert in a total volume of 20µl, containing 2µl 10x ligase buffer and 1µl T4 DNA ligase. The ligation reactions were allowed to proceed for four hours at room temperature, and control ligations of vector DNA alone were done in parallel. Although no attempt was made to quantify the molar ratio of insert to vector DNA, these procedures proved to be adequate. After four hours, 10µl of the ligation mixture was used to transform competent *E.coli* (XL1 Blue). ligated DNA was not stored.

2.5.6 Preparation of competent bacterial cells.

A 0.5ml aliquot of overnight culture of XL1blue cells was inoculated into 50ml LB medium. This was incubated at 37°C (with shaking) until the culture reached an optical density of approximately 0.3 at 600nm. The culture was centrifuged at 3000rpm for 10 minutes (IEC Centra-R) at 4°C. Cell pellets were resuspended in 5ml of sterile ice-cold 0.1M $MgCl_2$, and centrifuged as before. Cell pellets were resuspended in 2ml of sterile ice-cold 0.1M $CaCl_2$. The preparations were left on ice for at least 30 minutes before being used in transformations. XL1blue cell stocks were maintained on agar plates containing 100µg/ml tetracycline (Tet), at 4°C.

2.5.7 Transformation of competent bacteria.

Competent XL1blue cells (200µl aliquots) were kept chilled on ice, and 10µl of ligation mix (methods 2.5.5) or 1µl of purified plasmid (methods 2.5.9) were added. After 30 minutes (on ice) the samples were heat shocked in a water bath set at 42°C, for 90 seconds, and then immediately placed on ice for a further 5 to 10 minutes. Transformed cells and non-transformed competent cell controls were spread onto Amp/Tet agar plates using a sterilised glass rod, left for 15 minutes, and finally incubated overnight at 37°C.

2.5.8 Preparation of agar plates.

Molten LB/agar was kept at 55°C until equilibrated at this temperature. Ampicillin and Tetracycline were added to a final concentration of 0.1mg/ml, and the agar poured into sterile

petri-dishes (approximately 20ml/dish). After flaming the surface of the agar to remove bubbles, plates were left for one hour to solidify and used the same day.

2.5.9 Small scale plasmid preparation (miniprep).

The method used throughout is outlined in the Qiagen plasmid handbook. Single colonies from selected agar plates were used to inoculate 3ml of LB/Amp medium, then grown overnight at 37°C. Cells were pelleted (bench top microfuge), and resuspended in buffer P1 (10mM EDTA; Tris/HCl, pH 8.0) containing 100µg/ml A (Qiagen), and 0.3ml of buffer P2 (200mM NaOH; 1% (w/v) SDS), then incubated at room temperature for 5 minutes. Ice-chilled buffer P3 (3M Potassium acetate, pH 5.5) was added (0.3ml), then cell lysates were mixed gently and incubated on ice. After 10 minutes, lysates were centrifuged at 13000g (microfuge) for 15 minutes. The DNA was precipitated from the supernatant by adding 0.8 volumes of isopropanol, and centrifuged for 15 minutes at 130000g. DNA was washed twice with 70% ethanol and redissolved in 40µl ddH_2O.

To check for potential clones, 2µl of DNA was incubated with BamH1, EcoR1, and multicore buffer (1µl each) in a total volume of 10µl, and left for 1.5 hours at 37°C. Digests were examined by agarose gel electrophoresis, and positive clones used for expression of deletion mutants.

2.5.10 Expression and purification of deletion mutants.

Deletion mutant plasmids were transformed into *E.coli* BL21 (DE3) cells. A single colony was picked from a selective agar plate and used to inoculate 5ml LB/Amp medium, and grown overnight at 37°C. From the starter culture, 1ml was used to inoculate 250ml of LB/Amp and grown until an optical density of between 0.5 and 0.8 was observed at 600nm. Expression of deletion mutants was induced by the addition of IPTG at a final concentration of 0.1mM. After six hours, cells were harvested by centrifugation (10000rpm/10min), and washed once in STE buffer (section 2.1.1), then pelleted as before (methods 2.1.2). Pellets were stored at -20°C.

Thawed pellets were resuspended in 3ml STE buffer with Pefabloc (Boehringer Mannheim), added to a final concentration of 4mM, and supplemented with lysozyme (100µg/ml). The pellets were incubated on ice for 15 minutes. Triton X-100 was added (1% final

concentration), then lysates sonicated (3x 15 second bursts/2min on ice), and centrifuged at 15000g (JA-17 rotor, Beckman J2-21 centrifuge) for 5 minutes, at 4°C. Supernatant fractions were added to 0.5ml glutathione Sepharose-4B beads (pre-swollen in PBS) and incubated in 10ml plastic tubes, on ice, mixing periodically. After 30 minutes, the mixture was pelleted by centrifugation (1000g/2min) and supernatant aspirated off the beads. The glutathione Sepharose beads were washed 10 times with ice-cold PBS. Fusion proteins were eluted with 10mM reduced glutathione/PBS, and examined by Western blotting with appropriate monoclonal antibodies.

2.6 Epitope mapping: Overlapping peptides.

2.6.1. Design of overlapping peptides.

Synthesised peptides which extend over two regions of the Ad2 23kd protease (R48 to P101, and F133 to S19) are listed below:

1 (57/71) FAWNPRSKTCYLFE-S

2 (67/81) CYLFEPFGFSDQRLK-S

3 (77/91) DQRLKQVYQFEYESL-S

4 (87/101) EYESLLRRSAIASSP-S

6 (87/95) EYESLLRRS

7 (82/90) QVYQFEYES

8 (133/146) FANWPQTPMDHNPT-S

9 (142/156) DHNPTMNLITGVPNS-S

10 (151/164) TGVPNSMLNSPQVQ-S

11 (161/176) PQVQPTLRRNQEQLYS

12 (183/194) PYFRSHSAQIRS

13 (176/187) SFLERHSPYFRS

14 (171/182) QEQLYSFLERHS

15 (175/189) YSFLERHSPYFRSHS

All peptides were synthesised on serine linked Pepsyn resin, although in some instances the serine was not native to the Ad2 23kd protease (-S). The start and finish amino-acids indicate

the position of these residues in the intact protein. Peptide 5 (region 1) was previously synthesised (Webster, 1992) and has the sequence; RETGGVWHMAFAWN (48/61).
Overlapping peptides synthesised on cellulose support (SPOTs test; Genosys) were designed as follows:

For region 1 (R63 to I105) all peptides were of 13 residues in length, shifted by 2 amino acids i.e.;

RSKTCYLFEPFGF

KTCYLFEPFGFDQ

..... etc.

For region 2 (D102 to K202) peptides of 13 residues in length, overlapping by 5 amino-acids were synthesised i.e.;

DRCITLIKSTQSV

STQSVQGPNSAAC

.....etc.

2.6.2 Peptide synthesis.

The method used is essentially the same as that described by Webster (1992). All peptides were synthesised by solid phase fluorenyl methoxy carbonyl (Fmoc) polyamide chemistry. The Fmoc penta fluorophenyl derivatives of amino acids and Fmoc-L-Ser(But)-Pepsyn resin were purchased from Millipore. Plastic columns (1.5ml) and 10μm pore filters were obtained from Mobitec. Dimethylformamide (DMF), glacial acetic acid, acetonitrile, and trifluoracetic acid (TFA) were all HPLC grade from Rathburn. Piperidine was purchased from Applied Biosystems. Ethanedithiol, anisole, tertiary amyl alcohol, and 1-hydroxybenzotriazole (HOBT) were obtained from Aldrich. DMF was routinely tested for dimethylamine using fluorodinitrobenzene (FDNB) from Sigma, as descibed by Webster (1992). The apparatus used for synthesising peptides consisted of a plastic box with 5 columns with filters and a outlet for applying vacuum by reduced pressure.
Resin (75mg) was resuspended in 1ml DMF and transferred to a column and sucked dry using the vacuum line in a fume hood. Columns were washed three times with DMF (vacuum being applied each time), then filled with piperidine (20% in DMF), Dried, and filled again,

but allowing to percolate through (approximately 15 minutes). Amino-acids (30-40mg) were dissolved in 300µl DMF and 100µl HOBT (1.3g/10ml DMF), vortexed, and added to the column, after it had been washed 4 times with DMF to remove any residual piperidine. The whole apparatus was placed in an incubator (25°C) and left for 1 to 1.5 hours. This procedure was repeated until all amino-acids had been added.

The resin was deprotected and washed sequentially with DMF, t-amyl alcohol, glacial acetic acid,t-amyl alcohol (2x 0.5ml each) then ether (4x 0.5ml). An eppendorf tube was placed underneath each column, and 200µl cleavage reagent added (TFA containing a total of 5% of the appropriate scavengers such as anisole, or phenol if peptides contained arginines). Tubes were left for one to two hours or overnight if arginine was present, then TFA was vacuum filtered into the eppendorf tube, and resin washed with TFA. A stream of nitrogen gas was used to evaporate TFA, and 500µl of ether was added to precipitate peptides. Peptides were finally washed 5x with ether, then redissolved in water and freeze-dried.

2.6.3 Peptide purification using High Performance Liquid Chromatography (HPLC).

HPLC grade S-acetonitrile, TFA, and water were obtained from Rathburn. A Gilson HPLC connected to an Apple II computer with pre-set gradient programs was used throughout. Freeze-dried peptides were weighed, dissolved in 1ml 0.1% TFA/water, then filtered (0.2µm Acrodisc). An RsiL C18 HL column (5µm sylane particles packed into a total column volume of 4.15ml), was washed with 100% acetonitrile/0.1% TFA for 25 minutes, then equilibrated for 15 minutes with 0.1% TFA/water. Sample (1ml) was injected, and a continuous gradient applied (0 to 50% acetonitrile in 25 minutes), and 1ml fractions collected after 10 minutes (approximately 20% acetonitrile). The elution profile was monitored at 226nm, and purified peptides analysed by capillary electrophoresis. Aliquots of HPLC fractions (10µl) were added to 10µl CE buffer and 80µl filtered water then examined using the CZE method (methods 2.2.5). In addition, peptides were also sequenced (methods 2.2.4). Purified peptides were stored at -20°C.

2.6.4. Determination of epitopes by competitive ELISA.

Immulon microtiter plates (Dynatech ltd) were coated with 100µl of 1% glutaraldehyde (in PBS) and left overnight at 4°C. Plates were washed 3 times with PBS, and 100µl of purified 23kd protease (methods 2.1) were added to a final concentration of 5µg/well in PBS, then left overnight at 4°C. Plates were rinsed with 150µl wash buffer (0.5% (w/v) dried milk; 0.1% (v/v) Tween-20; PBS) three times and incubated in blocking buffer (5% (w/v) dried milk; PBS) for 3 hours at 37°C, or overnight at 4°C. ELISA plates were again rinsed with wash buffer 3 times. In a separate 96 well plate, a doubling dilution series of cell culture supernatant was added to an equal volume of peptide solution (100µg/ml in PBS) and incubated for one hour at 37°C. Antibody/peptide solutions were transferred to corresponding wells on the 23kd protease coated ELISA plate and left for an additional hour at 37°C. ELISA plates were rinsed 3 times (150µl each) with wash buffer, and 100µl of secondary antibody (anti-mouse Ig horseradish peroxidase linked whole antibody, Amersham), diluted 1/5000 with wash buffer, was added to each well. Incubations were at 37°C for 30 minutes, then plates were rinsed extensively with wash buffer, and finally with PBS alone. Peptide inhibition of antibody binding to 23kd protease was detected by the addition of 3,3',5',5-Tetramethylbenzidine (TMB) liquid substrate system (Sigma). TMB was added at 50µl/well and colour development read at 655nm after a one hour incubation at 37°C (in darkness).

2.6.5 Overlapping peptides bound to cellulose (SPOTs test).

Overlapping peptides synthesised on cellulose membranes by fluorenyl carbonyl (Fmoc) chemistry (Genosys,UK), were used for epitope mapping in accordance with manufacturers instructions.

Membranes were rinsed in methanol (HPLC grade, Rathburn) for 3 minutes, then incubated in 20mls of TBS (25mM Tris, pH 8.0; 144mM NaCl) for 10 minutes. Concentrated blocking buffer (supplied by Genosys) diluted 1/10 with T-TBS (0.1% (v/v) Tween-20; TBS, pH 8.0) was added, and membranes blocked overnight at 4°C. After blocking, membranes were washed 3 times (15 minutes each) in T-TBS, and monoclonal antibody solution added at a dilution of 1/200 in T-TBS. After a 3 hour incubation, membranes were washed 3 times as described above. The cellulose membranes were incubated with secondary antibody (anti-mouse Ig horseradish peroxidase linked whole antibody) diluted 1/5000 in T-TBS, for 30

minutes, with gentle agitation, followed by 3 washes in T-TBS and finally in TBS alone. The blots were developed as described in methods 2.2.3.

Cellulose membranes were re-probed with several monoclonal antibody supernatants. Regeneration of membranes was achieved by washing in 20ml ddH_2O, then 20ml DMF, and finally 20ml ddH_2O for 10 minutes each. Regeneration buffer A (8M Urea; 1% SDS; ddH_2O) was added for 10 minutes, followed by an incubation in regeneration buffer B (50% ethanol; 10% acetic acid; ddH_2O) for 10 minutes. Methanol was added for 10 minutes, and the SPOTs procedure described above repeated in full, for new antibody solutions.

2.7 Adenovirus (type 2) infection of HeLa cells.

2.7.1 HeLa monolayer and spinner cell culture maintenance.

Monolayer HeLa cells (generously provided by Prof.J.Lamb, University of St.Andrews, and originally purchased from Imperial Labs) were maintained in 75cm^2 flats (Sterilin) with 25ml G-MEM/10%NCS, at 37°C/5%CO_2. Cells were passaged every 3 days by washing the cell monolayer with trypsin/EDTA (5ml) and overlaying the monolayer with 2ml trypsin/EDTA. After approximately 2 minutes, 8ml of G-MEM/10%NCS was added and the flat gently tapped to release cells into suspension. Generally, 1/5 or 1/10 dilutions of cell suspension were seeded into new 75cm^2 flats. HeLa spinner cells were maintained in S-MEM/10%NCS at 37°C. When the cells reached a density of 5x10^5 cells/ml they were passaged to give a cell concentration of 2x10^5 cells/ml.

Periodically cell stocks were examined for mycoplasma contamination (methods 2.8.2).

2.7.2 Preparation of wild type Ad2 virus stocks.

i) Infection of HeLa spinner cells:

HeLa spinner cell cultures (6 litres) were grown to a density of 3x10^5 cells/ml, then centrifuged for 30 minutes at 3000rpm in a Mistral 6L centrifuge. Cell pellets were resuspended in 250ml of S-MEM and 1ml of Ad2 arcton extract added. After 2 hours at 37°C, S-MEM/2%NCS was added to a final volume of 6 litres. Cells were harvested at 72 hours post infection (h.p.i) by centrifugation (as before), the cell pellet was washed with PBS, and resuspended in 48ml of 10mM Tris/HCl, pH 7.0. Cell suspension (12ml) and

40ml of trichloro-trifluoro-ethane (arcton) were added to 4x 50ml sterile centrifuge tubes and shaken for 30 minutes at 4°C using a mechanical shaker. Extracts were centrifuged at 800g (IEC-Centra 3R) and the aqueous layer removed then clarified by centrifugation at 10000g for 30 minutes (JA-17 rotor, Beckman J2-21 centrifuge). Fractions were aliquoted (1ml) and stored at -70°C. Titre of virus stocks were determined by plaque assay.

ii) Plaque assay:

HeLa monolayer cells were grown to 90% confluence in $50mm^2$ petri dishes (sterilin). Media was aspirated from the cell monolayer and replaced with 0.1ml of serially diluted virus stock (range of 10^{-7} to 10^{-10} used) and incubated for one hour at 37°C/5%CO_2. Duplicate assays were performed for all dilutions, and uninfected controls were included. When the incubation was completed, 4ml of agar overlay (20ml 2.5% (w/v) Noble agar; 20ml 5x G-MEM(-glutamine); 10ml tryptose phosphate broth (2.95g/100ml); 9ml sodium bicarbonate (2.25g/100ml); 2ml NCS; 2ml 1M MgCl; 2ml glutamine (2.9g/100ml); 100 Units each of Penicillin and Streptomycin; ultrapure water to 100ml), cooled to 42°C, was added gently to the side of the petri dish (Precious and Russell, 1991). After the overlay had set, dishes were placed at 37°C/5%CO_2 for 4 days then 2ml of agar overlay was added. Cells were fixed after a further 4 days by adding 10% (v/v) formal saline and left overnight. After removing the agar overlay, monolayers were stained with 0.1% crystal violet solution for 20 minutes to observe plaques.

2.7.3. Ad2 infection of HeLa monolayer cells:

HeLa monolayer cells grown in $75cm^2$ flats were infected with Ad2 wild type virus stock, or Ad2ts1 mutant virus (kindly donated by Ailsa Webster and Ian Leith, University of St.Andrews) at approximately 10 p.f.u/cell. When cells were approximately 70% confluent, media was aspirated off, and cell monolayers washed with pre-warmed G-MEM. HeLa cells were incubated with virus (in 5ml G-MEM) for one hour at 37°C/5%CO_2. The virus solution was replaced with 25ml G-MEM/2%NCS and left at 37°C/5%CO_2 until harvesting at defined time points. Ad2ts1 infected cells were incubated at 39°C (non-permissive) or 33°C (permissive) temperatures.

HeLa monolayer cells for immunocytochemical studies were grown on Henley-Wessex multispot slides in G-MEM/10%NCS (3 slides/100mm^2 dish) and infected as described above. Cells were grown on slides for a minimum period of 24 hours before infection.

2.7.4. Preparation of nuclear and cytoplasmic extracts.

All protease inhibitors were obtained from Sigma (except PefablocSC which was purchased from Boehringer Mannheim), and stored at -20°C. Lysis buffers were stored at 4°C and protease inhibitors added when required.

i) From HeLa monolayer cells:

At fixed times post infection, HeLa monolayer cells were washed with ice-cold PBS, and removed from 75cm^2 flats (using a rubber cell scraper) into 1ml PBS/flat. Cells were centrifuged at 6000rpm for 2 minutes at 4°C (Eppendorf centrifuge S402), and the pellet washed in 0.5ml PBS, then re-centrifuged and stored at -70°C. Addition of 100µl lysis buffer (50mM sodium flouride; 5mM tetra sodium pyro-phosphate; 1mM sodium orthovanadate; 10mM ß-glycerophosphate; 0.5% NP40; 2mM EDTA; 20mM Na_2HPO_4; ddH_2O) containing protease inhibitors (1mM Leupeptin; 1mM Pepstatin; 100mM Pefabloc; 1mM Bestatin; 1mM TPCK), then centrifugation at 14000rpm for 10 minutes at 4°C, yielded cytoplasmic extracts (supernatant fraction) which were stored at -70°C. Nucleoplasmic extracts from pellets were obtained by adding 5M NaCl to lysis buffer to give a final salt concentration of 425mM. Lysates were incubated on ice for 20 minutes, then centrifuged at 14000rpm for 15 minutes at 4°C. The supernatant was stored at -70°C.

ii) Hypotonic lysis of spinner cells:

HeLa spinner cells (2 litres) were centrifuged at 1500g (Mistral 6L centrifuge) for 15 minutes, washed in PBS, and pelleted. The pellet was resuspended in 5ml hypotonic lysis buffer (10mM Hepes/NaOH, pH 7.9; 10mM KCl; 1.5mM $MgCl_2$) containing protease inhibitors (see above), and left on ice for 10 minutes to allow cells to swell. The cells were lysed by 15 strokes in a glass Dounce homogeniser (type B pestle). Large particulate matter, including nuclei, were sedimented at 1000g for 10 minutes at 4°C. The supernatant was centrifuged at 100000g for 30 minutes at 4°C (Beckman TL-100 Ultracentrifuge) to give the

soluble cytoplasmic extract (also referred to as the S100 extract). Nuclei were lysed by adding high salt buffer (20mM Hepes/NaOH, pH 7.9; 420mM NaCl; 25% glycerol; 1.5mM $MgCl_2$; 0.2mM EDTA) containing protease inhibitors, followed by 15 strokes of the Dounce homogeniser. In some instances, 0.5% NP40 was added to nucleoplasmic fractions to disrupt lipids (Stow and Hay, 1993). Lysates were centrifuged at 100000g for 30 minutes (4°C) and the supernatant stored at -70°C.

2.7.5 Fixation of Hela monolayer cells for immunocytochemistry.

Glutaraldehyde (25% aqueous stock stored at -20°C) and osmium tetroxide (2% aqueous stock stored at room temperature) were purchased from Sigma. Paraformaldehyde was obtained from BDH and 40% Formaldehyde from May and Baber ltd. Sheep serum was obtained from the Scottish Antibody Production Unit (SAPU).

Infected and uninfected cells grown on glass slides were washed three times with PBS to remove any traces of media prior to fixation. For light microscopy, cells were incubated with fixative (5% (v/v) formaldehyde; 2% (w/v) sucrose; 1% (v/v) sheep serum) for 10 minutes. In some instances, 4% paraformaldehyde solutions were prepared by adding 8 grams to 100ml ddH_2O, and heating in a fume hood until dissolved. After cooling, 100ml of 2x PBS was added. Paraformaldehyde solutions were prepared as required.

For electron microscopy, the above fixatives were used in addition to 1% (v/v) glutaraldehyde/PBS, pH 7.4. Mixtures of fixative solutions, such as 2.05% PfG (2% (w/v) paraformaldehyde; 0.05% glutaraldehyde; PBS, pH 7.4) were prepared as required (Griffiths, 1995). The duration of fixation ranged from 10 to 60 minutes for all fixatives used. Fixed monolayer cells to be treated with 1% (v/v) osmium tetroxide/80mM cacodylate buffer, pH 7.3, were first washed with 80mM cacodylate buffer alone (3x 15minutes) and then post-fixed with buffered osmium tetroxide for a further 30 minutes.

Fixed cells were washed 3 times with blocking buffer (1% (v/v) sheep serum; PBS, pH 7.4) and stored in blocking buffer containing 0.02% Sodium azide, at 4°C for a maximum period of one week.

2.8 Immunocytochemistry.

Methods used in light microscopy studies are derived from Antibodies: a laboratory manual (Harlow and Lane, 1988), and Immunocytochemistry: a practical approach (Monaghan and Robertson, 1993). The latter book was also a source of methods used during electron microscopy studies, in addition to Fine structure immunocytochemistry (Griffiths, 1993), which was a valued source of technical information.

2.8.1 Source and preparation of primary antibodies.

Monoclonal antibodies against cytokeratin peptide 18 (clone K5.B17.2) and vimentin (clone V9) were purchased from Sigma and used at a 1/40 dilution in PBS. Dr.A.Webster and Professor.R.T.Hay (St.Andrews University) kindly provided monoclonal antibodies 44E1, 11F11, and 3D11B1, specific for the Ad2 preterminal protein (pTP). Cell culture supernatants for these monoclonal antibodies, those against the Ad2 23kd protease (methods 2.2) and the promyelocytic leukaemia protein (PML), clone 5E10 (Stuurman *et al.* , 1992), were filtered (0.2μm Acrodisc) then used at dilution's ranging from 1/2 to 1/10. Dr.D.A.Mathews and Professor.W.C. Russell (University of St.Andrews) kindly donated rabbit polyclonal antiserum against the Ad2 V, pVI, and DNA binding protein (DBP). In addition, Prof.W.C.Russell generously donated aliquots of monoclonal antibodies recognising the Ad2 pVII, and DBP proteins. Dr.A.I.Lamond (University of Dundee) provided both monoclonal (SP10) and polyclonal (204/4) antibody solutions specific to p80 coilin. Stuart Annan (University of St.Andrews) donated polyclonal antiserum specific to the Ad2 pVIII protein.

Polyclonal antiserum against viral antigens were extensively pre-absorbed onto uninfected HeLa cell monolayers, and individual titres determined for both light and electron microscopy studies. HeLa cells were grown in $25cm^2$ flats and fixed when 90% confluent. Cell monolayers were permeabilised (10% (w/v) sucrose; 0.5% (v/v) NP40; 1% (v/v) sheep serum) for 5 minutes, then washed three times (5min each) with 1% sheep serum/PBS. Antiserum (100μl) of appropriate dilutions (1/500 to 1/5000) were added to the cell monolayers and incubated for one hour with gentle rocking. This procedure was repeated

three times. Pre-absorbed antiserum were filtered and stored at 4°C with 0.02% sodium azide, or kept at -20°C. Antiserum against cellular proteins were titred only.

2.8.2 Immunofluorescence.

Fixed HeLa monolayer cells were permeabilised (10% (w/v) sucrose; 1% (v/v) sheep serum; 0.5% (v/v) NP40; PBS) for 5 minutes then incubated in blocking buffer (1% sheep serum/PBS) three times (5 minutes each). The glass slides were dried around the wells using a P100 pipette tip wrapped in Medi-Wipe tissue, taking care to avoid the wells. Primary antibodies were added (10µl/well), and left in a humid chamber for one hour at room temperature. Microscope slides were quickly rinsed with PBS, permeabilised, then washed and dried as described above. Texas Red conjugated affinipure donkey anti-rabbit IgG, and Fluoroscein conjugated affinipure donkey anti-mouse IgG secondary antibodies (Jackson Immunoresearch) were added (10µl) at recommended dilutions (1/50 to 1/200), and incubated for one hour in a humid chamber (protected from light). Finally, slides were rinsed with PBS (3x 10min) in darkness, then dried around the edges. Citifluor (Chemical Laboratories, University of Kent) was added dropwise between the wells, then coverslips were gently applied onto the microscope slide. Often coverslips were sealed onto slides with nail varnish to prevent cell monolayers being disturbed when using oil immersion.

Fluorescence was examined using a Nikon Microphot-FXA microscope with either 20x,40x, or 100x (oil immersion) objectives at emission spectra of 525nm for fluorescein, and 620nm for Texas red. Cell fluorescence was photographed with an automatic exposure onto Ilford HPS 400 film. In addition, a BioRad Confocal Laser Microscope was used in colocalisation studies using a 100x oil immersion objective.

Periodically cells were examined for mycoplasma contamination. when adding second antibodies, the DNA-intercalating agent 4', 6-diamidino-2-phenylindole (DAPI) was added (a dilution of 1/1000 from a stock of 100µg/ml in PBS) directly with second antibody solutions.

2.8.3 Preparation of fixed cells for electron microscopy.

i) Embedment:

Fixed HeLa cell monolayers on Henley-Wessex slides were washed in 80mM cacodylate buffer for 15 minutes (3 times). Cells were dehydrated gradually in 50, 70, 80, and 90%

ethanol for 10 minutes each, then finally dehydrated in 100% ethanol 3 times (20min each), and left overnight in 100% ethanol. The araldite epoxy resin used (MY753) is not miscible with ethanol, therefore glass slides were left in 100% propylene oxide (3x 20min). Prior to infiltration of resin, the embedding medium was prepared by combining 19ml epoxy resin (MY753), 21ml of the hardener, dodecyl succinic anhydride (DDSA), and 0.6ml of the plasticiser, dibutyl phthalate, in a fume hood. After mixing the components thoroughly, 1.2ml of resin accelerator, benzyl dimethylamine (BDMA) was added. All components were obtained from Agar Scientific. Resin infiltration was performed gradually by adding 2 parts propylene oxide to 1 part resin for one hour, then 1 part propylene oxide to 2 parts resin for a further hour. Gelatine capsules were placed over wells and 100% resin added. Cells were embedded for 48 hours, and cured at 60°C in an oven within the fume hood. Embedded slides were dipped into liquid nitrogen briefly, and gelatine capsules snapped off.

ii) Thin sections:

Resin blocks were trimmed to a four sided pyramid, then cut using an ultramicrotome (Reichart Ultracut S) fitted with a diamond knife, to give sections of 50 to 70nm thickness. Thin sections were applied to hexagon 100-mesh copper grids (Agar Scientific), pre-coated with 1% pioloform in chloroform. Grids (with sections) were carbon coated using a Balzers coating machine (BA3), at high voltage and vacuum. Sections were then ready for immunolabelling or contrasting.

2.8.4 Immunolabelling thin sections:

Grids were immersed section down on drops of blocking buffer (5% (v/v) sheep serum; 0.1% (w/v) gelatine; 0.05% (v/v) Tween-20; PBS) for 30 minutes, then incubated on drops of 0.02M glycine for a further 10 minutes to block free aldehyde groups (Griffiths, 1993). Grids were then placed on 5ml of wash buffer (1% (v/v) sheep serum; 0.1% (w/v) gelatine; 0.05% (v/v) NP40; PBS) for 15 minutes on an orbital shaker, then transferred to 100µl drops of primary antibody on parafilm for one hour. After 3x 15 minute incubations in wash buffer (gently on an orbital shaker), thin sections were incubated with 1/20 dilutions of 6nm colloidal gold-affinipure goat anti-rabbit IgG, and 12nm colloidal gold-affinipure goat anti-mouse IgG, on parafilm at room temperature for one hour. Immunolabelled sections were

incubated (3x 15min) with wash buffer, PBS (3x 15min), then for one minute with ddH_2O on an orbital shaker (5ml each). Finally, grids were placed on drops of 2.5% glutaraldehyde for 1 minute to fix immunogold labelling, and stored overnight in ddH_2O with 0.02% sodium azide.

2.8.5 Contrasting thin sections.

Uranyl acetate (0.2g dissolved in 70% ethanol) and lead citrate (1.76g trisodium citrate and 1.33g lead nitrate dissolved in 30ml ddH_2O, then 8ml 1N NaOH pus ddH_2O to 50ml) were centrifuged for 10 minutes at 10000rpm (MSE benchtop centrifuge) and stored in foil at 4°C. Inverted grids were added to uranyl acetate drops on dental wax. Meanwhile, NaOH pellets were placed on filter paper within a petri dish and clean dental wax placed in the centre of the dish. Drops of lead solution were applied to the dental wax. After uranyl acetate staining, grids were washed in ddH_2O 3 times, then dried with tissue paper and transferred to the lead citrate solution. After 5 minutes, the grids were dipped in 0.02N NaOH twice, ddH_2O 3 times, and dried as before.

2.8.6 Transmission electron microscopy.

Contrasted thin sections were examined using a Phillips EM 301 Microscope at 80kv. The camera film used was Agfa Scientia EM film. For any particular antigen, a minimum of 5 grids were examined (prepared at different periods during the study). For viral antigens, primary antibodies were incubated with uninfected cell thin sections as a control for non-specific reactions. Secondary antibodies were incubated with thin sections not treated with primary antibodies. Controls were done throughout the whole study as stringent monitoring of background levels of gold particles, and artifactual structures arising from thin section preparation was essential. The magnification of thin sections necessary to detect immunogold labelling varied with the type of fixation used, but 34,000x was sufficient for most purposes.

2.9 Processing of viral and cellular proteins

2.9.1 Immunoprecipitation of 23kd protease from cell extracts.

i) Covalently coupling monoclonal antibodies to Dynabeads:

Dynabeads M-450 rat anti-mouse IgG1 (Dynal,UK) were used in accordance with manufacturers instructions. Beads were resuspended in the supplied vial for 1 minute by vortexing, then the required volume was aliquoted into a 0.5ml Eppendorf tube and separated from stock solution by applying to the Dynal MPC-E/E-1 magnetic particle concentrator. Beads were washed several times with 0.1% bovine serum albumin (BSA)/PBS.

For direct antigen capture, 10^7 dynabeads were added to crude cell culture supernatants (approximately 1.5µg of antibodies in total) and incubated at room temperature for 30 minutes with continuous slow rotation, followed by several washes (3x 15min) in 0.1%BSA/PBS. Crosslinking of bound antibody to beads was achieved firstly by washing in 0.2M triethanolamine, pH 9.0, and resupending in 10ml of this buffer. Solid dimethyl pimelidate dihydrochloride (DMP) was added (52mg) to the bead suspension to a final concentration of 20mM, and incubated at room temperature for 45 minutes with rotational mixing. The reaction was stopped by concentrating the beads in the MPC and resuspending several times in 0.2M triethanolamine, pH 9.0. After two hours, all non-covalently coupled antibody was removed by stringent washing in 1% Triton X-100 /PBS. Beads were finally washed with PBS (3x 15min) and stored at 4°C.

ii) Antigen capture from cell lysates:

Nuclear and cytoplasmic extracts (methods 2.7.4) were pre-cleared by mixing lysates and uncoated dynabeads for one hour, with continual rotation, at 4°C. Dynabeads were removed from cell lysates using the MPC. Pre-cleared lysates were added to antibody coated beads and incubated for one hour as described above. To 100µl of lysate supernatant, approximately 10^7 beads were added. The beads were washed 4x 15minutes with 0.1%BSA/PBS, and bound protein eluted from the beads either by resuspending the washed pellet in SDS-PAGE loading buffer, then boiling for 3 minutes, and applying to the MPC, or resuspending in

100µl 0.5M acetic acid then vortexing for 15 seconds, and applying to the MPC. Eluted protein was examined by Western blotting.

2.9.2 Preparation of polyclonal antiserum against the Ad2 L1-52kd protein.

i) Peptide synthesis and coupling to carrier protein:

The peptide GDYEPPRRRARMYL corresponding to residues 47 to 59 of the Ad2 L1-52kd protein, was synthesised from the carboxyl terminus as described in methods 2.6.2, using F-moc-L-Cys(Trt)PEG-PS. The peptide was purified by reverse phase HPLC (methods 2.6.3). The peptide was coupled to Human Serum Albumin (HSA) using N-succinimidyl-3-(pyridyl dithio)-propionate (SPDP) which couples the amino groups to the cysteinyl residue of the peptide. HSA (10mg) was dissolved in 1ml of 0.1M NaCl/0.1M sodium phosphate, pH 7.5, and then 225µl of 20mM SPDP in ethanol was added dropwise over 5 minutes. The solution was stirred for a further 30 minutes at room temperature before the free SPDP was removed using the fast desalting HR10/10 column (pre-equilibrated with 0.1M NaCl/0.1M sodium phosphate, pH7.5). Fractions containing HSA were pooled and mixed with 3mg peptide (3x molar excess of peptide to activated groups). The conjugated peptide was dialysed against PBS at 4°C overnight.

ii) Immunisations and test bleeds:

Emulsion for immunisation was prepared by mixing 0.75ml of peptide conjugated HSA (0.5mg/mlPBS) with 1ml of Freunds complete adjuvant and repeatedly sonicating (15 second bursts) with intermittent cooling on ice (2min each). An emulsion was known to be stable when droplets did not disperse on water. A Dutch rabbit was injected subcutaneously with 1ml emulsion (approximately 200µg of peptide/HSA) at 4 sites on the back. A booster injection (same concentration of conjugate) was given two weeks later, with incomplete Freunds adjuvant (again subcutaneously). A test bleed (5ml) from the rabbits ears was taken 7 days after the second injection. The sera was allowed to clot for one hour, placed at 4°C overnight, then centrifuged at 10000g for 10 minutes (benchtop microfuge), and stored in 0.5ml aliquots at -20°C.

Rabbits were kept and maintained in accordance with Home Office guidelines.

iii) Assessment of antiserum (direct ELISA):

The direct ELISA method is essentially the same as the competitive ELISA protocol described in methods 2.6.4. Unconjugated peptide was incubated with microtiter plates which had been treated with 1% glutaraldehyde (or carbonate buffer, pH 9.0) at a concentration of 10μg/well (150μl/well final volume). Microtiter plates were left overnight at 4°C, then washed 3 times with PBS (200μl/well). Non-specific binding was blocked by adding 150μl of 10% (w/v) dried milk/PBS to each well, and incubating for 3 hours at 37°C (or overnight at 4°C), before washing with 3x 200μl of wash buffer (1% (w/v) dried milk; 0.5% (v/v) Tween-20; PBS). A doubling dilution series of rabbit antiserum in wash buffer was prepared in a separate plate and then 50μl from each well was transferred to the peptide coated plate, which was then incubated at 37°C for one hour. The plate was rinsed extensively with 200μl wash buffer (4x 15min) then second antibody (anti-rabbit Ig horseradish peroxidase linked whole antibody, Amersham), diluted 1/5000 in wash buffer was added to each well (100μl). After 30 minutes, plates were incubated 4 times with 200μl wash buffer (15min each), and TMB added as described in methods 2.6.4.

Another method of screening antiserum, dot-blots (methods 2.3.2), was used to screen antiserum to the Ad2 L1-52kd protein. Pre-equilibrated PVDF sheets were incubated with non conjugated peptide solutions (1mg/ml in PBS), blocked and washed as described in methods 2.3.2. A doubling dilution series of polyclonal antiserum was used.

2.9.3 Cleavage of p80 coilin and pVIII.

i) *In vitro* transcription/translation systems:

The TNT coupled reticulocyte lysate system (Promega) was used in accordance with manufacturers instructions. The plasmid pBS751.2A (coilin cDNA in pBSSK-) was kindly donated by Dr.A.I.Lamond (Dundee University). The plasmid contains a T3 TNA polymerase promoter upstream of the coilin start codon. Plasmids for the wild type Ad2 23kd protease (pT7AD23K6), ts1 mutant (p250A, originally from Carl Anderson; Brookhaven, New York), and Ad2 pVIII (in pRSETA, from Stuart Annan; University of St.Andrews) all have T7 RNA polymerase promoter sites. All DNA templates were prepared using the QIAprep spin plasmid kit (Qiagen,UK) and stored at -20°C. The TNT lysate system reagents were stored at -70°C, rapidly thawed prior to use, and kept on ice throughout. Rabbit

reticulocyte lysates were not used if thawed twice.^{35}S-methionine was obtained from Amersham, stored at -70°C and used in accordance with radiation safety guidelines.

A typical *invitro* transcription/translation reaction was as follows:

TNT rabbit reticulolysate	25µl
TNT reaction buffer	2µl
TNT RNA polymerase (T3 or T7)	1µl
Amino-acid mixture minus methionine (1mM)	1µl
^{35}S-methionine (1000ci/mmol) at 10mci/ml	4µl
RNAsin ribonuclease inhibitor (40U/ml)	1µl
DNA templates (0.5 to 1.0µg/µl)	2µl
ddH_2O	34µl

All components were mixed in a siliconised 0.5ml eppendorf tube (Sigma) then incubated at 30°C for 90 minutes. Reaction mixtures were stored at -70°C if not used immediately. Non-DNA, and control DNA reaction mixtures were included throughout.

ii) Assays with recombinant Ad2 23kd protease:

Aliquots (10µl) of purified protease (50µg/ml) were incubated with 10µl of activating peptide (1mg/ml stock in ddH_2O) and assay buffer (25µl) in siliconised Eppendorf tubes. TNT lysate reaction mixtures (10µl) of wild type and ts1 mutant 23kd protease were treated identically. Digestion reactions were started by the addition of pVIII or p80 coilin TNT lysate mixtures, and the reaction allowed to proceed for two hours at 37°C (aliquots extracted at defined time points). Reactions were stopped by transferring aliquots to -70°C. All proteins were immunoprecipitated before loading onto 15% SDS-Page.

iii) Immunoprecipitation using polyclonal antisera:

Polyclonal antibodies against pVIII and p80 coilin were covalently coupled to Protein-A sepharose (Sigma) prior to immunoprecipitations, using methods described by Harlow and Lane (1988).

Protein-A Sepharose beads (250mg) were pre-swollen in 1ml PBS for one hour. An aliquot (100µl) of beads was incubated with 5 to 10µl of polyclonal antisera, then incubated for two hours at room temperature, with gentle rotation. The mixture was centrifuged briefly

(Microcentaur microfuge), washed twice with 10ml 0.2M borate buffer, and resuspended in the same buffer. DMP was added to a final concentration of 20mM, and the mixture was gently rotated for 45 minutes at room temperature. Beads were pelleted by centrifugation and resuspended in 1ml 0.2M ethanolamine, pH 9.0, rotated gently for two hours (washing in the same buffer periodically), then finally washed with 1% Triton X-100/PBS (3x 10min) to remove unbound material. Crosslinked antibody/protein A Sepharose beads were stored at 4°C in PBS.

TNT lysate reactions (and reaction digests) were pre-cleared with protein-A Sepharose beads (10µl of original stock) for one hour at 4°C, with rotation. Protein-A Sepharose beads were separated from the pre-cleared lysates by centrifugation through micropure-22 filters (Amicon) at 1000g for 1minute (Microcentaur microfuge). Antibody coupled protein-A beads were washed (4x 15min) in blocking buffer (0.1%BSA/PBS) then added to pre-cleared lysates and incubated for one hour at 4°C with gentle rotation. Beads were washed with blocking buffer (4x 15min) and PBS alone (15min), pelleted, and resuspended in SDS-Page loading buffer. Samples were boiled for 3minutes, and examined by 15% SDS-Page. Gels were stained/destained then dried (methods 2.2.2) and taped into a Fujix BAS IP cassette, a phospo-imager screen placed on top, then left overnight. Radiolabelled proteins were detected using the Fujix BAS 1000 Phosphorimager.

3 Results and Discussion.

3.1 Monoclonal antibody production.

3.1.1 Purification of recombinant 23kd protease from *E.coli*.

Webster (1992) cloned the Ad2 23kd protease gene into pGEX-2T and transformed *E.coli* JM101 cells with the pGEX23k construct. The author showed the level of GST-23kd fusion protein expression to be very high (approximately 20mg per litre of cell culture), although the majority of fusion protein appeared as insoluble inclusion bodies, making purification by affinity chromatography very difficult. Additionally, it was noted that a significant amount of proteolytic degradation had occurred, and that *E.coli* protease's may have been responsible.

Due to the high level of fusion protein expression, this system was reassessed for the purpose of obtaining enough recombinant 23kd protease for immunising Balb/c mice (section 3.1.2). The methodology of GST-23kd expression and purification is outlined in section 2.1, although initially, instead of sarkosyl addition, Triton X-100 was added to a final concentration of 1% prior to sonication. SDS-PAGE and Western blotting analysis revealed that much of the GST-23kd fusion protein (apparent molecular weight of 47kd) remained in the insoluble fraction of bacterial lysates. However, intact fusion protein and a 28kd co-purified degradation product were isolated from the soluble fraction of bacterial lysates (figures 3.1a and b). Additionally, both the intact and degraded forms of the GST-23kd fusion protein were cleaved after a 30 min incubation with 100ng of thrombin (Sigma) in cleavage buffer (150mM NaCl; 2.5mM $CaCl_2$; 0.1% ß-mercaptoethanol; 50mM Tris-HCl, pH 8.0) at 25°C (using the methods described by Guan and Dixon (1991)).

It is not uncommon for fusion proteins to appear as insoluble inclusion bodies (reviewed by Marston, 1986; Sassenfeld, 1990) and many purification protocols make use of solubilisation and refolding steps to increase the yield of expressed proteins. Frangioni and Neel (1993) adapted the GST purification system to solubilise fusion proteins from crude bacterial lysates. These authors utilised the alkyl anionic detergent sarkosyl (N-laurylsarcosine) to solubilise GST fusion proteins, and showed that subsequent treatment with nonionic detergent (Triton X-100) enhanced solubilised fusion protein affinity to glutathione-agarose. Similarly, the GST-23kd fusion protein was solubilised with a final concentration of 1.5% sarkosyl (from a 10% stock in STE buffer) being optimum (figure 3.1c). For sarkosyl sequestration, a final

10% stock in STE buffer) being optimum (figure 3.1c). For sarkosyl sequestration, a final concentration of 4% Triton X-100 (from a 10% stock in STE buffer) was required. Sarkosyl concentrations greater than 1.5% decreased fusion protein affinity for glutathione-Sepharose, despite increasing the concentration of Triton X-100 proportionately.

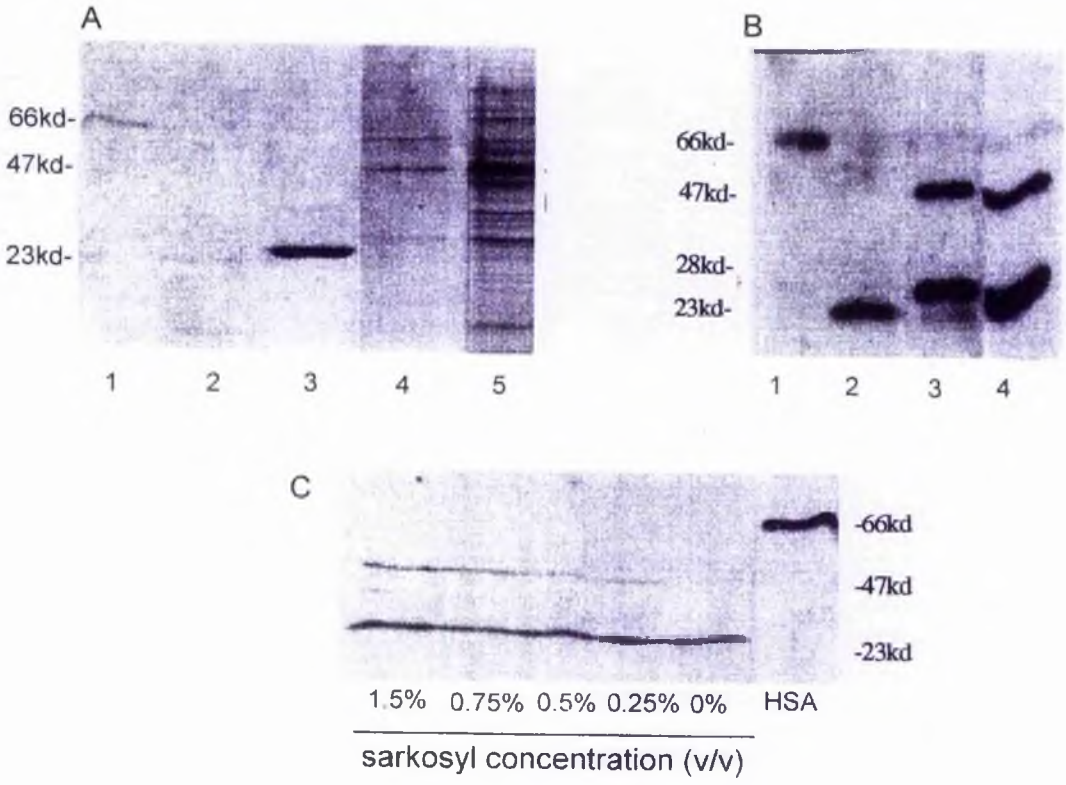

Figure 3.1: Expression of the Ad2 23kd protease as a fusion protein with GST. Samples of purified fusion protein were examined using 15% SDS-PAGE and either stained with Coomassie blue (part A) or electroblotted and probed with polyclonal antiserum R11 (raised against the N-terminal 15 amino acid residues of the Ad2 23kd protease, Webster (1992)) at a 1/5000 dilution (parts B and C). The samples were IPTG induced JM101 cells transformed with plasmids pGEX-2T (for GST protein alone) and pGEX23k (GST-23kd fusion protein). The methodology of purification is described in section 2.1. Part A: Human serum albumin (lane 1), purified recombinant 23kd protease (lane 2), purified GST protein (lane 3), purified GST-23kd (lane 4), and GST-23kd (soluble fraction from cell lysates) (lane 5). Part B: Human serum albumin (lane 1), purified recombinant 23kd protease (lane 2), Purified GST-23kd after incubation with thrombin (lane 3), and purified GST-23kd (lane 4). Part C: Western blot showing effect of increasing sarkosyl concentrations on GST-23kd purification.

Addition of Phenylmethanesulphonyl fluoride (PMSF) to a final concentration of 1mM (from a 50mM stock in methanol) did not prevent proteolytic degradation of GST-23kd fusion

degradation was also evident when GST-23kd fusion protein was expressed in *E.coli* BL21 (DE3) cells. These cells are deficient in the lon protease, and ompT outer membrane protease (Rosenberg *et al.*, 1987). Nakano *et al.* (1988) noted that *E.coli* strains such as AD202 which are deficient in ompT protease, exhibit a reduction in proteolytic degradation of fusion proteins.

The pET expression system was also assessed for large scale production of recombinant 23kd protease required for monoclonal antibody production. A four hour induction of E.coli BL21 (DE3) cells transformed with pT7AD23k6 (the Ad2 23kd protease gene cloned into pET11-C) has been shown to yield approximately 1mg of soluble 23kd protease per litre of M9 media (Webster, 1992; Grierson *et al.*, 1994). The methodology of expression and purification outlined in section 2.1 is essentially the same as that described by these authors. After a 6 hour induction, cells from 1 litre cultures were pelleted, then disrupted by addition of lysozyme and freeze/thawed (frozen for 10 minutes in liquid nitrogen then incubated at 37°C for 15 minutes). Following DNAase 1 treatment and centrifugation, clarified supernatant was applied to a DEAE-Sepharose anion exchange column, and the elution profile monitored (figure 3.2a). SDS-PAGE and Western blotting analysis revealed that flow through fractions 19 to 35 (inclusive) contained 23kd protease, which when pooled, was applied to either a CM-Sepharose or Mono-S cation exchange column. Following elution (section 2.7.1ii), recombinant protein was detected by SDS-PAGE and/or Western blotting (figures 3.2b and c).

Three proteins co-purified with the 23kd protease have apparent molecular weights of 35kd, 18kd, and 14kd. The 35kd *E.coli* protein was partially removed when pooled DEAE-Sepharose flow through was applied to a ssDNA-Sepharose column, eluting with 200mM NaCl (figure 3.2d).

However, a significant reduction in overall yield of 23kd protease was evident when using the ssDNA-Sepharose column. In contrast, the Mono-S column has a binding capacity of 20mg per ml of matrix. This served as a useful concentration step, with an estimated 3.75mg of recombinant protein (derived from 5x one litre cultures) being eluted into a final volume of 5ml (figure 3.3). This in turn was concentrated further by lyophilisation. Because of possible harmful effects of Trisma base and high salt concentration on Balb/c mice, the freeze-dried

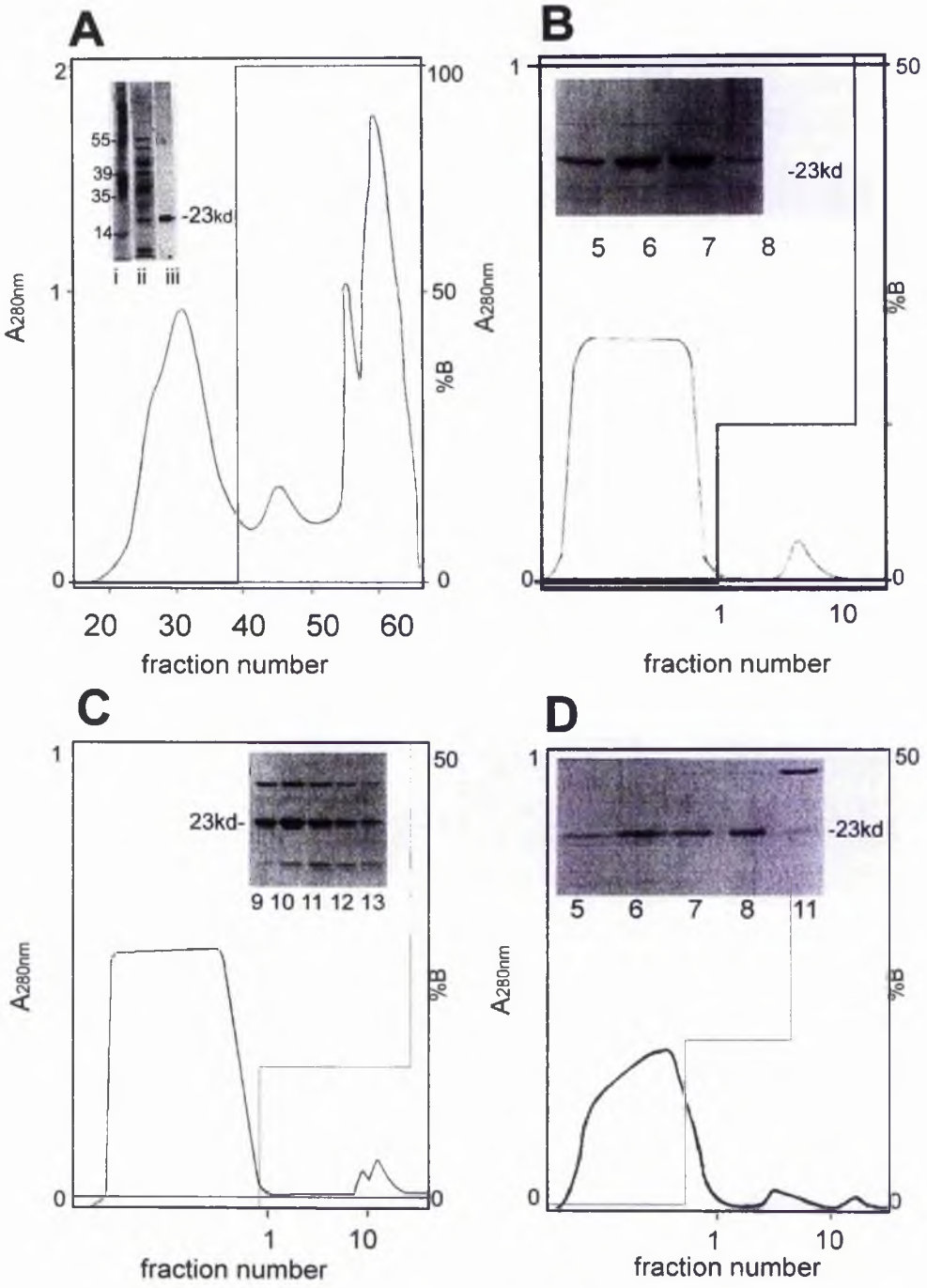

Figure 3.2: Purification of expressed 23kd protease from E.coli lysates.

23kd protease was purified from IPTG induced BL21 (DE3) cells transformed with the plasmid pT7AD23k6 using the methods described in section 2.1.The elution profile from the DEAE-Sepharose column is shown in part A with a Coomassie blue stained 15% Polyacrylamide gel (ii) and Western blot (iii) of pooled fractions (19 to 35 inclusive) superimposed with prestained Mr markers (i). The pooled eluate was injected into either the CM-Sepharose (B), Mono-S (C), or ssDNA-Sepharose (D) columns. Coomassie blue stained 15% Polyacrylamide gels showing eluted fractions containing 23kd protease are included with respective elution profiles. Absorbance at 280nm (---), and percentage of buffer B (--).

powder was resuspended in 1ml of 0.1M ammonium bicarbonate buffer and applied to a pre-equilibrated (same buffer) fast-desalting HR10/10 column (Pharmacia). Eluted fractions were pooled then lyophilised. After the addition of 1ml PBS, it was evident that the majority of recombinant 23kd protease was rendered insoluble through desalting/freeze-drying. This final concentration step was replaced with Amicon ultrafiltration (section 2.1.8), with Mono-S eluate gradually concentrated into 1ml PBS.

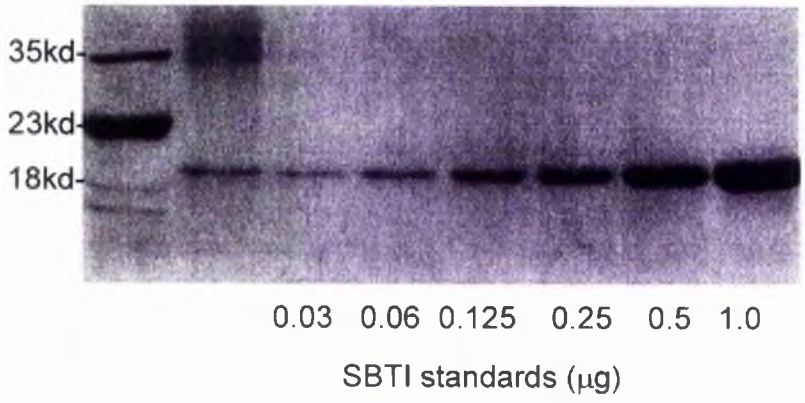

figure 3.3: Final yield of purified 23kd protease. Coomassie blue stained 15% Polyacrylamide gel of SBTI standards and a 10μl sample of pooled Mono-S fractions containing 23kd protease. Prestained molecular weight markers were also included.

3.1.2 Immunisations and test bleeds.

Five mice received an estimated 50μg of soluble 23kd protease which was known to be enzymatically active (figure 3.4a), whilst another five mice received a mixture of 35μg soluble and 15μg insoluble 23kd protease throughout the immunisation regime. Western blot analysis of test bleeds against the original source of immunogen revealed that all mice raised an immune response against the 23kd protease and the co-purified 35kd *E.coli* protein (figure 3.4b). Antibodies specific for the 23kd protease were detected by immunoblotting against recombinant 23kd protease purified from insect cells (figure 3.5a and b).

This source of antigen was used to screen test bleeds prior to cell fusion (figure 3.5c). Mice S2, S3 and S5 (immunised with soluble antigen only), and M2, M3 and M4 (immunised with the soluble/insoluble mix) were the most responsive to the immunisation regime and were given an intravenous boost of soluble antigen (without adjuvant) three days prior to cell

fusion. Interestingly, M1 and M5 appeared to have been the least responsive to the immunisation regime. This was unexpected as aggregated antigens (or antigens immobilised to a particulate matrix) have been shown to induce prolonged and more effective immune response if incorporated within an immunisation schedule (Harlow and Lane, 1988).

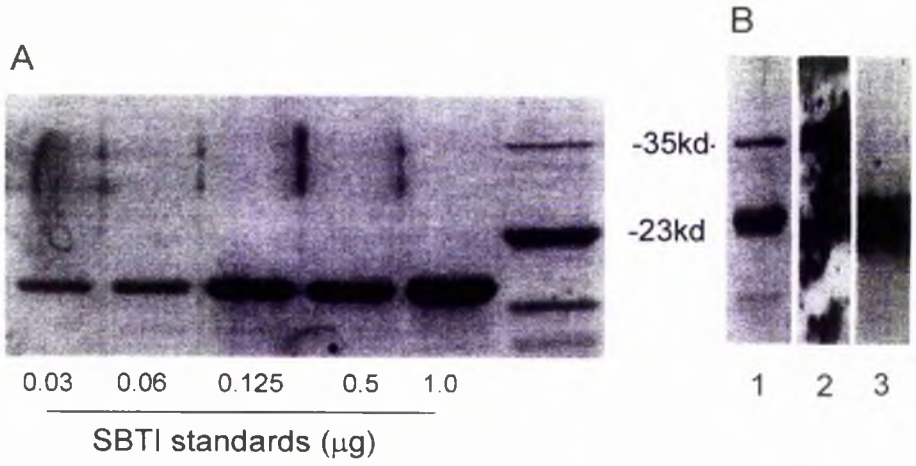

Figure 3.4: Recombinant 23kd protease used for immunisations. Part A: 15% Polyacrylamide gel stained with Coomassie blue showing SBTI standards and a 10μl sample of 23kd protease which was known to be enzymatically active. Stock solutions of 23kd protease were prepared fresh prior to each immunisation and analysed for enzyme activity. Part B: Lane 1: Purified 23kd protease (Coomassie blue stained 15% SDS-PAGE). Lanes 2 and 3: Electroblotted purified 23kd protease probed with a test bleed from mouse S2 and antiserum R11 respectively.

3.1.3 Screening hybridoma cell lines for antibody production.

Spleens were removed from mice M2 and S2 and splenocytes fused with myeloma SP2/0 cells. The cell mixture was aliquoted into 96 well tissue culture plates as an undiluted stock (plates A to F) or diluted 1/5 in selective media (plates G to T). Excess cells from the diluted stock were aliquoted into two 96 well plates containing a recommended (Dr.P.W.Szawlowski, pers.comm.) final concentration of interleukin-2 (Sigma), then prefixed IL1 and IL2 for identification. When cells reached approximately 70% confluence (1 to 2 weeks), 50μl of supernatant from appropriate wells was transferred into another 96 well plate and used for screening antibodies specific to the 23kd protease (section 2.3.2).

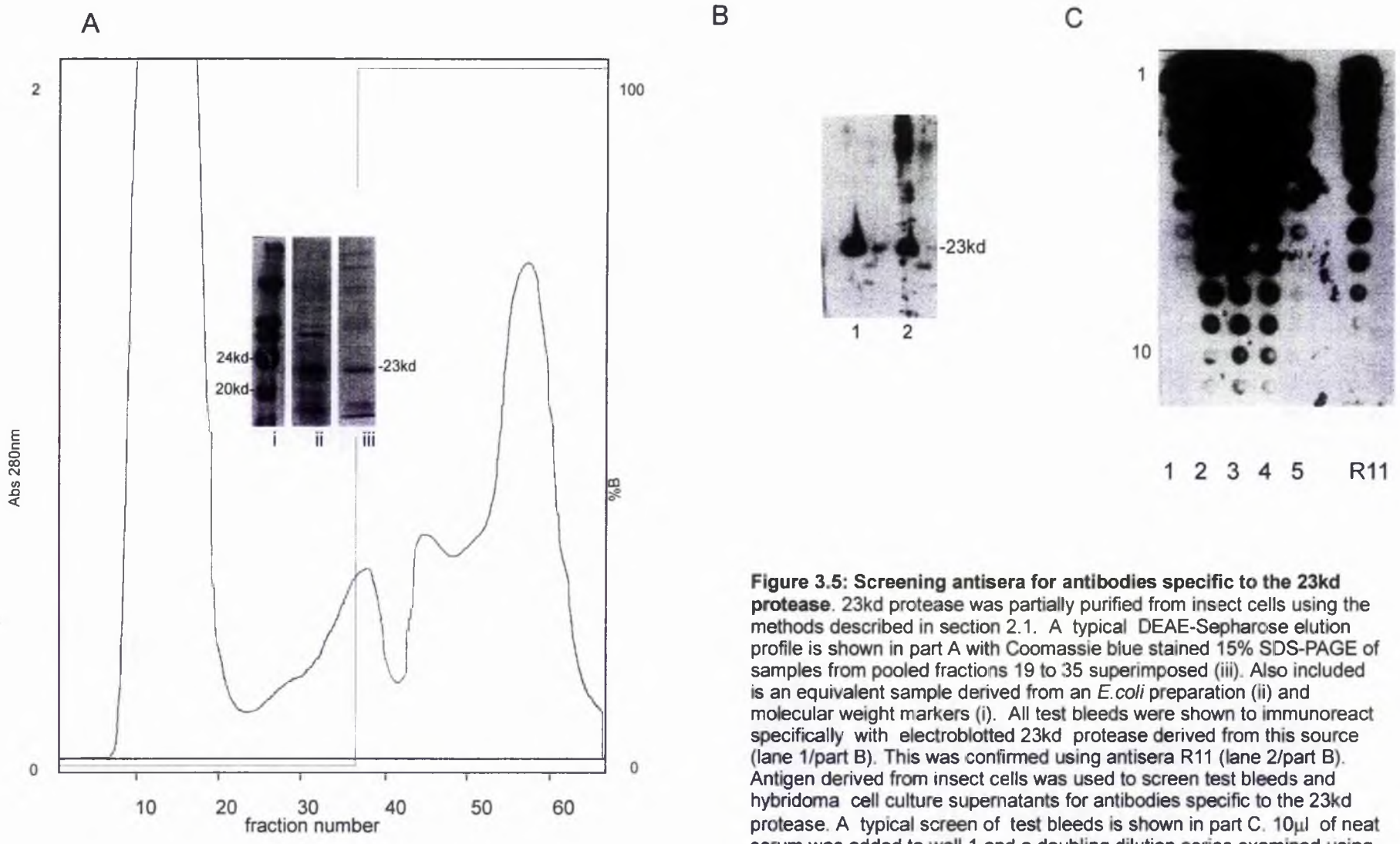

Figure 3.5: Screening antisera for antibodies specific to the 23kd protease. 23kd protease was partially purified from insect cells using the methods described in section 2.1. A typical DEAE-Sepharose elution profile is shown in part A with Coomassie blue stained 15% SDS-PAGE of samples from pooled fractions 19 to 35 superimposed (iii). Also included is an equivalent sample derived from an *E.coli* preparation (ii) and molecular weight markers (i). All test bleeds were shown to immunoreact specifically with electroblotted 23kd protease derived from this source (lane 1/part B). This was confirmed using antisera R11 (lane 2/part B). Antigen derived from insect cells was used to screen test bleeds and hybridoma cell culture supernatants for antibodies specific to the 23kd protease. A typical screen of test bleeds is shown in part C. 10µl of neat serum was added to well 1 and a doubling dilution series examined using the methods described in section 2.3.2. Similar results were observed with mice immunised with the soluble/insoluble mixture of antigen (results not shown).

Absorbance at 280nm (---). Perecentage buffer B (---).

A total of 80 hybridoma colonies from plates A to F (figure 3.6a) were identified as being positive for antibody production, and an aliqout of cells from each colony was transferred to a single well in a 24 well tissue culture plate. These hybridoma colonies were re-screened in the case that false positives had originally been detected. Although splenocytes do not grow in standard tissue culture medium, they do not die immediately, and will continue to secrete antibodies which may be detected in early screens. After confirmation that hybridoma colonies were positive for antibody production, aliquots of cells from separate colonies were pooled and stored (section 2.3.5). None of the hybridoma cell lines from plates A to F were used for single cell cloning.

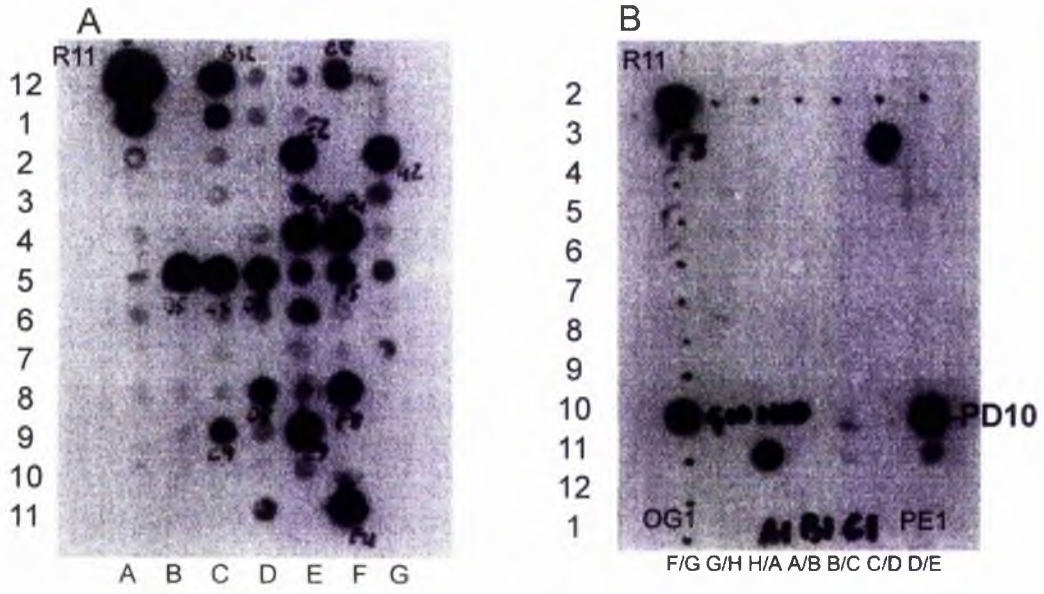

Figure 3.6: Screening hybridoma cell culture supernatants. Cell culture supernatants were screened for antibodies using the methods described in section 2.3.2. Antiserum R11 was added to the top left well in the Teraski plate for all screens (shown in parts A and B) to ensure correct identification of positive immunoreactions. Cell culture supernatants (10µl) from colonies in plate A were added to appropriate wells and are shown in part A. Colonies from plates O and P are shown in part B, with colony PD10 highlighted. Exposure times were approximately 30 seconds.

A further 58 hybridoma colonies from plates G to T and 6 colonies each from IL1 and IL2 were detected (figure 3.6b). These colonies were also expanded into 24 well plates, re-screened, and stored. From the 70 colonies (table 3.1), 33 were single cell cloned after re-screening in batches of 11 staggered over an interval of 3 days. Four days after subcloning, individual wells were marked and screened where it was clear that groups of cells had arisen

from an individual cell. This procedure was repeated for colonies screened positive. It was evident that many hybridoma cell lines could not tolerate single cell cloning, for instance, no subclones were isolated from plates I and L. However, many single cell clones were isolated from plates O, J, and IL2 (table 3.1).

3.1.4 Characterisation of monoclonal antibodies.

i) Isotyping and Immunoblotting:

Using the Serotec isotyping kit, either IgM or IgG1 antibody variants were detected from cell culture supernatants of appropriate hybridoma subclones (table 3.1). IgM's are the major component of the primary immune response and are generally considered to be unsuitable for immunocytochemical studies due to the lower affinity for antigens compared to IgG's (Griffiths, 1993). It is noteworthy that in this study, monoclonal antibodies of the IgM class failed to recognise recombinant 23kd protease following electroblotting, and therefore, were not characterised further.

In contrast, monoclonal antibodies subclassed as IgG1 recognised electroblotted recombinant 23kd protease, with the notable exceptions being antibodies derived from RG2, MD7, and JB4 hybridoma cell lines (figure 3.7/table 3.1). Cell culture supernatants from these hybridoma cell lines also exhibited poor immunoreactivity with 4% (v/v) formaldehyde fixed (figure 3.8), or 4% (v/v) paraformaldehyde fixed Ad2 infected HeLa cells in immunofluorescence microscopy studies. Additionally, no immunoreactions were detected when cell culture supernatants were screened with GST-(Ad4)23kd fusion protein bound to nitrocellulose membranes (purified fusion protein (50µg/ml) was kindly donated by Dr Ailsa Webster, University of St.Andrews). These results suggested that monoclonal antibodies derived from RG2, MD7, and JB4 hybridoma cell lines were specific to conformation dependant epitopes. Monoclonal antibodies isolated from subclones of OA10, OF10, GB4, IL2G5, PD10, IL2E4 and OC11 were amenable with electroblotting studies (table 3.1/figure 3.7) and exhibited distinctive punctate immunofluorescent staining patterns with Ad2 infected HeLa cells (figure 3.8).

Stock plate	Positive wells	Subcloned colonies	Isotype	Western blotting
IL1	A1 **C7** D1 **E2** F5 **G8**	none	n/d	n/d
IL2	**A3** A4 A7 **E4** G1 **G5**	**E4-** (b3 e8 d6 h6 g2 d2 g6 c4 f3) **G5-**(h9 c2 g2 e11 c12 b6 f3 e4) **A3-**(a6)	IgG1 IgG1 IgM	+ + -
G	**A9** A10 **B4** **C5** G4 **G5** G6	**B4-**(f3 g7 b11 g4)	IgG1	+
H	A2 **A5** A6 B2 **B3** B9 **C9**	**B3-**c3	IgM	-
I	**A3** A6 C6 C10	none	n/d	n/d
J	B3 **B4** **D3** E6 F4 H8	**B4-**(f6 h4 e8 b8 b10 e10 g8 c9 c6) **D3-**(e4)	IgG IgM	- -
K	**C1** D3 **F10** **H5**	**H5-**(b3 f3 e4 f4)	IgM	-
L	G11 **H2**	none	n/d	n/d
M	**B5** **D7** D11 G4	**D7-**(e10 d10 h6 b12)	IgG1	-
N	D6 **E10**	none	n/d	n/d
O	A6 A9 **A10** **C11** E1 **F10** H11	**A10-**(a4 h3 e11 f11 b2 b5 f12 e1 h10 b3) **F10-**(c5) **C11-**(b11 d8 d11 g11)	All IgG1	All +
P	C3 **D10** G10 **H10**	**D10-**(g5 c4)	IgG1	+
Q	C4 **C7** D7 E2	**C7-**(e5 f10)	IgM	-
R	A5 B3 **G2**	**G2-**(h11)	IgG1	-
S	A8 **C9** E6	none	n/d	n/d
T	**F2**	**F2-**(f8 f10)	IgM	-

Table 3.1: Derivation and partial characterisation of monoclonal antibody secreting cell lines. Hybridoma colonies within stock plates (after cell fusion) which were screened positive for antibody production were re-plated and re-screened then single cell cloned as described in methods section 2.3.4. Colonies that were subcloned are highlighted in bold. Single cell cloned colonies determined to be positive for antibody production are listed in brackets. Antibodies were not isotyped or characterised further (n/d) in cases where no subclones were isolated from stock hybridoma colonies.

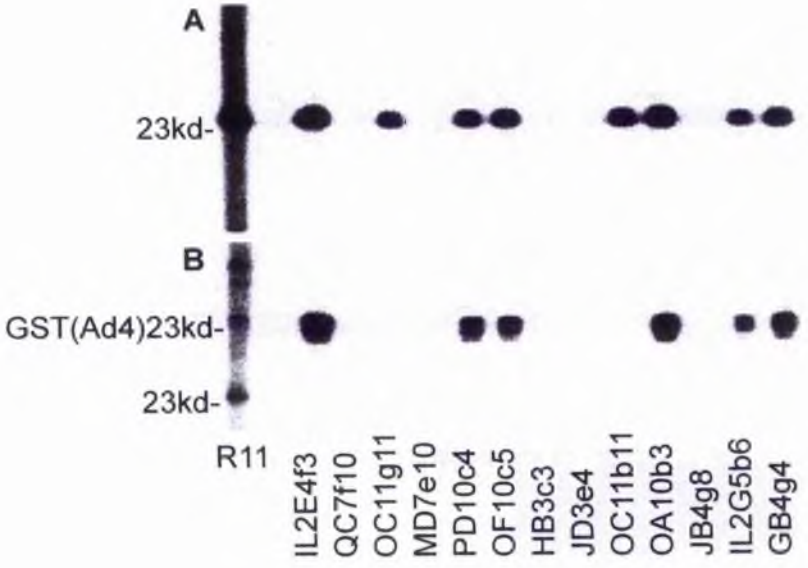

Figure 3.7: Monoclonal antibodies that recognise electroblotted 23kd protease. Recombinant Ad2 23kd protease (part A) and GST(Ad4)23kd fusion protein (part B) were electroblotted (15% SDS-PAGE) and probed with specific antibodies using the methods described in section 2.4.3. Prestained molecular weight markers and 23kd protease were added in lane 1 and probed with antiserum R11. Antibody titres were determined for individual cell culture supernatants prior to immunoblotting. Exposure time of 30 seconds.

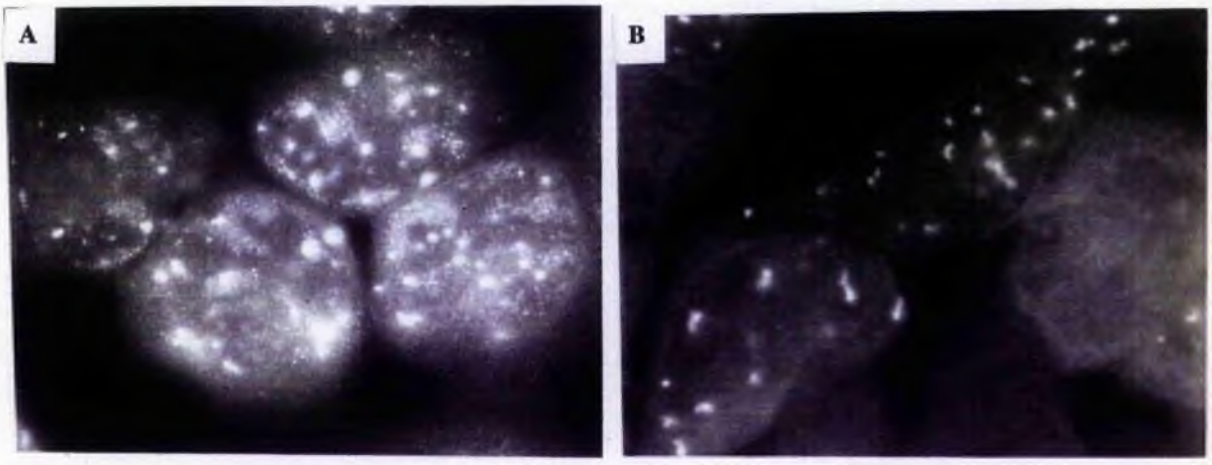

Figure 3.8: Immunofluorescent staining of Ad2 infected HeLa cells. A typical fluorescent cell staining pattern using antibody OC11b11 (part A) shows a diffuse nucleoplasmic staining in addition to the speckled pattern also present in cells stained with antibodies OA10b3 (part B), GB4g4, PD10c4 and OF10c5. Cells were fixed at 28 h.p.i and processed using the methods described in section 2.7. FITC conjugated second antibody was preabsorbed onto permeabilised non-infected cells prior to fluorescent staining at recommended dilution's. None of the monoclonal antibodies showed any fluorescent staining in non-infected cells. Automatic exposure times were typically of between 60 to 120 seconds.

ii) Specificity of Mabs OC11b11 and OA10b3:

The specificity of monoclonal antibodies derived from OC11 subclones differed from the others in several respects. For instance, OC11b11 did not recognise denatured or nitrocellulose bound GST-(Ad4)23kd fusion protein, but did immunoreact with denatured Ad2 23kd protease (figure 3.7). Of particular interest was the diffuse immunofluorescent staining of infected HeLa cell nuclei which was additional to the punctate patterns also observed with monoclonal antibodies OA10b3 and GB4g4. To determine whether cross-reactions with other viral antigens were being detected, extracts of infected HeLa cells were immunoprecipitated (figure 3.9) using OC11b11 and OA10b3 cell culture supernatants with monoclonal antibodies cross-linked to Dynabeads (section 2.9.1). All monoclonal antibodies specifically recognised 23kd protease with no cross reactions being detected.

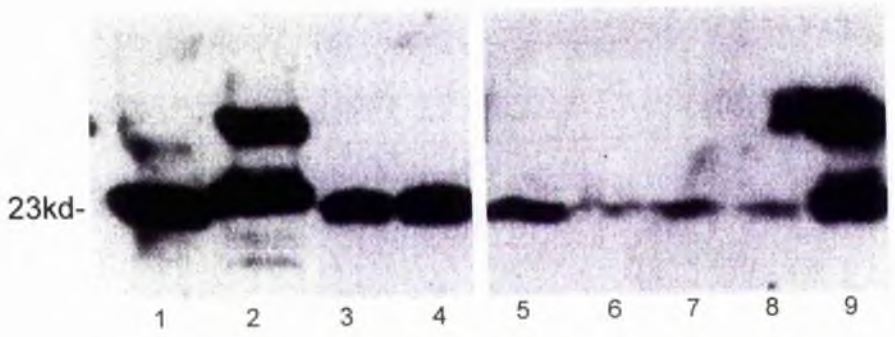

Figure 3.9: Immunoprecipitation of Ad2 infected cell extracts. Nuclear and cytoplasmic cell extracts were prepared from infected HeLa cells (grown as a monolayer) using the methods described in section 2.7.4i. Antibodies OA10b3 and OC11b11 were coupled to Dynabeads using the method recommended by the manufacturer (section 2.9.1i). Lysates were precleared using Dynabeads prior to immunoprecipitation and electroblotting (15% SDS-PAGE). 23kd protease (lane 1), OA10b3 (lanes 2) and prestained molecular weight markers were used as standards. OA10b3 and OC11b11 immune-complexed with purified recombinant 23kd protease (lanes 3 and 4 respectively), and specifically recognised 23kd protease from nuclear extracts (lanes 5 and 6 respectively), and cytoplasmic extracts (lanes 7 and 8 respectively) of infected HeLa cells (28 h.p.i). An immunoprecipitation of purified recombinant 23kd protease using non-coupled OA10b3 is shown in lane 9.

It is likely that the immunofluorescent staining patterns observed with antibodies OA10b3 and OC11b11 are due to the availability of different epitopes for immunoreaction within infected

cells. This might occur through physical loss of epitopes (which can result from extraction of molecules and structures), or that epitopes recognised by antibodies OA10b3 and GB4g4 are non-immunoreactive within particular nuclear subcompartments following chemical fixation (possibly due to steric hindrance of epitopes by fixative-induced cross-links). Similarly, chemical alteration of epitopes by direct reactions with fixatives may also account for fixative-induced denaturation effects that render conformation dependant epitopes non-immunoreactive.

iii) Affect of antibody binding on proteolytic activity:

Observed differences in immunofluorescent staining may also be a direct consequence of the physical nature of the antigen in lytically infected cells. For instance, the activity of recombinant 23kd protease *in vitro* has been shown to be dependent on the addition of activating peptide, and it has been proposed that activation *in vivo* is required for production of infectious particles. Therefore, specific protein-protein interactions may affect epitope binding within post-fixed infected HeLa cells. In determining whether monoclonal antibodies could distinguish between the activated and non-activated forms of the 23kd protease, antibodies OA10b3, GB4g4 and OC11b11 were used to immunoprecipitate both forms of the recombinant enzyme . It was evident that all three antibodies recognised both forms of the enzyme *in vitro* (results not shown), which suggested that the antibodies might recognise the non-activated and activated viral protease *in vivo*.

The same antibody solutions were used to determine whether antibody binding to recombinant 23kd protease affected enzyme activity *in vitro*. Cell culture supernatants (protein free media) from $75cm^2$ flats were filtered, then concentrated into 23kd protease elution buffer (150mM NaCl/50mM Tris-HCl, pH 8.0) by ultrafiltration to a final volume of 0.5ml. The approximate concentrations of antibody and antigen were determined by SDS-PAGE (figure 3.10). Appropriate volumes of both solutions were mixed briefly, then incubated on ice for one hour before addition of pVI-ct and assessment of enzymatic activity. Similarly, assays were performed one hour after antibody solutions had been added to pre-activated 23kd protease.

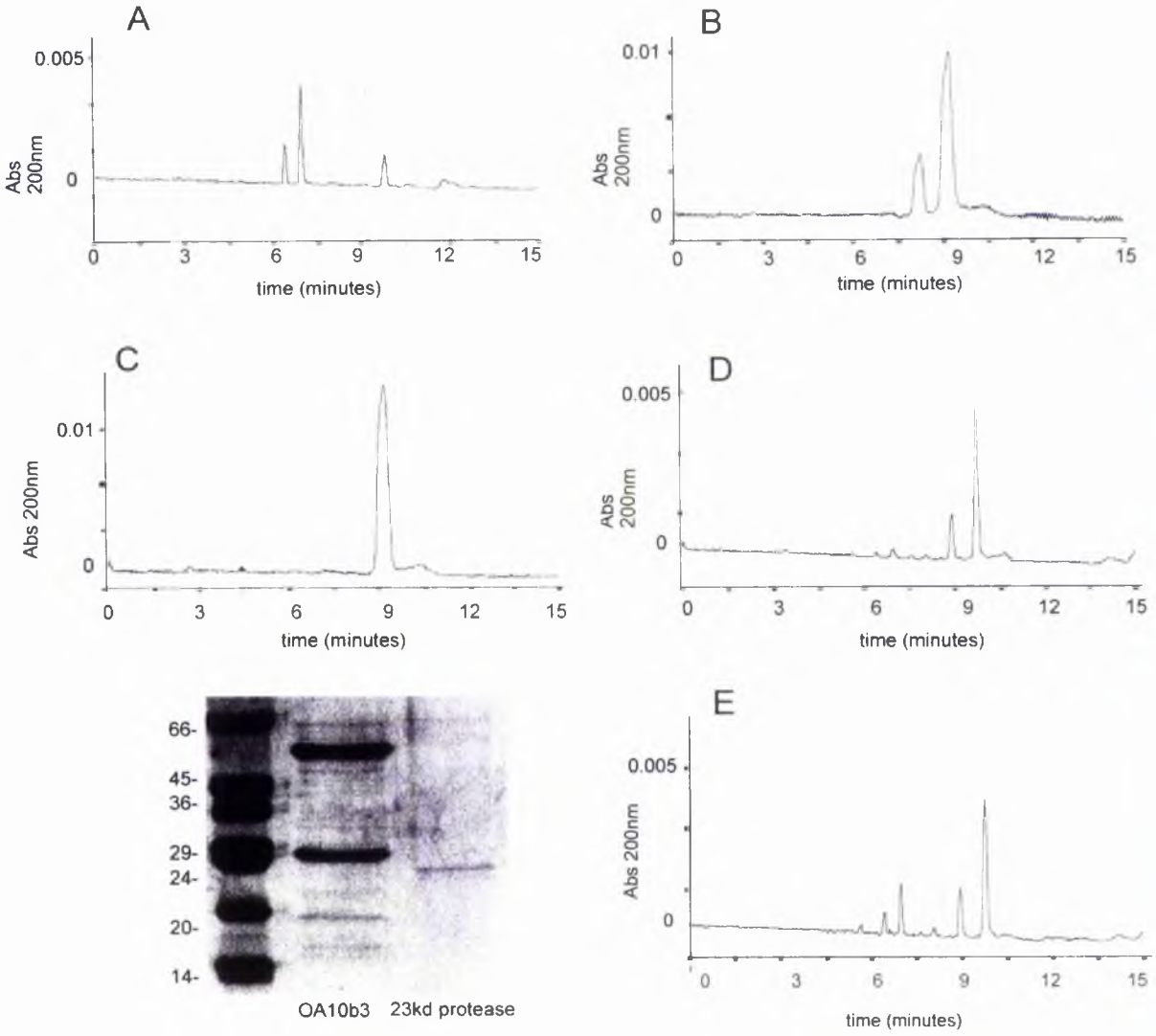

Figure 3.10: Effect of antibody binding on enzyme activity. Approximate concentrations of antibody and 23kd protease were estimated by 15% SDS-PAGE. Assays were performed as described in methods section 2.2.5. 10µl of 23kd protease was incubated with 10µl of antibody solution (in 23kd elution buffer/methods section 2.3.8) and kept on ice for one hour before addition of 25µl assay buffer and pVI-ct to a final concentration of 0.2mM. Substrate peptide LSGAGFSW was added (5µl from a stock of 2mg/ml) after 5 minutes and the assay allowed to proceed for one hour at 37°C. Reactions were stopped by addition of 10µl 0.1% TFA. Part A: A capillary electrophoresis trace showing peaks corresponding to LSGAGFSW (approximately 9 minutes (also shown in part C)), LSGA and GFSW (between 6 and 7.5 minutes). Peaks corresponding to cleavage products were absent when OA10b3 was added to non-activated 23kd protease (part D), however an additional peak was evident at approximately 8 minutes. This peak was also evident when antibody solution was incubated with the assay mixture in the absence of 23kd protease (part B). Peaks corresponding to cleavage products were evident when OA10b3 was added to activated enzyme as shown in part E (antibody solution added after assay buffer/pVI-ct).

Capillary electrophoresis traces (measured at 200nm) indicated that addition of OA10b3 to non-activated 23kd protease resulted in the inhibition of enzymatic activity (figure 3.10). A minimal level of activity was consistently observed when the same antibody solution was added to pre-activated enzyme. Initially it was thought possible that the epitope for OA10b3 might be located at the site of activation, however, epitope mapping results later indicated that inhibition through antibody binding was likely due to steric interference of pVI-ct binding (section 3.1.5iii). None of the other antibodies tested (OC11b11, GB4g4, JB4b8, PD10c4, IL2G5b6 and IL2E4f3) appeared to have any effect on enzyme activity (results not shown).
It is noteworthy that cell culture supernatants contained cellular aminopeptidases that partially digested the LSGAGFSW peptide substrate. This non-specific digestion was eliminated if acetylated synthetic substrate Ac-LRGAGRSR was added in place of LSGAGFSW (results not shown). Anti-pVII monoclonal antibody supernatants (protein free media) exhibited similar aminopeptidase activity when the non-acetylated substrate was used. Non-specific digestion was also eliminated if monoclonal antibodies were purified using a Q-Sepharose column, which also acted as a useful concentration step, or using a DEAE-Sepharose ion exchange column (figure 3.11 on page 112).

3.1.5 Epitope Mapping.

i) Chemical cleavage and limited proteolysis:

In acidic conditions, cyanogen bromide specifically cleaves methionine containing proteins and peptides at the carboxylic side of methionine in the amino acid chain (Carrey, 1990). CNBr reacts with the sulphur-containing side chain and generates a mix of homoserine, homoserine lactone, and methylcyanate. The Ad2 23kd protease has six Met-X bonds (including the N- and C-terminal methionines), which if cleaved, would generate 6 peptides of 55, 72, 6, 13, 10 and 47 amino acid residues in length (figure 3.12). Synthetic peptides (15 residues in length) corresponding to sequences within the 55 residue (N-terminal) and 47 residue (C-terminal) cleavage products have previously been used to generate polyclonal antiserum against the 23kd protease (Webster, 1992).

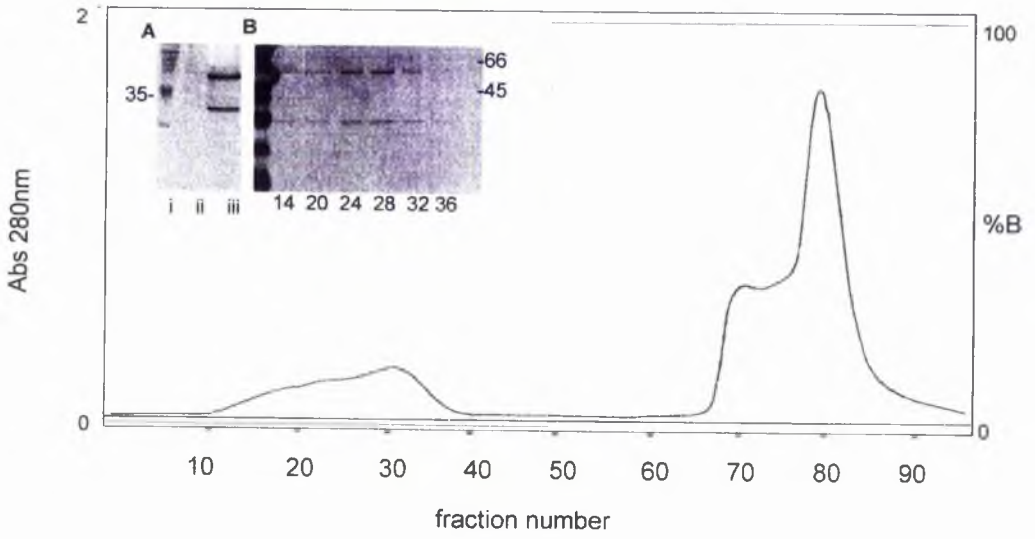

Figure 3.11: Monoclonal antibody purification. OA10b3 cell culture supernatants (500ml/protein free media) were purified using a pre-equilibrated (50mM Tris-HCl, pH 8.8) Mono-Q column as described in section 2.3.8. A sample of eluted antibody is shown in gel A (lane iii) with a sample of the original supernatant (ii) and prestained molecular weight markers (i) included for comparison. Concentrated OA10b3 cell culture supernatants (5ml total volume) were also injected into a pre-equilibrated DEAE-Sepharose column. A typical elution profile is shown with a Coomassie blue stained 15% Polyacrylamide gel (gel B) containing flow through fractions 14 to 36 superimposed. At pH 8.0, some antibody was retained by the matrix and eluted as described in section 2.3.8. Abs 280nm (---). % of buffer B (---).

MGSSEQELKA IVKDLGCGPY FLGTYDKRFP GFVSPHKLAC
AIVNTAG**RET** GGVHWMAFAW NPRSKTCYLF EPFGFSDQRL
KQVYQFEYES LLRRSAIASS PDRCITLEKS TQSVQGPNSA
ACGLFCCMFL HAFANWPQTP MDHNPTMNLI TGVPNSMLNS
PQVQPTLRRN QEQLYSFLER HSPYFRSHSA QIRSATSFCH
LKNM

Figure 3.12: CNBr cleavage sites within the Ad2 23kd protease. Potential CNBr cleavage sites are indicated by arrows. Regions of the 23kd protease which are recognised by specific polyclonal antiserum (Webster, 1992) are highlighted in bold.

Recombinant 23kd protease (estimated final concentration of 0.8mg/ml) was purified from a one litre culture of *E.coli* BL21 (DE3) cells using DEAE-Sepharose and Mono-S columns, then freeze dried over a period of 24 hours. The lyophilised powder was resuspended in 0.5ml of 0.1M ammonium bicarbonate buffer (pH 8.0), then injected into a pre-equilibrated (same buffer) fast-desalting HR 10/10 column, with eluted protein again freeze-dried for a further 24 hours. Resuspended protein was subjected to chemical cleavage (section 2.4.2), and samples of the reaction mix, and original protein stock, examined by SDS-PAGE (figure 3.13a).

It was clear from the Coomassie blue stained gel that chemical cleavage of the 23kd protease, and co-purified *E.coli* proteins, resulted in the generation of numerous low molecular weight products, the most prominent being a polypeptide of approximately 16kd. However, the multiscreen immunoblot (figure 3.13b) indicated that a fraction of the enzyme remained uncleaved. Partial hydrolysis may have occurred because the desalting/freeze-drying step rendered a proportion of the purified protein insoluble, thereby burying potential cleavage sites within a hydrophobic environment. Additionally, some reactions do not go to completion because of competition from nearby side chains, or because residual folded structures in the protein reduce access of CNBr to susceptible bonds. Nevertheless, the panel of monoclonal antibodies used immunoreacted with 3 major cleavage products, with antibody OA10b3 immunoreacting with 2 major cleavage products, and OC11b11 exclusively recognising the third, lower molecular weight peptide.

Interestingly, none of the polyclonal antisera immunoreacted with the 3 major reaction products, which suggests that none of the monoclonal antibodies recognised epitopes within either the 55 or 47 residue peptides, which contain epitopes for polyclonal antiserum R11 and R12/R13 respectively. This suggested that epitopes for OA10b3 and OC11b11 could be located within region M56 to M157 of the enzyme. To determine whether the epitopes were within this region, aliquots of the reaction mix, and original protein stock, were electroblotted for protein sequencing (section 2.4.4). After comparing the immunoblot (figure 3.13c), and amido black stained blot (not shown), it was evident that neither of the 2 major cleavage products recognised by OA10b3 corresponded to the 16kd polypeptide (which was not sequenced). Instead, both co-migrated with several lower molecular weight peptides and

therefore could not be accurately identified. Similarly, the peptide recognised by OC11b11 was not identified, and therefore not isolated for sequencing.

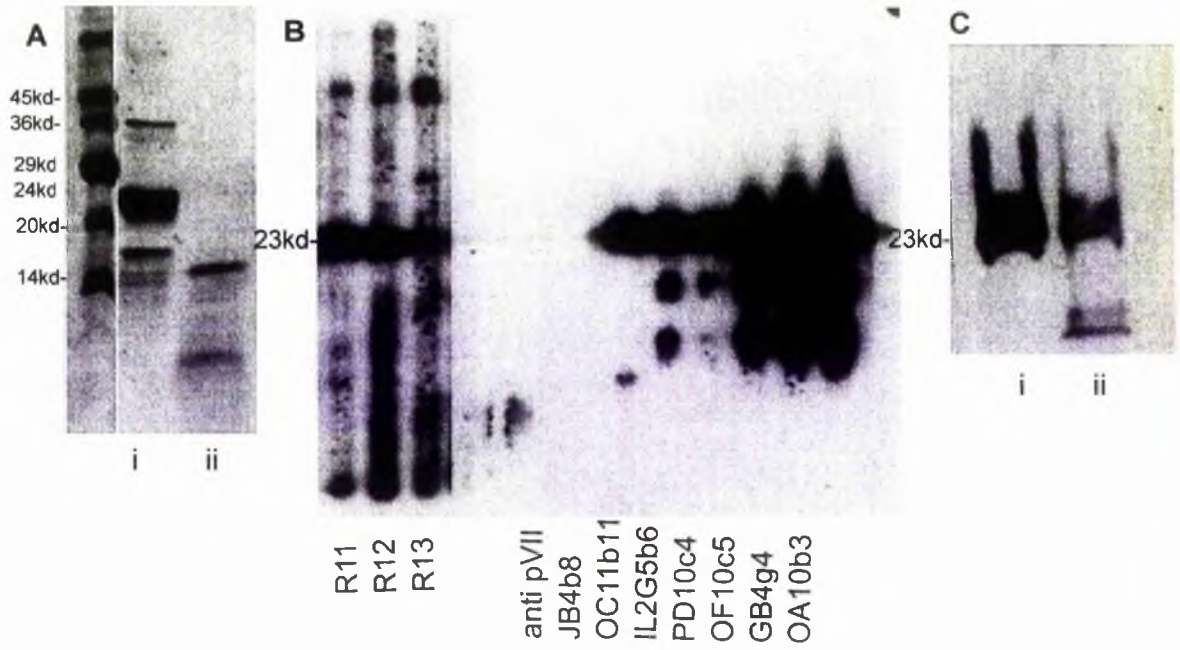

Figure 3.13: CNBr cleavage of the 23kd protease. Part A: 10µl samples of the original protein stock solution (lane i) and reaction mix (lane ii) were electrophoresed (20% SDS-PAGE) with molecular weight standards then stained with Coomassie blue. CNBr cleavage reactions were performed as described in section 2.4.2. Part B: a 100µl sample from the same reaction mix was electrophoresed (20% SDS-PAGE), then electroblotted and probed (within a Protean II multiscreen apparatus/section 2.4.3) using a panel of monoclonal antibodies. Polyclonal antisera (see text) and anti-pVII monoclonal antibody (kindly provided by Professor W.C.Russell) were included as controls. Part C: Two 20µl samples of the original 23kd protease stock solution (lane i) and cleavage reaction mix (lane ii) were electrophoresed simultaneously (12.5% SDS-PAGE) and electroblotted for sequencing (section 2.4.4). The electroblot was divided and one part probed with antibody OA10b3 and the other amido black stained (not shown).

Limited proteolysis is much less predictable than chemical cleavage and is dependant on the experimental conditions used. In the native conformation, most proteins are almost entirely resistant to attack by low concentrations of protease's, with proteolysis occurring only at the most exposed, or disordered regions of the polypeptide backbone (Carrey, 1990). In this study, a panel of enzymes with contrasting specifities were chosen that included endoproteinase Glu-C (cleaves at Glu-Y and Asp-Y), and the pancreatic enzymes, trypsin

(Arg-Y and Lys-Y), and α-chymotrypsin (Phe-Y, Trp-Y and Tyr-Y). The enzymes were diluted from stock solutions with 23kd protease elution buffer (all enzymes exhibiting optimum activity at pH 7.5 to 8.5) to give a ratio of enzyme to substrate (w/w) of 1/1000 (section 2.4.1). Cleavage reactions were maintained at 37°C for 1 hour, then stopped by addition of SDS-PAGE loading buffer. After boiling for 5 minutes, the reaction mix was electroblotted as described in section 2.4.3. The multiscreen immunoblots of α-chymotrypsin, trypsin, and endoproteinase Glu-C cleavage reactions are shown in figures 3.14a, b and c respectively.

Although the immunoblots do not provide any information regarding the location of particular epitopes, they do indicate which epitopes are likely to be shared by antibodies of interest. For instance, following α-chymotrypsin cleavage, all of the monoclonal antibodies (with the exception of OC11b11) recognised the same 5 cleavage products, 2 of which, were also recognised by polyclonal antiserum R11 (lane 1in figure 3.14a). However, following trypsin cleavage of the 23kd protease, GB4g4 and OF10c5 recognised an additional peptide not detected by OA10b3. These results indicated that epitopes for GB4g4, OF10c5 and OA10b3 may be located within the same region of the 23kd protease, possibly adjacent to each other, yet the epitope for OA10b3 may have been cleaved directly, or elements of secondary structure required for antibody binding may have been removed. It was thought that low antibody titres were likely to be responsible for poor immunoreactions exhibited by antibodies PD10c4 and IL2G5b6.

Despite using low concentrations of all three enzymes, proteolysis resulted in the generation of numerous cleavage products which hindered the accurate identification of peptides of interest. For instance, although 2 major cleavage products of the 23kd protease were recognised by OA10b3 after endoproteinase Glu-C proteolysis (figure 3.14c), an examination of the reaction mix by SDS-PAGE (results not shown), indicated that these peptides could not be isolated for sequencing using the methods outlined in section 2.4.4.

In order to isolate these peptides, reaction mixtures (50µl) were diluted with 350µl of 0.1% TFA/water, then filtered (0.2µm Acrodisc) and cleavage products seperated by HPLC purification (section 2.6.3). The elution profile of an α-chymotrypsin and 23kd protease (1/1000) reaction mixture is shown in figure 3.16. Collected fractions were vacuum dried (Howe Gyrovap GT) and contents resuspended in 50µl PBS. The fractions were incubated

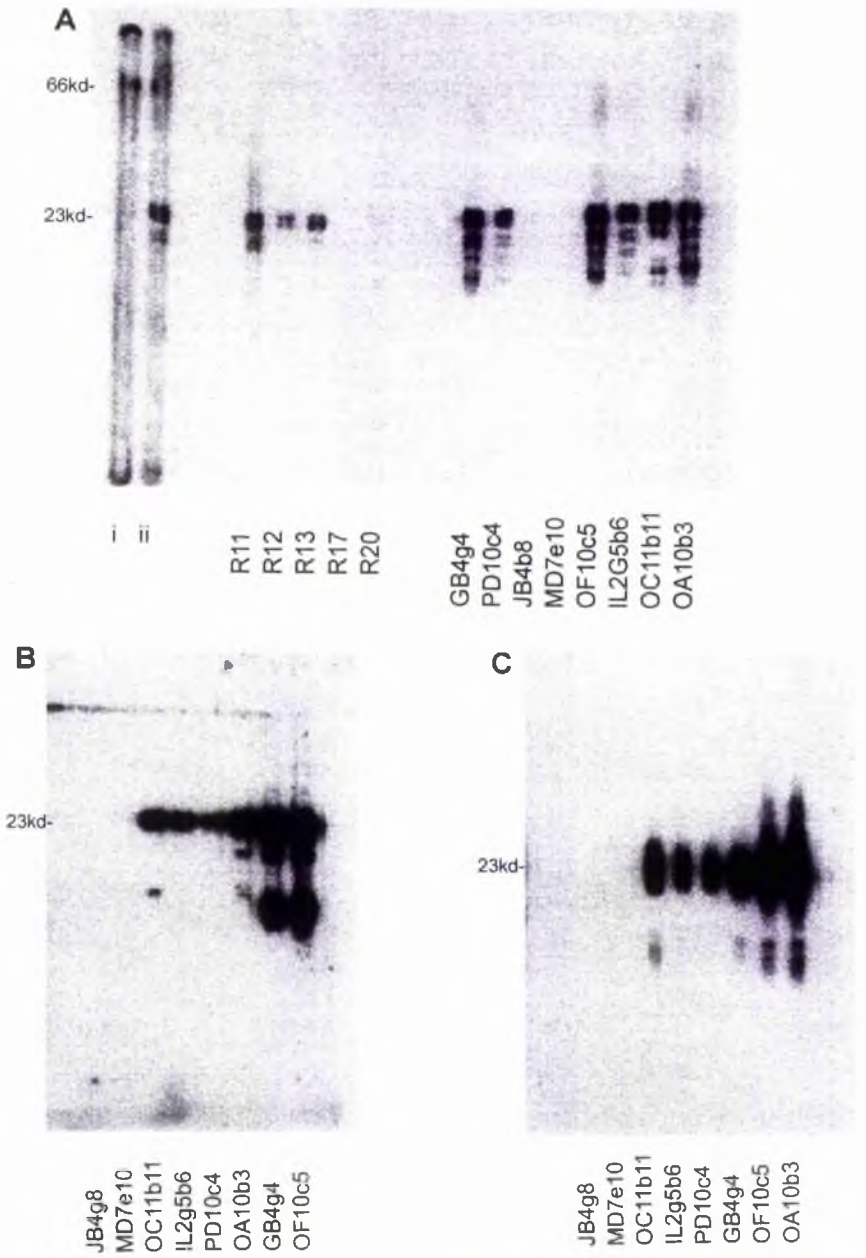

Figure 3.14: Limited proteolysis of the 23kd protease. 100µl samples from a stock solution of 23kd protease (estimated concentration of 0.8mg/ml) were incubated with chymotrypsin, trypsin, and endoproteinase Glu-C (all for one hour at 37°C) at a 1/1000 dilution (methods section 2.4.1). The reaction mixtures were electrophoresed (20% SDS-PAGE), then immunoblotted within the multiscreen apparatus using a panel of monoclonal antibodies and polyclonal antisera. Lanes which were probed with polyclonal antisera are included in the immunoblot of the chymotrypsin reaction mixture only (part A). Prestained molecular weight markers were added to lane one of the gel and probed later in the multiscreen apparatus using antisera R11 (lane i). Antiserum R11 was also added to lane ii to ensure correct identification of other positive immunoreactions. Some cleavage products associated with trypsin (part B), and endoproteinase Glu-C (part C) reaction mixtures were difficult to identify, and consequently immunoblots were typically overexposed (approximately 30 min).

with a pre-equilibrated PVDF membrane strip, within the multiscreen apparatus for 2 hours, then the strip was incubated with blocking buffer and processed as described in section 2.4.3.

Peptides containing the epitope for OA10b3 were not detected in any of the fractions screened, despite the antibody recognising peptides from the original reaction mix. It seemed likely that addition of 0.1% TFA/water to the reaction mix rendered some of the peptides insoluble, which in turn, would have been removed by filtration prior to HPLC purification. Similar results were obtained from trypsin, endoproteinase Glu-C, and CNBr cleavage mixtures.

The panel of monoclonal antibodies were also screened against the four peptides that were previously used to generate the polyclonal antisera against the 23kd protease. The peptides were resuspended from lyophilised powder (1mg/ml in PBS), then incubated with 1% glutaraldehyde treated 96 well microtitre plates at a final concentration of 1µg/well (overnight at 4°C) and/or incubated with pre-equilibrated PVDF membranes at a concentration of 100µg/ml for 2 hours. Monoclonal antibodies were screened using the methods outlined in sections 2.9.2 and 2.3.2, with appropriate polyclonal antisera included as controls. None of the monoclonal antibodies immunoreacted with any of the peptides (results not shown) and it was assumed that corresponding sequences of the 23kd protease did not contain epitopes for antibodies used.

ii) Deletion mutagenesis:

All of the protease deletion mutants that were expressed as GST fusion proteins (with the C-terminal PK tag) are schematically presented in figure 3.15. Monoclonal antibody 336, that specifically recognises the 14 amino acid PK tag (Hanke *et al.*, 1994), was used to determine whether full length fusion proteins had been expressed (figure 3.16). Polyclonal antiserum R11 was used to verify that deletion mutants containing the N-terminal 15 amino acids of the 23kd protease had been cloned in reading frame with the PK tag (figure 3.17). In addition, purified fusion proteins were examined by SDS-PAGE and compared with standard molecular weight markers (figure 3.18).

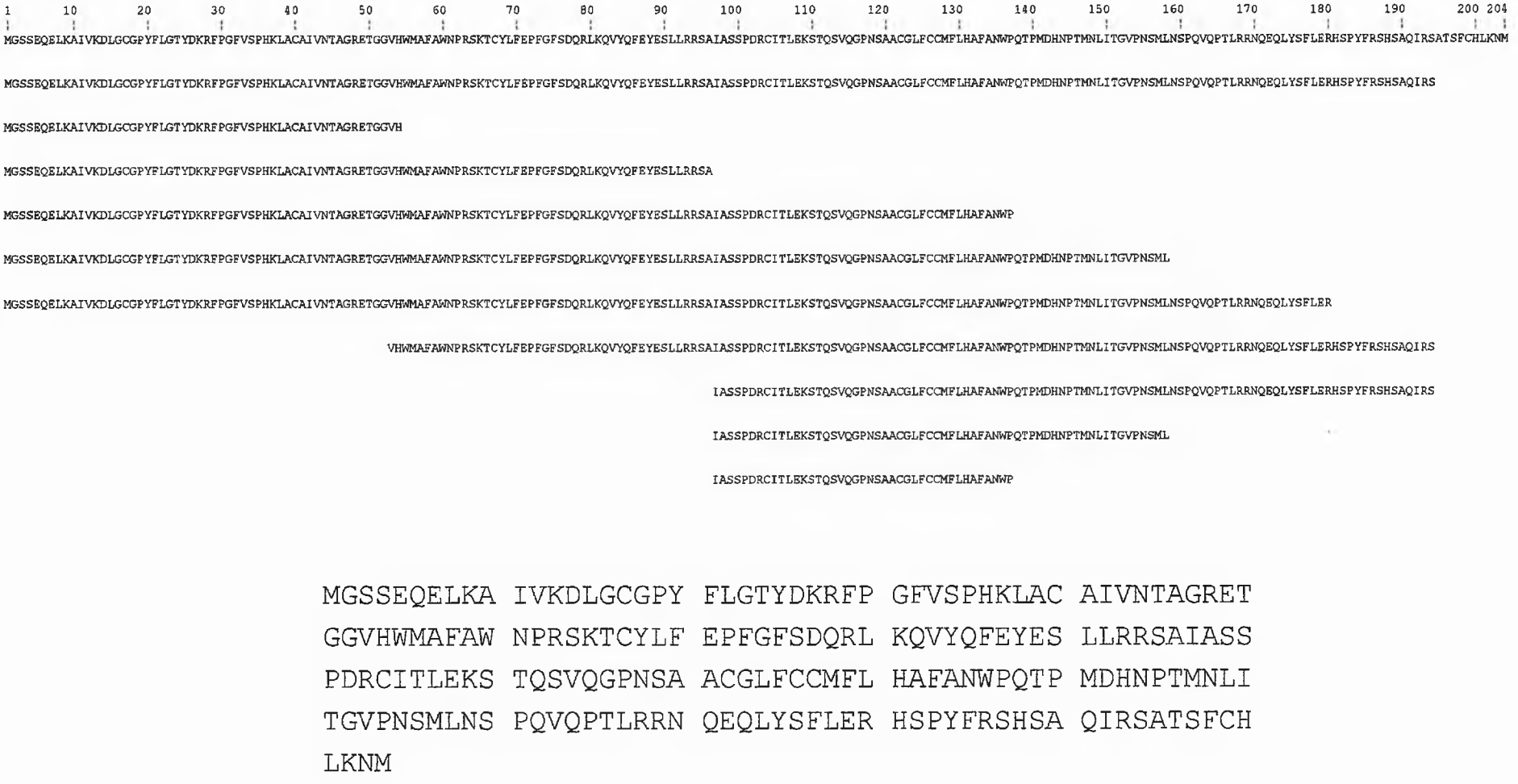

Figure 3.15: Schematic representation of deletion mutants. Deletion mutants were cloned into the pGEX-cPK vector (section 2.5) with the N-terminus and C-terminus of mutants linked to GST and the PK tag respectively.

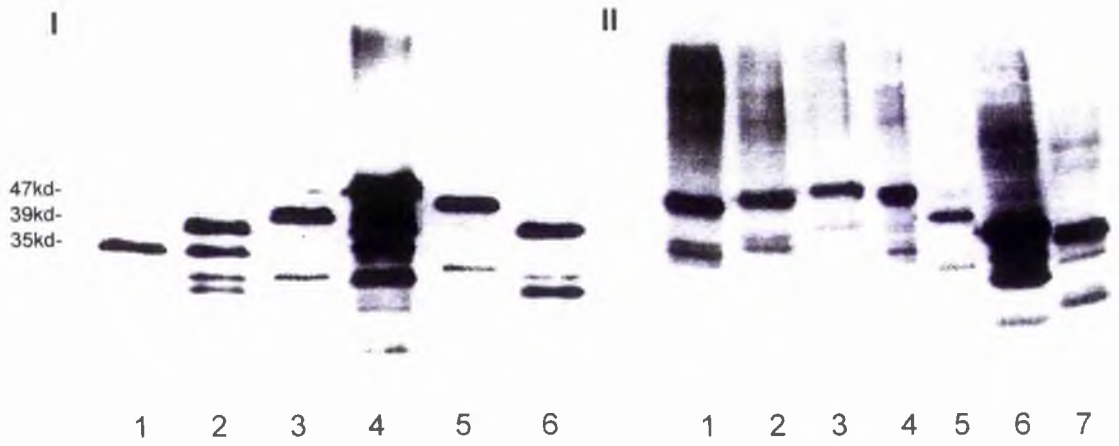

Figure 3.16: Detection of intact deletion mutants using Mab 336. Fusion proteins were expressed, purified and electroblotted (15% SDS-PAGE) as described in section 2.5.10. Part I: Initially, deletion mutants M1-H54 (33.6kd), M1-A96 (38.3kd), M1-P137 (42.9kd), M1-S194 (49.4kd), V53-S194 (43.4kd) and I97-S194 (38.5kd) (lanes 1, 2, 3, 4, 5 and 6 respectively) were used for screening monoclonal antibodies. Part II: Deletion mutants M1-L158 (45.3kd), M1-R180 (47.8kd), I97-L158 (34.4kd) and I97-P137 (32kd) (lanes 2, 3, 6 and 7 respectively) were later cloned and expressed to identify the region containing the epitope for OC11b11 (see text). Included in immunoblot II are deletion mutants M1-P137 (lane 1), V53-S194 (lane 4) and I97-S194 (lane 5). The Mr of GST was assumed to be 26kd and the PK tag to be approximately 1.5kd.

Although full length fusion proteins for all the deletion mutants were isolated, it was evident that all were susceptible to proteolytic degradation, in particular fusion proteins of deletion mutants M1-A96, I97-S194 and M1-S194 (figure 3.16). A significant reduction in proteolytic degradation was observed when Pefabloc was added to cell lysis buffer (4mM final concentration). Additionally, it was evident that a significant amount of expressed fusion protein was retained in the insoluble fraction of bacterial cell lysates (results not shown). However, sufficient quantities of deletion mutants were purified for the purpose of screening monoclonal antibodies. Purified fusion proteins were subjected to thrombin cleavage (30 minutes at 25°C in cleavage buffer) and analysed using monoclonal antibody 336 and polyclonal antiserum R11 (where appropriate).

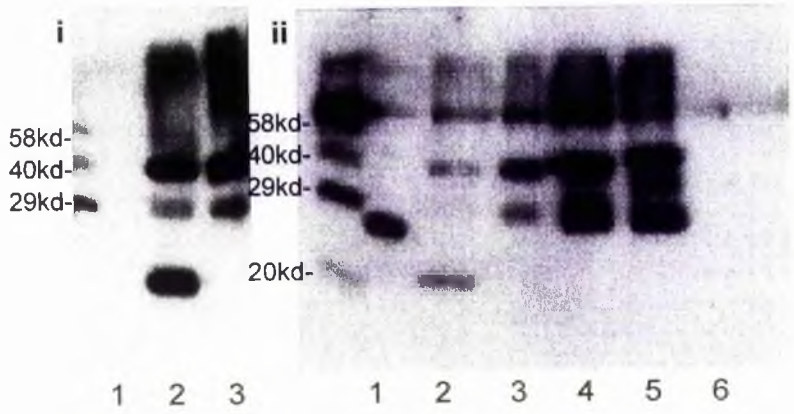

Figure 3.17: Identification of intact fusion proteins and thrombin cleavage products using antiserum R11 and Mab 336. Part I: Immunoblot using with Mab 336: 23kd protease standard (lane 1), and purified M1-P137 fusion protein plus thrombin (lane 2) and minus thrombin (lane 3). Part II: 23kd protease standard and M1-P137 (+/- thrombin in cleavage buffer) are shown in the R11 probed immunoblot (lanes 1, 2, and 3 respectively). The R11 antisera also immunoreacted with mutants M1-L158 (lane 4) and M1-R180 (lane 5), but did not detect V53-S194 (lane 6). The cleavage product in lane 2 (parts I and II) was assumed to be the intact M1-P137-PK polypeptide with an approximate Mr of 16.9kd (see text). All samples were electrophoresed using 15% SDS-PAGE with Biotinylated molecular weight markers, and prestained molecular weight markers included. Biotinylated markers were detected using streptavidin linked peroxidase (Sigma) at recommended dilution's.

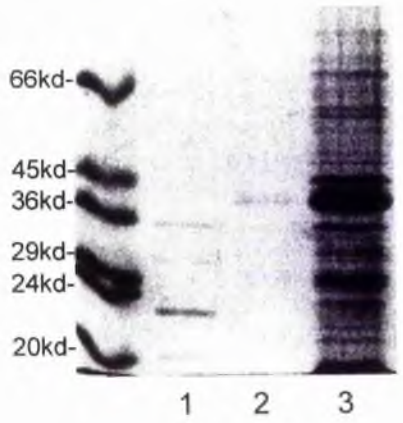

Figure 3.18: Purification of deletion mutant M1-P137. All deletion mutants were purified as described in section 2.5.10, then resolved by 15% SDS-PAGE, and Coomassie blue stained. 23kd protease standard (lane 1) and Dalton V molecular weight markers were included. A sample of purified fusion protein M1-P137 is shown in lane 2 and a sample of the soluble lysate extract shown in lane 3. The molecular weight of deletion mutant M1-P137 was estimated to be approximately 42.9kd.

Thrombin cleavage of mutant M1-S194 resulted in the generation of a polypeptide of approximately 23kd (presumed to be M1-S194-PK) as shown in figure 3.19. Similarly, cleavage of the fusion protein containing region M1-P137 would be expected to generate a

16.9kd product (M1-P137-PK). This appeared to be the case when the relative mobility of the cleavage product was compared to biotinylated molecular weight markers (figure 3.17 parts I and II). These protein markers were compared with prestained markers, and Dalton V molecular weight markers (used in figure 3.18), to determine whether biotinylation had altered the relative mobilities of proteins involved. The biotinylated 20kd marker protein had the correct mobility, although the 40kd marker protein migrated slower giving an apparent Mr of approximately 45kd (result not shown).

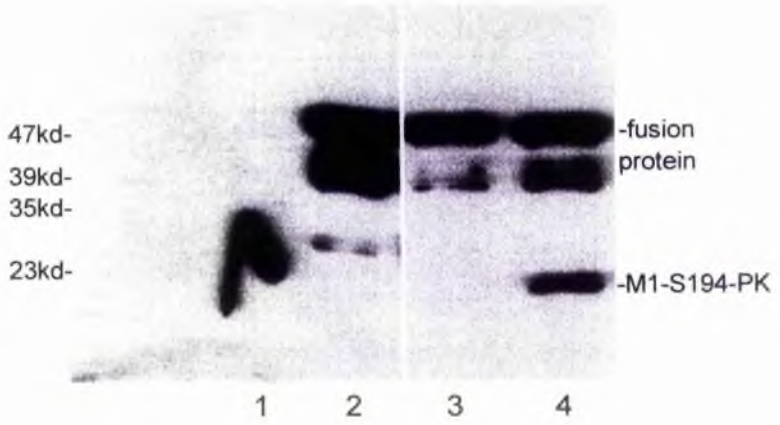

Figure 3.19: Thrombin cleavage of mutant M1-S194. The fusion protein considered to represent the full length 23kd protease (minus the C-terminal 10 amino acids which were known not to comprise any epitopes of interest (section 3.1.5i)) was incubated with 100ng of thrombin in cleavage buffer (section 3.1.1), then electroblotted and probed using antibody OA10b3. 23kd protease standard is shown in lane 1 and a sample of soluble extract from the bacterial lysate shown in lane 2. A degradation product with an approximate Mr of 28 to 30kd (which was also detected using the 33bc antibody and the R11 antisera) was not evident after purification (lane 3), although two degradation products of higher molecular weight were co-purified and also detected using the R11 antisera and 33bc antibody (results not shown). Thrombin cleavage resulted in the generation of a polypeptide with an approximate Mr of 23kd (lane 4), which was also detected using antibody 33bc and the R11 antisera.

None of the monoclonal antibodies immunoreacted with M1-H54 (figures 3.20a, b and c), which was consistent with CNBr cleavage results. Instead, all the monoclonal antibodies (with the exception of OC11b11) immunoreacted with deletion mutants containing the region V53 to A96. Antibody IL2E4f3 differed from the rest in that no immunoreaction with deletion mutant V53-S194 was detected. This was unexpected as the antibody did not recognise M1-H54, but did immunoreact with deletion mutant M1-S194. This suggested that critical

residues required for antibody binding may have been missing from deletion mutants M1-H54 and V53-S194, or that elements of secondary structure necessary for antibody binding were not present. It is noteworthy that IL2E4f3 had previously been shown not to immunoreact with the peptide ^{48}RETGGVHWMAFAWN.

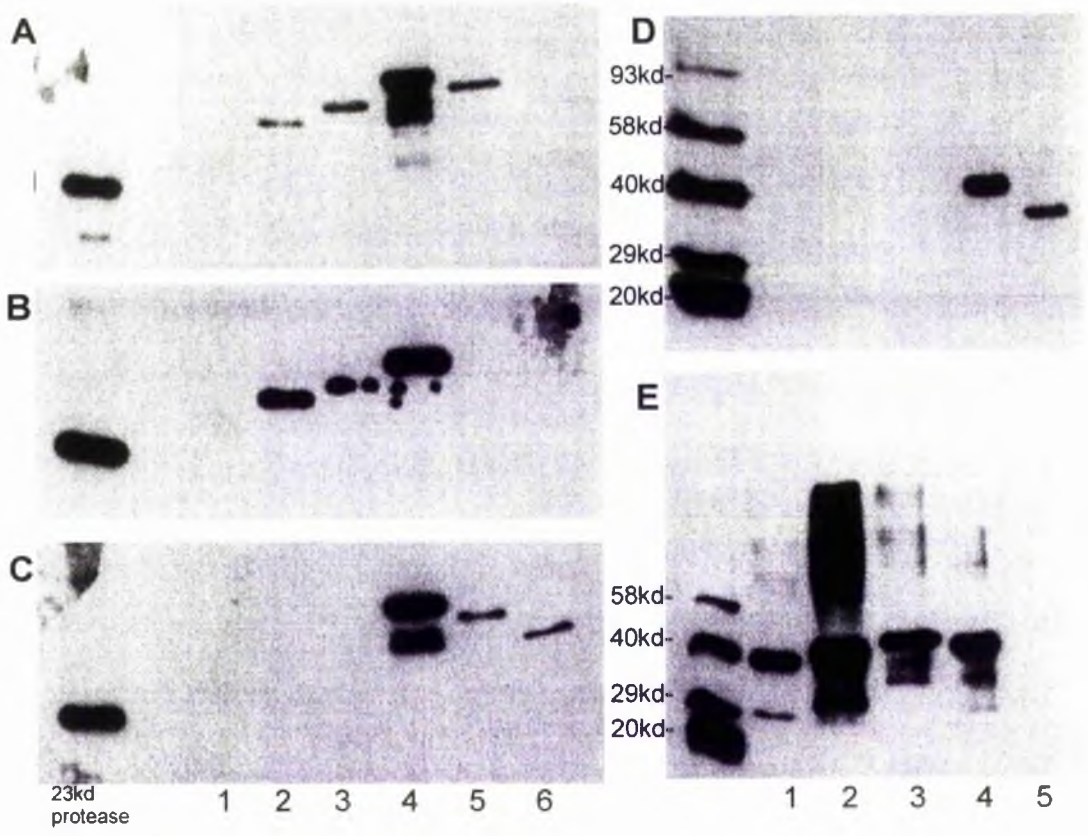

Figure 3.20: Screening monoclonal antibodies against deletion mutants. Purified fusion proteins were resolved by 15% SDS-PAGE then electroblotted and probed using titred antibody solutions. Part A: Mab's OA10b3 (shown), GB4g4, PD10c5, IL2g5b6 and OF10c5 immunoreacted with deletion mutants M1-A96, M1-P137, M1-S194 and I97-S194 (lanes 2, 3, 4 and 5 respectively). Part B: IL2E4f3 detected the same fusion proteins with the exception of V53-S194. Part C: OC11b11 recognised M1-S194, V53-S194 and I97-S194 only. Part D: OC11b11 was also screened against deletion mutants M1-L158 and M1-R180 (lanes 2 and 3 respectively). Deletion mutants M1-P137 (lane 1), V53-S194 (lane 4), and I97-S194 (lane 5) were also included. OC11b11 only immunoreacted with electroblotted V53-S194 and I97-S194 or either deletion mutant immobilised to nitrocellulose (result not shown). Part E: OA10b3 immunoreacted with M1-L158 and M1-R180. None of the monoclonal antibodies immunoreacted with deletion mutants M1-H54 (lane 1 in parts A,B, and C) or I97-L158 and I97-P137 (results not shown).

The epitope for antibody OC11b11 was initially localised to region P137 to S194 (figure 3.20c). However, the antibody did not immunoreact with synthetic overlapping peptides corresponding to this region, and therefore the antibody was subsequently screened against fusion proteins containing the sequences I97-L158, I97-P137, M1-L158 and M1-R180 (figure 3.20d). None of these deletion mutants were recognised by OC11b11, which suggested that the epitope for this antibody was in the region R180 to S194. None of the other antibodies immunoreacted with mutants containing regions I97-L158 and I97-P137 (figure 3.20e), which was consistent with previous results which indicated that epitopes were within the region V53 to A96.

iii) Overlapping peptides:

Peptides which extended over two regions of the 23kd protease (R48 to P101 and F133 to S194) were designed and synthesised as outlined in section 2.6. All the peptides used are schematically presented in figure 3.21. Freeze-dried peptides were dissolved in 0.1% TFA/water (1mg/ml), then filtered (0.2µm Acrodisc) and purified by HPLC. The elution profile was monitored at 226nm (figure 3.22a) and collected fractions analysed by capillary electrophoresis (figure 3.22b, c, d and e). When appropriate, peptide sequences were confirmed using the Procise Protein Sequencer. Several peptides that were relatively insoluble were also resuspended in PBS (1mg/ml) and used without HPLC purification.

Monoclonal antibodies OA10b3, OC11b11, GB4g4, PD10c4, IL2G5b6 and IL2E4f3 were initially screened against appropriate peptides which had been immobilised in 96 well microtitre plates (1µg/well) and nitrocellulose (100µl/ml in PBS), using the methods outlined in sections 2.9.2 and 2.3.2 respectively. None of the antibodies immunoreacted with peptides using these methods, irrespective of whether peptides had been HPLC purified, or simply resuspended in PBS (results not shown). Because immobilisation of peptides resulted in loss of antigenicity, antibodies were re-screened using the competitive ELISA method. A doubling dilution series of antibody solution (50µl/well) was incubated with peptide (5µg/well in PBS) for one hour at 37°C before being transferred to a 96 well microtitre plate pre-coated with purified recombinant 23kd protease (0.05µg/well). After a one hour incubation at 37°C, microtitre plates were processed as described in section 2.6.4.

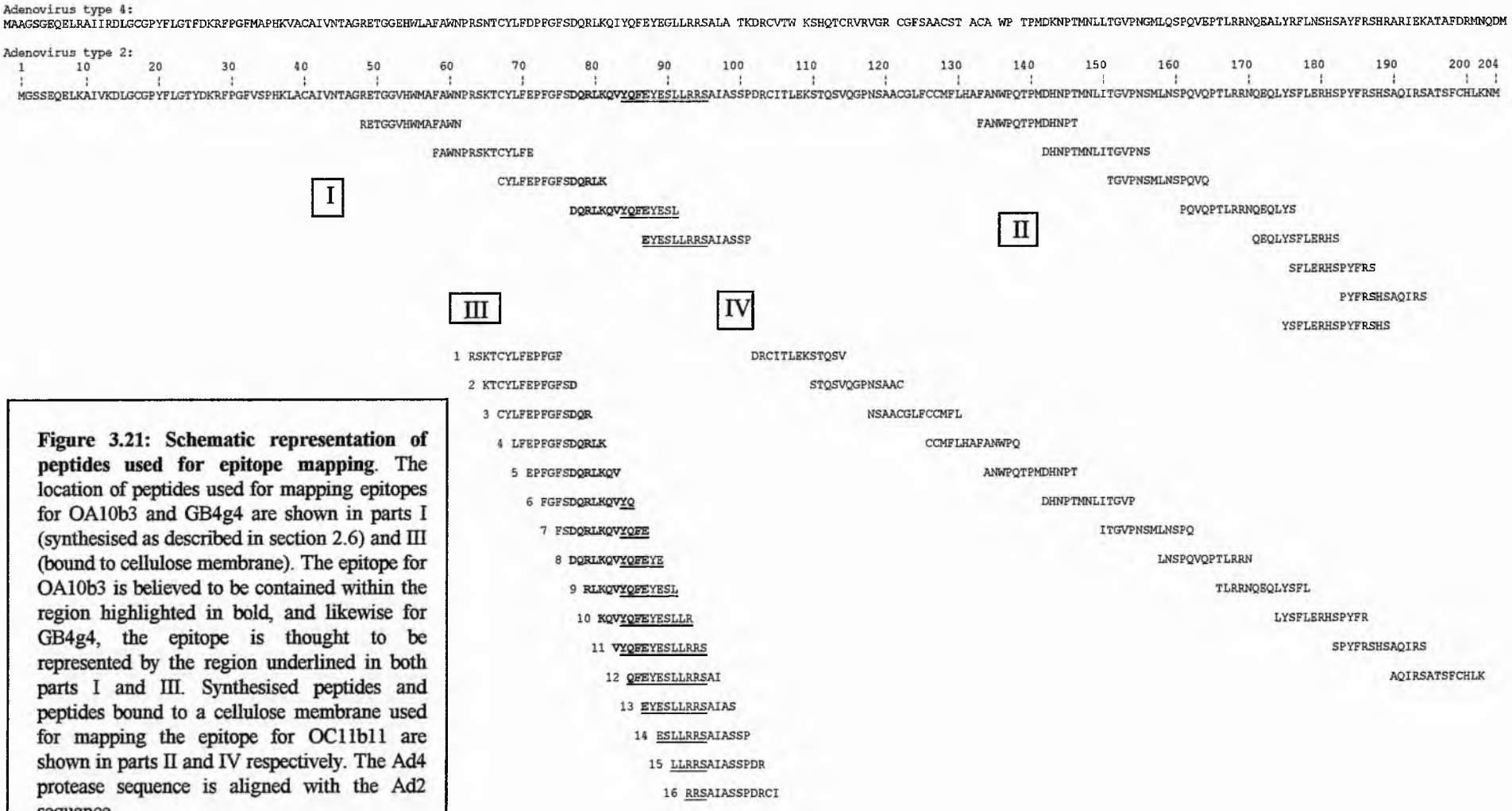

Figure 3.21: Schematic representation of peptides used for epitope mapping. The location of peptides used for mapping epitopes for OA10b3 and GB4g4 are shown in parts I (synthesised as described in section 2.6) and III (bound to cellulose membrane). The epitope for OA10b3 is believed to be contained within the region highlighted in bold, and likewise for GB4g4, the epitope is thought to be represented by the region underlined in both parts I and III. Synthesised peptides and peptides bound to a cellulose membrane used for mapping the epitope for OC11b11 are shown in parts II and IV respectively. The Ad4 protease sequence is aligned with the Ad2 sequence.

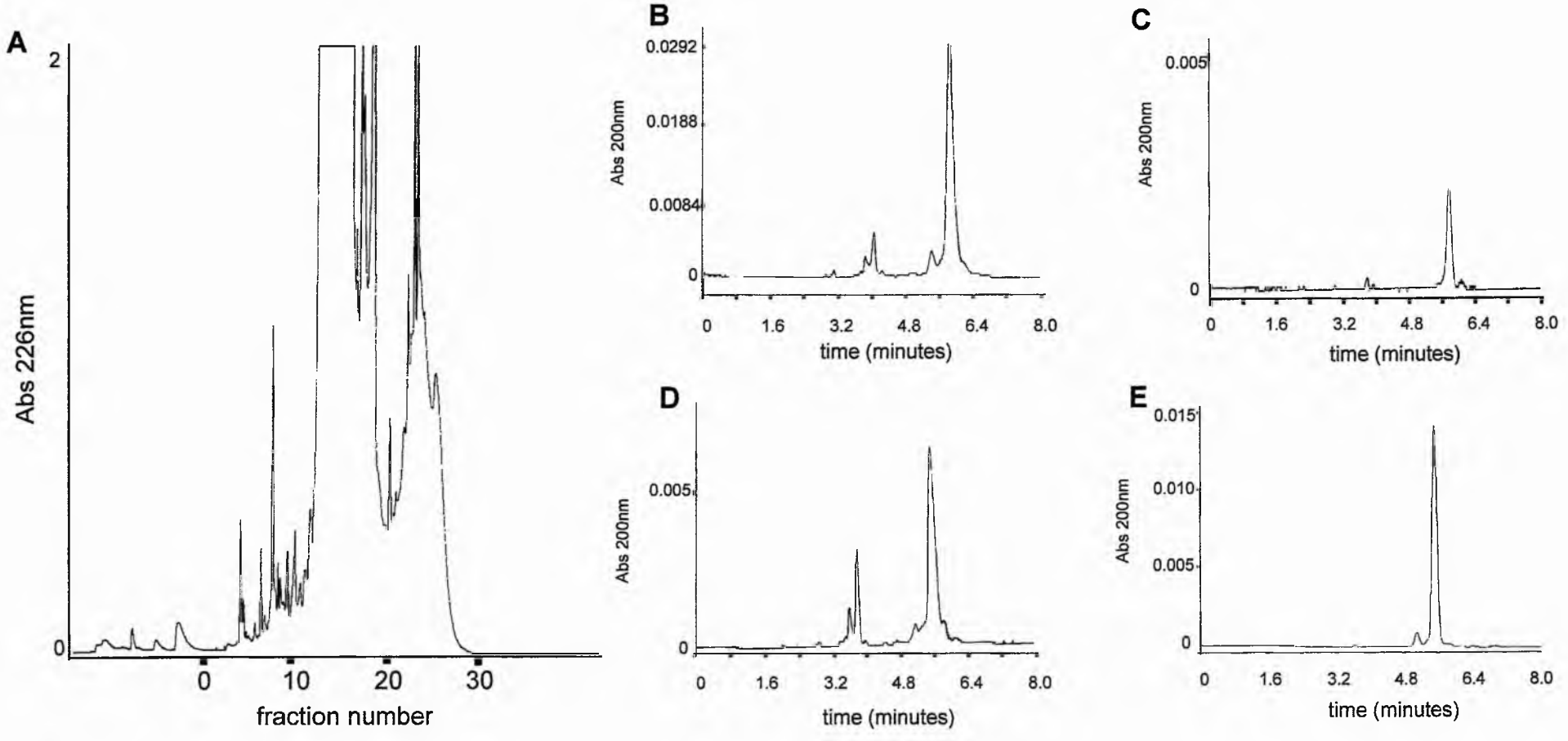

Figure 3.22: Typical purification and assessment of a synthesised peptide. Peptides were synthesised as described in section 2.6.2 (final yields typically of 5mg lyophilised powder), then resuspended in 1ml 0.1% TFA/water, filtered and injected into a pre-equilibrated Rsil C18 HL column (section 2.6.3). Part A: the HPLC elution profile for peptide FANWPQTPMDHNPT. 1ml fractions were collected then samples analysed by capillary electrophoresis. A sample of the peptide solution prior to HPLC purification is shown in part B. Fractions 13, 14 and 15 from the HPLC are shown in parts C, D and E respectively.

None of the overlapping peptides corresponding to sequences within the region F133 to S194 affected OC11b11 binding to immobilised 23kd protease (figures 3.23a and b).

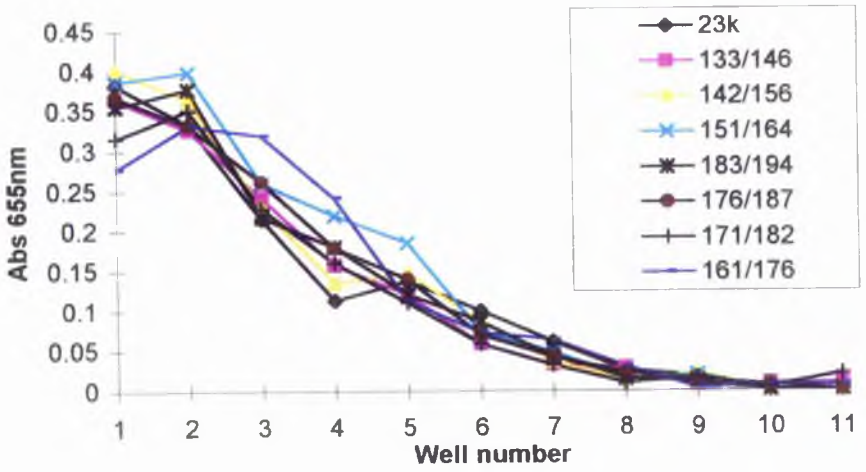

Figure 3.23: Determination of the epitope for OC11b11 by competitive ELISA. Overlapping peptides which corresponded to sequences within the region F133 to S194 (shown in figure 3.21ii and listed within the legend) were incubated with cell culture supernatants containing antibody OC11b11 for one hour at 37°C before addition of antibody to immobilised 23kd protease (section 2.6.4). As a control, OC11b11 was added directly to immobilised 23kd protease (labelled as 23k within the figure). None of the peptides affected antibody binding to immobilised 23kd protease when compared to the control immunoreaction. An identical result (not shown) was determined for peptide 175/189.

As deletion mutagenesis results indicated that the epitope for OC11b11 may be located within the region R180 to S194, it was of interest that the antibody did not immunoreact with any of the synthesised peptides corresponding to this region (figure 3.21ii).

Overlapping peptides of 15 residues in length corresponding to region D102 to K202, synthesised on cellulose membranes, were probed using the method outlined in section 2.6.5 (Spots test). A faint immunoreaction was detected with peptides 10 and 11 (figure 3.24a) which correspond to peptides ^{174}LYSFLERHSPYFR and ^{182}SPYFRSHSAQIRS (figure 3.21iv). This suggested that the epitope for OC11b11 was in the region L174 to S194, which partially confirmed results from the deletion mutagenesis studies (localised to R180 to S194). However, it is noteworthy that the immunoreaction detected using the Spots test was weak and that the peptides ^{175}YSFLERHSPYFRSHS, ^{183}PYFRSHSAQIRS and ^{176}SFLERHSPYFRS were not recognised.

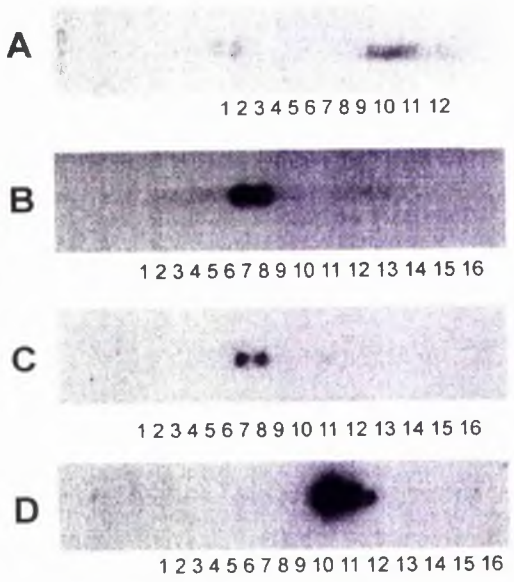

Figure 3.24: Determination of epitopes using the Spots test. Part A: peptides shown schematically in figure 3.21iv were screened (using the method described in section 2.6.5) with titred OC11b11 cell culture supernatant. Fuji RX film was placed over the cellulose membrane strip and pierced using a needle at each end of the membrane to aid identification of positive immunoreactions. Cellulose membranes were treated with the peroxidase linked antibody alone, and anti-pVII monoclonal antibody then peroxidase linked antibody as controls for non-specific immunoreactions. A separate membrane (figure 3.21iii) was probed by the same methods with antibodies OA10b3 (part B), PD10c4 and IL2B5b6 (part C), and GB4g4 and OF10c5 (part D). The membrane was regenerated according to the methods specified by the manufacturer (Genosys).

It is possible that the epitope for OC11b11 is composed of non-contiguous amino acid sequences that are not fully represented by the synthesised peptides used. For instance, the epitope for a monoclonal antibody generated against lysozyme was shown to be composed of two distant stretches of the primary amino acid sequence (residues 18-27 and 166-129). Although separated from each other in the primary sequence, these stretches of amino acids are adjacent on the protein surface (Harlow and Lane, 1988). Similarly, the 3 α-helices that comprise the secondary structure of region L158 to R180 (figure 3.25) may contain residues that, although separated on the amino acid sequence, are spatially oriented to comprise the epitope recognised by OC11b11. It is has been shown that elements of secondary structure (in particular α-helices) are not completely unfolded/disordered during the course of thermal, or chemical denaturation (Pace *et al.*, 1990). Therefore, it is possible for OC11b11 to

immunoreact with denatured antigen, but not synthesised peptides that are missing elements of secondary structure necessary for antibody binding. It is noteworthy that OC11b11 did not recognise native or denatured GST-(Ad4)23kd fusion protein. Differences in the amino acid sequence between Ad2 and Ad4 23kd protease within the L158 to S194 region (figure 3.21) might confer subtle changes in secondary structure and/or involve the substitution of residues that are critical to antibody binding. It is best to consider the epitope for OC11b11 to be within the region L158 to S194 in the absence of data which would confirm its location within region R180 to S194.

Five overlapping peptides corresponding to region R48 to P101 (figure 3.21i) were used in competitive ELISA's to determine the location of epitopes for the remainder of the monoclonal antibodies. Although OA10b3 did not recognise immobilised peptide 3 (^{77}DQRLKQVYQFEYESL), an immunoreaction with this peptide was detected using the competitive ELISA method (figure 3.26). The epitope was confirmed by screening peptides corresponding to region R63 to I105 (figure 3.21iii) using the SPOTs test. OA10b3 recognised peptides ^{75}FSDQRLKQVYQFE and ^{77}DQRLKQVYQFEYE (figure 3.24b), which suggested that the N- and C-termini of peptide ^{77}**DQRLKQVYQFE** were essential for antibody binding. The epitope for OA10b3 appears to span α-helix H2 and part of the loop extending to α-helix H3 (figure 3.25). The residues which appear to be essential for antibody binding are located at the N-terminal end of H2 (Asp-77 and Gln-78), and those which comprise the H2 to H3 loop (Tyr-84, Gln-85, Phe-86 and Glu-87).

The peptide ^{77}**DQRLKQVYQFE** also contained antigenic determinants for antibodies PD10c4 and IL2G5b6, although immunoreactions were relatively weak (figure 3.26 and 3.24c), which suggested that epitopes on the native antigen comprised of conformational elements not presented on synthesised peptides.

The epitopes for antibodies GB4g4 and OF10c5 were not determined using the competitive ELISA method (figure 3.26). However, immunoreactions with peptides ^{83}VYQFEYESLLRRS, ^{85}QFEYESLLRRSAI and ^{87}EYESLLRRSAIAS were detected using the SPOTs method (figure 3.24d). It was significant that immunoreactions were progressively weaker as residues VY and then QF were removed, and also that neither antibody recognised the peptide ^{81}KQVYQFEYESLLR. This suggests that the N- and C-termini of the peptide ^{84}**YQFEYESLLRRS** were important for antibody binding. This may

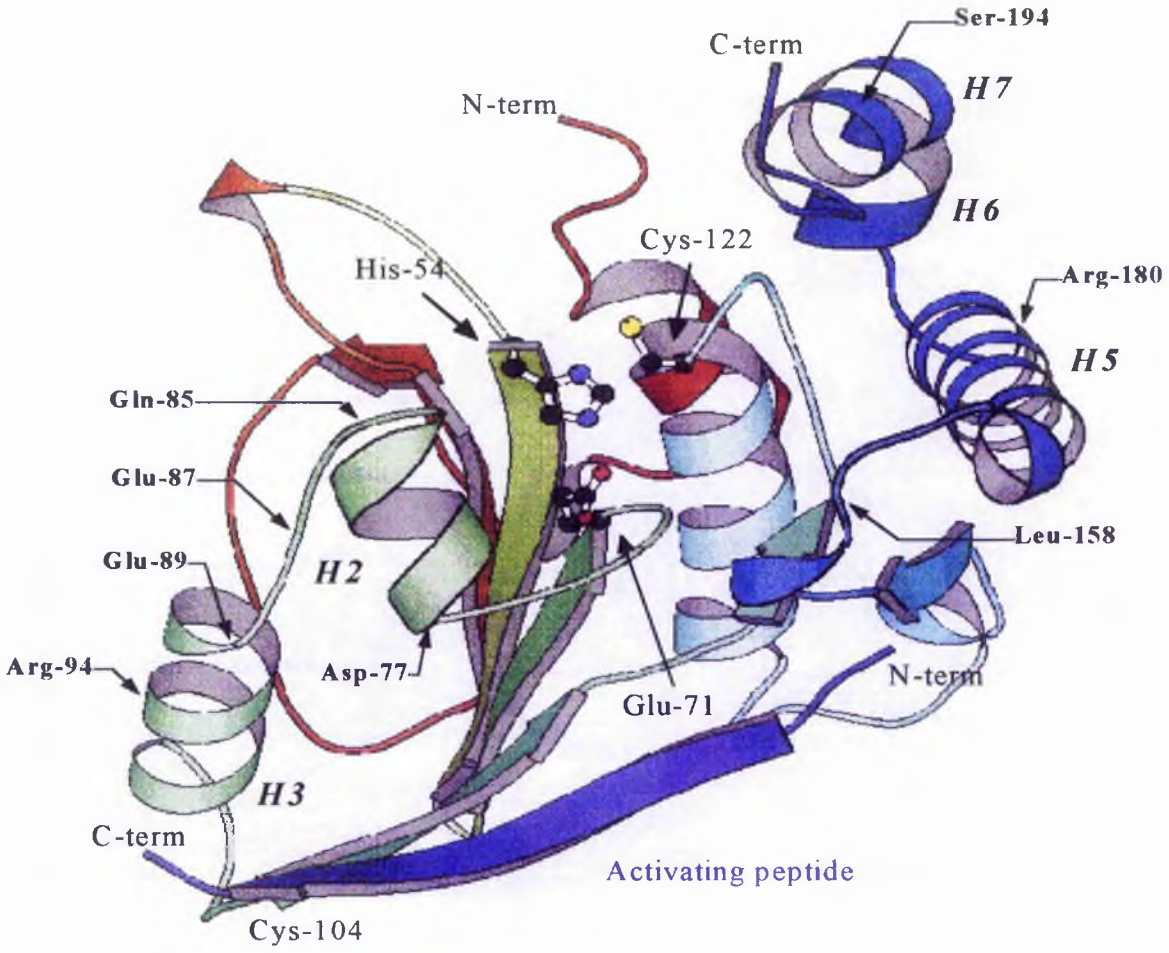

H1

MGSSEQEL**KA IVKDL**GCGPY FLGTYDKRFP GFVSPHKLAC AIVNTAGRET GGVHWMAFAW

H2 *H3*

NPRSKTCYLF EPFGFS**DQRL KQVY**QFEY**ES LLRRSAIAS**S PDRCITLEKS TQSVQGPNSA

H4 *H5*

A**CGLFCCMFL HAFA**NWPQTP MDHNPTMNLI TGVPNSMLNS PQVQ**PTLRRN QEQLYSFLER**

H6 *H7*

HSPYFRSHSA QIRSATSFCH LKNM

Figure 3.25: Location of epitopes within the 23kd protease. The epitope for OC11b11 is thought to be within the H6 to H7 region although residues within H5 may be involved in antibody binding. The location of residues Leu-158, Arg-180 and Ser-194 are indicated. The epitope for OA10b3 is believed to span α-helix H2 (77-DQRLKQVYQFE) and comprise part of the H2-H3 loop. The positions of Asp-77, Gln-85 and Glu-87 are indicated. The epitopes for antibodies GB4g4 and OF10c5 (84-YQFESLLRRS) are thought to span α-helix H3 and part of the H2-H3 loop. Residues that may be involved in antibody binding include Arg-94 and 95, Gln-85 and Glu-87 and 89. His-54 is located at the end of the loop extending between β-sheets S2 and S3 (not labelled) and Cys-122 is located at the N-terminal end of α-helix H4. The precise location of residues indicated on the structure was possible through the invaluable assistance of Gonzalo Cabrita (University of St.Andrews). The schematic representation was originally derived from Ding *et al* (1996).

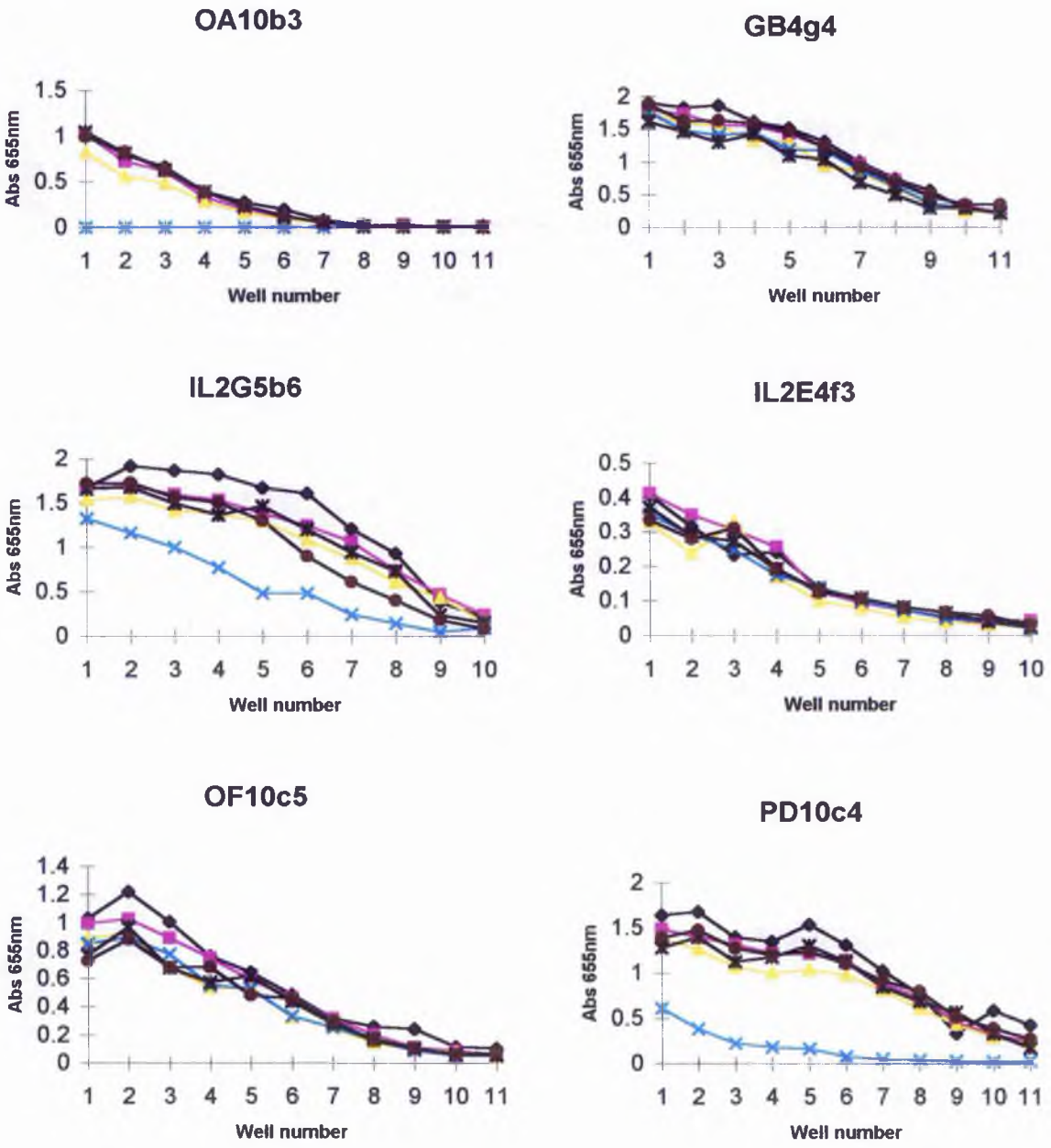

Figure 3.26: Competitive ELISA of monoclonal antibodies with epitopes within region R48 to 101. Peptide solutions were incubated with titred antibody cell culture supernatants before addition of antibody solution to microtitre plates containing 23kd protease. A decrease in absorbance at 655nm (in comparison to the non-peptide control) was detected in instances were immunoreactions with peptides had occurred.

be partly supported by the competitive ELISA results which indicated that neither peptide 3 (^{77}DQRLKQV**YQFEYESL**) or peptide 4 (^{87}**EYESLLRRS**AIASSP) were recognised by antibodies GB4g4 or OF10c5. However, it is possible that the two arginines in peptide 4 may not have been deprotected, and therefore, not recognised by either antibody. The Mtr protecting group on arginine is removed slowly and requires longer cleavage times and the presence of phenol as a scavenger. The sequence ^{84}**YQFEYESLLRRS** corresponds to part of α-helix H3 (LLRRS) and the loop linking H2 and H3 (figure 3.25).

None of the peptides used in the competitive ELISA, or included in the Spots test were recognised by antibody IL2E4f3. These results, and those from the deletion mutagenesis study, suggest that the epitope for this antibody, like others that have been partially characterised, may comprise of elements of secondary structure or non-contiguous amino acid sequences.

3.1.6 Discussion.

Although antibodies OA10b3, PD10c4, GB4g4, and IL2G5b6 share common antigenic determinants within region H2 to H3, only OA10b3 binding affected activation of the enzyme. This may be due to steric hindrance of pVI-ct binding, although it would be expected that GB4g4, PD10c4, and IL2G5b6 would exert similar effects after binding. Alternatively, OA10b3 may 'trap' the 23kd protease in a transient conformational state, in a manner similar to which pVI-ct binding stabilises the proteolytic apparatus by aligning two distant mini-domains of the enzyme (figure 3.25). Binding of OA10b3 to α-helix H2 (and the loop between H2 and H3) may inhibit pVI-ct induced realignment of α-helix H4 and render the enzyme in an inactive conformational state. Similarly, Goldberg (1991) showed that Mab-93, which preferentially recognised denatured *E.coli* tryptophan synthase, inactivated the enzyme after a long period of time. The author proposed that the protein exists in solution in an equilibrium between the native and locally dissociated state (in which the epitope becomes available). Antibody binding appeared to inhibit enzyme activity by preventing or restricting the molecular movements that accompanied pyridoxal-5'-phosphate binding during the catalytic cycle.

It was of particular interest that epitopes for all the monoclonal antibodies (with the exception of OC11b11) were initially localised to region V53 to A96, yet only the epitope for OA10b3

was accurately identified using synthetic overlapping peptides. Constraints imposed by the dimensions of the antigen binding sites of antibodies limits the size of antigenic determinants to 6 to 8 amino acid residues, and therefore, it was expected that the remaining monoclonal antibodies would immunoreact against epitopes on appropriate synthesised peptides. However, other studies which have involved the determination of epitopes on Ad2 DBP (Cleghon *et al.*, 1993), myoglobin, lysozyme, and influenza virus haemagglutinin (HA)(Harlow and Lane, 1988; Griffiths, 1993), have indicated that many antigenic states may be dependant upon secondary, tertiary and even quaternary structure since they may be composed of discontinuous segments which are often found to incorporate loops or turns in the polypeptide chain. Cleghon *et al* (1993) have shown that a panel of monoclonal antibodies generated against DBP recognise both the native and denatured forms of the protein, suggesting that their epitopes consist of primary or limited secondary structures that are exposed on the native molecule. Additionally, these authors have shown (via limited proteolysis experiments) that the epitope for one of these antibodies (Mab B6) was discontinuous, being ascribed to the C-terminal domain of DBP and the hinge between the N- and C-terminal domains. It is possible that the epitopes for OC11b11, IL2E4f3, PD10c4, and IL2G5b6 are likewise composed of discontinuous segments of the 23kd protease.

It was clear from a comparison of the amino acid sequence and of the crystallographic structure of hens egg white lysozyme that the epitope for a monoclonal antibody generated against this protein was formed by Lys-116, Arg-114, Asn-113, and, Phe-34 and Lys-33 (Harlow and Lane, 1988). The epitopes for all the antibodies appeared to be composed of charged or polar amino acids, for instance, out of the 16 amino acids that were mapped to these sites, nine were either lysine or arginine. Likewise, ^{77}**DQRLKQVYQFE** contains three glutamines, an arginine and a lysine that may constitute the antigenic determinants for OA10b3. It is possible that this peptide does not contain all of the antigenic determinants for PD10c4 and IL2G5b6, and therefore, like OC11b11, it was assumed that these antibodies recognised non-contiguous amino acid sequences. As previously mentioned, the antigenic determinants for antibodies GB4g4 and OF10c5 were not easily determined, however, it is possible that the arginines in α-helix H3, and residues within the H2 to H3 loop, are recognised by these antibodies. The residues which are suspected to be critical for OA10b3

and GB4g4 binding are highly conserved amongst human serotypes which have been sequenced (figure 3.27).

```
                        71                                  100                 120
Bovine   type    7   YQMFIFDPLG WKNDQLMKYY KFSYSNLIKR SALSS.PDKC VKVIKNSQSV
Ovine    strn  287   YKLFIFDPLG WKDTQLIKFY NFSLNSLIKR SALNN.SDRC ITVERNTQSV
Avian    strn  127   YTIYMFDPLG WKEKDLFKLY GFSYKTMIKR SALQS.DNRC VKLVKNTEAV
Human    type    2   KTCYLFEPFG FSDQRLKQVY QFEYESLLRR SAIASSPDRC ITLEKSTQSV
Human    type    5   KTCYLFEPFG FSDQRLKQVY QFEYESLLRR SAIASSPDRC ITLEKSTQSV
Human    type   40   RTCYLFDPFG FSDERLKQIY QFEYEGLLKR SALASTPDHC ITLIKSTQTV
Human    type   41   HTCYLFDPFG FSDERLKQIY QFEYEGLLKR SALASTPDHC ITLVKSTQTV
Human    type   12   HTCYLFDPFG FSDQRLKQIY QFEYESLLRR SALAATKDRC VTLEKSTQTV
Human    type    3   NTCYLFDPFG FSDERLKQIY QFEYEGLLRR SALA.TKDRC ITLEKSTQSV
Canine   type    1   KTFYMFDPFG FSDSKLKQVY SFEYEGLLRR SAIASTPDRC VTLAKSNETI
Bovine   type    3   QTFYMFDPFG FSDQKLKQIY NFEYQGLLKR SALTSTADRC LTLIQSTQSV
Human    type    4   NTCYLFDPFG FSDQRLKQIY QFEYEGLLRR SALA.TKDRC VTW.KSHQTC
Murine   type    1   STFYLFDPFG FSDRKLQQVY KFEYERLLKR SAVSSSSSKC VTLVKSHQTV
Porcine  type    3   RTFYFFDPFG FSDRELAQVY DFEYQRLLRK SAIQSTPDRC LTLVKSTQSV
Avian    type    1   GRCYMFDPFG WSDQKLWELY RVKYNAFMRR TGL.RQPDRC FTLVRSTEAV
```

Figure 3.27: Comparison of the sequence that comprises the Ad2 H2 to H3 region with 14 other adenovirus serotypes. Protease sequence alignments and numbering are based on Ad3. Conserved residues are highlighted in red. Residues that are not conserved are highlighted in green if they are similar in respect to charge or polarity, and in bold if they do not share any characteristics with the conserved residues. The Serine residue which is not conserved (but present within the Ad2 sequence) is highlighted in blue.

It is evident that the epitopes for OA10b3 and GB4g4 are highly conserved amongst the human serotypes. The Ad2 enzyme contains 2 residues that are not considered to be conserved (Val-83 and Ser-90) that are located within α-helices H2 and H3 respectively. Residues that compose the loop between these helices (Tyr-84 to Glu-89) are highly conserved, particularly Tyr-84 which is totally conserved amongst all the serotypes shown in figure 3.27. Other residues which have been thought to be essential for antibody binding are highly conserved in particular Asp-77 (for OA10b3 binding), and Arg-95 and Ser-96 (for GB4g4 binding).

It is noteworthy that none of the monoclonal antibodies generated against the Ad2 23kd protease immunoreacted with electroblotted Avian strain 127 recombinant protease (Lewis Murray, University of St.Andrews, pers.comm.). It is evident from figure 3.27 that residues

which are thought to be required for antibody recognition are absent in this enzyme. The extent to which these differences affect the conformation of the H2 to H3 region is unclear. Both native (known to be active) and denatured forms of the 23kd protease were injected into Balb/c mice throughout the immunisation regime, and it was expected that a broad range of antibody specificities would be isolated. However, the finding that the majority of monoclonal antibodies recognised antigenic determinants within the H2 to H3 region may be significant. For instance, other studies have also shown that native proteins possess only a very limited number of sites against which antibodies are preferentially made during an immune response. In the case of influenza HA, most antibodies were found to be directed against particular regions of the protein and it was surmised that many segments of the protein were non-immunogenic. Likewise, a panel of monoclonal antibodies which were generated against adenovirus core proteins pVII and mu, all recognised common antigenic determinants within arginine rich regions of both proteins (Lunt *et al.*, 1988). It is noteworthy that none of the monoclonal antibodies generated against the 23kd protease were mapped to region T45 to H54, which forms an extended loop between S2 and S3 (figure 3.25). Webster (1992) immunised rabbits with peptide RETGGVHWMAFAWN conjugated to HSA, which contains residues corresponding to part of the loop region. The resultant polyclonal antiserum was shown to immunoreact poorly with the native and denatured form of the antigen.

Only antibodies that were used in immunocytochemical studies were characterised, however, several of the monoclonal antibodies which recognised conformation dependant epitopes (such as JB4b8 and MD7e10) can be epitope mapped to a limited extent now that other epitopes have been determined. For instance, The ELISA additivity test (Friguet *et al.*, 1990) could be utilised to determine the number of antigenic sites simultaneously available to two antibodies on the antigen. As the epitopes for antibodies OA10b3 and OC11b11 have been localised to regions H2 to H3 and H5 to H7 respectively, the approximate location of the conformation dependant epitope of JB4b8 could be determined with relative ease, although care should be taken when interpreting results as antibody binding may be subject to steric hindrance, even though epitopes may be located on apparently distinct regions of the 23kd protease. Once characterised, antibodies JB4b8 and MD7e10 could be powerful tools for investigating conformational changes that are assumed to occur when the 23kd protease

interacts with DNA (Ding *et al.*, 1996), and peptides containing the VEGGS motif (Diouri *et al.*, 1996). Although these antibodies did not immunoreact with 23kd protease in 4% formaldehyde fixed virus infected HeLa cells, they can be used to immunoprecipitate the enzyme from infected cell lysates, and therefore, may prove useful in distinguishing isoforms of the protease *in vivo*.

3.2 Isoforms of the 23kd protease.

Several recent reports have indicated that isoforms of the 23kd protease can be detected *in vivo* and *in vitro* (Webster *et al.*, 1993; Greber *et al.*, 1996; Keyvani-Amineh *et al.*, 1996). In order to determine whether monoclonal antibodies would preferentially immunoreact with one isoform over another, recombinant Ad2 and Ad2(ts1) 23kd enzymes were first expressed in E.coli BL21 (DE3) cells (cells were transformed with plasmid p250A for Ad2(ts1) 23kd protease expression, Anderson (1992)), then purified using the methods outlined in section 2.1.7.

It was evident that the level of Ad2(ts1) 23kd protease expression was poor in comparison to the wild type equivalent (results not shown). However, 10µl samples from fraction 25 (from the Mono-S column) of the Ad2(ts1) protease (hereafter referred to as ts1 25), and fraction 18 of Ad2 wild type protease (wt 18), were both shown to digest approximately 50% of the synthetic peptide substrate LSGAGFSW over a period of one hour at 37°C (figure 3.28) using the conditions described in section 2.2.5. A similar level of activity was observed with ts1 25 at 39°C (the non-permissive temperature) after one hour. 10µl samples from wt 18 and ts1 25 were examined by SDS-PAGE (figure 3.28), from which it was evident that a higher concentration of the ts1 enzyme, over the wild type equivalent, was required to digest the same amount of substrate. This is consistent with results described elsewhere (Rancourt *et al.*, 1995). These authors determined that recombinant Ad2 ts1 enzyme was active regardless of the temperature of synthesis, or the temperature of the enzyme reaction, and like the wild type recombinant enzyme, was dependent on the addition of pVI-ct for activity. These authors also noted the level of recombinant Ad2 ts1 protease expression was poor in comparison to recombinant wild type. Keyvani-Amineh *et al* (1995) provided additional

information to suggest that the ts1 mutation destabilises protein structure, and therefore renders the protein less soluble.

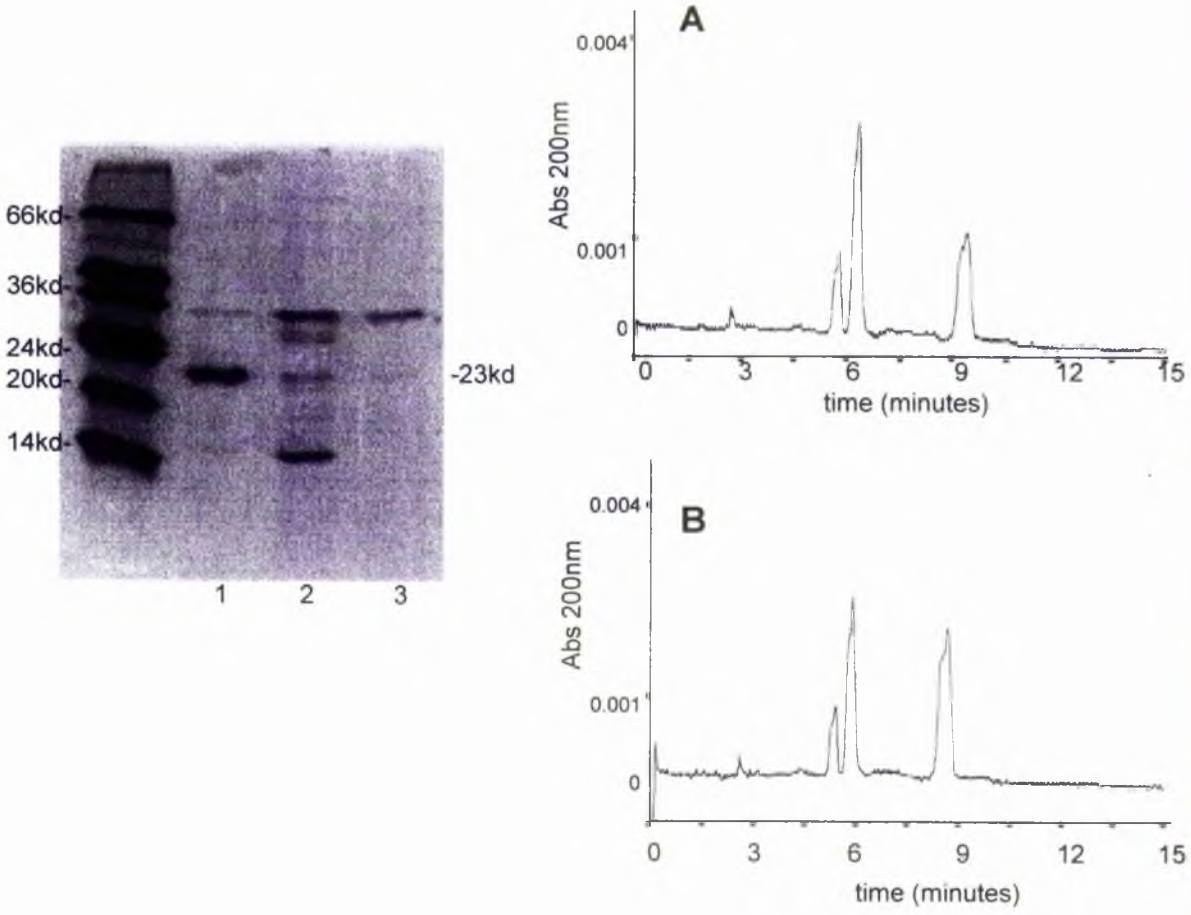

Figure 3.28: Relative activities of recombinant wild type (wt) and ts1 enzymes. Recombinant wt and ts1 23kd protease enzymes were expressed and purified as described in section 2.1.3. The wt enzyme was examined by 15% SDS-PAGE (lane 3 of the Coomassie blue stained gel) together with molecular weight markers and 23kd protease standard (lane 1). The fraction (referred to as wt 18) was estimated to contain approximately 10µg/ml 23kd protease (using SBTI standards as a comparison). 10µl of this source of 23kd protease was estimated to cleave approximately 50% of the synthetic substrate LSGAGFSW (using the methods outlined in section 2.2.5) over a period of one hour at 37°C (part A). Recombinant ts1 23kd protease (referred to as ts1 25) is shown in lane 2 (estimated final concentration of approximately 30µg/ml). A 10µl sample was determined to cleave approximately 50% of LSGAGFSW at both 37°C and 39°C (the latter is shown in part B).

To determine whether any of the monoclonal antibodies affected ts1 25 activity, or indeed, whether the P137L substitution affected antibody binding, monoclonal antibodies OA10b3, OC11b11 and GB4g4 were incubated with 10µl fractions of wt 18 and ts1 25 for one hour

on ice, and, at 37°C and 39°C for 30 minutes. After addition of pVI-ct and substrate (LSGAGFSW), assay mixtures were left for one hour at 37°C or 39°C then analysed by capillary electrophoresis. Both wt 18 and ts1 25 enzyme activities were inhibited by OA10b3 binding at 37°C and 39°C (figure 3.29a and c). Neither OC11b11 or GB4g4 affected enzyme activity (figures 3.29c, d, e and f) regardless of the temperature of antibody-antigen incubation, or temperature of the enzyme reaction.

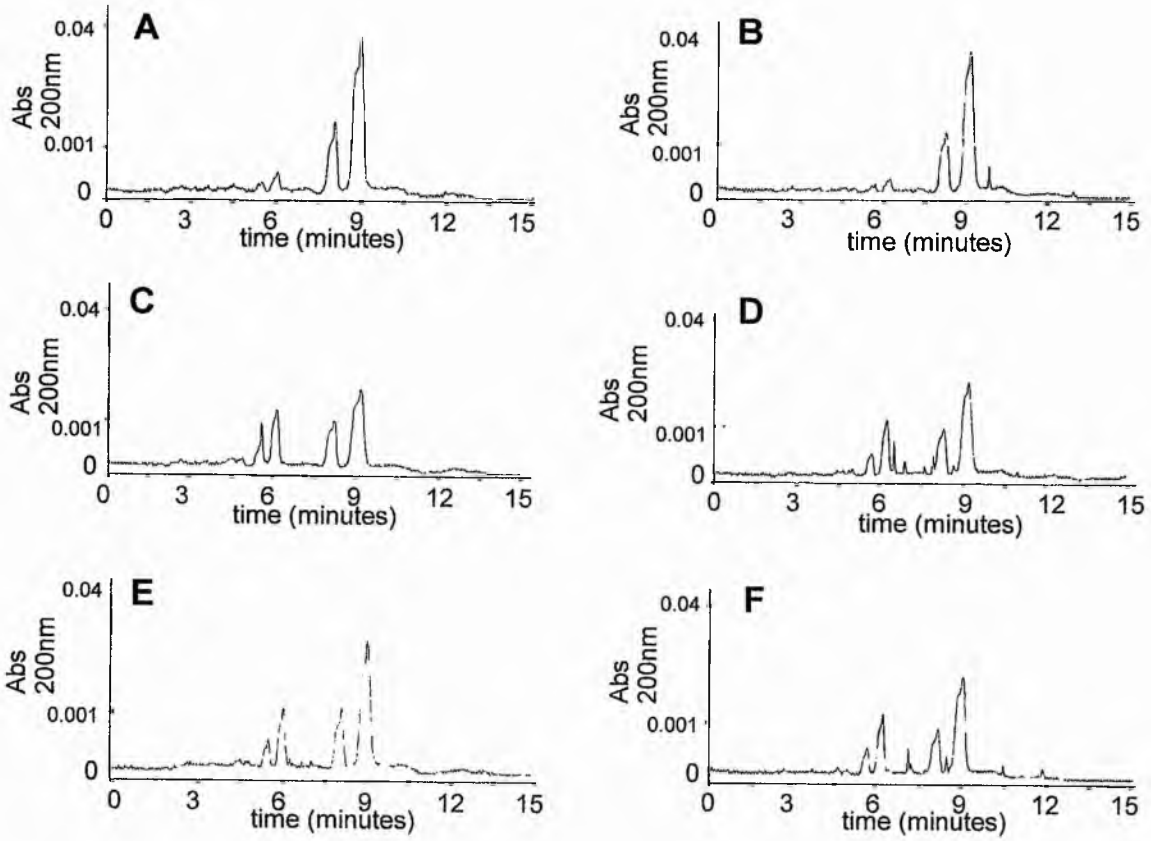

Figure 3.29: Effect of antibody binding on recombinant wt and ts1 enzyme activity. Antibody solutions were incubated with samples of wt 18 and ts1 25 for one hour on ice prior to peptide assay (section 2.2.5). OA10b3 was shown to inhibit wt 18 and ts1 25 protease activity (parts A and B respectively) whilst OC11b11 (parts C and D) and GB4g4 (parts E and F) did not appear to significantly affect activity of either enzyme. Several other peaks evident on capillary electrophoresis traces shown in parts B, D and F (ts1 profiles), but not those of the wt enzyme, suggest that aminopeptidases present within concentrated cell culture supernatants may have cleaved co-purified polypeptides in the ts1 25 sample.

None of the antibodies were added to the pre-activated wt 18 or ts1 25 using the above assay system, although all three monoclonal antibodies were shown to recognise immobilised

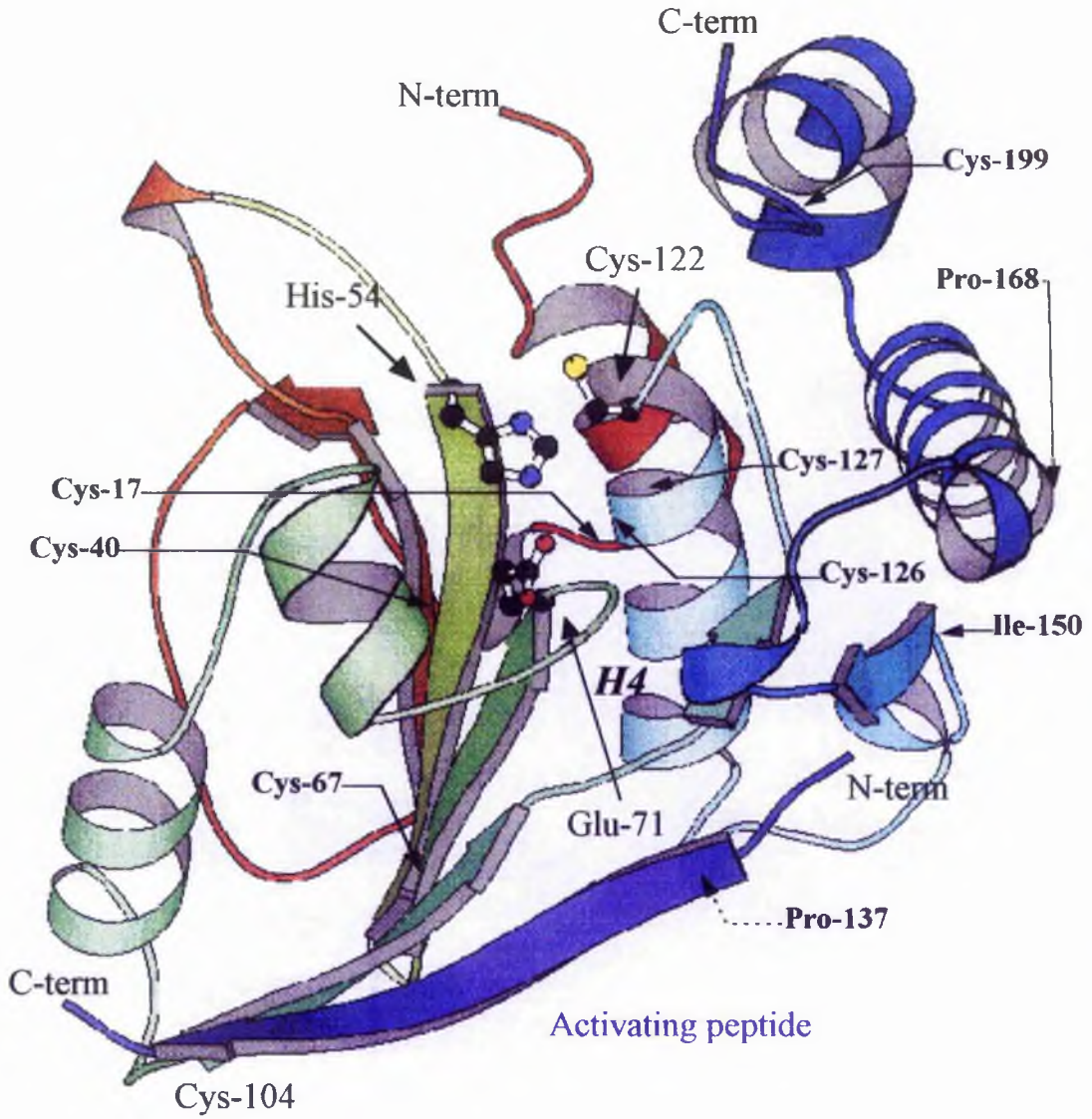

Figure 3.30: Location of cysteines and P137 within the 23kd protease. Cysteines involved in the activation (Cys-104) and known to comprise the active site triad (Cys-122) are highlighted in appropriate locations (Ding *et al*, 1996). Other cysteines are highlighted in bold at predicted sites (locations predicted by Gonzalo Cabrita, University of St.Andrews). Proline-137 is believed to be located within the loop hidden from view by the N-terminal region of the activating peptide. The proline rich region extends from Pro-137 to Pro-168 (Ile-150 is highlighted). A portion of this region appears to fold around a loop extending from Cys-104 to Cys-122.

activated, and non-activated wt 18 and ts1 25 using the direct ELISA method (results not shown). It was evident that any changes in the enzymes conformation as a consequence of the P137L substitution did not affect regions H2 to H3 and H5 to H7 which contained the epitopes for the antibodies used. Keyvani-Amineh *et al* (1995) suggested that the ts1 mutation could alter the size, shape and stability of the proline rich region (P137 to P165) that stretches from a-helices H4 to H5 (figure 3.30 on the previous page). Interestingly, the authors proposed that this region may be an important regulatory signal in determining the lifetime and degradation rates of the enzyme. The region forms a surface loop that may be required for protein trafficking *in vivo*.

Oxidising and reducing agents were used to investigate the effects of redox modulation on wt 18 and ts1 25 sulphydryl groups. The thiol oxidising agent diamide [diazinedicarboxylic acid bis (N,N-dimethylamide), Aldrich] was prepared fresh as a 50mM stock solution in 10mM Tris-HCl, pH 8.0, and added to recombinant 23kd protease (10µl samples of wt 18 and ts1 25) to a final concentration of 10mM. Likewise, pVI-ct and ß-mercaptoethanol (ß-MeSH) were added to final concentrations of 0.2mM and 1mM respectively. Treated and non-treated samples were left at room temperature for 5 minutes, then electrophoresed under denaturing conditions (without reduction) and either electroblotted (then examined using antibodies OA10b3 and OC11b11, figure 3.31a) or silver stained (figure 3.31b).

Two isoforms were detected when both wt 18 and ts1 25 were pre-incubated with 1mM ß-MeSH and 0.2mM pVI-ct/ 1mM ß-MeSH, with the slower migrating form assumed to be the 23kd protease/pVI-ct heterodimer. Greber *et al* (1996) showed that protease extracted from reduced virus particles migrated faster than protease from non-reduced virus particles (when electrophoresed under denaturing conditions) and suggested that the aberrant gel mobility was due to the inter-chain disulphide that connects the protease with pVI-ct. unexpectedly, both forms were detected in the non-treated wt 18 and ts1 25 samples, which suggested that pVI-ct binding alone was not responsible for the differences in migration. In addition, the non-treated wt 18 sample contained what was presumed to be a dimeric form of the enzyme. This form was not detected in the non-treated ts1 25 sample, nor has it been described elsewhere. Keyvani-Amineh *et al*(1996) also observed two closely migrating forms of the non-treated recombinant wild type protease, and also a faster migrating form (appeared at 12kd) which they assumed contained one or more disulphides. Differences between results presented here

and those provided by Keyvani-Amineh *et al* (1996) may be a consequence of different purification protocols used. For instance, Keyvani-Amineh *et al* (1996) included ß-MeSH (5mM final concentration) in all buffers used throughout their purification regime, to increase the overall yield of soluble protease. ß-MeSH was not included in buffers used in this study and as a consequence, recombinant protease may have been subject to oxidation throughout the course of the lengthy purification.

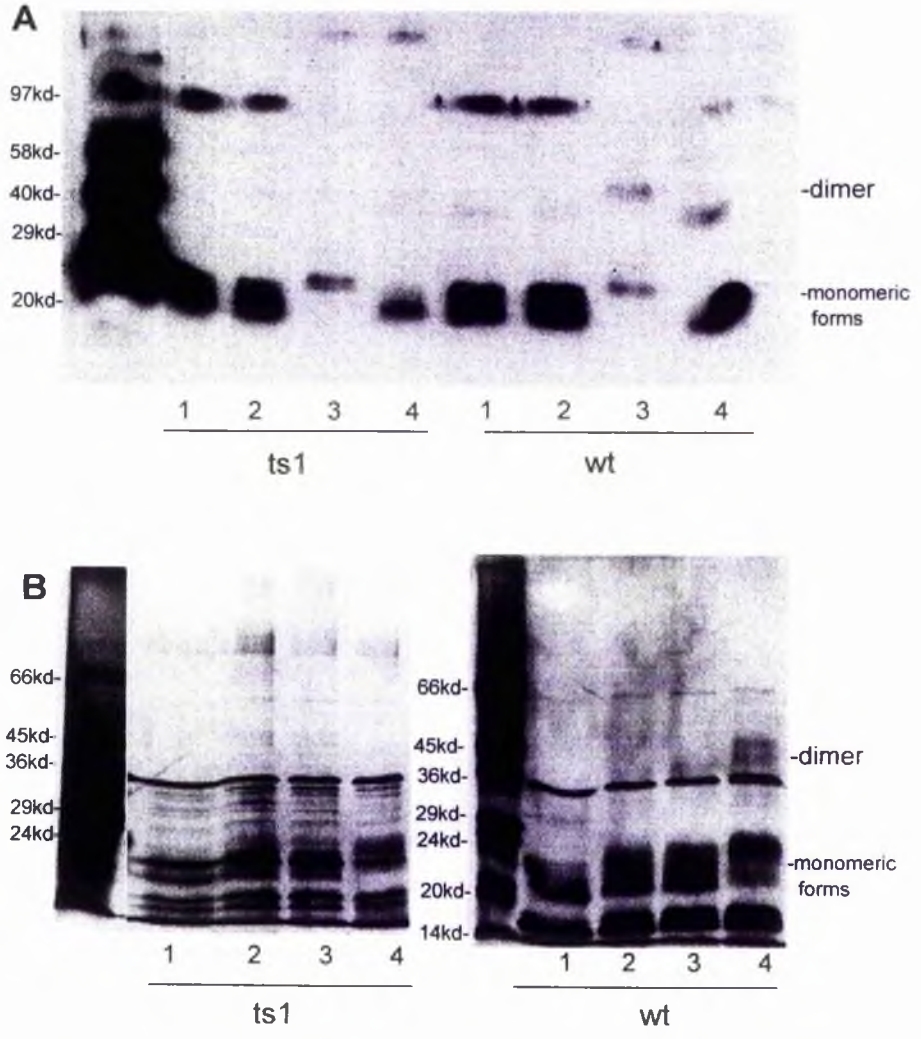

Figure 3.31: Isoforms of recombinant wt and ts1 protease. Part A: 10µl samples of wt and ts1 were reduced (1mM ß-MeSH/assay buffer) (lane 1), incubated with pVI-ct (0.2mM final concentration in 1mM ß-MeSH/assay buffer)(lane 2), treated with diamide (10mM final concentration)(lane 3), or non-treated (assay buffer added without ß-MeSH)(lane 4). Treated and non-treated samples (all 20µl total volume) were left at room temperature for 5 minutes, then electrophoresed (15% SDS-PAGE without ß-MeSH), probed using OA10b3. Immunoblots were over-exposed (approximately 1 hour) and consequently some levels of background were evident. Part B: silver stained 15% Polyacrylamide gel (samples prepared for electrophoresis as outlined above) of fully reduced (5mM ß-MeSH)(lane 1), pVI-ct treated (lane 2), non-treated (0.2mM)(lane 3) and diamide treated (10mM)(lane 4) wt and ts1 recombinant enzymes.

A slow migrating dimeric form of wt 18 (but not ts1 25) was detected after diamide treatment. Additionally, one other isoform was detected for both wt 18 and ts1 25 which appeared to have migrated slower than the two close migrating isoforms detected in the non-treated, and ß-MeSH treated samples. It is generally accepted that oxidised proteins migrate faster than reduced equivalents when electrophoresed under denaturing conditions (Creighton, 1990). It is unclear why in this instance the oxidised form has migrated more slowly. It is possible that 10mM diamide in the sample may affect the migration of proteins during electrophoresis. However, if this was the case then co-purified *E.coli* proteins did not appear to be affected (figure 3.31b). The dimeric form of wild type (but not ts1 mutant) was consistently detected from several batches of purified enzyme. It is possible that the geometry of cysteine residues in the ts1 mutant enzyme are disturbed, and consequently, has affected the occurrence of inter-chain disulphides.

In an attempt to isolate the dimeric isoform, 200µl of recombinant wild type protease (from an estimated 0.5mg/ml stock solution, figure 3.32a(i)) was injected into a pre-equilibrated (150mM NaCl; 50mM Tris-HCl, pH 8.0) Superdex-75 gel filtration column (section 2.1.7iii). The flow rate was 0.5ml/min, with 0.5ml fractions collected. Fractions 12 to 16 were examined by Western blotting using antibody OA10b3 (figure 3.32a(ii)). The same fractions were examined in the absence of ß-MeSH (figure 3.32b) and after the addition of pVI-ct (figure 3.32c). It was evident that fractions 12 and 13 contained the dimeric form of the enzyme only, which after pVI-ct addition, appeared to be converted into a monomeric form that was presumed to represent the activated enzyme. This was suggestive that Cys-104 was involved in the inter-chain disulphide exchange required for pVI-ct binding and dimerisation. In addition to the isoform that migrated at 23kd, fractions 14 and 15 also contained a faster migrating form that was assumed to contain one or more intra-molecular disulphides. Only this form and the dimeric form were detected in fraction 16. It was unclear whether pVI-ct addition affected the gel mobility of the fast migrating oxidised isoform. Fraction 14 was found to be active after pVI-ct addition, and exhibited minimal activity in the absence of pVI-ct. No activity was detected from fractions 12 and 16 after pVI-ct addition, although this was likely due to the low concentrations of enzyme present in both samples.

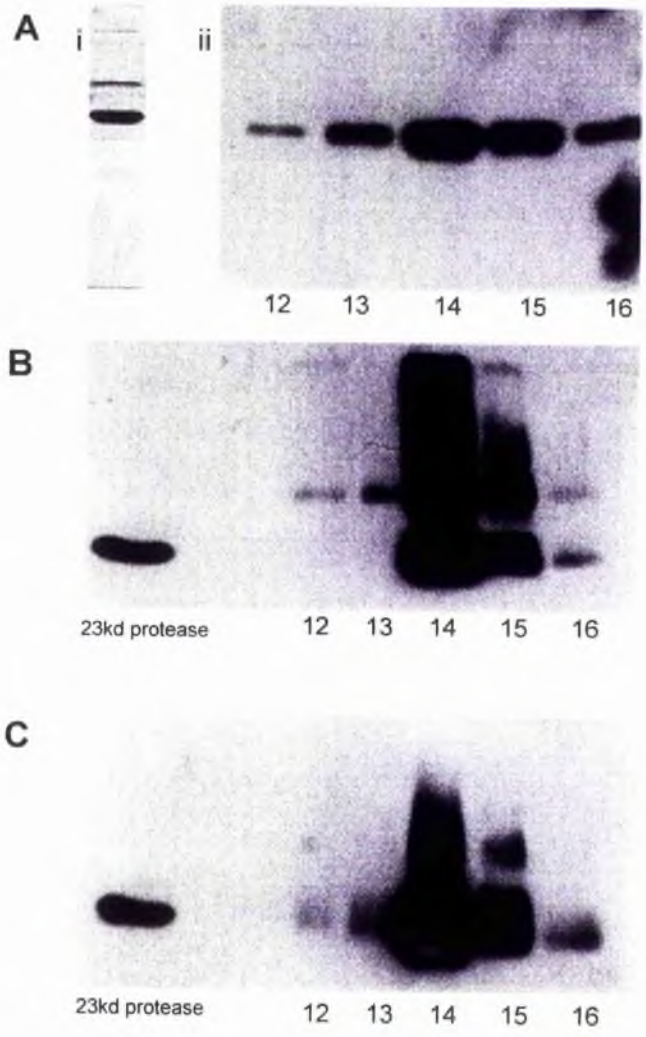

Figure 3.32: Isolation of the dimeric form of recombinant wt 23kd protease. Part A (i): 10µl sample of recombinant wt 23kd protease (Coomassie blue stained 15% SDS-PAGE). Part A (ii): Immunoblot (OA10b3) of eluted fractions 12 to 16 (section 2.1.7iii). 10µl samples from the same fractions were also electrophoresed under denaturing conditions without reduction (immunoblot B) and after addition of pVI-ct (final concentration of 0.2mM)/without addition of ß-MeSH (immunoblot C).

Further evidence to support the suggestion that Cys-104 may be directly involved in dimerisation is given in figure 3.33. Wt 18 and ts1 25 were treated with diamide, pVI-ct, and ß-MeSH as described previously. When diamide (10mM final concentration) was added to pre-activated enzyme no dimers were detected. However, it was clear from the immunoblots that diamide addition had caused the pre-activated wt 18 and ts1 25 enzymes to migrate more slowly than the non-activated diamide treated wt 18 and ts1 25 equivalents. Interestingly,

addition of pVI-ct to diamide treated protease did not lead to the conversion of the dimeric form to the activated monomer as previously observed in non-treated samples, although again, an aberrant gel mobility was evident. It is possible that the inter-chain disulphide is extremely stable in the presence of diamide resulting in the inability of pVI-ct to convert the protease to the inactive form. It was of particular interest that there did not appear to be any difference in mobilities of the fast migrating forms of wt 18 and ts1 25. This suggested that both contained the same number of intra-chain disulphides and/or free thiols in both the diamide treated and non-treated samples. It was also apparent that fully reduced/denatured wt 18 and ts1 25 enzymes exhibited the same gel mobility as the non-reduced/denatured heterodimer.

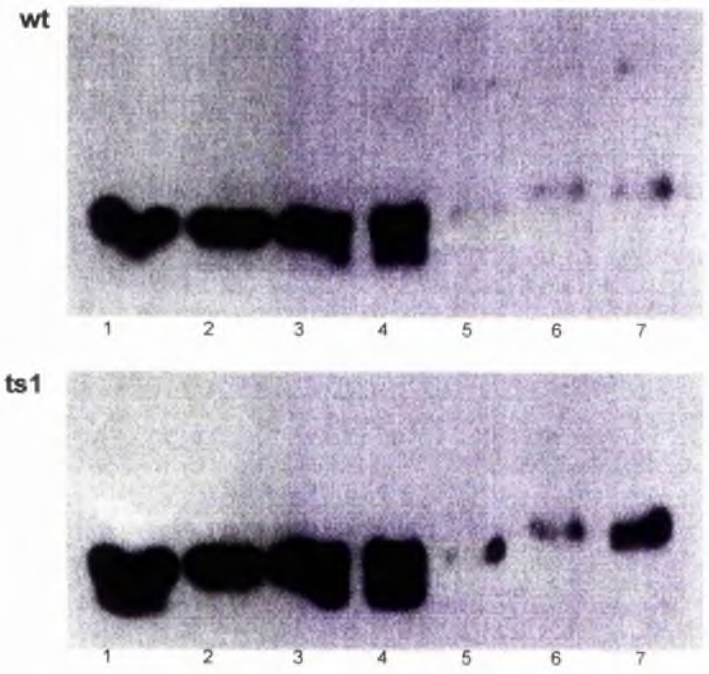

Figure 3.33: Redox modulation of recombinant wt and ts1 23kd protease. 10µl samples of wt 18 and ts1 25 were electrophoresed (15% SDS-PAGE) as non-treated (lane 1), reduced (ß-MeSH added to gel loading buffer)(lane 2), activated (0.2mM pVI-ct/1mM ß-MeSH in assay buffer)(lane 3), non-activated (1mM ß-MeSH in assay buffer)(lane 4), oxidised (10mM diamide)(lane 5), activated then oxidised (0.2mM pVI-ct added then incubated for 5 minutes before addition of 10mM diamide)(lane 6), and oxidised (10mM diamide added and sample incubated for 5 minutes) before addition of pVI-ct (0.2mM pVI-ct)(lane 7). All incubations prior to electrophoresis were 5 minutes in duration at room temperature. Except for fully reduced samples, no ß-MeSH was added to gel loading buffer. The exposure time was approximately one hour.

The Ad2 protease contains eight cysteines (figure 3.30), three of which are highly conserved (Cys-104,-122, and -126), four others are less conserved (Cys-17, -40, -67, and -127), and one is unique to the Ad2 protease (Cys-199). In order to determine which cysteines were involved in intra- and/or inter-chain disulphides, protease mutants C17A, C40A, C67A, C104S, C104/122S, C122S, C126A, C104/126A, C126/127A, C127A, and C199A (site directed mutagenesis had previously been carried out by Grierson *et al* (1994)) were expressed, then purified using the methods outlined in section 2.1.7. It is noteworthy that low yields of purified mutants C67A and C126A were obtained. It was not determined whether this was due to low levels of expression, or if mutants were insoluble and retained in lysed cell pellets. All of the protease mutants (including ts1 25), and two sources of wild type enzyme (wt 18 and wt 6 (donated by Dr.Munir Iqbal, University of St.Andrews)) were electrophoresed under denaturing conditions, then electroblotted, and examined using an antibody mix of OA10b3/OC11b11. As expected, the two close migrating isoforms of wt 18 and ts1 25, and the dimeric form of wt 18 were detected from the non-treated samples (figure 3.34). The three isoforms were also detected with mutants C199A, C17A, C40A, C127A and surprisingly C104S. This suggesed that these cysteine residues were not required for intra- and/or inter-chain disulphides. The faster migrating isoform of the protease (which was assumed to be the oxidised monomer) was absent with mutants C67A, C126A and the double mutant C126/127A. It was less apparent whether this isoform was absent with mutants C122S and C104/122S. The absence of the oxidised monomer was suggestive that these cysteine residues were required for intra-chain disulphides. In addition, the dimeric form of the enzyme was not detected with mutants C67A, C126A or C126/127A.

Keyvani-Amineh *et al* (1996) noted that the fast migrating (apparent 12kd) isoform was absent when mutants C67G, C126G and C104G (later re-identified as C122G) were electrophoresed under denaturing conditions. The authors did not specify whether or not this was due to low levels of expression and/or insolubility of the enzyme, but did suggest that these residues may be important for disulphide bond formation. An examination of the atomic structure of the activated 23kd protease revealed that Cys-122 and Cys-126 are in close proximity, and therefore may form an intra-chain disulphide upon oxidation. Interestingly, the proline rich region (P137-P165) loops around ß-sheet S6, and therefore the ts1 mutant

P137L substitution in this region, may exert conformational constraints on a-helix H4, and consequently affect the orientation of Cys-122.

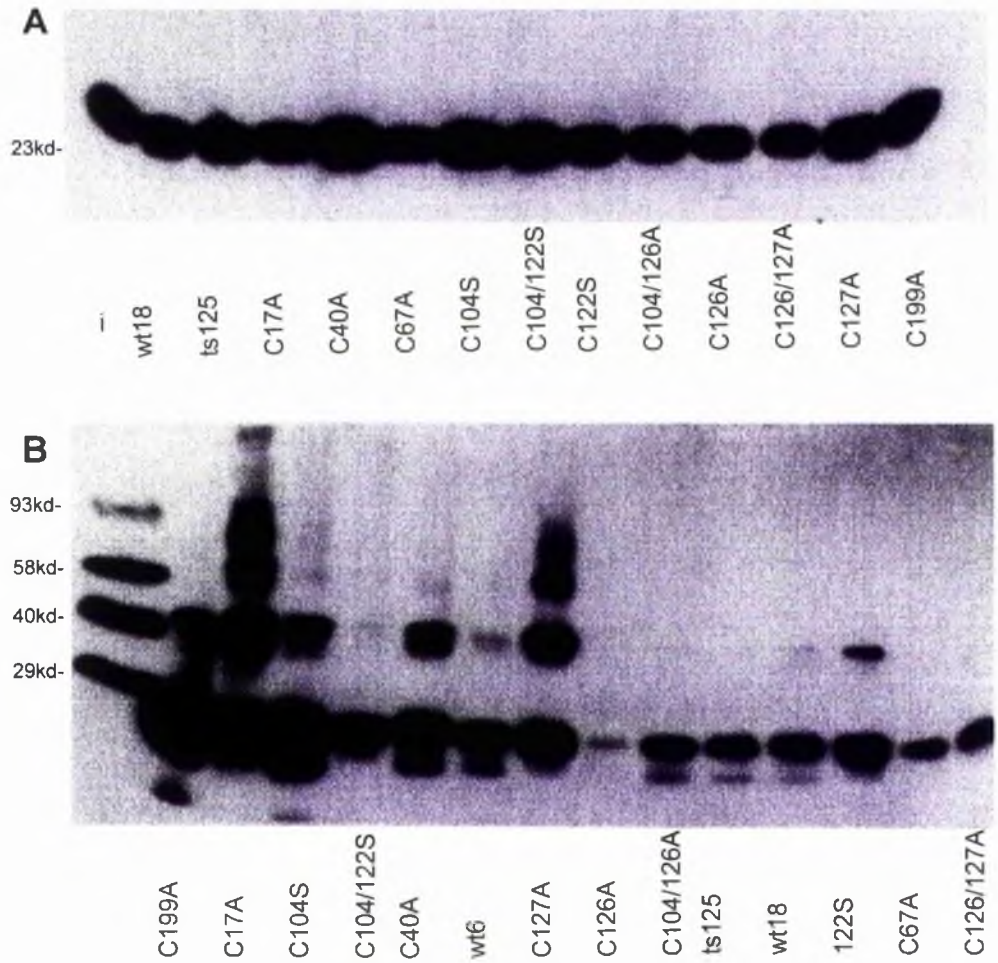

Figure 3.34: Isoforms of site directed mutants. Cysteine mutants were expressed and purified using the methods described in section 2.1.3 and 2.1.7. Samples were electrophoresed after addition of ß-MeSH to the gel loading buffer (part A), or in the absence of reducing agent (part B). Prestained molecular weight markers (lane i) in immunoblot A (probed with OA10b3) confirmed that all protease samples had an Mr of 23kd. Biotinylated molecular weight markers are included in blot B.

Results presented in this section have suggested that the likely candidates for intra- and/or inter-disulphide bond formation are Cys-67, Cys-122, Cys-126 and Cys-104. These results were based solely on SDS-PAGE and immunoblotting analysis, and to implicate these cysteine residues directly requires other methodological approaches. For instance, chemical

determination of disulphides involves the disruption of protein conformation, and degradation of the protein into peptides, whilst ensuring that manipulations do not alter the disulphide bonds that were initially present. Thiols are blocked using thiol reagents such as iodoacetate or iodoacetamide, thus minimalising the likelihood of disulphide rearrangements before identifying peptides that contain cysteine residues of interest. This type of approach may provide further information regarding the involvement of particular cysteines in intra-chain disulphide bond formation, and consequently, the effects of the P137L substitution on ts1 mutant protease structure.

The relevance of results presented in this section to the role of the protease in virus infected cells is discussed in section 4.

3.3 Subcellular localisation of the Ad2 23kd protease.

3.3.1 Morphology of an adenovirus infected cell.

i) Determination of intranuclear structures by electron microscopy (EM):

The eukaryotic cell nucleus performs a series of tasks including replication and packaging of DNA and transcription, splicing, polyadenylation, and transport of RNA. The nucleus is organised into a series of structural domains of which the nucleolus is best characterised. Much of the nuclear interior is occupied by chromatin (in various degrees of condensation) and interchromatin regions that contain several characteristic structures, including perichromatin fibrils and granules, interchromatin granules, and other nuclear bodies including coiled bodies (Brasch and Ochs, 1992; Chaly and Chen, 1993; Puvion-Dutilleul and Puvion, 1995; Bridge and Pettersson, 1995). In this study, mock infected cells, and non-infected cells, were examined to form a basis for comparison with nuclei of infected cells. By conventional EM, the nuclei of mock infected HeLa cells exhibited few distinctive features (figures 3.35 and 3.36). The nucleoplasm was quite homogenous in appearance with condensed chromatin, nucleoli and nuclear bodies detected. It was beyond the scope of this study to accurately identify specific structures within non-infected HeLa cell nuclei (for instance coiled bodies), however, based on comparisons with micrographs presented in publications by Brasch and Ochs (1992) and Chaly and Chen (1993), it appears likely that

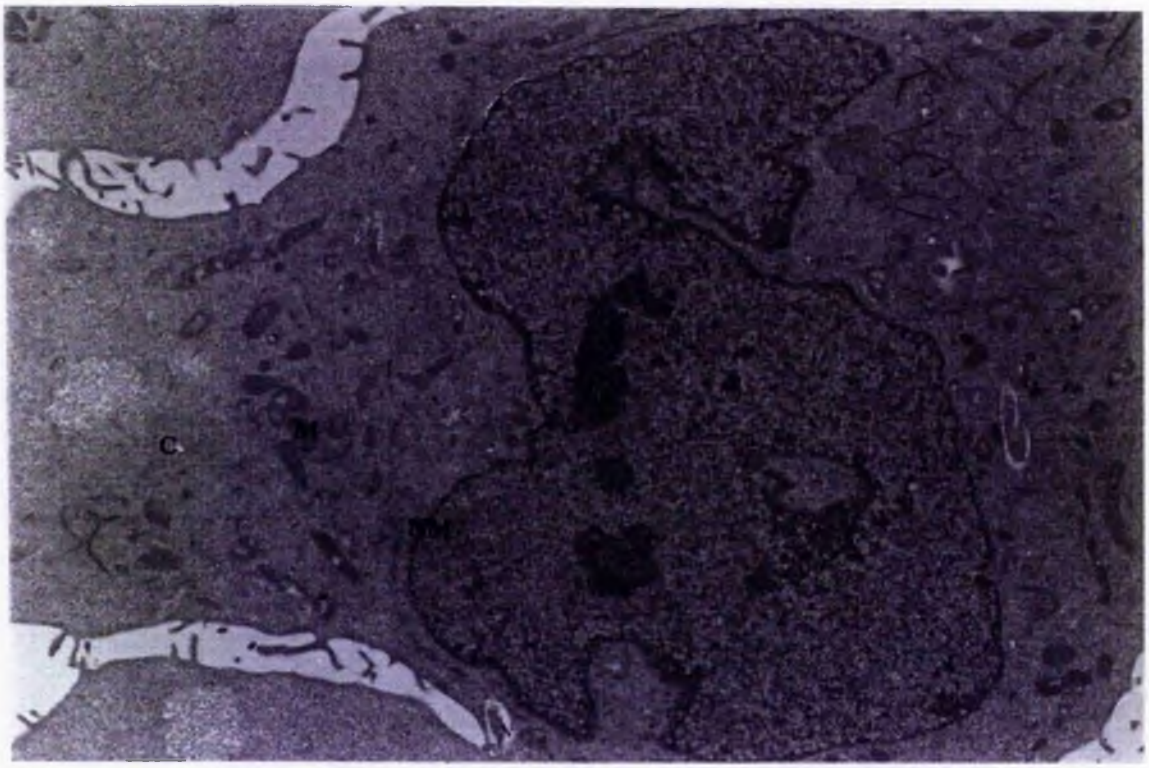

Figure 3.35: Electron micrograph of a mock-infected HeLa cell. Mock-infected HeLa cells were fixed with 2% paraformaldehyde/ 0.05% glutaraldehyde (pH 7.4) for one hour then dehydrated and embedded in epon as described in section 2.8. Thin sections were contrasted with uranyl acetate/lead citrate then viewed at 80kv. The nucleolus (Nu), regions containing condensed chromatin (CC), nuclear membrane (NM), cytoplasm (C), and mitochondria (M) are easily identified. Automatic exposure at x5700 magnification.

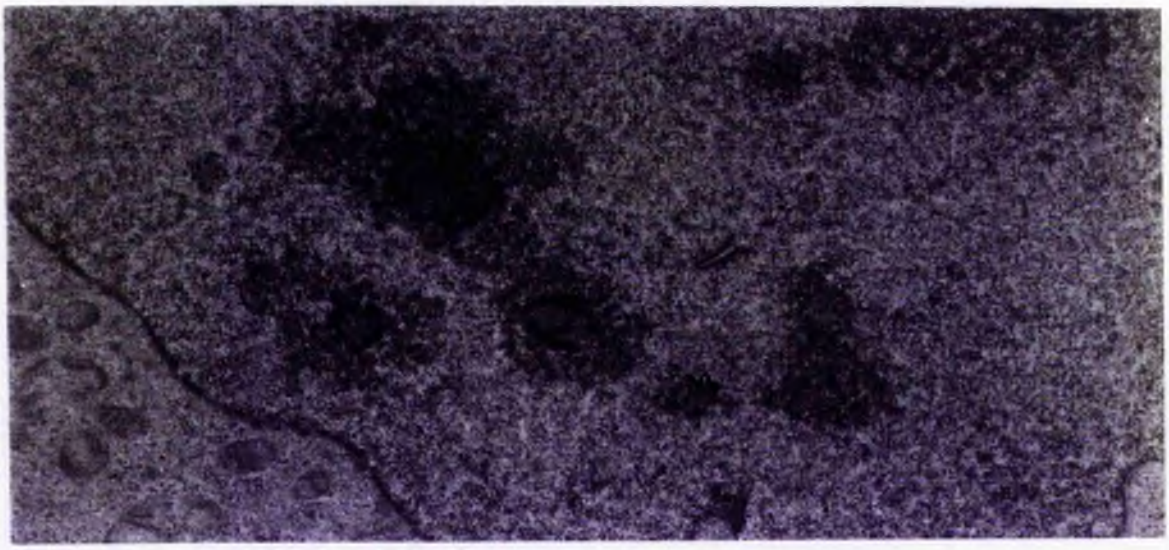

Figure 3.36: Intranuclear domains of the non-infected HeLa cell. Higher magnification (x25000) view of the nucleus of a HeLa cell from the same thin-section as that shown in figure 3.35. Nucleoli (Nu), condensed chromatin (CC), and possible nuclear bodies (Nb). Automatic exposure.

many of the domains shown in figures 3.35 and 3.36 are genuine and are not artefacts of fixation methods, or dehydration and/or embedding in hydrophobic resin.

Nuclei of adenovirus infected cells progressively accumulate new induced structures as a consequence of viral replication. Due to the low multiplicity of infection (10 p.f.u/cell) used during the course of this study, some of these structures were detected, and are highlighted in figures 3.37 and 3.38.The earliest ultrastructural changes detected are small, irregularly shaped masses of thin fibrils (Puvion-Dutilleul and Puvion, 1995) that rapidly increase in size and become pleomorphic, appearing as crescents, rings and spheres (figure 3.37). These fibrillar inclusions contain DBP-ssDNA (ssDNA accumulation sites are discussed in more detail in section 3.3.4) and are present in the fibrillogranular network of the peripheral replicative zone, which appears to be the main site of viral replication and transcription. At late stages of nuclear transformation, DBP-ssDNA accumulation sites are located at the periphery of the viral genome storage sites (which are frequently associated with crystalline arrays of virus particles), and become smaller and more homogenous in shape, appearing as globular inclusions rather than crescents and rings (figure 3.38). Viral genome storage sites are typically detected within nuclei after 20 h.p.i (Bridge and Pettersson, 1995), and it has been suggested that DNA from these compartments may be incorporated into virions. Structures which are thought to be viral genome storage sites (VGSS) are highlighted in figures 3.37 and 3.38, although it should be noted that the identification of these structures is based only on comparisons with data presented by Chaly and Chen (1993) and Puvion-Dutilleul and Puvion (1995). However, a viral genome storage site identified by Puvion-Dutilleul *et al* (1995b) is shown in figure 3.53 (page 163).

Clusters of interchromatin granules are more discernible as infection progresses (figure 3.37) and have been shown to contain snRNP proteins, regardless of the stage of infection (Puvion-Dutilleul *et al.*, 1994). Electron microscopic studies of non-infected HeLa cells (Puvion-Dutilleul *et al.*, 1994; Rebelo *et al.*, 1996) have shown that snRNPs are present in clusters of interchromatin granules, interchromatin granule-associated zones, coiled bodies and perichromatin fibrils. It was not possible to accurately identify these structures in this study (figures 3.35 and 3.36), although in late-phase adenovirus infected cells the interchromatin granules and less commonly observed compact rings (not shown) were easily identified after comparing data presented here, and that provided by Chaly and Chen (1993)

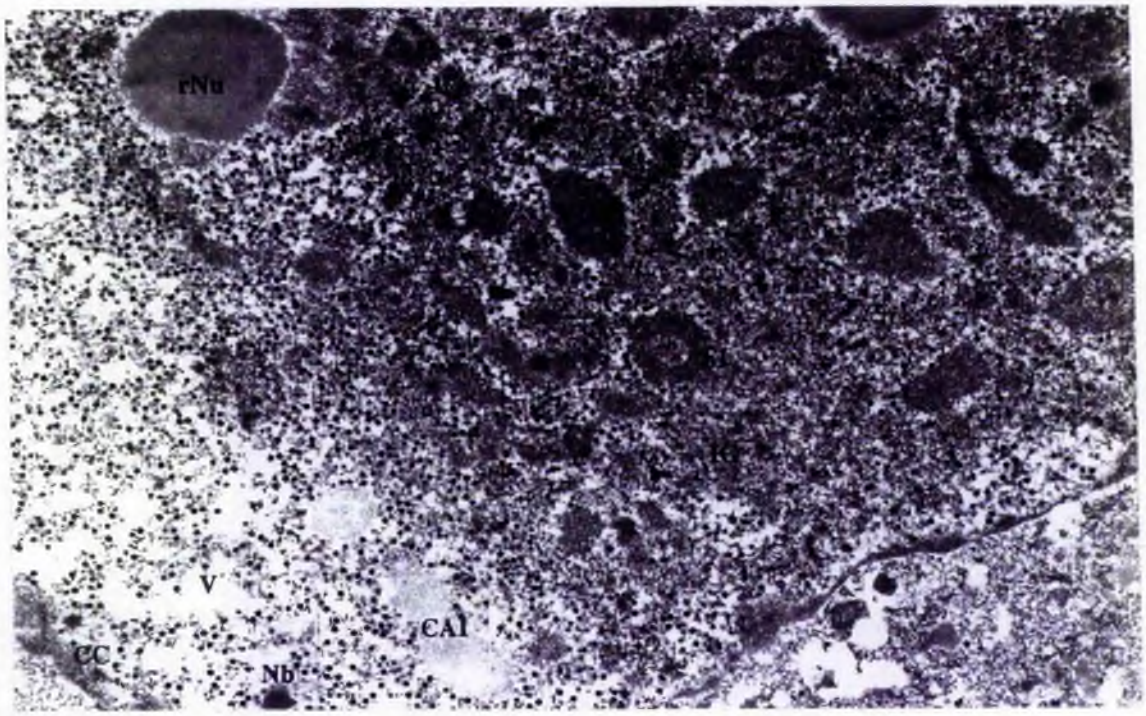

Figure 3.37: The nucleus of an adenovirus infected cell (I). Adenovirus infected HeLa cells (28 h.p.i) were fixed with 4% formaldehyde (pH 7.4) for 10 minutes then dehydrated, embedded, and contrasted as described in section 2.8. Thin-sections were viewed at 80kv. Residual nucleolus (rNu), ssDNA-accumulation sites (fibrillar inclusions; FI), interchromatin granules (IG),viral genome storage site (possible)(VGSS), clear amorphous inclusions (CAI), condensed chromatin (CC), and virions (V). Automatic exposure at x9100 magnification.

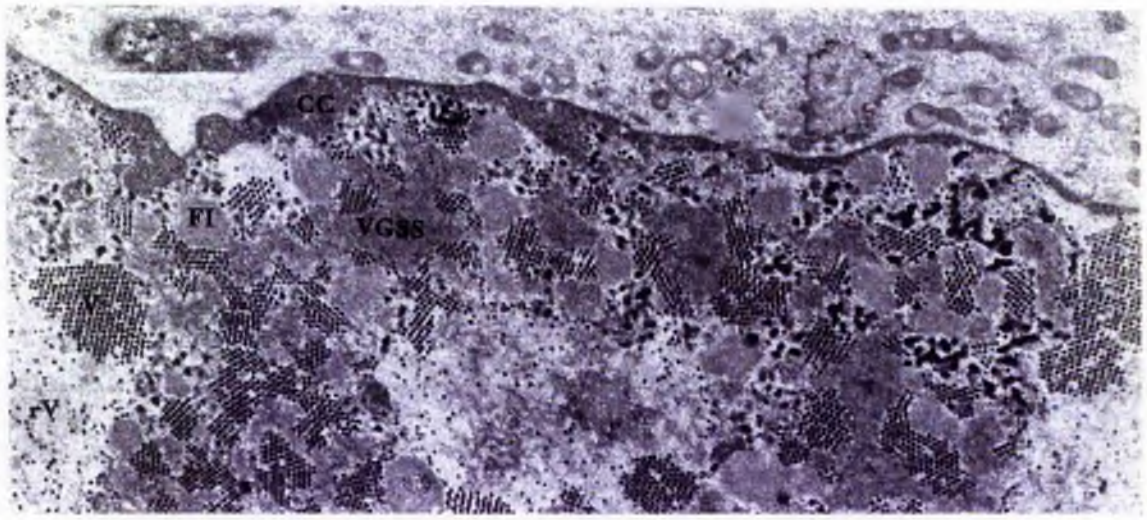

Figure 3.38: The nucleus of an adenovirus infected cell (II). Ad2 infected HeLa cells (28 h.p.i), were fixed with 2% paraformaldehyde/ 0.05% glutaraldehyde (pH 7.4) for one hour then dehydrated, embedded, and contrasted as outlined in section 2.8. Crystalline arrays of virions (V), randomly distributed virions (rV), condensed chromatin (CC), viral genome storage site (possible)(VGSS), and fibrillar inclusions (FI). viewed at 80kv, automatic exposure at x7100 magnification.

and Puvion-Dutilleul *et al* (1994). The latter authors have detected spliceosome components, viral RNA and poly(A)$^+$ RNA within the fibrillogranular network and clusters of interchromatin granules and suggest that these could be the sites of active splicing and/or post-splicing events. Pulse-chase labelling studies undertaken by the same authors (Puvion-Dutilleul *et al.*, 1992 and 1994) have also indicated that clusters of interchromatin granules might contribute to some sorting of viral RNA molecules before their transport to the cytoplasm.

During the course of an adenovirus infection nucleolar proteins (B23, NOR90, Pol1, and NuF1; Bridge and Pettersson, 1995) and nucleolus-associated proteins such as fibrillarin (Puvion-Dutilleul and Christensen, 1993) and P80-coilin (Rebelo *et al.*, 1996) are redistributed, some of which are later detected within and/or near ssDNA accumulation sites. Data is consistent with idea that adenovirus infection disrupts the organisation of the nucleolus (figure 3.37), with viral replication being associated with pseudonucleoli.

Many of the cellular and virus-induced structures emphasised within the micrographs presented so far, have been tentatively compared with published data from studies which have been primarily focused on the elucidation of structure-function relationships of specific cellular compartments involved in the replicative cycle of the virus. Comparisons are made difficult for several reasons. Firstly, other studies have described the formation of several types of nucleoplasmic inclusions that differ in size, morphology, and in some instances, whether they incorporated [^{3}H]uridine, [^{3}H]thymidine, or neither. Since these studies used different cell types, Ad strains, stages of infection (most studies have focused on events occurring from 1 to 20 h.p.i), and inclusion body nomenclatures, it is difficult to compare the results directly.

Comparisons were made more difficult when different methods of fixation (in particular if cryo-fixation was used instead of chemical fixation), or different types of embedding media were utilised (in most studies hydrophilic acrylic resins or hydrophobic epoxy resins were used, although in a few cases cryo-electron and embedment-free section electron microscopy techniques were employed), and whether or not thin sections were contrasted, or post-fixed with osmium tetroxide. Even during the course of this study there were observed differences in the apparent structure of clear amorphous inclusions (figure 3.37), which appeared to be

dependant on the chemical fixative used, and/or the duration time of fixation. This is discussed in detail below.

ii) The balance between fine structure preservation and immunolabelling:

Chemical fixation of non-infected, and adenovirus infected, HeLa cells is the only method by which intracellular structure can be preserved to as near as possible the 'native' organisation, as well as protecting the intracellular structure against later stages of preparation for immunocytochemical analysis. However, treatment with many chemical fixatives can lead to the physical loss of epitopes such as by extraction of molecules and structures (which can occur with osmium tetroxide treatment), volume and shape changes in cellular architecture, steric hindrance of epitopes by fixative-induced cross-links, and chemical alteration of epitopes by direct reaction with fixatives (fixative-induced denaturation effects).

It was thought possible that any one of these effects might be observed during the course of this study and therefore several chemical fixatives were utilised. 4% formaldehyde, 4% paraformaldehyde, 1% glutaraldehyde and 2% paraformaldehyde/0.05% glutaraldehyde (prepared fresh prior to use as described in section 2.7.5) were all used, with the duration times of fixation being 10, 30 and/or 60 minutes. In some instances, fixed cells were post-fixed osmium tetroxide prior to embedment.

The fine structural preservation of 4% formaldehyde fixed (10 minutes fixation time) infected (figure 3.39) and non-infected (not shown) HeLa cells was poor in comparison with 1% glutaraldehyde and 2% paraformaldehyde/0.05% glutaraldehyde fixed cells. This may be in part due to the extraction of soluble antigens from the cytoplasmic and nucleoplasmic compartments. For instance, although formaldehyde penetrates both the cytoplasmic and nucleoplasmic compartments relatively quickly, the time taken for optimal fixation is slow in comparison to glutaraldehyde fixation. There appears to be two different modes by which formaldehyde cross-links amino groups of proteins, depending on the concentration of fixative (Griffiths, 1993). At concentrations (below 2%) where the monomer methylene glycol predominates, the major types of cross-links are methylene bridges. Evidence suggests that methylene bridges form relatively slowly and inneficiently in comparison to polyoxymethylene cross-bridges which are rapidly formed when high (>10%) concentrations of formaldehyde are used.

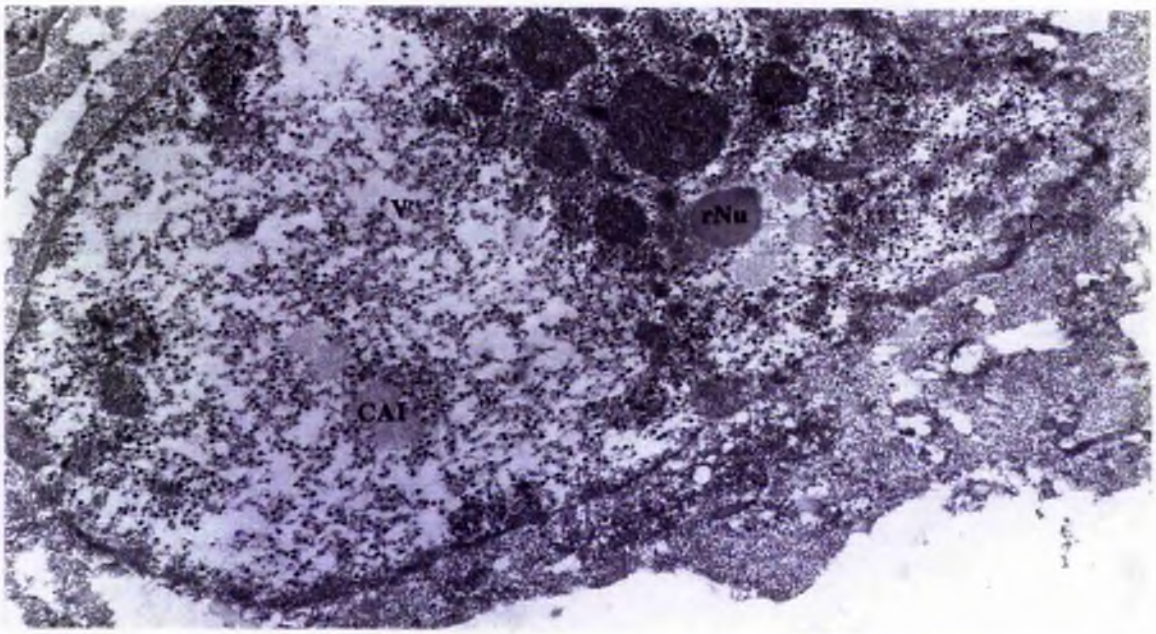

Figure 3.39: Preservation of nuclear structure after 4% formaldehyde fixation. Ad2 infected HeLa cells (28 h.p.i) were fixed with 4% formaldehyde (pH 7.4) for 10 minutes then dehydrated, embedded, and contrasted as described in sections 2.7.5 and 2.8. Residual Nucleolus (rNu), virions (V), condensed chromatin (CC), and clear amorphous inclusions (CAI). Viewed at 80kv. Automatic exposure at x7100 magnification.

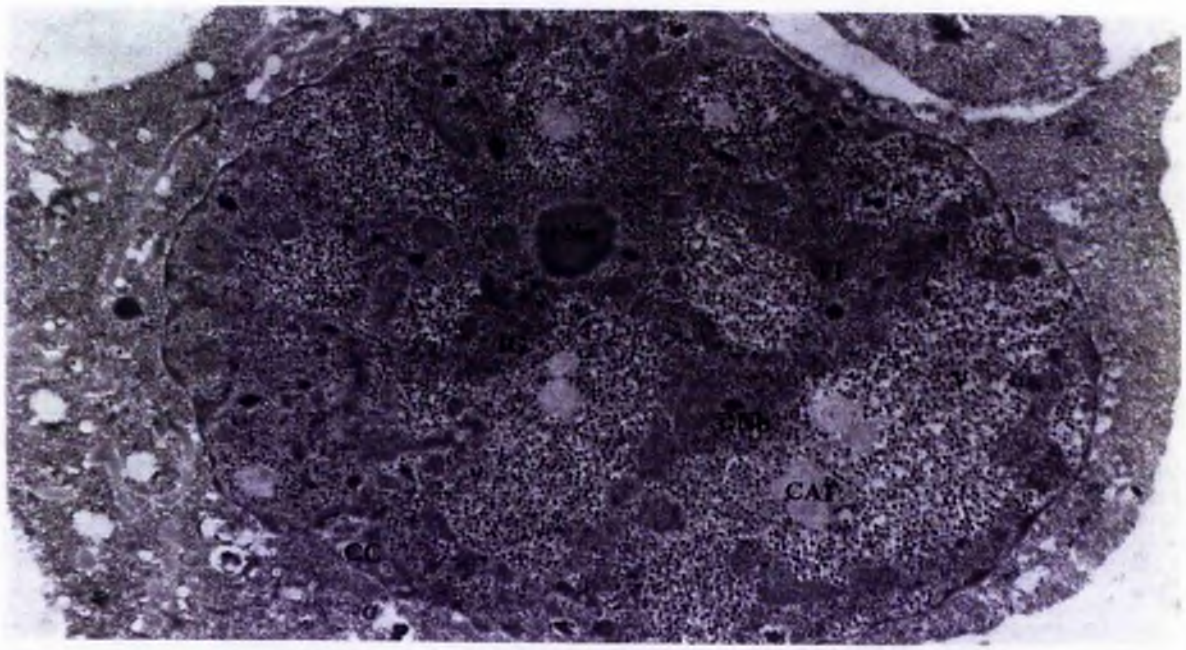

Figure 3.40: Fine structural preservation after 2% paraformaldehyde/ 0.05% glutaraldehyde fixation. Infected HeLa cells (28 h.p.i) were fixed as described in section 2.7.5 for 10 minutes prior to dehydration and embedding. Residual nucleolus (rNu), clear amorphous inclusions (CAI), electron dense nuclear bodies (DNb), interchromatin granules (IG), fibrillar inclusions (FI),condensed chromatin (CC), and virions (V). Viewed at 80kv. Automatic exposure at x7100 magnification.

Formaldehyde cross-links tend to be less stable than those of glutaraldehyde, as formaldehyde will most likely give rise to networks of linear cross-links as opposed to the branched cross-links that predominate within glutaraldehyde fixed cells. The linear cross-links are generally thought to be more amenable to access of antibodies to antigen, and therefore there is a balance between access of antibody to available antigen and preservation of fine structure to determine the localisation of the antigen of interest.

Many of the intranuclear structures that were identified in figures 3.37 and 3.38 are less discernible in figure 3.39. However, it is possible to distinguish clusters of interchromatin granules, ssDNA accumulation sites, and what is thought to be the late-phase nucleolus. The clear amorphous inclusions are also evident (typically found within regions of high virion density, and interestingly, close to the nucleolus), and have a fibrillar appearance. Typically, several clear amorphous inclusions were observed to be joined together, often in pairs, although in many instances 'chains' of several inclusions were detected. The nature and possible function of these structures is discussed in more depth in section 3.3.2. It is also noteworthy that many of the intracytoplasmic structures are missing and/or difficult to identify within 4% formaldehyde fixed cells.

Fine structural preservation was improved with the 2% paraformaldehyde/0.05% glutaraldehyde mixture (10 minutes fixation time), with very little extraction of intracellular antigens (figure 3.40). All the virus-induced structures which had been previously identified were observed. Importantly, the clear amorphous inclusions had a fibrillar appearance, and were surrounded by high densities of virus particles. The clear amorphous inclusions had a different appearance within cells fixed (same fixative) for 60 minutes instead of 10 minutes (figure 3.41). The inclusions appeared to be less fibrillar, appearing as opaque circles that either appeared as single inclusions or joined with other identical inclusions. Likewise, in 1% glutaraldehyde fixed cells (10 minutes duration) the amorphous inclusions also had an opaque appearance (figure 3.42) with no discernible fibrillar structure.

Glutaraldehyde in solution is uncharged and can rapidly cross all biological membranes. It can produce significant intracellular cross-linking in a matter of seconds and forms a large, three-dimensional network of cross-links in the cytoplasm in tenths of seconds (Griffiths, 1993). The observed differences in the structural composition of clear amorphous inclusions using the different fixatives is difficult to explain. The differences are more evident

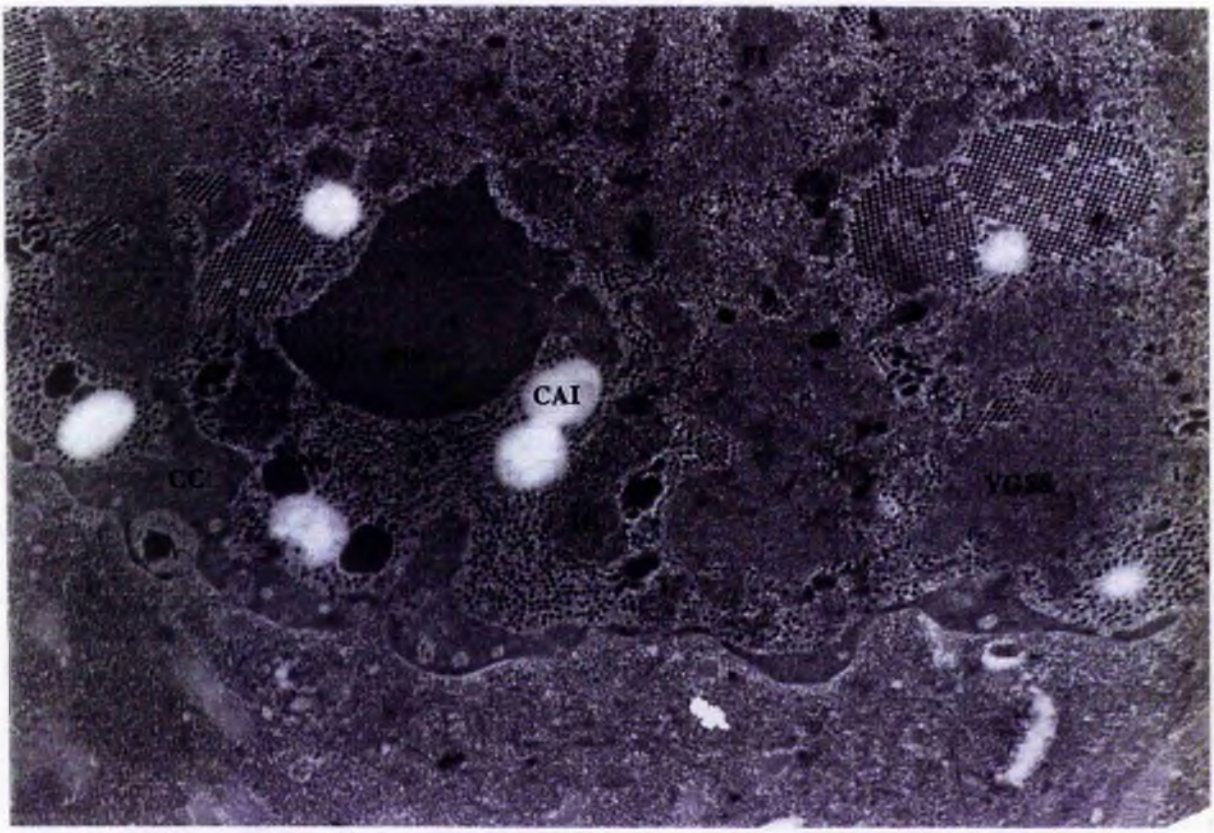

Figure 3.41: Fine structure of virus-induced inclusions. Ad2 infected HeLa cells (28 h.p.i) were fixed with 2% paraformaldehyde/0.05% glutaraldehyde (pH 7.4) for one hour, then dehydrated, embedded, and contrasted as described in sections 2.7.5 and 2.8. Residual nucleolus (rNu), clear amorphous inclusions (CAI), electron dense nuclear bodies (DNb), interchromatin granules (IG), ssDNA-accumulation sites (FI), possible site of condensed cellular chromatin (CC),possible viral genome storage sites (VGSS) , randomly distributed virions (rV) and crystalline arrays of virion particles (V). Viewed at 80kv. Automatic exposure at x9100 magnification.

after post-fixation with osmium tetroxide. Clear amorphous inclusions within 2%paraformaldehyde/0.05% glutaraldehyde fixed cells (10 minutes) that were post-fixed with osmium tetroxide (section 2.7.5) were darker and more fibrillar in appearance (figure 3.43). The characteristic appearance of many structures, in particular membranes, in epoxy resin sections depends to a large extent on the effect of osmium tetroxide. Although it is unclear what protein(s) clear amorphous inclusions are comprised of, osmium tetroxide is known to be reactive to nucleophiles such as amino and sulphydryl groups and with unsaturated acyl chains of membrane lipids (Griffiths, 1993).

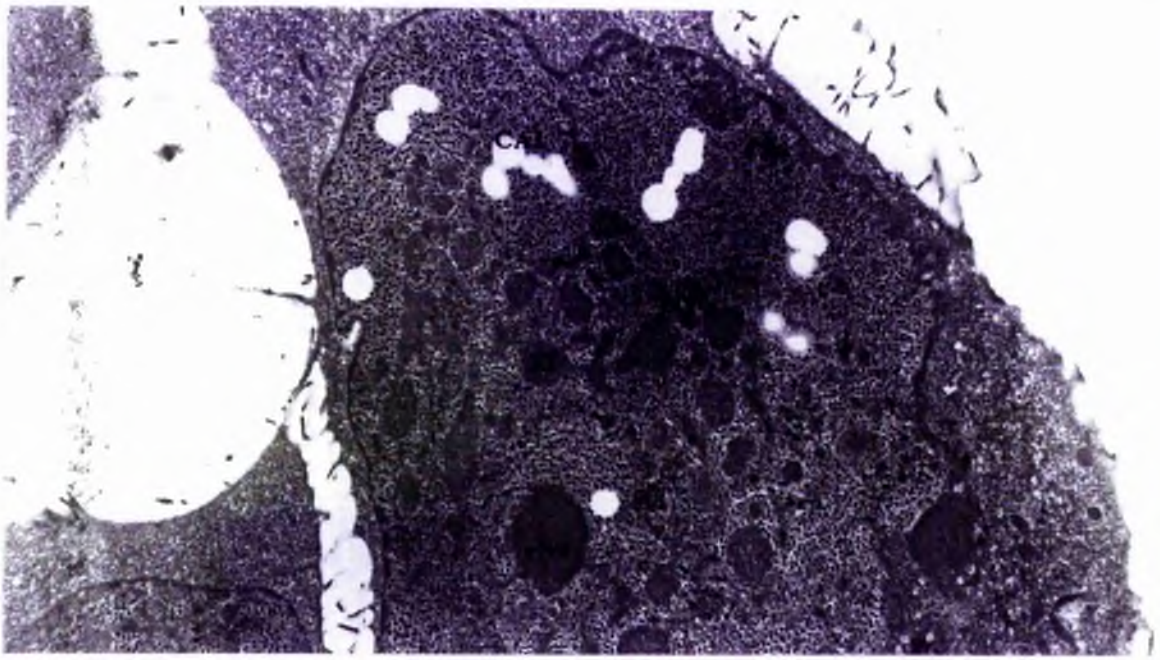

Figure 3.42: Fine structural preservation with 1% glutaraldehyde fixation. Infected HeLa cells (28 h.p.i) were fixed as described in section 2.7.5 for 10 minutes. Residual nucleolus (rNu), electron dense nuclear bodies (DNb), clear amorphous inclusions (CAI), fibrillar inclusions (FI). Viewed at 80kv. Automatic exposure at x5700 magnification.

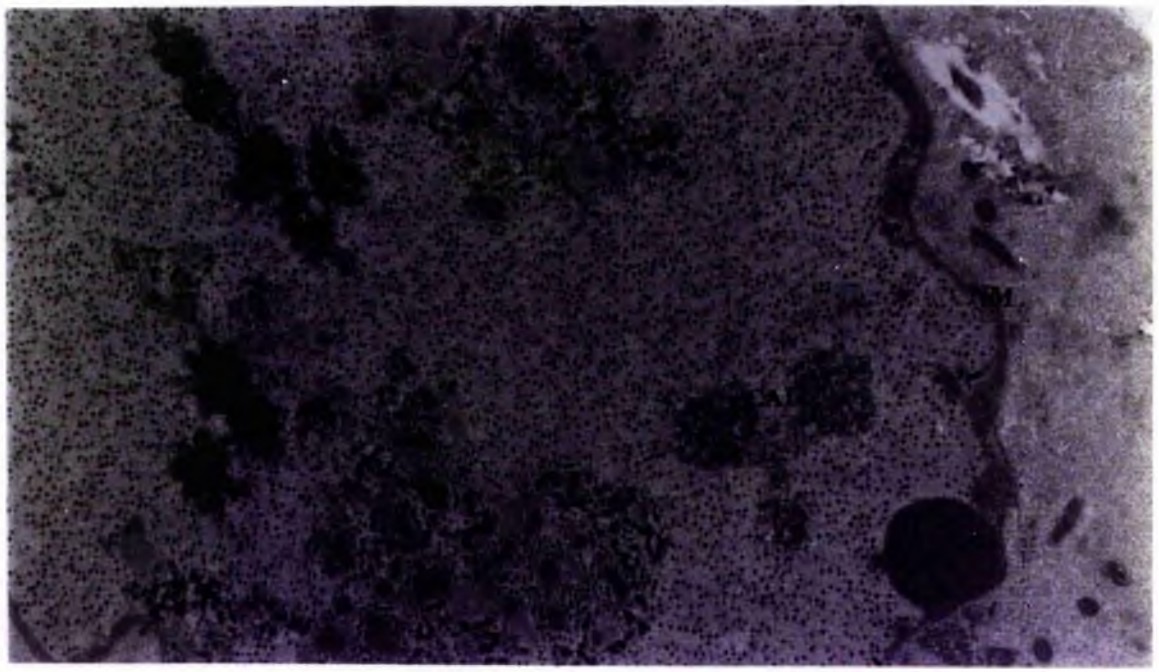

Figure 3.43: Post-fixation with osmium tetroxide. Ad2 infected HeLa cells (28 h.p.i) were fixed with 2% paraformaldehyde/0.05% glutaraldehyde (10 minutes) then post-fixed with osmium tetroxide as described in section 2.7.5. Electron dense fibrillar structures thought to correspond to clear amorphous (CAI) and the 'classical' railway track appearance of the nuclear membrane (NM) are changes thought to be dependent on osmium tetroxide fixation. Viewed at 80kv. Automatic exposure at x7100 magnification.

The ability of most antibodies to bind antigens is generally considered to be far less affected by formaldehyde treatment when compared to glutaraldehyde treatment (Griffiths, 1993). This was found to be the case in this study with the level of immunolabelling of 23kd protease and protein pVIII on thin sections of 4% formaldehyde fixed cells (figure 3.44a) significantly greater than that of cells that had been fixed with 1% glutaraldehyde (figure 3.44b) (fixation times of 10 minutes). The double immunolabelling technique for electron microscopy (Monaghan and Robertson, 1993) was used throughout the immunocytochemical study (section 3.3.2). It is clear from figure 3.44b that pVIII was not immunodetected within 1% glutaraldehyde fixed cells despite a significant level of immunolabelling being detected within cells fixed with 4% formaldehyde.

It has been estimated (Griffiths, 1993) that approximately 15% of epitopes presented on the surface of thin sections of cells fixed by 1% glutaraldehyde are available for antibody binding, partly as a consequence of the nature of cross-links, but also because glutaraldehyde, like osmium tetroxide, can significantly affect the secondary and tertiary structures of many proteins. However, because the fine structural preservation within formaldehyde fixed cells was relatively poor in comparison to glutaraldehyde fixed cells (particularly within nucleoplasmic regions containing high densities of virions), a compromise was made with the fixative 2%paraformaldehyde/0.05% paraformaldehyde (10 and 60 minutes fixation times) being preferred for immunolabelling studies. The results of these studies are presented and discussed in the following sections. It is noteworthy that neither the 23kd protease or pVIII were detected in infected cells that were fixed with 2% paraformaldehyde/ 0.05% glutaraldehyde (10 minute fixation) then post-fixed with osmium tetroxide (figure 3.44c).

3.3.2 Colocalisation of the viral protease and pVIII/VIII.

i) Intranuclear colocalisation within clear amorphous inclusions:

Intranuclear and/or nucleus associated punctate spot and 'thread like' immunofluorescent staining patterns were detected using antibodies OA10b3 and GB4g4 within 4% formaldehyde fixed (10 minutes)/detergent permeabilised Ad2 infected HeLa monolayer cells late in infection (figure 3.45a). An identical immunofluorescent staining pattern for pVIII was

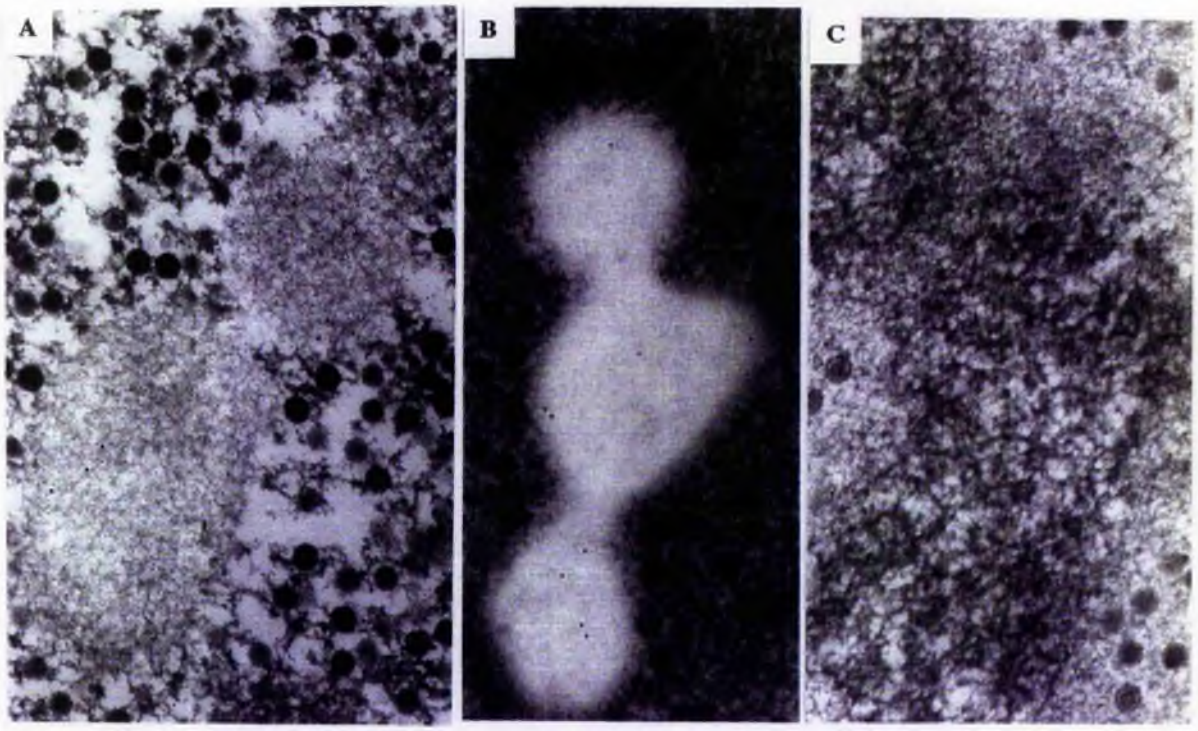

Figure 3.44: Immunocytochemical detection of pVIII and the 23kd protease. Ad2 infected HeLa cells (28 h.p.i) were fixed (10 minutes) with 4% formaldehyde (part A), 1% glutaraldehyde (part B) or 2% paraformaldehyde/0.05% glutaraldehyde and post-fixed with osmium tetroxide (part C). Double immunolabelling against pVIII (6nm gold particles) and 23kd protease (10nm gold particles) was performed as described in section 2.8.4. All thin-sections viewed at 80kv. Automatic exposures at x34000 magnification.

observed within the same cells (figure 3.45b), when both proteins were examined using the double immunolabelling technique for light microscopy (Jackson and Blythe, 1993).

The two step indirect method was used with unlabelled primary antibody (rabbit polyclonal antiserum specific for pVIII was kindly donated by W.S.A. Annan, University of St.Andrews) and labelled secondary antibody (Texas-red conjugated anti-rabbit immunoglobulin and FITC conjugated anti-mouse immunoglobulin). This method is generally considered to be more sensitive than the direct method because several secondary antibodies may react with different antigenic sites on the primary antibody . Additionally, the technique is more versatile than the direct method as the same labelled secondary antibody can be used with a variety of primary antibodies raised from the same animal species, as was the case throughout the course of this study.

The colocalisation of both proteins was examined further using the BIO-RAD MRC-600 laser scanning confocal imaging system. The fluorescent staining patterns of both proteins were

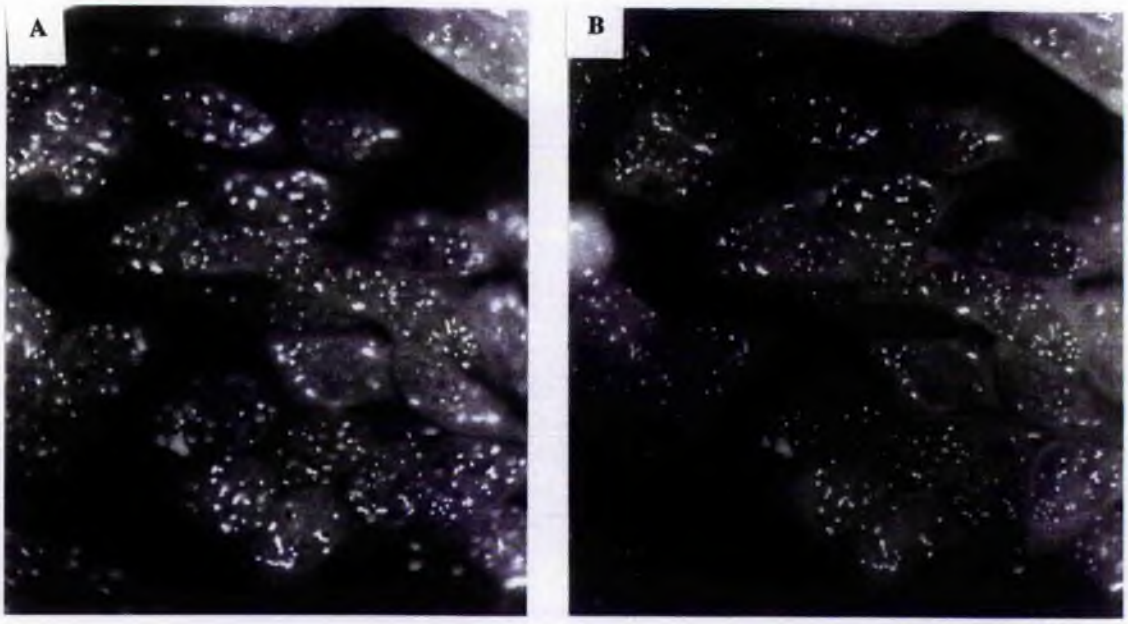

Figure 3.45: Colocalisation of pVIII and the 23kd protease (I). Ad2 infected HeLa cells (28 h.p.i) were fixed for 10 minutes using 4% formaldehyde. The methodology of immunofluorescent staining is descibed in section 2.8.2. Part A: Immunostaining of pVIII using anti-pVIII polyclonal antiserum and Texas-Red conjugated anti-rabbit IgG. Part B: immunodetection of the viral protease using cell culture supernatant containing antibody OA10b3 and FITC conjugated anti- mouse IgG. Automatic exposure times were typically 30 seconds for pVIII and 1.5 minutes for the viral protease. x40 objective.

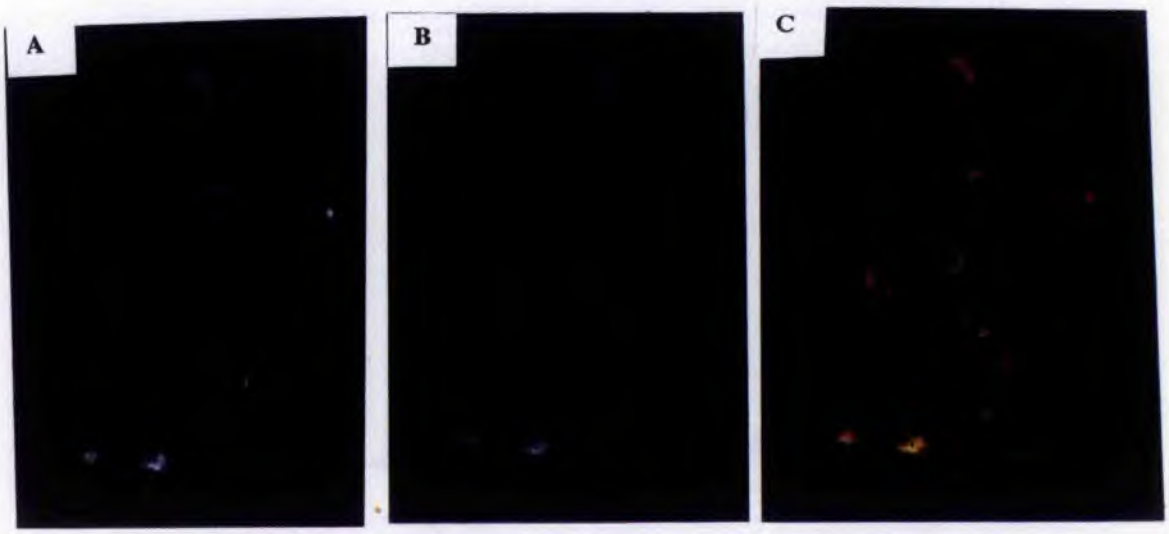

Figure 3.46: Colocalisation of pVIII and the 23kd protease (II). Ad2 infected HeLa cells (28 h.p.i) were fixed and treated as outlined in figure 3.45 and section 2.8.2. Immunolabelled cells were examined using the BIO-RAD MRC-600 laser scanning confocal imaging system at x100 magnification (oil immersion). Part A: pVIII. Part B: 23kd protease (stained using OA10b3). Part C: merge of both images with pVIII stained red, the viral protease stained green and colocalisation of both antigens identified through yellow fluorescent staining.

examined using a 100x oil immersion objective, recorded, stored (figure 3.46a and b) and merged (figure 3.46c). Colocalisation of pVIII and the viral protease was clearly evident and is indicated in regions of the cell highlighted in yellow. A disadvantage of the laser confocal system over conventional light microscopy is that fluorescent staining patterns within a single plane are recorded. Therefore, the threads of fluorescent staining characteristic to the 23kd protease and pVIII were less obvious. However, it was thought these images were more likely to resemble sections of ultrathin cell slices examined using immunocytochemistry.

As previously mentioned, both proteins were immunolocalised to clear amorphous inclusions (figure 3.47). The 23kd protease was not detected within or (associated with) any other nuclear structures using antibody OA10b3, with the exception of minor levels of immunolabelling at regions of high virion density (section 3.3.3). pVIII/VIII was also localised exclusively to clear amorphous inclusions, although similar to the viral protease, some immunolabelling of virions was detected. This suggested that the punctate spots and/or thread immunofluorescent staining patterns shown in figures 3.45 and 3.46 were likely to be immunolabelling of both proteins within these inclusions.

Interestingly, there appeared to be observable differences in the infrastructure of clear amorphous inclusions as highlighted in figure 3.47. Two inclusions with fibrillar arrangements of different contrasts appear to be linked, with the 23kd protease being localised (using antibody OA10b3) predominantly to the darker contrasted inclusion (dai). Significant immunolabelling of pVIII is observed in both, although the majority is associated with the light contrasted amorphous inclusion (lai). As mentioned in section 3.3.2, the fibrillar infrastructure was absent within clear amorphous inclusions after 2% paraformaldehyde/ 0.05% glutaraldehyde fixation (60 minutes). Significant immunolabelling of pVIII/VIII and 23kd protease was detected within these structures (figure 3.48) which had a 'thread like' appearance and were surrounded by virions.

The shape of clear amorphous inclusions within Ad2ts1 infected HeLa cells at 28 h.p.i differed markedly from the wild type equivalent (figure 3.49). The inclusions had an irregular appearance and perhaps more importantly were not immediately surrounded by virus particles. Although the 23kd protease (detected using OA10b3) and pVIII/VIII were immunolocalised to these domains (figure 3.50), the apparent levels of both proteins within these structures was significantly reduced.

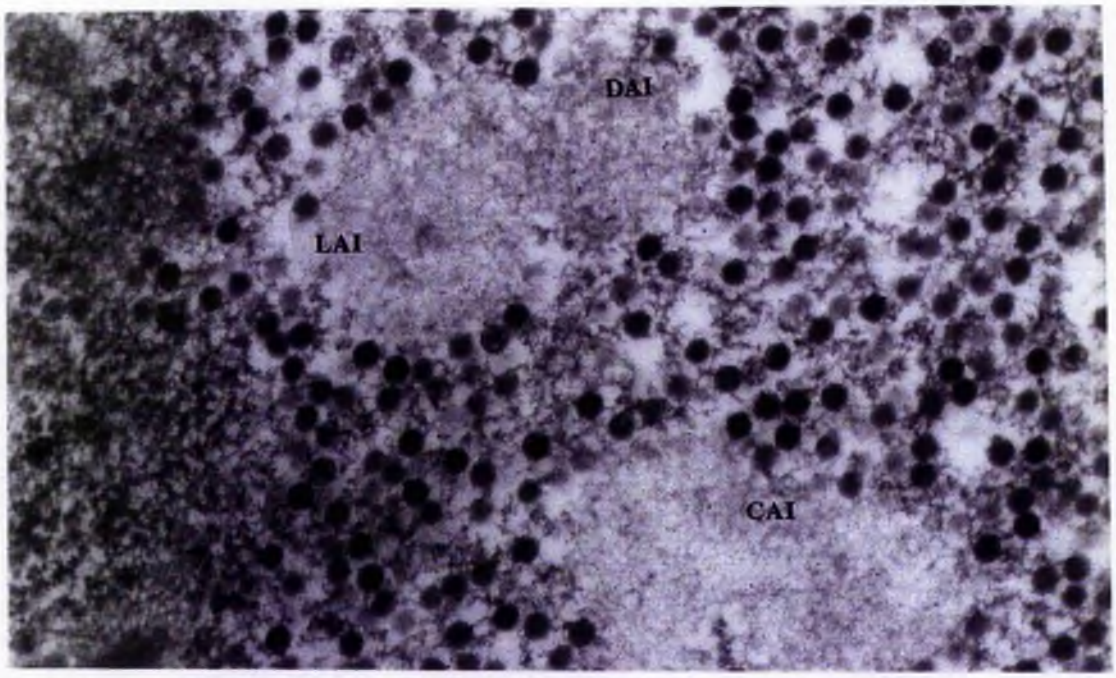

Figure 3.47: Colocalisation of pVIII and the viral protease within clear amorphous inclusions (I). Ad2 infected HeLa cells (28 h.p.i) were fixed using 2% paraformaldehyde/0.05% glutaraldehyde (pH 7.4) for 10 minutes, then dehydrated and embedded as descibed in section 2.8. Thin-sections were treated as described in section 2.8.4. pVIII and the 23kd protease are immunolabelled with 6nm and 10nm gold particles respectively. Clear amorphous inclusions (CAI) are subdivided into dark contrasted (DAI), and light contrasted inclusions (LAI). Viewed at 80kv. Automatic exposure at x34000 magnification.

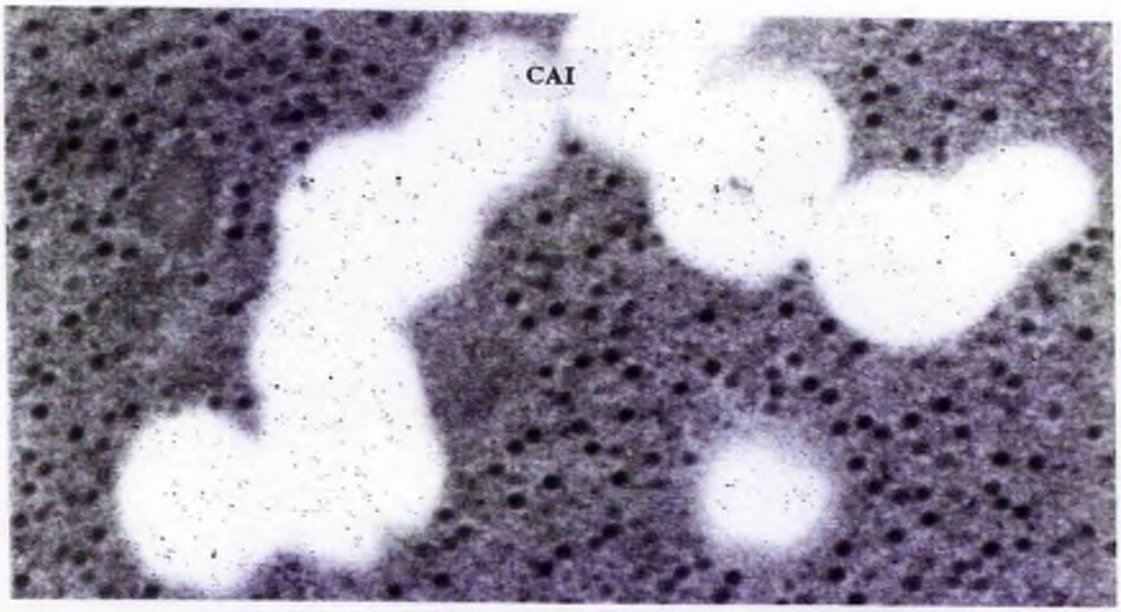

Figure 3.48: Colocalisation of pVIII and the viral protease within clear amorphous inclusions (II). Ad2 infected HeLa cells (28 h.p.i) were fixed with 2% paraformaldehyde/0.05% glutaraldehyde (pH 7.4) for 60 minutes (section 2.7.5) then dehydrated and embedded (section 2.8). pVIII and the viral protease are immunolabelled with 6nm and 10nm gold particles respectively within the elongated clear amorphous inclusion (CAI). Viewed at 80kv. Automatic exposure at x34000 magnification.

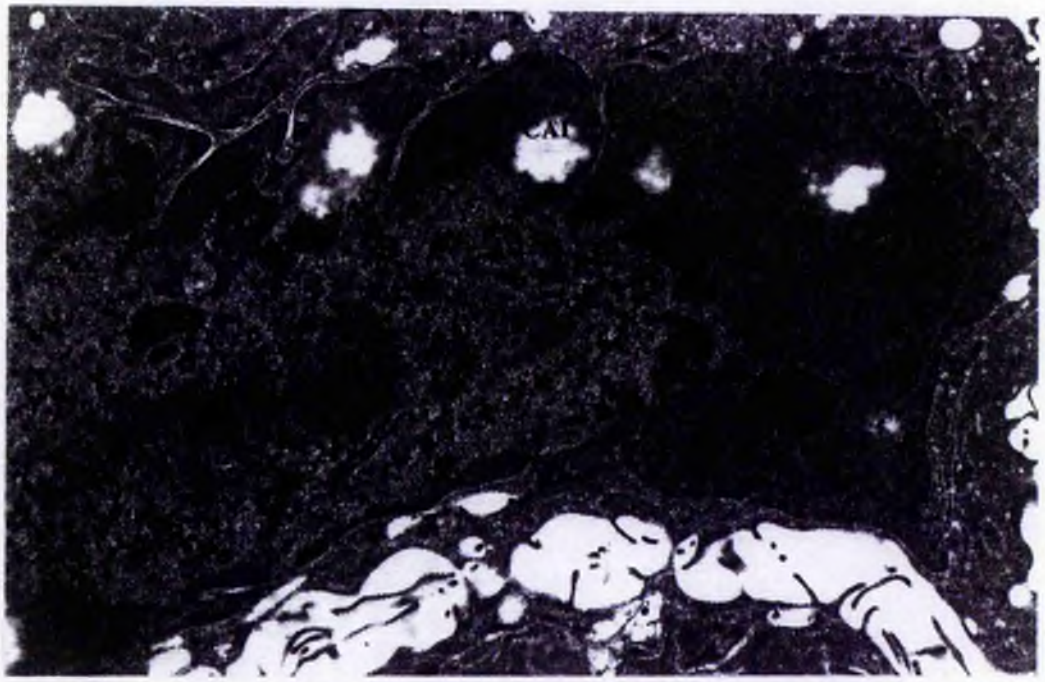

Figure 3.49: Alterations in nuclear structure upon Ad2ts1 infection. HeLa cells were infected with Ad2ts1 arcton extract at approximately 10 p.f.u/cell and maintained at the non-permissive temperature (39.5°C). Monolayers were fixed at 28 h.p.i with 2% paraformaldehyde/0.05% glutaraldehyde (pH 7.4) for one hour, then dehydrated and embedded (section 2.8). Clear amorphous inclusions are highlighted (CAI). Viewed at 80kv. Automatic exposure at x7100 magnification.

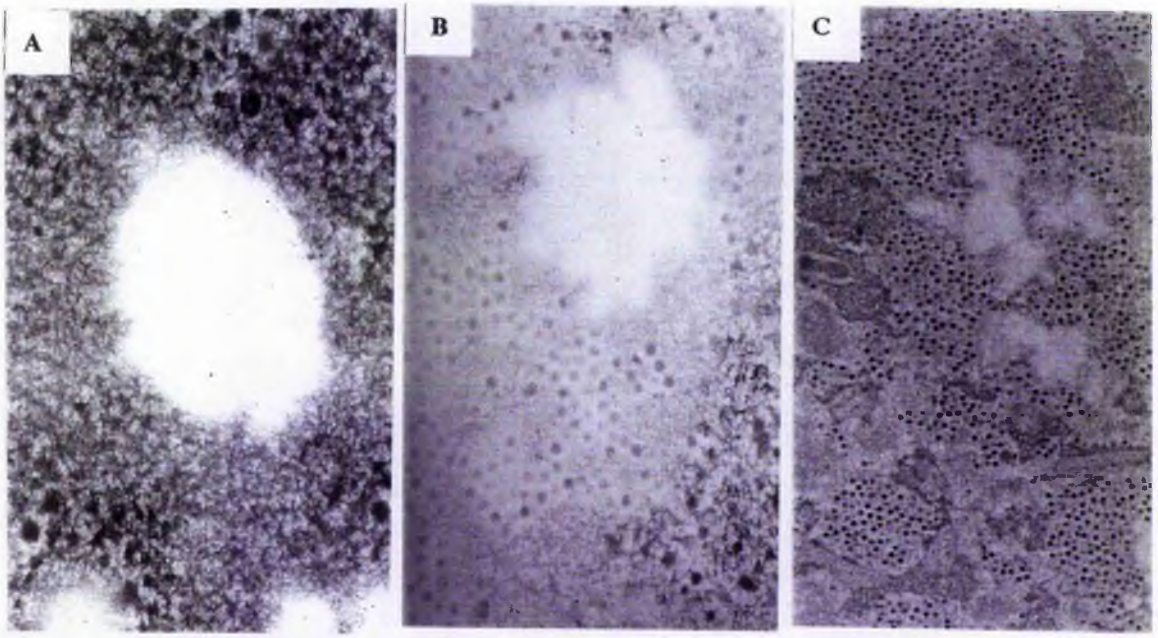

Figure 3.50: Colocalisation of pVIII and the viral protease within inclusions of Ad2ts1 infected cells. HeLa cells (same thin sections as shown in figure 3.49) were immunolabelled as described in section 2.8.4. Part A: Irregular shaped inclusion containing the viral protease and pVIII (immunolabelled with 10nm and 6nm gold respectively) but not immediately surrounded by virions (x34000 magnification). Part B: Immunolabelled clear amorphous inclusion with virions in close proximity (x25000 magnification). Part C: Lower magnification of clear amorphous inclusions (x9100) within regions of high virion density. All viewed at 80kv. Automatic exposures.

It was of interest that even when the clear amorphous inclusions within Ad2ts1 infected cells were in the proximity of regions containing high densities of virions, the virions were not observed to be closely associated with the virus-induced structures (figure 3.50 parts a and b) as observed within wild type Ad2 infected cells.

Immunofluorescent staining patterns of both pVIII and the 23kd protease in Ad2ts1 infected cells (28 h.p.i) maintained at the non-permissive temperature (39.5°C) and permissive temperature (33°C) are shown in figure 3.51 (parts a and b respectively). The punctate spots and threads observed within wild type infected HeLa cells were detected using OC11b11, however, the diffuse nucleoplasmic immunofluorescent staining patterns also detected in wild type Ad2 infected cells using antibody OC11b11 (figure 3.8a), were not detected in the Ad2ts1 (non-permissive) infected cells (figure 3.51a). A similar nucleoplasmic distribution of the 23kd protease to the wild type infection was detected within Ad2ts1 infected HeLa cells maintained at the permissive temperature for 48 h.p.i (discussed in more depth in section 3.3.3). Interestingly, the structural integrity of clear amorphous inclusions also appeared to be restored within Ad2ts1 infected cells maintained at the permissive temperature for 48 h.p.i, with clusters of virus particles observed to be in close proximity (figure 3.52).

ii) The origin of clear amorphous inclusions:

The clear amorphous inclusions to which pVIII and the 23kd protease have been shown to be localised to late in infection, are believed to be identical to the amorphous inclusions which Puvion-Dutilleul *et al* (1995b) determined to be the sites of PML accumulation during the course of Ad5 infection (figure 3.53). However, as cells were only examined at 28 h.p.i, only speculations can be made as to their origin.

A direct comparison can be made with the amorphous inclusions described in this study with those of Puvion-Dutilleul *et al* (1995b) because no other inclusions in either study were identified as having the same electron translucent appearance. In addition, the amorphous inclusions reported by these authors were also identified as being in close proximity to virus-induced protein crystals, which the authors noted, also contained redistributed PML protein. Puvion-Dutilleul *et al* (1995b) noted that as soon as virus-induced intranuclear changes became visible, clear amorphous inclusions were present in infected nuclei, and persisted until cell lysis. These structures which although were initially small and irregularly shaped,

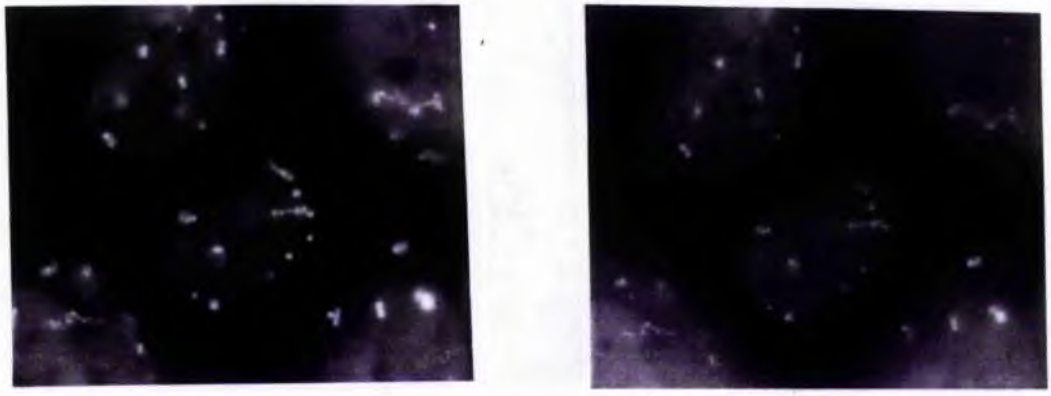

Figure 3.51: Immunofluorescent staining of pVIII and the 23kd protease within Ad2ts1 infected cells at the nonpermissive temperature. Ad2ts1 infected HeLa cells were fixed and double-immunolabelled as described in section 2.8.2. Localisation of pVIII (left) and 23kd protease (right) within Ad2ts1 infected HeLa cells (28 h.p.i) maintained at 39.5°C

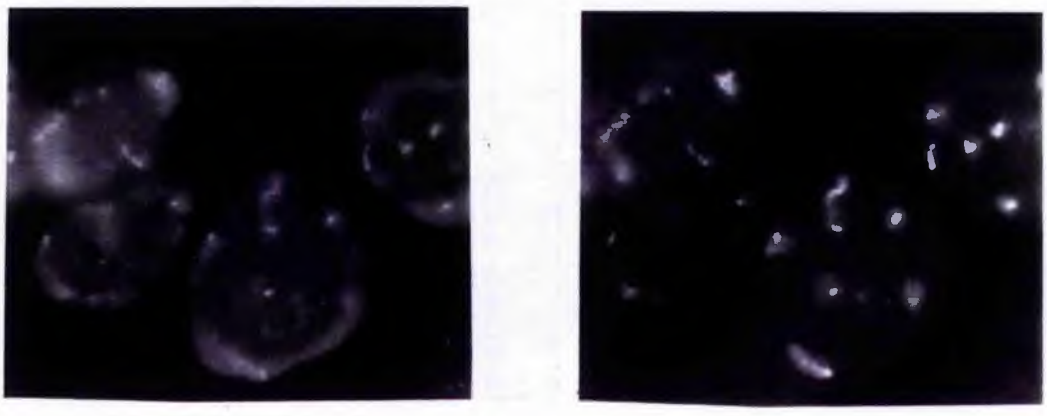

Figure 3.52: Immunofluorescent staining of pVIII and the 23kd protease within Ad2ts1 infected cells at the permissive temperature. Localisation of pVIII (left) and the viral protease (right) within Ad2ts1 infected cells (48 h.p.i) maintained at 33°C. OC11b11 was used to immunodetect the viral protease. x100 magnification (oil immersion).

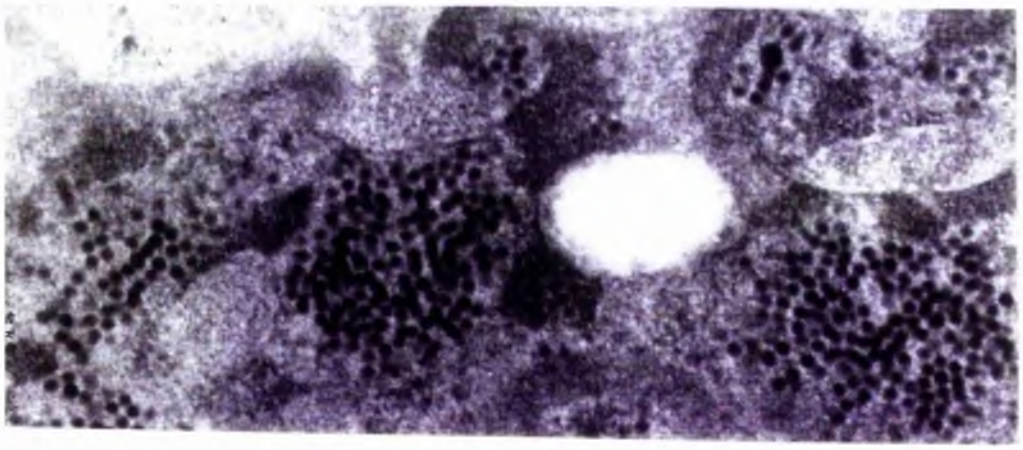

Figure 3.53: The morphology of clear amorphous inclusions within Ad2ts1 (permissive) infected cells. Infected HeLa cells were fixed at 48 h.p.i using 2% paraformaldehyde/0.05% glutaraldehyde (pH 7.4) for one hour, then dehydrated, embedded and contrasted (section 2.8). Viewed at 80kv. Automatic exposure at x34000 magnification.

became larger, spherical, and more abundant as the infection progressed. It was uncertain whether the inclusions were derived from nuclear bodies of non-infected cells. At the late phase of nuclear transformation (when virus clusters were numerous) clear amorphous inclusions were excluded from the region of the nucleus occupied by the viral genome storage site and were localised to the nuclear periphery.

The significance of the simultaneous presence of PML within clear amorphous inclusions and among the regular arrays of viral capsids is unknown. The authors noted that cellular hnRNP proteins were also localised to these virus-induced structures which suggested that crystal structures probably resulted from the assembly of both viral and cellular proteins. The authors speculated that the delocalisation of PML to these structures might facilitate the intranuclear development of progeny genomes and viruses. In that sense they demonstrated

that PML was a target gene of interferon and induces an antiviral state. Therefore, sequestration of PML into clear amorphous inclusions and crystal structures might indicate that PML is inactivated during adenovirus infection.

Protein crystals were not detected in this study, although it is clear from all the electron micrographs presented within this report, that the amorphous inclusions are located in regions of the nucleus containing high densities of virus particles.

A study undertaken by Wills and Russell (1973) involved the examination of the fine structure of Ad5 induced-protein crystals using temperature sensitive mutants for hexon, fibre and penton base. An electron micrograph of an intranuclear crystal published by these authors is shown in figure 3.54a together with an electron micrograph (from this study) of a clear amorphous inclusion in the proximity of crystalline arrays of virus particles (figure 3.54b). These authors have shown that there is a direct relationship with capsid synthesis and intranuclear crystal formation, with crystal formation being related to fibre, but not hexon, antigen expression. It was apparent that although the hexon deficient mutant ts17 was unable to form virus particles at the non-permissive temperature, crystal formation could still take place. Interestingly, the authors also observed the formation of irregularly shaped intranuclear inclusions when the temperature sensitive mutant ts36 (the fibre, hexon and penton base defect is a consequence of the Ad5 polymerase mutation (Professor R.T. Hay, pers.comm)) was maintained at the non-permissive temperature. It is thought possible that the intranuclear inclusions described by these authors (and highlighted in figure 3.54a) are early-phase clear amorphous inclusions.

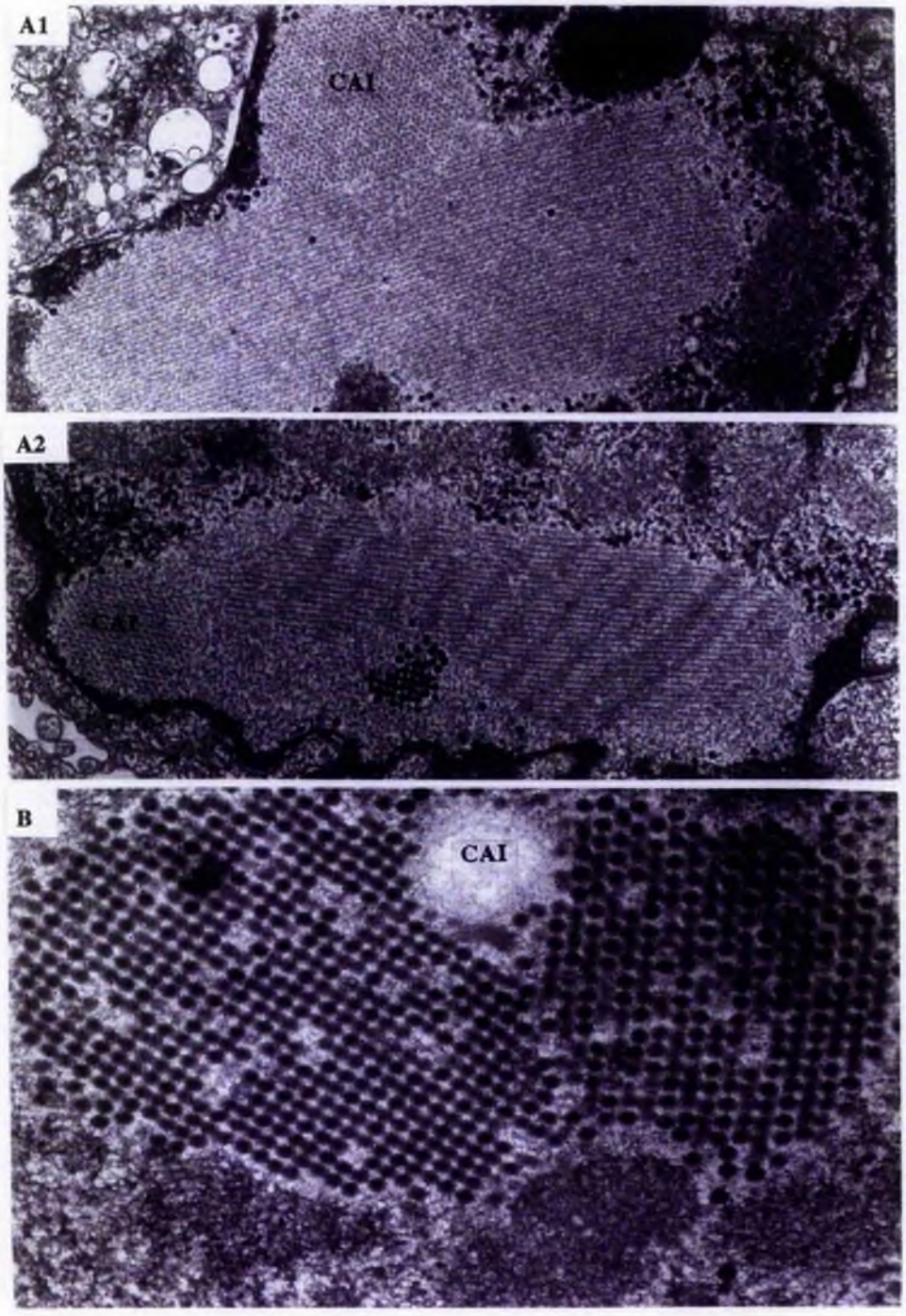

Figure 3.54: Adenovirus-induced protein crystals. Part A (1): Portion of a nucleus early after infection with wild strain Ad5 at 38°C, showing crystaline inclusions. Part A (2): Crystals in the nucleus of a cell infected with ts36 at 33°C (48 h.p.i at the permissive temperature). Reproduced from Wills and Russell (1973). Inclusions which are thought to be early forms of the clear amorphous inclusions presented within this study are highlighted (CAI) Part B: Arrays of virus particles (immunolabelled with anti-pVII) at 28 h.p.i (this study, x34000 magnification). A lower magnification (x9100) of this section is shown in figure 3.41.(highlighted as V).

It is noteworthy, that many of the clear amorphous inclusions detected during the course of this study, were observed to be in close proximity to electron dense nuclear bodies (figure 3.55). None of the cellular or viral antigens examined during the course of this study were localised to these structures and it is presently unclear what functional significance (if any) they have on virus assembly.

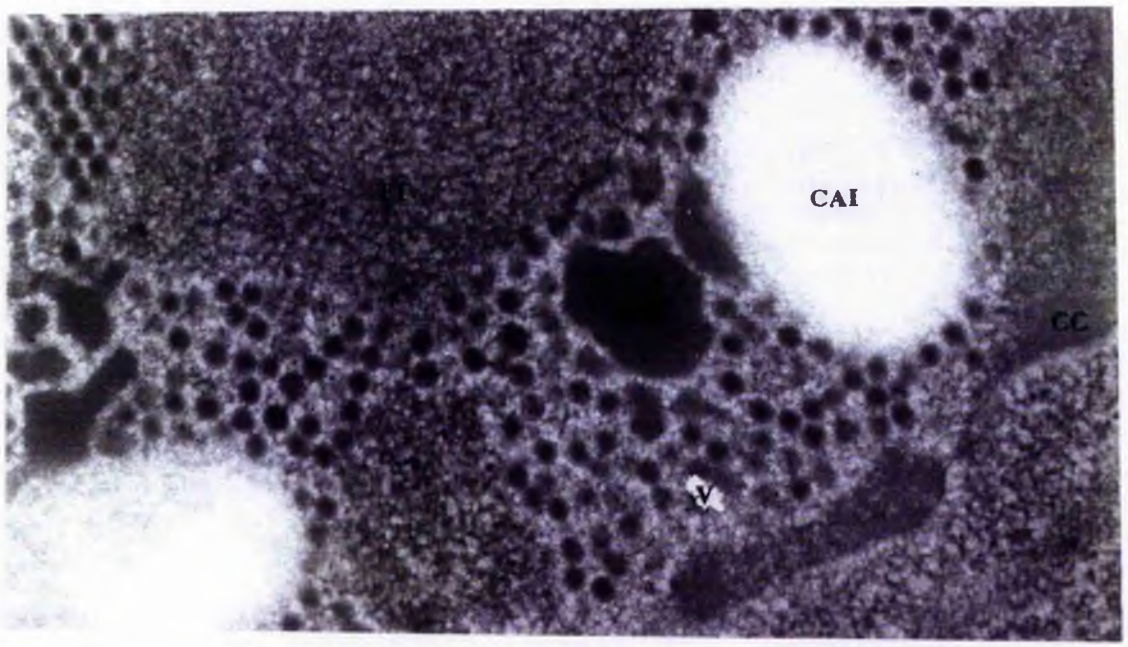

Figure 3.55: Ad2-induced inclusions at the nuclear periphery. Higher magnification (x34000) of the infected HeLa cell presented in figure 3.41. The thin section was immunolabelled with anti-pVII monoclonal antibody. 10nm Gold particles are evident within regions containing virions (V) and condensed cellular chromatin found at the nuclear priphery (CC), but not within clear amorphous inclusions (CAI) or electron dense nuclear bodies (DNb), and fibrillar inclusions (FI). The electron dense structures were commonly found to be in close proximity with clear amorphous inclusions at the nuclear periphery.

iii) The redistribution of PML and P80-Coilin:

Doucas *et al* (1996) have shown that at least two early transcribed viral proteins namely, the E4 ORF3 (11kd protein) and the E1B 55kd protein, are targeted to PML nuclear bodies, which in turn, undergo reorganisation into novel structures which the authors referred to as tracks. These structures had an identical appearance to the thread-like structures which were shown to contain pVIII/VIII and the 23kd protease late in infection.

Interestingly, prolonged infection of HeLa cells with HSV-1 results in the localisation of PML, and another nuclear autoantigen SP100, to translucent patches of fine granular

material, and viral capsids, at the nuclear border (Puvion-Dutilleul *et al.*, 1995c). These authors also determined that HSV-1 infection induces the redistribution of at least some of the components of interchromatin granule-associated zones and coiled bodies, in particular U1 snRNA, U2 snRNA and P80-coilin, to translucent patches. The translucent patches are detected only at the late stage of nuclear transformation, and contain a high concentration of capsid proteins (and also viral capsids), which suggested a possible role for these structures in the assembly of capsid proteins into capsid shells. Direct comparisons were made with the adenovirus induced clear amorphous inclusions, which the authors noted did not contain redistributed P80-coilin and snRNAs.

It was thought possible that 23kd protease may play an active role within clear amorphous inclusions in the inactivation of cellular proteins relocated to these intranuclear structures. A SWISSPROT findpatterns database search of all human proteins containing the consensus cleavage sequences for the Ad2 23kd protease ((M,L,I)xGxG and (M,L,I)xGGx, with zero mismatches) revealed that PML, P80-coilin, SP100, fibrillarin and U1 snRNP proteins all had potential cleavage sites for the viral enzyme. For PML, the potential cleavage sites are ^{679}-LWGPG and the C-terminal ^{869}-LAGRG. Likewise, P80-coilin has two potential cleavage sites which are ^{61}-LEGGL and ^{512}-MRGRG. Polyclonal antiserum and monoclonal antibody cell culture supernatant generated against P80-coilin were generously provided by Dr.C. Lyons and Dr.A.I. Lamond from the University of Dundee. Cell culture supernatant containing Mab 5E10, which specifically recognises PML protein (Stuurman *et al.*, 1992) was kindly donated by Professor Roel Van Driel (University of Amsterdam).

The distribution of both PML and P80-coilin within non-infected HeLa cells was examined using the BIO-RAD MRC-600 laser scanning confocal imaging system (figure 3.56). Both proteins were immunolocalised to specific foci within non-infected nuclei, with partial colocalisation observed within most cells examined. This was not surprising as Schul *et al* (1996) have described trios of coiled bodies, PML bodies and cleavage bodies (not examined here) which partially overlap within nucleoplasmic domains.

The distribution of both proteins late in infection (28 h.p.i) was markedly different (figure 3.57), with the track-like staining patterns of PML described by Doucas *et al* (1996) easily identified. P80-coilin was likewise shown to be redistributed, but was not shown to colocalise with PML.

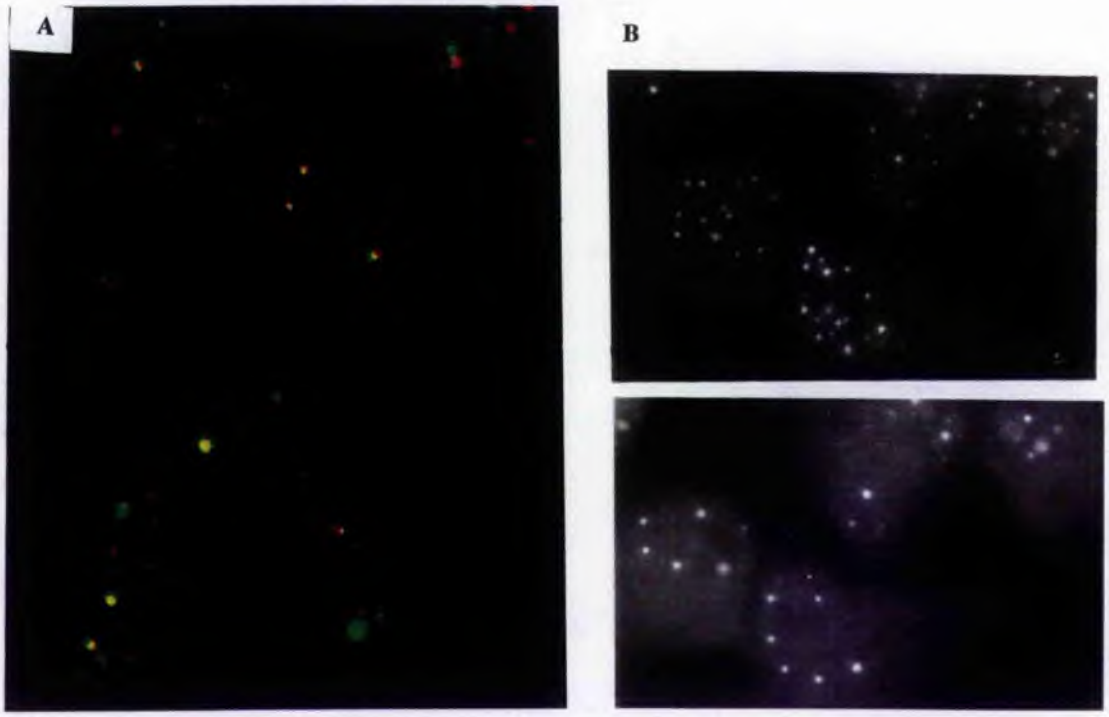

Figure 3.56: Immunofluorescent staining of PML and P80-coilin within non-infected HeLa cells. Part A: BIO-RAD MRC-600 laser scanning confocal image of PML (green) and P80-coilin (red) partial colocalisation within non-infected cells. Part B: Immunolocalisation of PML (top right) and P80-coilin (bottom right) using the Nikon-microphot light microscope. Mab 5E10 (anti-PML) and polyclonal antiserum 204/4 (anti-P80-coilin) were immunodetected using FITC and Texas-red conjugated anti-mouse and anti-rabbit IgG respectively (section 2.8.2). Both parts x100 magnification (oil immersion).

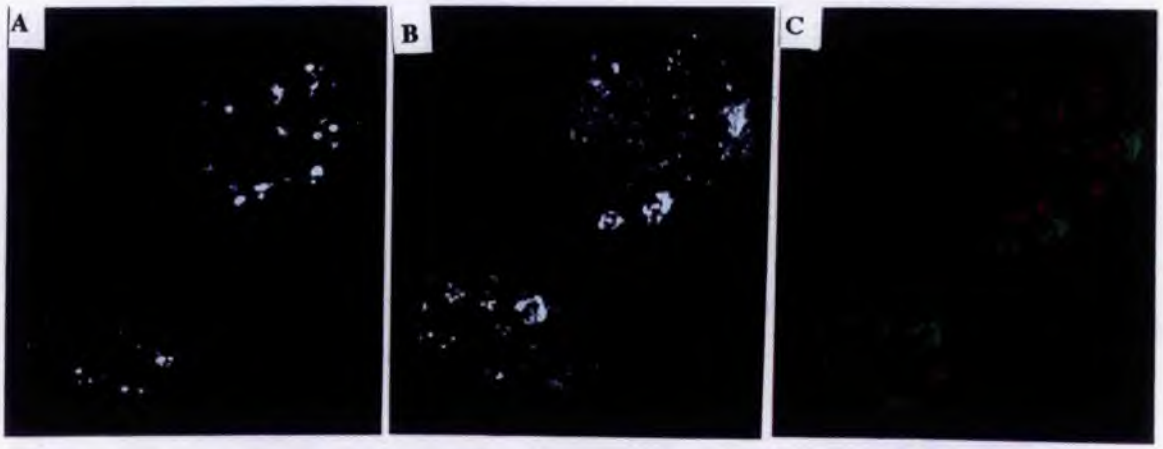

Figure 3.57: The distribution of PML and P80-coilin within Ad2 infected HeLa cells (28 h.p.i). BIO-RAD MRC-600 laser scanning confocal image of PML (part A) and P80-coilin (part B). The merge of both images is shown in part C with PML showing as red and P80-coilin as green (channel leads reversed). The same antibody solutions were used as outlined in figure 3.56. Viewed at x100 magnification (oil immersion).

Surprisingly, PML and pVIII were also found to be differentially localised within infected cell nuclei at 28 h.p.i (figure 3.58). Puvion-Dutilleul *et al* (1995b) detected PML within clear amorphous inclusions at 17 h.p.i, and it may be that PML inactivation during the subsequent later phases of infection has resulted in the protein (or cleaved products of the protein) being relocated from these structures.

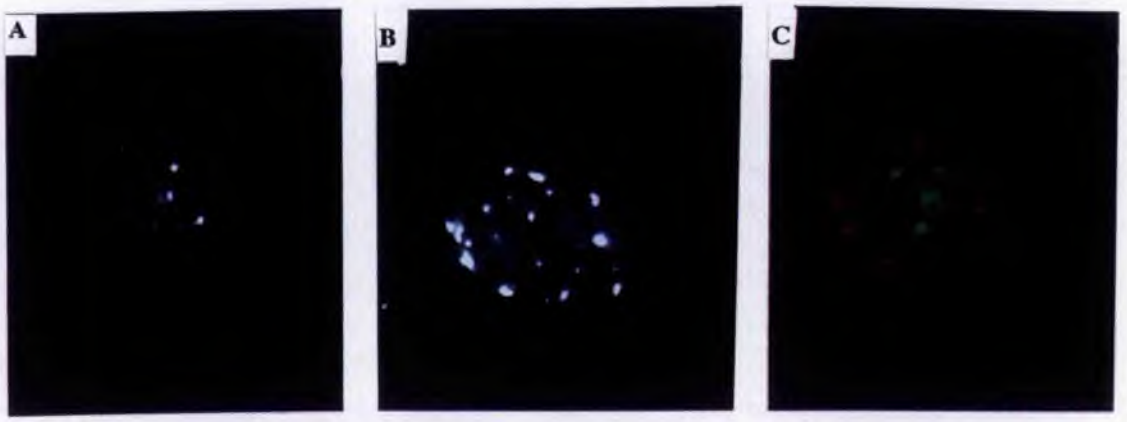

Figure 3.58: Immunolocalisation of PML and pVIII within Ad2 infected HeLa cells (28 h.p.i). BIO-RAD MRC-600 laser scanning confocal image of PML (part A) and pVIII (part B). The merge of both images is shown in part C with PML shown as green and pVIII as red. Viewed at x100 magnification (oil immersion).

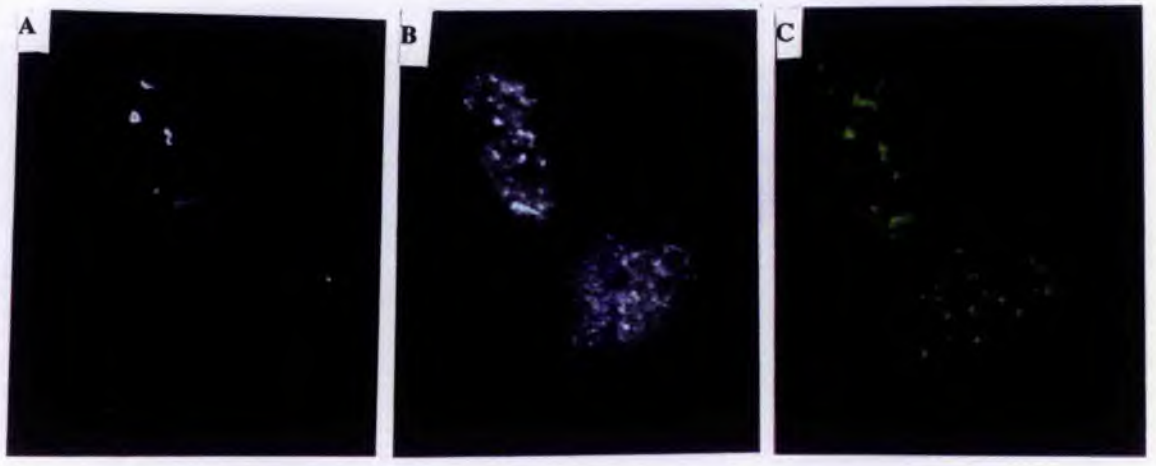

Figure 3.59: Immunolocalisation of the 23kd protease and P80-coilin within Ad2 infected HeLa cells (28 h.p.i). BIO-RAD MRC-600 laser scanning confocal image of the 23kd protease (detected using OA10b3)(part A) and P80-coilin (part B). The merge of both images is shown in part C with the 23kd protease shown as green and P80-coilin as red. Viewed at x100 magnification (oil immersion).

These authors also noted that P80-coilin was not localised to the clear amorphous inclusions during adenovirus infection. However, some colocalisation of the 23kd protease and P80-coilin was detected in this study (figure 3.59). Colocalisation appeared to occur at specific foci which contain the viral protease. It is possible that both proteins are localised to different intranuclear structures, which may overlap during the late stages of nuclear transformation. Rebelo *et al* (1996) have shown that coiled bodies are disassembled during adenovirus infection into microfoci, which they have determined using electron microscopy to be electron dense microbodies which contain both P80-coilin and fibrillarin. It is unclear whether these dense microbodies are the same electron dense nuclear structures which have been found in this study to be in close proximity to the clear amorphous inclusions at the nuclear periphery (figure 3.55). These electron dense nuclear bodies are discussed in more detail in section 3.3.6.

PML and P80-coilin were not detected in 4% formaldehyde or 2% paraformaldehyde/0.05% glutaraldehyde fixed (10 minutes) non-infected or infected HeLa cells. The post-embedding technique for immunocytochemistry which was used throughout this study has also been found to be unsuitable for immunodetection of P80-coilin in other studies (Dr.Carol Lyons, University of Dundee, pers.comm.). The pre-embedding technique, with immunolabelling of P80-coilin prior to infiltration of hydrophilic acrylic resins such as Lowicryl K4M, was found to be more suitable. Likewise, Stuurman *et al* (1992) used the pre-embedding technique to determine the intranuclear distribution of PML within permeabilised T24 and HeLa cells.

iv) Cleavage of P80-coilin, PML and pVIII:

In order to determine whether PML and/or P80-coilin were cleaved during the later stages of infection, nuclear extracts of infected cells (prepared at 28 h.p.i using the methods described in section 2.7.4) were electroblotted and examined using Mab 5E10 and antiserum specific to P80-coilin (figure 3.60 parts a and b respectively).

A major polypeptide was detected from both the Ad2 wild type and Ad2ts1 nuclear extracts using Mab 5E10, which may be a cleavage product of PML. The intact protein has an approximate Mr of 126kd (Stuurman *et al.*, 1992), however, the authors have noted that

small quantities of higher and lower molecular mass polypeptides are recognised by Mab 5E10.

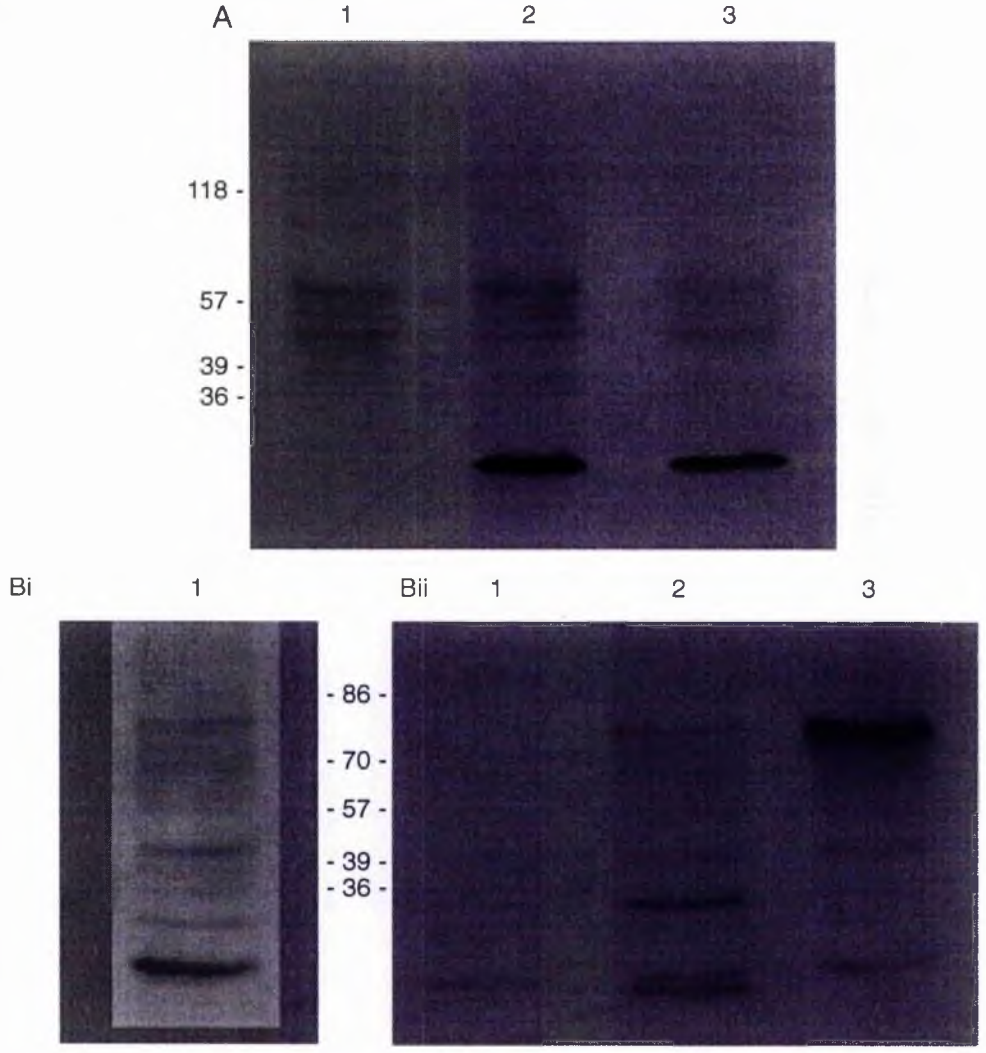

Figure 3.60: Possible cleavage of PML and P80-coilin. HeLa cell nuclear extracts (28 h.p.i) were prepared as described in section 2.7.4ii, then electroblotted (with prestained molecular weight markers). Samples of extracts from non-infected cells (lane 1), wild type infected cells (lane 2) and Ad2ts1 infected cells (lane 3). Part A: Immunoblot using Mab 5E10 (anti PML) at a 1/100 dilution. Part B: Immunoblot using anti-P80-coilin polyclonal antiserum 204/4 (1/1000 dilution). 10 minute exposure times (except part Bi/lane 1 which was an overnight exposure of Bii/lane 1).

The intact protein was not easily identified from the non-infected HeLa cell nuclear fraction and unfortunately, because there was only a limited quantity of Mab 5E10 available for these experiments, it was not possible to repeat the immunoblot presented in figure 3.60. As a consequence, it is also unclear whether the polypeptides detected in both wild type and ts1 infected nuclear extracts correspond to a cross-reaction of Mab 5E10 with a viral antigen. The immunoblot is by no means conclusive evidence that PML is cleaved during infection,

however, if the major polypeptides detected in the Ad2 wild type and Ad2ts1 nuclear extracts do correspond to a cleavage product of PML, then this might suggest that the viral protease is active within clear amorphous inclusions, and therefore possibly play some part in PML inactivation. This would be of particular interest in the context of the Ad2ts1 protease, which until relatively recently was thought to be inactive at the non-permissive temperature (Rancourt *et al* (1995). Additionally it is possible that cleavage products may be relocated from clear amorphous inclusions prior to the late-stages of infection as PML has not been observed to be colocalised with pVIII (and therefore potentially with the 23kd protease) at 28 h.p.i.

Intact P80-coilin, like PML, was difficult to identify from immunoblotted nuclear extracts of non-infected cells (10 minute exposure time), although a major polypeptide with an Mr of approximately 80kd was detected in wild type and ts1 infected cell nuclear extracts and over-exposed non-infected cell nuclear extracts. There also appeared to be a significant level of degradation despite the addition of a cocktail of protease inhibitors to lysis buffers (kept at 4°C). Similar levels of degradation have been observed elsewhere (Dr. Carol Lyons, pers.comm.). However, two additional bands were detected from the wild type Ad2 infected cell nuclear extract, which were not present in the equivalent non-infected, or the Ad2ts1 nuclear extracts. The upper band had an Mr of approximately 35kd and the lower band of approximately 20 to 25kd. It is unclear whether these polypeptides are cleavage products of P80-coilin, although their absence (and the higher concentration of the intact protein) within the Ad2ts1 nuclear extract suggested that the viral protease may be in part responsible for their occurrence.

The possible cleavage of P80-coilin was investigated further using *in vitro* transcribed/translated protein (plasmid pBS 751.2A (coilin cDNA in pBSSK-) was donated by Dr. Carol Lyons, University of Dundee), which in turn, was incubated with purified recombinant Ad2 23kd protease (section 2.9.3). Using the polyclonal antiserum specific to P80-coilin, the intact protein was immunoprecipitated from rabbit reticulolysates which also contained approximately 10µl (from a 50µg/ml stock solution) of non-activated recombinant protease (figure 3.61). The intact protein was not isolated from reticulolysates in which activated protease was added (section 2.93ii). Although no cleavage products were immunopecipitated from the reaction mixture, it appeared likely that the viral protease had

cleaved the intact protein. Additionally, the cleavage products were not detected within the original reticulolysate reaction mixture which was examined using 15% SDS-PAGE (20µl sample of the 100µl). However, two additional polypeptides were detected from a crude reaction mixture containing 5µl of activated protease and 25µl of rabbit reticulolysate containing P80-coilin (one hour incubation/37°C). It is unclear whether these correspond to cleavage products of P80-coilin, or other proteins present within the reticulolysate which were ^{35}S-methionine labelled.

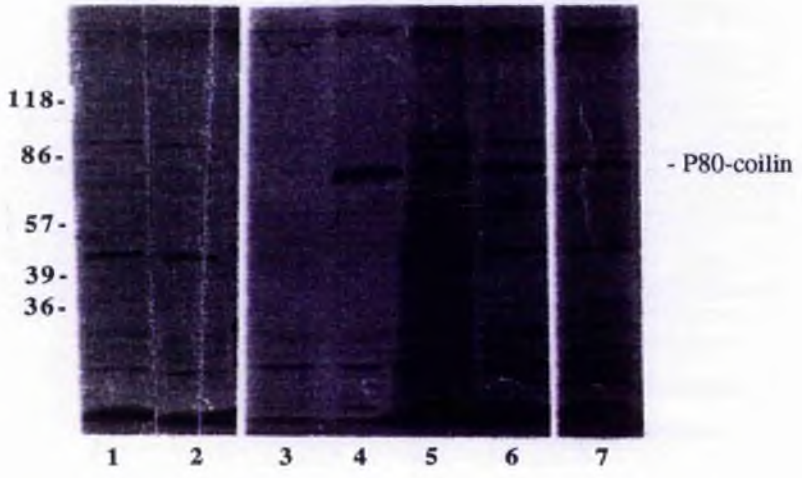

Figure 3.61: ***In vitro*** **cleavage of P80-coilin.** *In vitro* translated P80-coilin was incubated with activated and non-activated recombinant 23kd protease as described in section 2.9.3. 20µl samples from a crude TNT lysate containing P80-coilin, and P80-coilin plus non-activated and activated 23kd protease are shown in lanes 7, 6 and 5 respectively. P80-coilin was immuneprecipitated using polyclonal antiserum 204/4 from the TNT lysate/non-activated reaction mixture (lane 4), but not from the TNT lysate/activated protease reaction mixture (lane 3). 20µl samples from both reaction mixtures after immuneprecipitations are shown in lanes 1 and 2 respectively. Samples were electrophoresed (15% SDS-PAGE), then Coomassie blue stained/destained and dried prior to examination using the Fujix phosphoimager (section section 2.9.3iii)..

In the absence of cleavage products which can accurately be identified as being the result of 23kd protease activity, it is still uncertain whether cleavage does occur *in vivo*. However, if cleavage does occur then this might suggest that the both proteins are spatially distributed within nuclei of cells infected with Ad2ts1. As mentioned previously, the clear amorphous inclusions and electron dense bodies (which are thought to contain P80-coilin) were only found in close proximity with each other in wild type infected cells during the late-phase of nuclear transformation. The distribution of P80-coilin within Ad2ts1 infected cells was not determined using the laser scanning confocal imaging system. It may be that the partial

colocalisation observed within nuclei of wild type infected cells does not occur within nuclei of Ad2ts1 infected cells which in turn would explain why the possible cleavage products were not isolated from Ad2ts1 nuclear extracts.

It was of interest that P80-coilin cleavage was only detected when activated 23kd protease was added to reticulolysates, particularly as non-activated protease has been shown to cleave pTP (Webster *et al.*, 1994), and ovalbumin (Keyvani-Amineh *et al.*, 1995c).

The pVI-ct dependent activation of recombinant 23kd protease was examined further with *in vitro* transcribed/translated pVIII (pVIII cDNA in pRSET provided by W.S.A. Annan, University of St.Andrews) incubated with activated and non-activated recombinant 23kd protease as described above. Cleavage products of pVIII (assumed to be VIII with an approximate Mr of 15kd) were detected only after addition of the activated enzyme (figure 3.62). The *in vitro* requirement for pVI-ct activation of the 23kd protease suggests that pVIII may not be cleaved at sites of colocalisation (for instance the nuclear clear amorphous inclusions) which do not contain pVI during the late-phase of nuclear transformation.

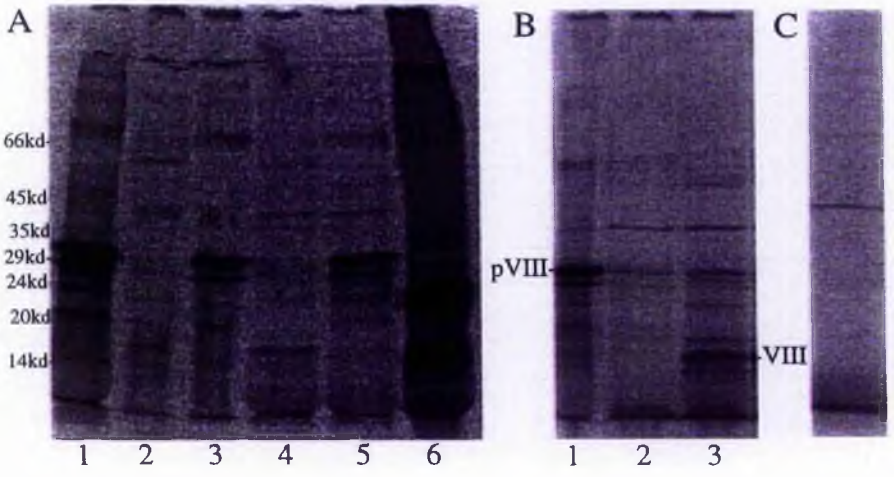

Figure 3.62: *In vitro* cleavage of pVIII. pVIII cleavage reactions and immunoprecipitations were carried out as described in section 2.9.3. Samples were resolved using 15% SDS-PAGE (Coomassie blue stained/destained) and bands examined using the Fujix Phosphoimager. Part A: Crude TNT lysate containing pVIII (lane 1). Immunoprecipitated products from reaction mixtures of pVIII incubated with activated 23kd protease, and non-activated 23kd protease are shown in lanes 2 and 3 respectively. Samples of these reaction mixtures which were not immunoprecipitated are shown in lanes 4 and 5 respectively. TNT lysate containing *in vitro* translated 23kd protease (lane 6). Part B: Samples of crude TNT lysates (samples were not immunoprecipitated) containing pVIII (lane 1), pVIII and non-activated 23kd protease (lane 2), and activated protease (lane 3). Part C: Sample of crude TNT lysate (no cDNA)/activated 23kd reaction mixture.

v) Colocalisation of pVIII and the protease within the cytoplasm:

The 23kd protease and pVIII were found to colocalise within the cytoplasm of infected cells from 24 h.p.i onwards (figure 3.45). One of the cytoplasmic structures that was immunolabelled during the course of the cytochemical study were the irregularly shaped electron dense structures shown in figure 3.63a. Although infrequently observed, these virus-induced structures were intensely labelled and detected only within infected cells fixed with 2% paraformaldehyde/0.05% glutaraldehyde, with extraction of components of these structures assumed to have occurred with 4% formaldehyde fixation. The significance of pVIII and 23kd protease colocalisation at these structures is unknown, as is the relevance to the functional roles both proteins have late in infection.

The protease and pVIII were more frequently detected within clear fibrillar structures that were typically found within close proximity to the nuclear membrane (figure 3.63b). Again, it is unclear what functional significance these structures have in relation to late-phase development of Ad2 infection, although their proximity to the nuclear membrane, and retention within 4% formaldehyde fixed/epon embedded cells, suggested that these structures were probably those most frequently detected by immunofluorescent staining. Rarely, and only within 4% formaldehyde fixed cells, clusters of 10nm colloidal gold particles were detected within the cytoplasm but did not appear to be localised to any specific structure (figure 3.63c). It was thought possible that these clusters may have been sites of cytokeratin cleavage, although these intermediate filaments were never identified.

Although after 24 h.p.i the viral protease is almost exclusively colocalised with pVIII within the cytoplasm, it is still unclear whether the protease is active (or available for activation) but unable to perform proteolytic cleavages on pVIII. Very little is known regarding the function of protein VIII apart from its proposed role in 'cementing' the capsid of the intact virion. Proteolytic cleavage pVIII is generally considered to occur within the maturing virion after pVI mediated activation of the viral protease.

vi) Cleavage of Cytokeratin K18:

It was of interest that the spheroid globules and cytoplasmic clumps associated with

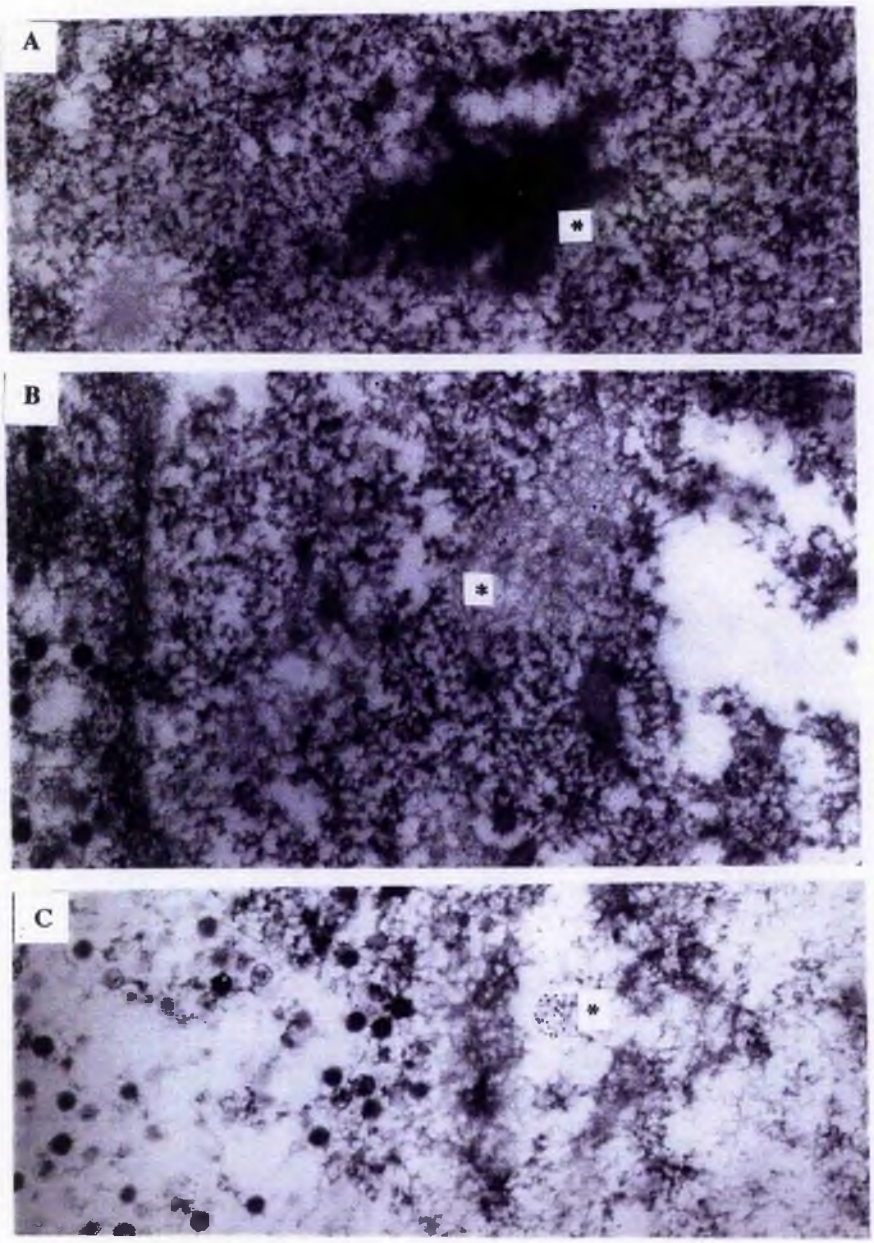

Figure 3.63: Cytoplasmic colocalisation of pVIII and the 23kd protease. Ad2 infected HeLa cells (28 h.p.i) were fixed with 2% paraformaldehyde/0.05% glutaraldehyde (part A) and 4% formaldehyde (parts B and C) for 10 minutes then dehydrated, and embedded in epon (section 2.8). Thin-sections were immunolabelled (OA10b3 used for detection of the 23kd protease) as described in section 2.8.4, then contrasted. Colocalisation of pVIII (6nm gold particles) and the viral protease (10nm gold particles) was detected at irregularly shaped electron dense structures (part A; asterisk), and clear fibrillar structures (Part B; asterisk). Clusters of the viral protease alone were also detected (part C; asterisk). All viewed at 80kv. All automatic exposures at x34000 magnification.

cytokeratin K18 cleavage (Chen *et al.*, 1993) were detected within the infected cells as early as 22 h.p.i (figure 3.64). The viral protease was normally detected within infected cells from

approximately 24 h.p.i onwards, with intracellular levels of the enzyme assumed too low to be detected by immunofluorescence prior to this stage in the development of infection. The distribution of pVIII prior to 24 h.p.i was almost exclusively intranuclear, appearing as punctate spots (figure 3.64). Nuclear and cytoplasmic colocalisation of pVIII and the 23kd protease was observed from 24 h.p.i onwards. pVIII was never detected within regions of the cytoplasm which were shown to contain cytokeratin spheroid globules and clumps, which initially suggested that the capsid protein was colocalised with the inactive form of the enzyme.

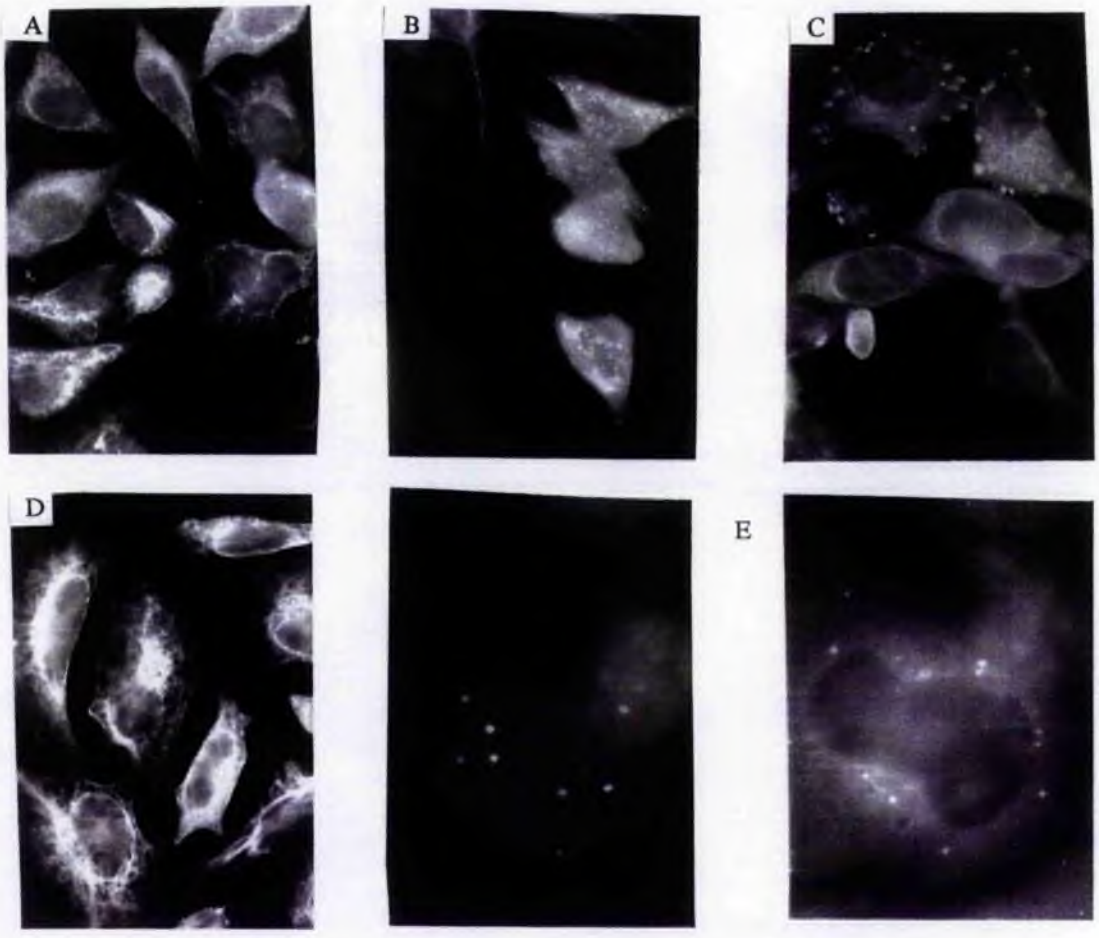

Figure 3.64: Cytokeratin cleavage during the late-phase of Ad2 infection. Ad2 infected HeLa cells were examined for cytokeratin K18 cleavage by direct-immunofluorescent staining (FITC-conjugated Mab K5.B17.2 is specific for cytokeratin peptide K18) at 12 h.p.i (part A), 22 h.p.i (part B) and 28 h.p.i (part C). Non-infected HeLa cells were also stained (part D). All were viewed at x60 magnification with approximately 30 second exposure times (automatic). Part E: Double immunolabelling of infected cells (22 h.p.i) showing pVIII (left) and cytokeratin K18 (right). x100 magnification (oil immersion).

It was of interest that the fluorescent staining pattern of pVI was entirely intranuclear from 16 h.p.i onwards (section 3.3.3). This suggested that other factors, either of viral or cellular origin, might be required for the activation of the protease *in vivo*. A database search (FASTA) of cellular proteins that contain sequences that might mimic the activating peptide (GVQSLKRRRCF), indicated that the activin receptor precursor protein is currently the only known human protein which contains a similar sequence (YGDKDKRRHCF). As this sequence does not have the N-terminal glycine and valine residues which have been shown to be important in binding of pVI-ct to the 23kd protease (Cabrita *et al*, 1997), it is unlikely that intracytoplasmic protease activity is regulated via this cellular protein. It is noteworthy that proteolytic activity *in vitro* has been determined in the absence of the activating peptide (reviewed within Weber, 1995).

As expected, cytokeratin cleavage was not detected within Ad2ts1 infected cells maintained at 39°C, but was detected within these cells maintained at the permissive temperature (figure 3.65). These observations were consistent with those presented by Chen *et al* (1993). Interestingly, Rancourt *et al* (1995) have shown that the temperature-sensitive phenotype was rescued by the provision of pVI-ct to the cell culture medium. The authors suggested that at 39°C the P137L mutation causes a small but crucial structural change in the protein that prevents it being in a position to be activated by cleavage of the pVI-ct peptide from the pVI protein. As activation is thought to occur within the immature virion, the significance of this finding is not absolutely clear in respect to cleavage of cytokeratin K18.

3.3.3 The intranuclear distribution of pVI.

i) Colocalisation of the 23kd protease and pVI/VI at assembly centres:

Using the anti-pVI/VI rabbit antiserum (kindly donated by Dr.D. Mathews, University of St.Andrews) it was evident that distribution of pVI/VI within Ad2 (wt) infected cells was exclusively intranuclear, with a diffuse nucleoplasmic immunofluorescent staining pattern consistently observed at 28 h.p.i (figure 3.66). It was not surprising that pVI/VI localised to the nucleus as Ad2 pVI has two potential nuclear localisation sequences, ^{246}-KRRR (within the C-terminal 12 amino acids), and ^{132}-KRPRP (a known targeting sequence from the C-terminus of Ad2 E1A proteins, Shin Hong and Engler, 1991). A comparison of known

mammalian adenovirus pVI sequences (human types 2, 5, 12, 31, 40 and 41 from the GenEMBL databases) indicates that these sequences are highly conserved.

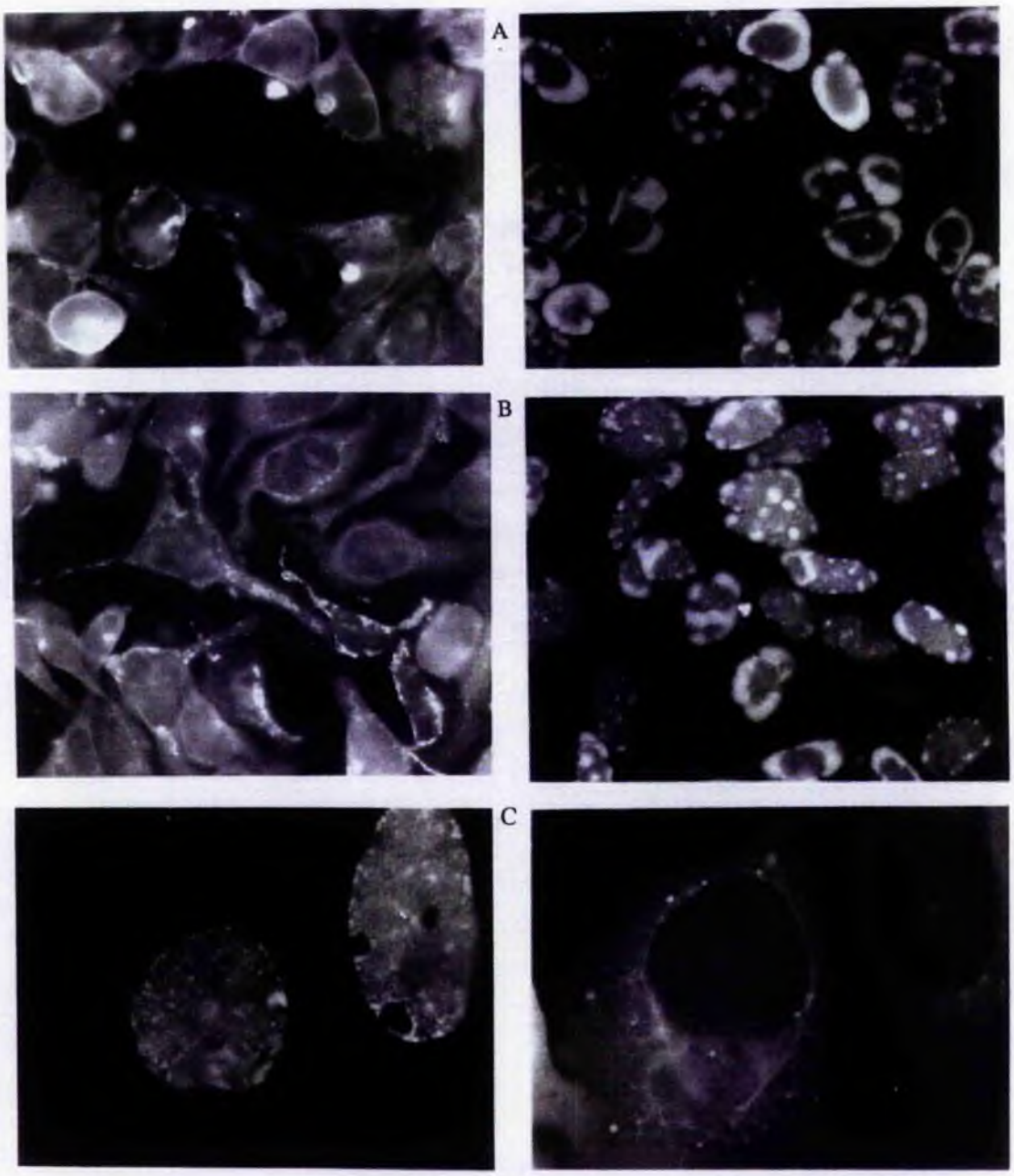

Figure 3.65: Cytokeratin is not cleaved within Ad2ts1 infected cells maintained at 39°C. AD2ts1 infected HeLa cells were maintained at 39°C and 33°C, then fixed with 4% formaldehyde at 28 h.p.i and 48 h.p.i respectively. Parts A (Ad2ts1 (39°C)) and B (Ad2ts1 (33°C)): Double immunofluorescence of cytokeratin K18 (left) and pVI (right)(using the polyclonal antiserum provided by Dr.D.Mathews (section 3.3.3)). x60 magnification. Part C: Corresponding Ad2 wild type infection (28 h.p.i) with staining of pVI (left) and cytokeratin K18 (right). x100 magnification (oil immersion). Automatic exposure times for pVI were approximately 15 to 30 seconds.

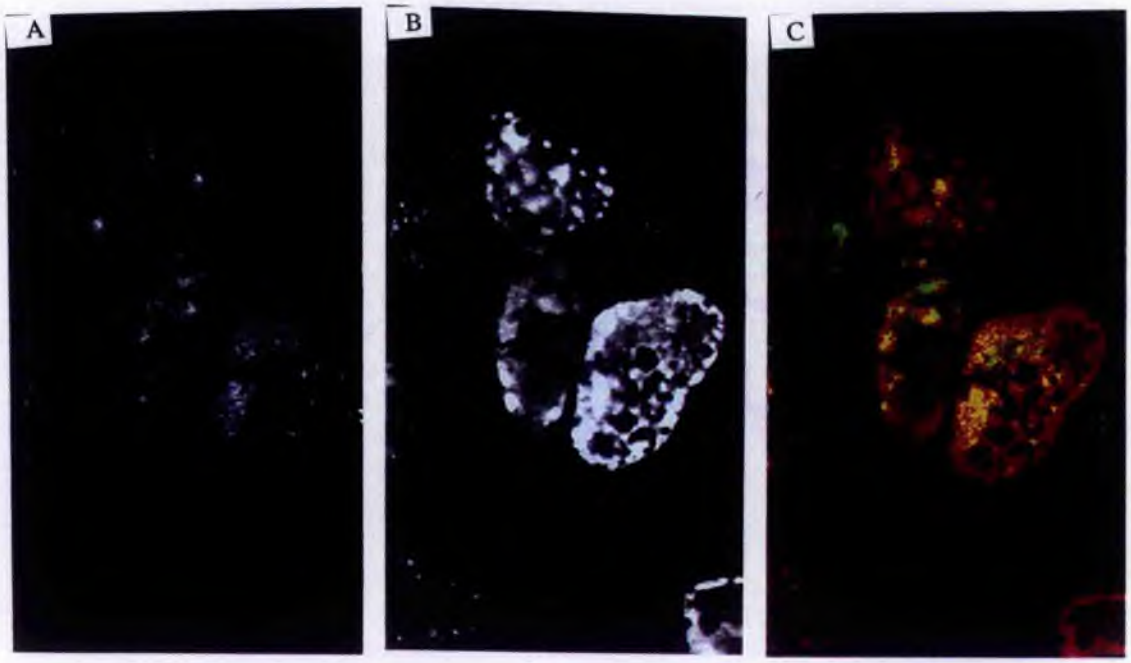

Figure 3.66: Intranuclear colocalisation of pVI and the 23kd protease. BIO-RAD MRC-600 laser scanning confocal image of the 23kd protease (detected using OC11b11)(part A) and pVI (part B). The merge of both images is given in part C with the viral protease showing as green and pVI showing as red (with yellow representing colocalisation). Viewed at x100 magnification (oil immersion).

From figure 3.66 it is clear that the 23kd protease (stained using OC11b11) and pVI/VI do colocalise within specific subnuclear domains late in infection, although it is unclear whether both proteins are in direct association. The distribution of the 23kd protease and pVI/VI within infected cell nuclei was further investigated at a series of time points during the course of Ad2 infection (from 12 to 28 h.p.i). At early-late times post infection (16 to 20 h.p.i) pVI appeared to accumulate at sites distinct from those which have been identified as containing DBP (figures 3.67a), and had the appearance of punctate spots and/or doughnut shaped spheres. These structures are also evident in figure 3.66 within infected cell nuclei where the 23kd protease was not detected. As infection progressed, the distribution of pVI/VI within the nucleus became more diffuse, with intense labelling observed at the nuclear periphery (from 20 h.p.i to 28 h.p.i). It was assumed that these were sites of virion assembly as they were distinct from regions containing pTP and DBP (figures 3.67b).

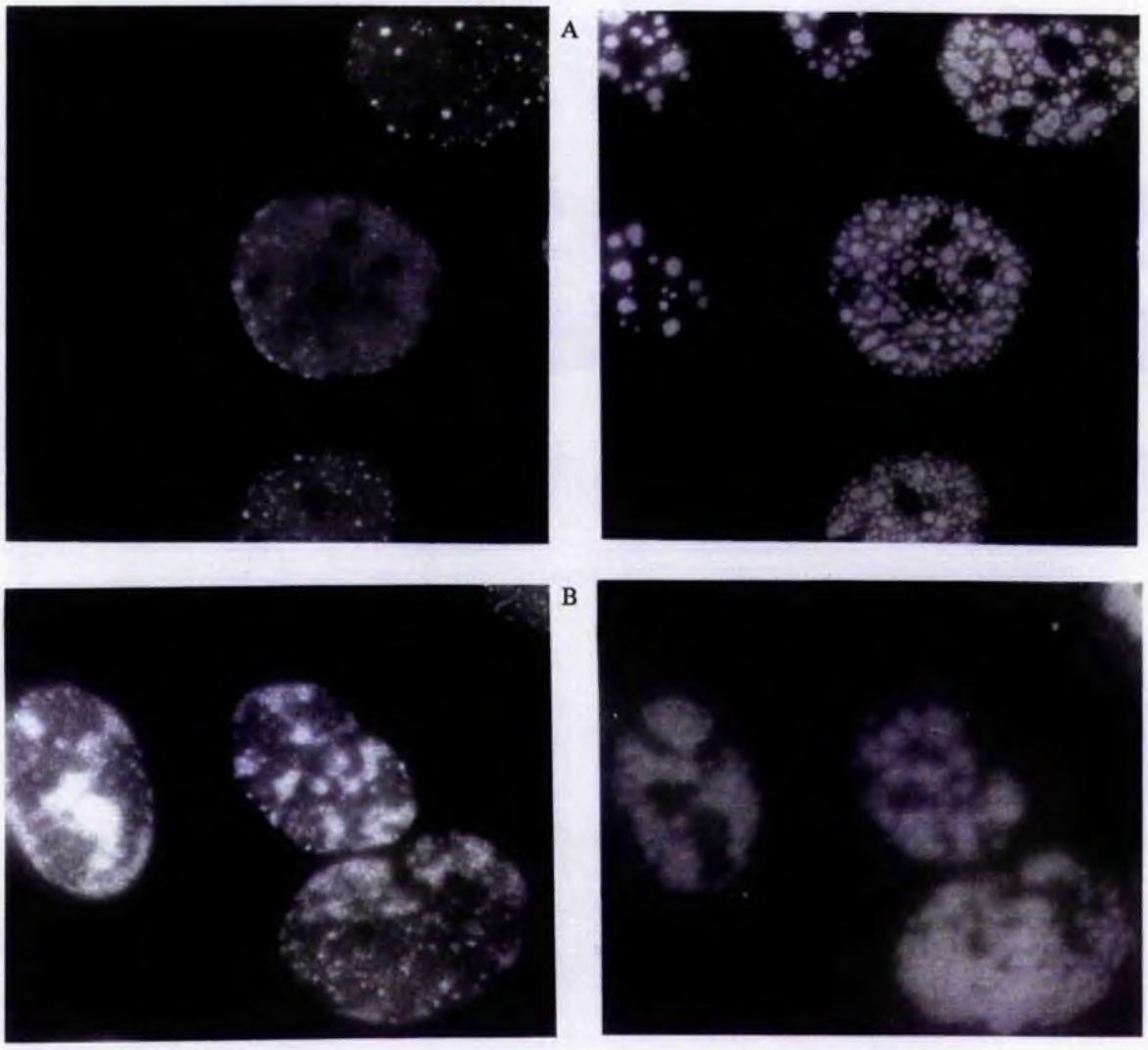

Figure 3.67: pVI/VI distribution within Ad2 infected HeLa cells. Part A: Ad2 infected HeLa cells (18 h.p.i) were fixed with 4% formaldehyde then double immunolabelled using the methods described in section 2.8.2. pVI (left) and DBP (right). Part B: pVI (left) and pTP (right) distribution within late-phase Ad2 infected cells (28 h.p.i) was examined using the same methodology. Mab 3D11b11 (anti-pTP) was kindly provided by Dr. Ailsa Webster (University of St.Andrews). pVI did not colocalise with pTP at 18 h.p.i, or DBP during the late-phase. Viewed at x100 magnification (oil immersion).

Immunogold labelled pVI/VI was detected in nuclear domains that contained high densities of virions (figure 3.68). Using antibody OC11b11, 10nm immunogold labelled 23kd protease was also detected within these assembly centres and within the clear amorphous inclusions which were usually in close proximity. It is likely that these virion containing assembly centres are the nuclear domains in which pVI/VI and 23kd protease were shown to colocalise in figure 3.66. OC11b11 did not detect 23kd protease within any other intracellular structures

apart from the virus induced clear amorphous inclusions and electron dense cytoplasmic structures.

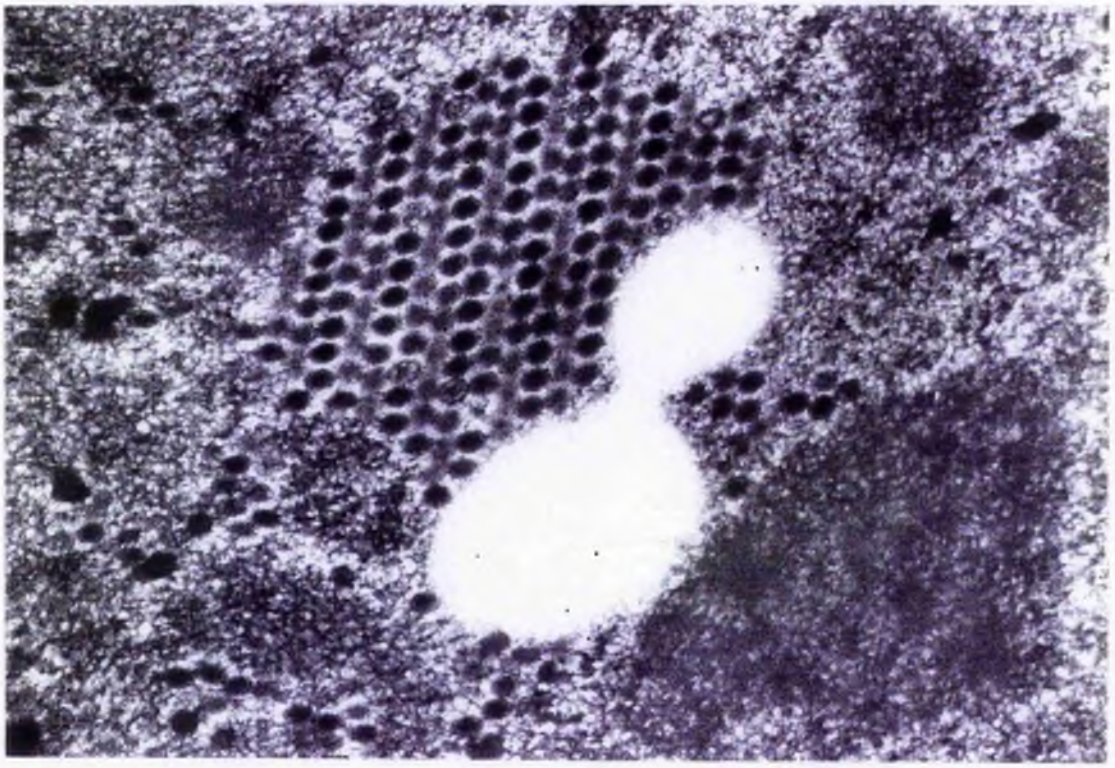

Figure 3.68: pVI/VI and the viral protease colocalise at assembly centres. Ad2 infected HeLa cells (28 h.p.i) were fixed (2% paraformaldehyde/ 0.05% glutaraldehyde, pH 7.4; for one hour), dehydrated and embedded as described in section 2.8, then immunolabelled using the anti-pVI polyclonal antiserum and Mab OC11b11. Viral protease (10nm gold particles) is distributed within the regions containing arrays of virions and within clear amorphous inclusions. pVI/VI (6nm gold particles) is distributed within the regions of high virion density only. Viewed at 80kv. Automatic exposure at x34000 magnification.

Mathews and Russell (1995) investigated the role of the protease in the processing of pVI to VI (via iVI which is thought to be pVI minus the C-terminal 11 amino acids (pVI-ct)), and found that no other factors were required *in vitro*. Their results led them to suggest that the protease might become closely associated with pVI within the 'young virion', and following activation, cleave the C-terminus of pVI to produce iVI. The authors noted that processing of pVI to iVI and finally to VI improved hexon binding and may therefore be important during assembly to prevent VI from prematurely associating with gestating hexon trimers.

Although pVI was not detected within clear amorphous inclusions during the late-phase of nuclear transformation, some colocalisation with the 23kd protease was detected (albeit infrequently) using antibody OA10b3, which appeared to specifically recognise the viral

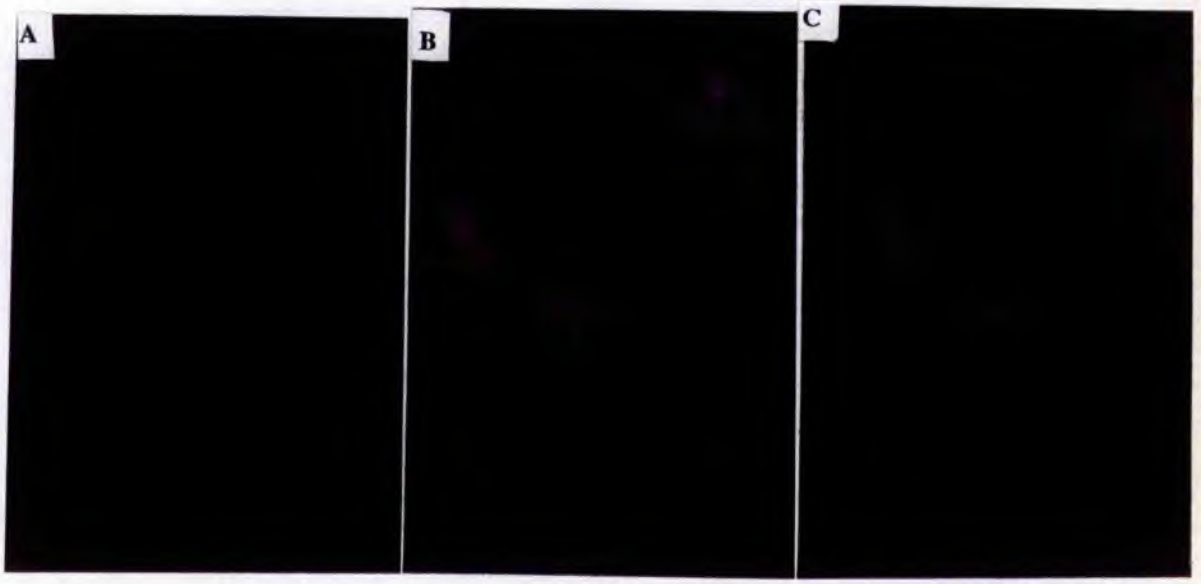

Figure 3.69: Localisation of pVI within intranuclear inclusions (I). BIO-RAD MRC-600 laser scanning confocal image of the 23kd protease (detected using Mab OA10b3)(part A) and pVI (part B). The merge of both images is given in part C with the viral protease showing as green and pVI showing as red (with yellow representing colocalisation). Infected HeLa cells (28 h.p.i) were fixed and immunolabelled as described in sections 2.7.5 and 2.8.2. Viewed at x100 magnification (oil immersion).

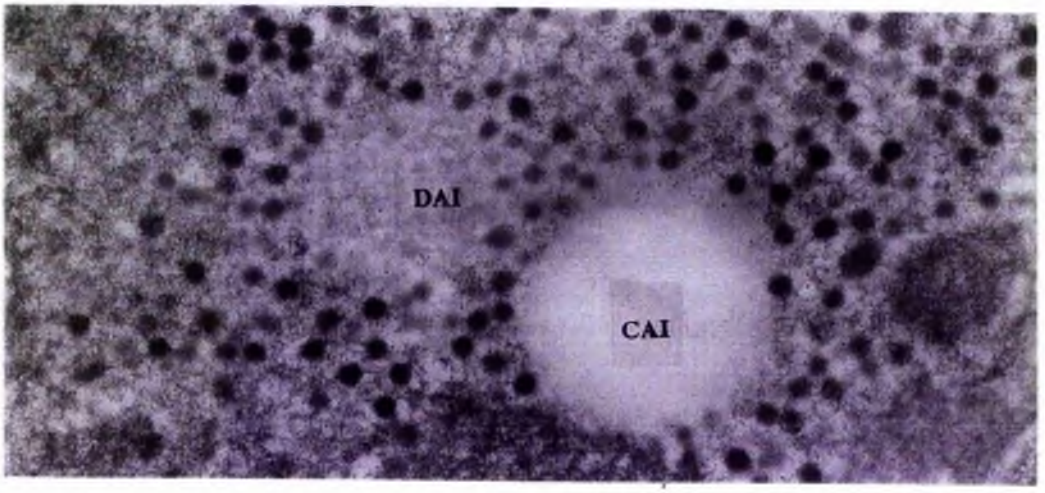

Figure 3.70: Localisation of pVI within intranuclear inclusions (II). Ad2 infected HeLa cells (28 h.p.i) were fixed with 2% paraformaldehyde/0.05% glutaraldehyde (pH 7.4)(one hour) and treated for immunocytochemistry as described in section 2.8. pVI detected (6nm gold particles) at the periphery of the clear amorphous inclusion (CAI), and present within the darker contrasted amorphous inclusion (DAI). Automatic exposure at x34000 magnification. Viewed at 80kv.

protease within the threads and/or punctate spots (figure 3.69) as well as cytoplasmic structures. Although the sites of colocalisation are unknown, pVI was detected (again

infrequently) within amorphous inclusions (figure 3.70) which may be similar in composition to the dark contrasted clear amorphous inclusions (dai) previously shown to contain the viral protease (figure 3.47).

ii) Intranuclear distribution of pVI/VI and PML:

From the immunofluorescence results it was unclear what intranuclear structures pVI localised too during the early-late phase of infection (16 to 20 h.p.i). It was initially thought that the punctate spot fluorescent staining of pVI might correspond to the proteins localisation within adenovirus-induced crystals (and/or clear amorphous inclusions) as pVI has been implicated to be directly involved in the transport of hexon capsomers to the nucleus (reviewed by D'Halluin, 1995). Some colocalisation with PML was detected within infected cell nuclei which showed a diffuse nucleoplasmic staining of pVI/VI, however, no colocalisation was observed within nuclei where punctate spot pVI staining was observed (figure 3.71).

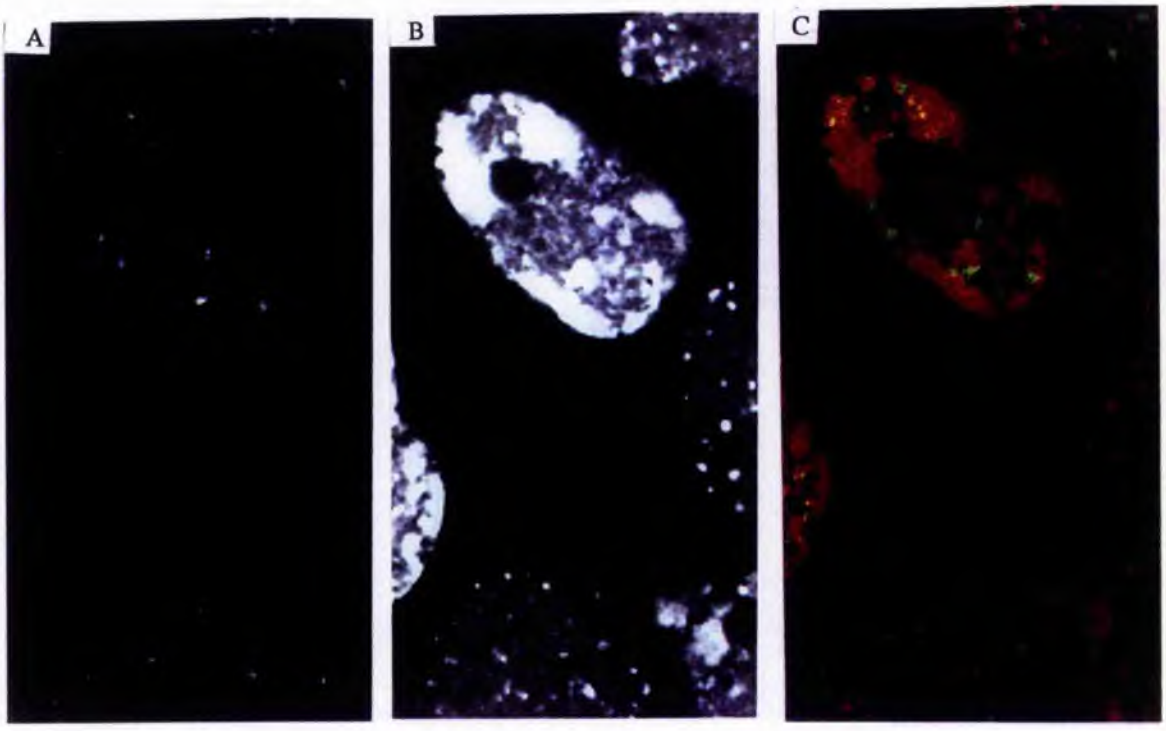

Figure 3.71: The distribution of pVI/VI and PML within Ad2 infected HeLa cells. BIO-RAD MRC-600 laser scanning confocal image of PML (detected using Mab 5E10)(part A) and pVI (part B). The merge of both images is given in part C with PML showing as green and pVI showing as red (with yellow representing colocalisation). Infected HeLa cells (28 h.p.i) were fixed and immunolabelled as described in sections 2.7.5 and 2.8.2. Viewed at x100 magnification (oil immersion).

iii) Intranuclear distribution of pVI/VI within Ad2ts1 infected cells:

The distribution of pVI/VI within Ad2ts1 infected cells (28 h.p.i) maintained at the non-permissive temperature differed markedly from the wild type equivalent, with the protein predominantly localised to the nuclear periphery (Figures 3.72a). The diffuse nucleoplasmic staining pattern of 23kd protease was detected only within Ad2ts1 infected cells maintained at the permissive temperature, albeit at reduced levels in comparison to wild type infection (figure 3.72b). The distribution of pVI within Ad2ts1 infected cells maintained at the permissive temperature resembled that detected during the wild type infection, although there was still intense peri-nuclear fluorescent staining similar to that observed within cells maintained at the non-permissive temperature.

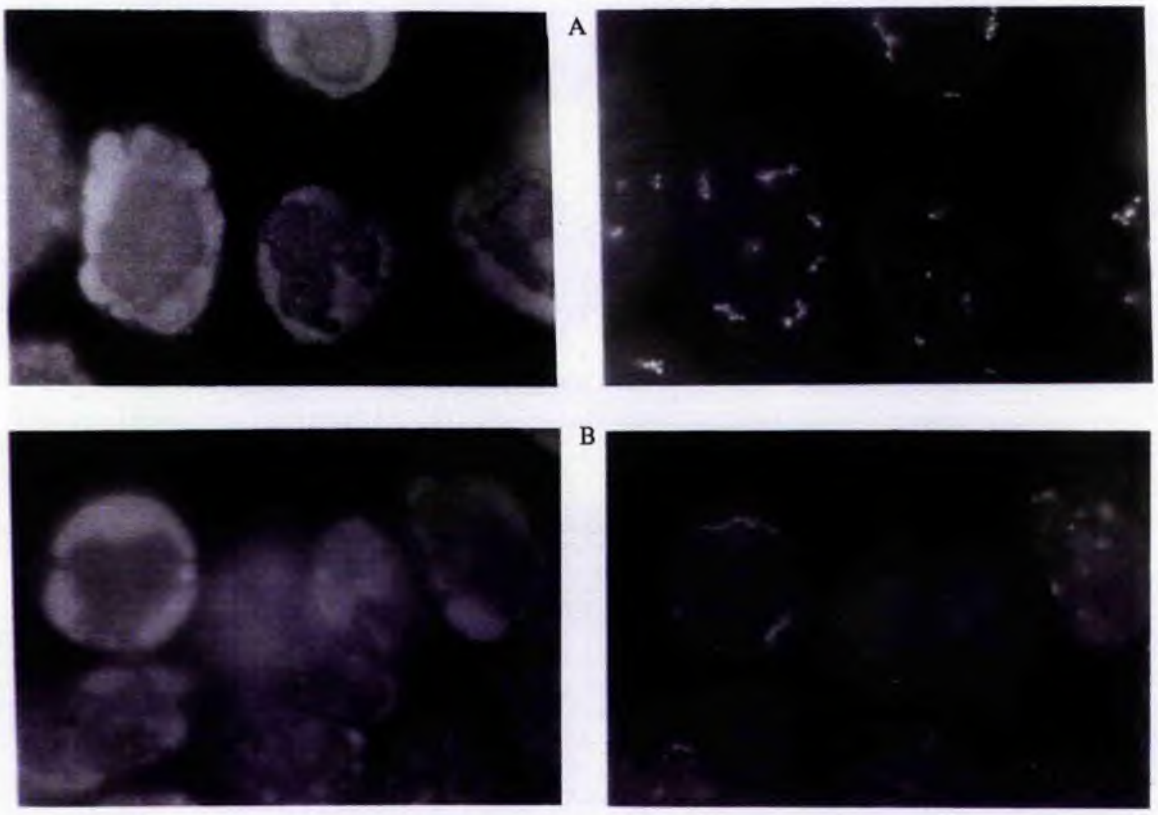

Figure 3.72: Intranuclear distribution of pVI during Ad2ts1 infection. Ad2ts1 infected HeLa cells were maintained at 39°C (fixed at 28 h.p.i) and 33°C (fixed at 48 h.p.i) then double immunolabelled as outlined in section 2.8.2. Part A: pVI fluorescent staining (left) is predominantly peri-nuclear within Ad2ts1 infected cells (non-permissive temperature). Only 'thread like' structures are detected using Mab OC11b11 (right). Part B: The intranuclear distribution of pVI (left) and the viral protease (right) within Ad2ts1 infected cells (permissive temperature). Viewed at x100 magnification (oil immersion).

The absence of the diffuse nucleoplasmic distribution of the 23kd protease within Ad2ts1 (non-permissive) infected cells suggested that the viral protease does not colocalise with pVI within regions of high virion density at the non-permissive temperature. Similarly, Rancourt *et al* (1995) have shown using extracts of Hep-2 cells infected with wt (37°C) and ts1 (33°C and 39°C) that the synthesis, stability and the transport of the enzyme to the nucleus appears to be normal in Ad2ts1 (39°C) infected cells. However, the authors did not detect protease within virions produced at 39°C, and suggested that the ts1 defect resides in a failure of enzyme activation and encapsidation at the non-permissive temperature. Interestingly, the authors noted that immature virions did contain protease (albeit 25% of that found in wt immature virion equivalents).

3.3.4 Immunolocalisation of replication and transcription sites:

The localisation of pTP and DBP to specific domains as shown in figure 3.73 is consistent with results derived elsewhere (Murti *et al.*, 1990). These authors detected regions in late-phase infected cells which labelled heavily with Adpol and TP but had less DBP. The centres heavily labelled with DBP likewise contained only small amounts of Adpol and TP and the authors suggested that replication initiates in locations that contain Adpol and TP, while elongation, which requires the 72kd DBP, takes place in the ssDNA accumulation sites. Collectively, results from other sources suggest that transcription and DNA replication of the virus take place in overlapping compartments (Pombo *et al.*, 1994; Besse and Puvion-Dutilleul, 1994; and Bridge and Pettersson, 1995) with transcription occurring almost exclusively in the peripheral replicative zone where it partially overlaps with areas of ongoing DNA synthesis. It is likely that the nuclear structures which are heavily labelled with 6nm gold particles in figure 3.74 are late-phase ssDNA accumulation sites. pTP was not detected within thin sections despite using solutions of pooled cell culture supernatants containing monoclonal antibodies specific to the protein (kindly donated by Dr.Ailsa Webster). Perhaps hydrophilic resins such as LR white or Lowikryl K4M would be more suitable for immunodetection of this protein in thin sections. In addition, several of the monoclonal antibodies (with the exception of 3D11) were found to cross-react with cellular proteins within non-infected cells.

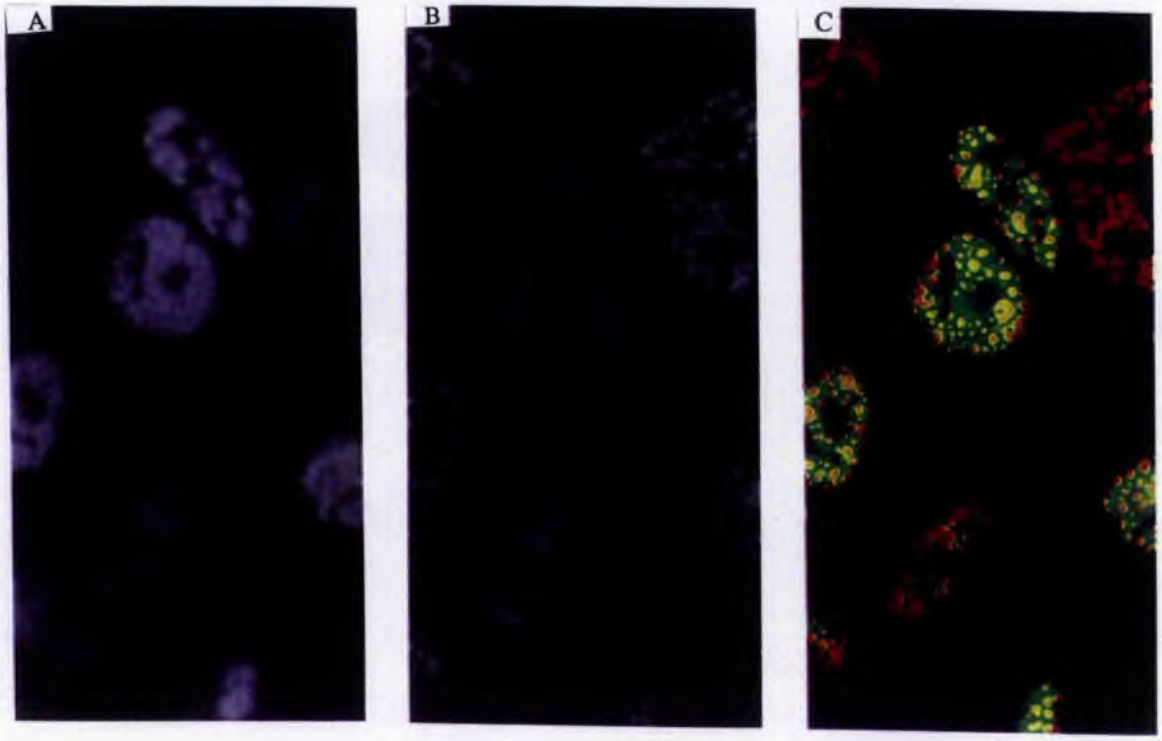

Figure 3.73: Distribution of pTP and DBP during the late-phase of infection. BIO-RAD MRC-600 laser scanning confocal image of pTP (detected using Mab 3d11)(part A) and DBP (part B). The merge of both images is given in part C with pTP showing as green and DBP showing as red (with yellow representing colocalisation). Infected HeLa cells (28 h.p.i) were fixed and immunolabelled as described in sections 2.7.5 and 2.8.2. Viewed at x100 magnification (oil immersion).

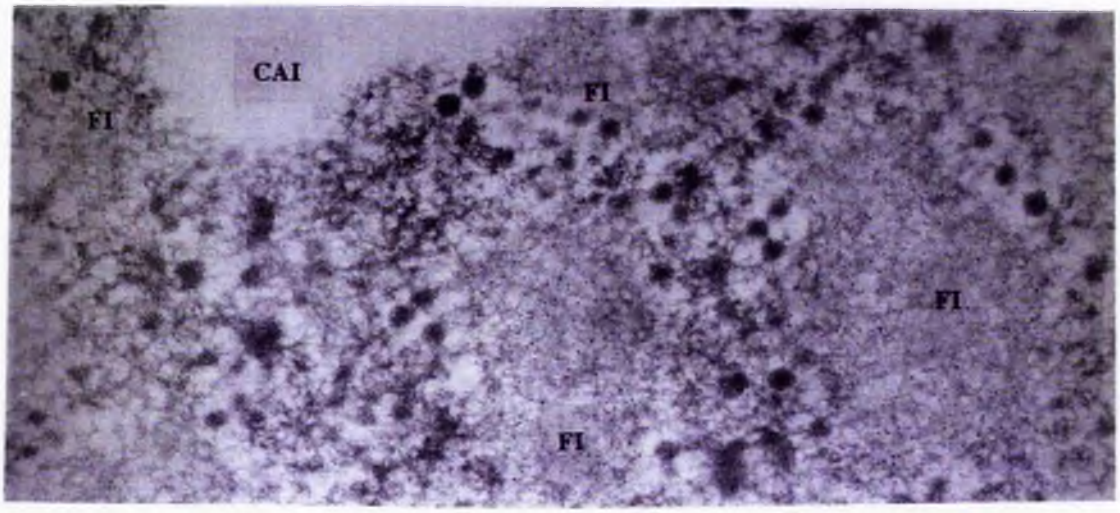

Figure 3.74: Identification of ssDNA accumulation sites. AD2 infected HeLa cells were fixed using 2% paraformaldehyde/0.05% glutaraldehyde (pH 7.4) for 10 minutes, then dehydrated, and embedded as described in section 2.8. ssDNA accumulation sites (fibrillar inclusions) were intensely labelled with DBP (6nm gold particles) and are highlighted (FI). Clear amorphous inclusion (CAI). Viewed at 80kv. x34000 magnification.

Partial colocalisation of the viral protease (detected using OA10b3) and DBP was observed in late-phase infected cell nuclei (figure 3.75). It is possible that there is some overlap between clear amorphous inclusions and ssDNA accumulation sites during the later stages of nuclear transformation. DBP was not detected within clear amorphous inclusions (figure 3.74), instead being detected within darker contrasted inclusions often found in the peripheral regions of the nucleus that contained high densities of virions.

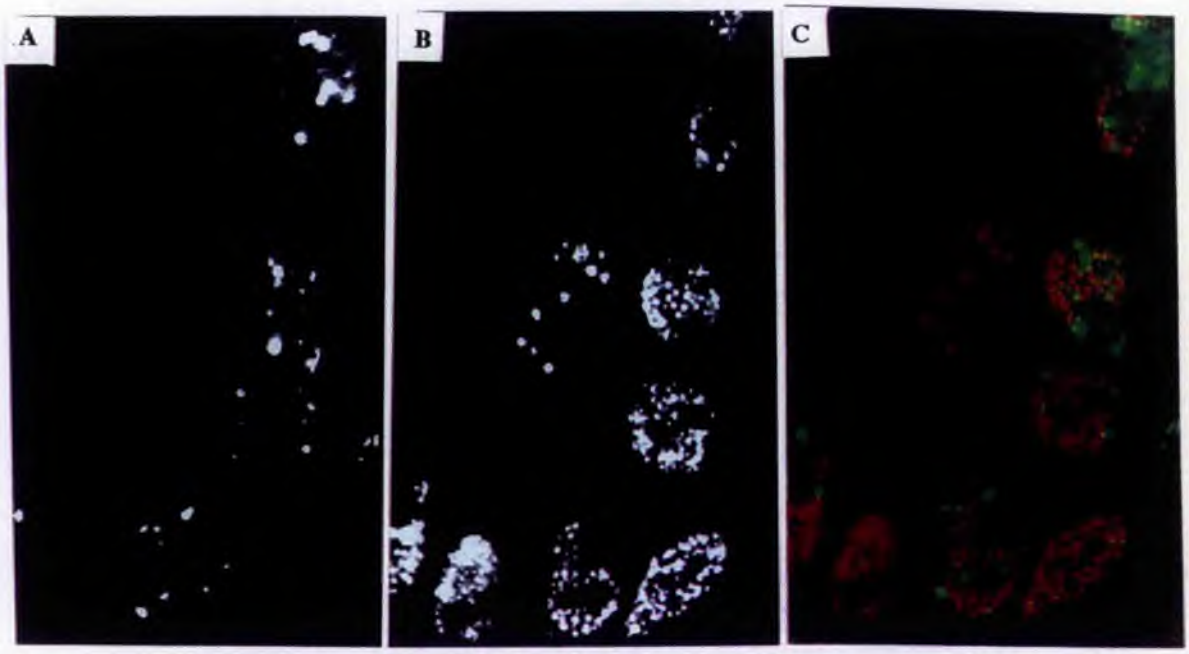

Figure 3.75: Distribution of DBP and the 23kd protease during Ad2 infection. BIO-RAD MRC-600 laser scanning confocal image of the viral protease (detected using Mab OA10b3)(part A) and DBP (part B). The merge of both images is given in part C with the 23kd protease showing as green and DBP showing as red (with yellow representing colocalisation). Infected HeLa cells (28 h.p.i) were fixed and immunolabelled as described in sections 2.7.5 and 2.8.2. Viewed at x100 magnification (oil immersion).

Bosher *et al* (1992) have shown that in Ad2 infections (but not Ad4) nuclear factor 1 (NF1) is colocalised with DBP at intranuclear centres which they identified as being sites of viral DNA replication. Their results suggested that host proteins needed for viral replication are recruited from their normal locations to sites where viral replication is taking place. In this context the partial colocalisation of the 23kd protease with DBP late in infection (possibly at sites where specific nuclear domains overlap) is of interest, as NF1 does contain a potential cleavage site. Likewise, the Ad2 E1B 55kd protein, which also has a potential cleavage site (^{199}-ISGNG), has been shown to colocalise with DBP at clear fibrillar inclusions (CFI) believed to be

ssDNA accumulation sites (Ornelles and Shenk, 1991). Doucas *et al* (1996) have shown that the E1B 55kd protein (and the E4 ORF3 11kd protein) colocalises with PML early in infection, which in turn undergoes reorganisation into the 'track' structures. During this process, some host components are recruited from PML bodies into the viral replication domain.

3.3.5 Immunolocalisation of core proteins pVII/VII and V.

In addition to the colocalisation with the 23kd protease, pVI/VI was also observed to colocalise with pVII/VII at assembly centres late in infection (figure 3.76). As was the case with immunodetection of pTP, the anti-pVII monoclonal antibody used cross-reacted with cellular antigen(s). The epitope for the antibody used has been determined as RNYPTP (Dr. Paul Szawlowski, pers.comm.). A similar sequence within DNA-directed RNA polymerase (PNYTPT) suggests that this protein may have been detected within non-infected cells. pVII/VII was predominantly detected within regions of high virion density (figure 3.54b on page 165), in particular regions of the nucleus which comprised of crystalline arrays of virus particles. Immunolabelling of pVII/VII was significantly lower in regions of the nucleoplasm which contained a random distribution of virus particles (figure 3.79). Some immunolabelling of condensed material (most likely cellular chromatin) located at the nuclear periphery was also detected (figure 3.55 on page 166). Cellular chromatin is condensed and relocated to the nuclear periphery during the late stages of nuclear transformation (Puvion-Dutilleul and Puvion, 1995b; Lutz *et al*, 1996), and it is possible that the anti-pVII monoclonal antibody cross-reacted with antigens present within this intranuclear domain.

Results described elsewhere indicate that the core proteins (V and pVII/VII) appear within intact virions 15 minutes after their synthesis (reviewed by D'Halluin, 1995), which is in sharp contrast to the lag period of 60 minutes required for the assembly of hexon polypeptides into virions (Horwitz *et al.*, 1969). Collectively, the results from studies on kinetics of labelling and protein composition suggest that empty capsids contain precursor polypeptides, and possibly scaffolding proteins, with viral DNA and core proteins V and pVII then incorporated either separately or together, with the final step involving proteolytic cleavage of precursor polypeptides. This implies that core proteins become rapidly associated with DNA after their synthesis and that DNA and core protein(s) (complexes) are somehow

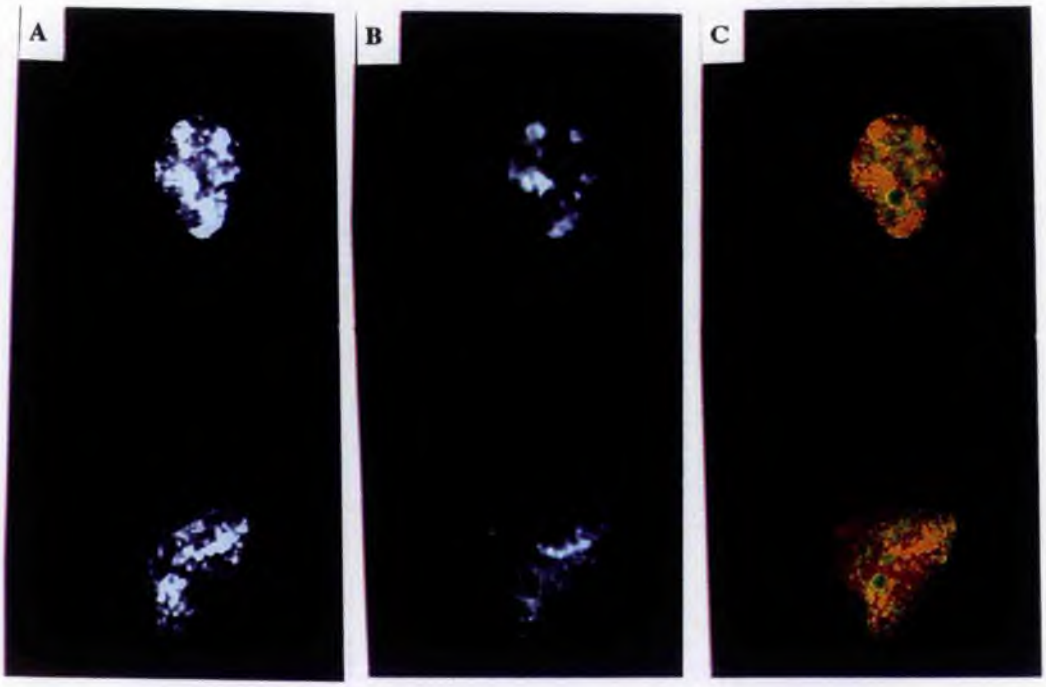

Figure 3.76: Colocalisation of pVI/VI and pVII/VII within Ad2 infected HeLa cells. Infected Hela cell monolayers were fixed at 28 h.p.i then prepared for immunofluorescence as described in section 2.8.2 and examined using the BIO-RAD MRC-600 laser scanning confocal microscope. Part A: pVII. Part B: pVI. The merge of both images is given in part C with the pVII showing as green and pVI showing as red (with yellow representing colocalisation). Viewed at x100 magnification (oil immersion).

inserted into previously assembled capsids. Interestingly, core proteins pVII and V only colocalised within particular subdomains of the nucleus at 28 h.p.i (figure 3.77). To a large extent the proteins appeared to be spatially distributed, colocalising at what appeared to be border regions between specific intranuclear structures. Phosphoprotein V appeared to be in close proximity to ssDNA accumulation sites during the late-phase of nuclear transformation (figure 3.78) and has also been detected within small electron dense nuclear bodies which have a similar composition to that of the residual nucleolus (figure 3.79).

Studies which have utilised bismuth staining of phosphorylated proteins (Chaly and Chen, 1993; Puvion-Dutilleul and Puvion, 1995) have primarily focused on the intranuclear distribution of DBP (which contains about a dozen phosphorylated sites which are concentrated in the smaller 25kd fragment of the protein). However, other intranuclear structures, in particular the dense (and very dense) fibrillar inclusions described by Chaly and Chen (1993) also contain significant levels of phosphoproteins. It is unclear whether

structures described by these authors correspond to the sites of protein V localisation shown here.

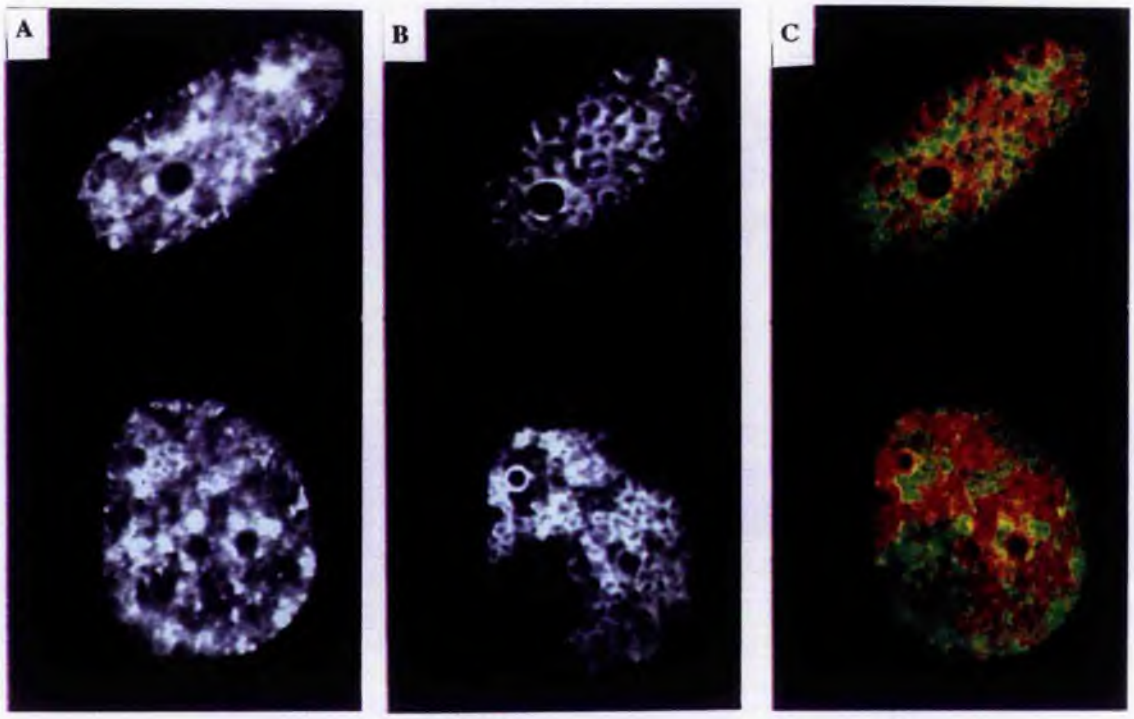

Figure 3.77: Intranuclear localisation of proteins V and pVII/VII. BIO-RAD MRC-600 laser scanning confocal image of pVII (part A) and V (part B). The merge of both images is given in part C with the pVII showing as green and V showing as red (with yellow representing colocalisation). Infected HeLa cells (28 h.p.i) were fixed and immunolabelled as described in sections 2.7.5 and 2.8.2. Viewed at x100 magnification (oil immersion) then stored at x1.7 magnification.

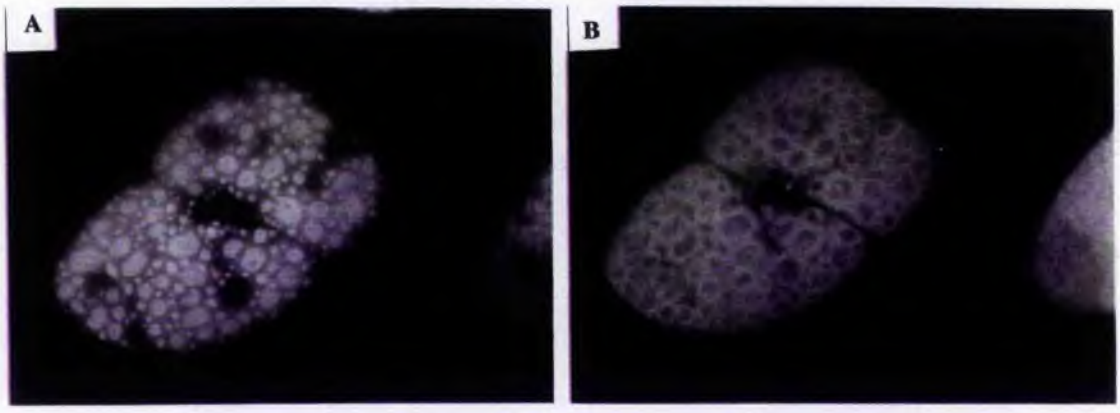

Figure 3.78: Intranuclear distribution of protein V and DBP. Ad2 infected HeLa cells (28 h.p.i) were fixed and double immunolabelled as described in section 2.8.2. DBP (left) and Protein V (right) were viewed at x100 magnification (oil immersion). Antibodies specific to both proteins were generously provided by Professor W.C.Russell (University of St.Andrews).

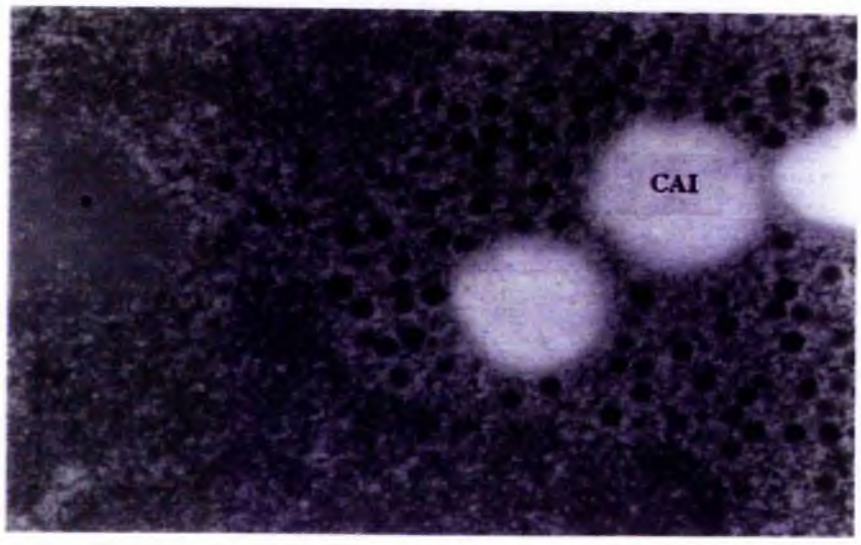

Figure 3.79: Protein V localises to specific nuclear structures. Infected HeLa cells (28 h.p.i) were fixed with 2% paraformaldehyde/0.05% glutaraldehyde (one hour)(pH 7.4), then dehydrated and embedded as described in section 2.8. Protein V (6nm gold particles) was detected within irregularly shaped electron dense structures (asterisk). Low levels of pVII/VII were detected within regions of the nucleoplasm containing random distributions of virions (10nm gold particles), and at the periphery of clear amorphous inclusions (CAI), viewed at 80kv. x34000 magnification.

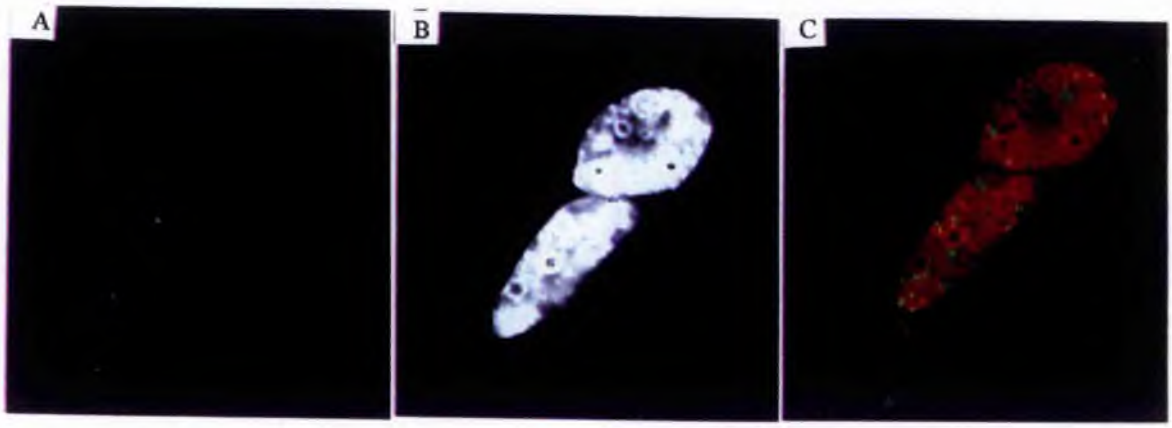

Figure 3.80: Distribution of protein V and the 23kd protease. BIO-RAD MRC-600 laser scanning confocal image of the 23kd protease (detected using OA10b3)(part A) and V (part B). The merge of both images is given in part C with the protease showing as green and V showing as red (with yellow representing colocalisation). Infected HeLa cells (28 h.p.i) were fixed and immunolabelled as described in sections 2.7.5 and 2.8.2. Viewed at x100 magnification (oil immersion).

Kinetic labelling studies carried out by Weber and Khitoo (1983) suggested that the protein V was incorporated into immature virions prior to DNA encapsidation with the disappearance of label being concomitant with DNA encapsidation. Interestingly, these authors have also

found that the Ad2ts1 mutation results in a failure of protein V dephosphorylation within the maturing virion. Although protein V was not detected within clear amorphous inclusions, some colocalisation with the 23kd protease was detected within nuclei of wt Ad2 infected cells (figure 3.80) using the laser scanning confocal imaging system (Ad2ts1 infected cells were not examined). The sites of colocalisation may be overlapping nuclear domains which are in close proximity to virion assembly centres.

3.3.6 Distribution of the 23kd protease and the L1 52/55kd proteins.

The adenovirus L1 region encodes several proteins important for assembly of infectious virus particles namely, the 52kd and 55kd proteins, and the IIIa protein (which is a structural component of the virion). The 52/55kd proteins are nuclear phosphoproteins (that are highly related in amino acid sequence), which have not been detected in virions. Mutations in either the 52/55kd proteins leads to an accumulation of intermediate particles that are blocked in viral genome compaction and encapsidation (Hasson *et al.*, 1989 and 1992). Hasson *et al* (1992) have proposed several possible roles for the L1 52/55kd proteins during infection. Firstly, the proteins may have a structural role as scaffolding proteins, and function to mediate recognition between capsid and chromosome at the initiation of encapsidation. They could also play a catalytic role in the compaction of the viral genome, or they could form a portal structure through which the viral genome must enter the virion capsid. Loss of any one of these functions could disrupt virion assembly. These authors also proposed that a major 40kd (doublet) breakdown product detected within empty capsids and intermediate particles may result from the cleavage of the 52/55kd proteins (at the consensus cleavage site ^{348}-LAGTG) at a late stage during encapsidation by the viral protease. This breakdown product can form homodimers with another 40kd cleavage product or with full length 52/55kd proteins (which can also dimerise).

In order to determine whether the 23kd protease and the L1 52/55kd proteins colocalised within infected cell nuclei, a monospecific polyclonal antiserum was generated against a synthetic peptide corresponding to the region ^{46}-DGYEPPRRRARHYL of both proteins, using the methods outlined in section 2.9.2. The antiserum immunoreacted with a doublet corresponding to apparent molecular weights of 52kd and 55kd from nuclear extracts of Ad2 infected cells (28 h.p.i), and a single form of approximately 52kd from cytoplasmic extracts

from the same cell lysates. No immunoreactions were detected with equivalent extracts from non-infected cells (figure 3.81).

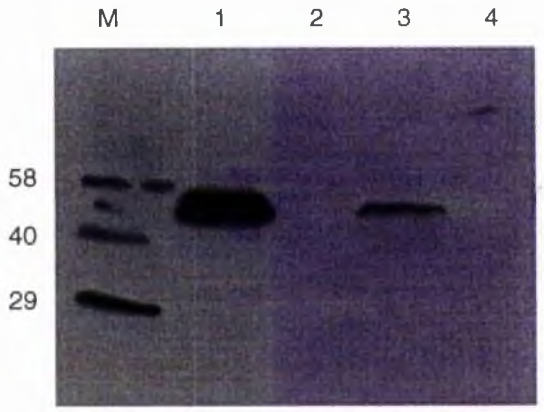

Figure 3.81: Immunoprecipitation of the L1 52/55kd proteins from Ad2 infected cell lysates. polyclonal antiserum was added to precleared nuclear and cytoplasmic extracts of Ad2 infected HeLa cells (28 h.p.i) and mock infected cells (sections 2.7.4ii and 2.9.3iii). Samples and biotinylated molecular weight markers were electroblotted (15% SDS-PAGE) and stained using the same polyclonal antiserum (1/3000 dilution). Ad2 Infected nuclear (lane 1) and cytoplasmic (lane 3) extracts. Non-infected nuclear (lane2) and cytoplasmic (lane 4) extracts.

Immunofluorescent staining of Ad2 infected HeLa cells (28 h.p.i) revealed that the L1 52/55kd proteins had a diffuse nuclear staining pattern (similar to that of pVI), with the proteins observed to be localised predominantly at the nuclear periphery. Colocalisation of the 52/55kd proteins and the viral protease was detected within domains likely to correspond to assembly centres and amorphous inclusions (figure 3.82). It was of interest that in the apparent absence of 23kd protease, the 52/55kd proteins exhibited a punctate staining pattern. The L1 52/55kd protein staining patterns shown here are identical to those published by Hasson *et al* (1992). These authors noted that sites of 52/55kd protein staining were distinct from replication centres, and appeared to colocalise with assembling virions. They proposed that virus assembly begins at multiple sites which coalesce as the infection proceeds, eventually filling much of the nuclear periphery. Interestingly, the apparent distribution of the 23kd protease and 52/55kd proteins within Ad2ts1 infected cells (28 h.p.i) was determined to be identical to that of the wild type (figure 3.83). This is markedly different to the observed pVI/VI distribution which was found to be less diffuse and more intense at the nuclear periphery.

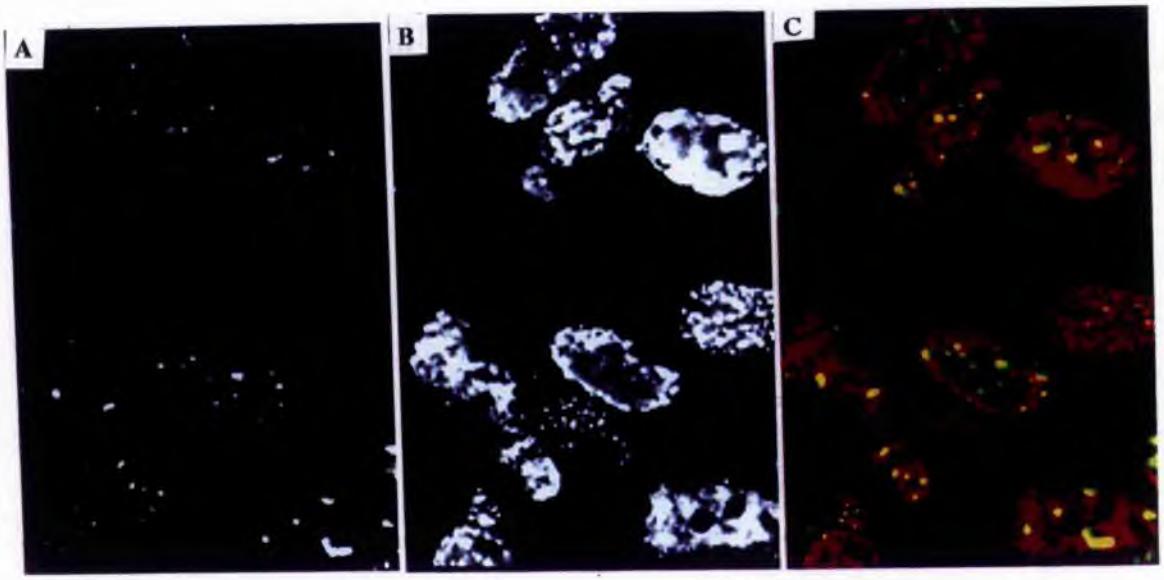

Figure 3.82: Distribution of the 23kd protease and L1 52/55kd proteins within Ad2 infected cells. BIO-RAD MRC-600 laser scanning confocal image of the viral protease (detected using Mab OA10b3)(part A) and the L1 52/55kd proteins (part B). The merge of both images is given in part C with the protease showing as green and the L1 52/55kd phosphoproteins showing as red (with yellow representing colocalisation). Infected HeLa cells (28 h.p.i) were fixed and immunolabelled as described in sections 2.7.5 and 2.8.2. Viewed at x100 magnification (oil immersion).

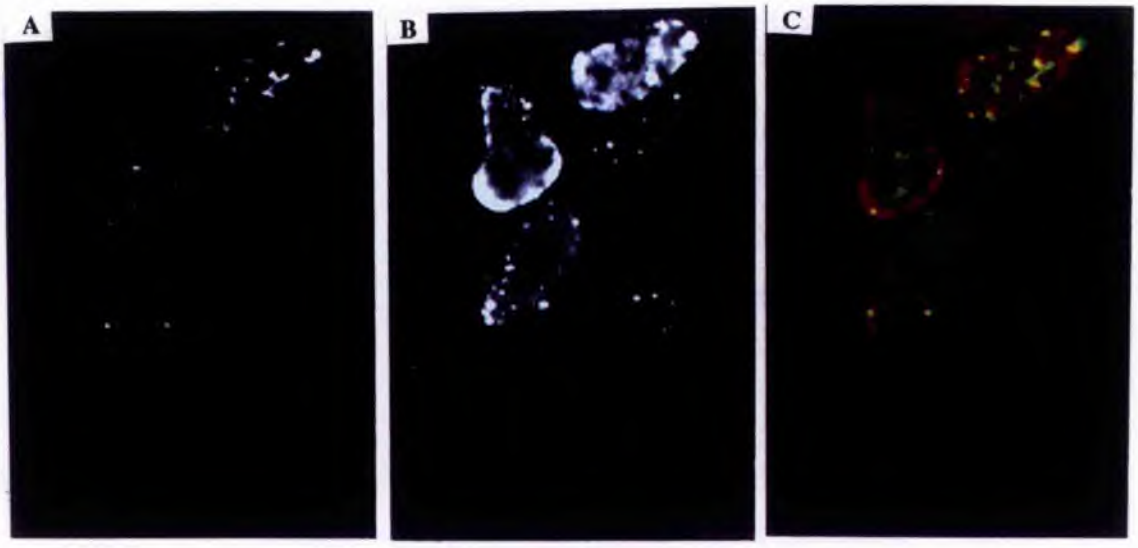

Figure 3.83: Distibution of the 23kd protease and L1 52/55kd proteins within Ad2ts1 infected cells. BIO-RAD MRC-600 laser scanning confocal image of the viral protease (detected using Mab OA10b3)(part A) and the L1 52/55kd proteins (part B). The merge of both images is given in part C with the protease showing as green and the L1 52/55kd phosphoproteins showing as red (with yellow representing colocalisation). Infected HeLa cells (28 h.p.i) were fixed and immunolabelled as described in sections 2.7.5 and 2.8.2. Viewed at x100 magnification (oil immersion).

The observed colocalisation of the 23kd protease and the 52/55kd proteins within Ad2ts1 infected cells suggested that the viral protease is unable to cleave the scaffolding proteins at these sites, as Hasson *et al* (1992) have determined that cleavage does not occur within Ad2ts1 infected cells. The authors have proposed that cleavage occurs within assembly intermediates, and therefore prior to maturation cleavages involved in converting young virions into mature virions.

Thin sections were not immunolabelled, however Hasson *et al* (1992) did localise the proteins to three different structures using the pre-embedding technique. The first, and probably the most relevant in terms of the observed colocalisation with the 23kd protease, was the immunolocalisation of the 52/55kd proteins to what these authors termed loading centres, which were always surrounded by numerous virions (which were also immunolabelled), and may correspond to the clear amorphous inclusions described in this study.

The 52/55kd proteins were also localised to circular electron dense bodies which may be the same structures as those shown in figure 3.55 (referred to as DNb), which were often found to be in close proximity to the clear amorphous inclusions. Electron dense bodies have been shown to contain protein IVa2 (figure 3.85; Lutz *et al.*, 1996).

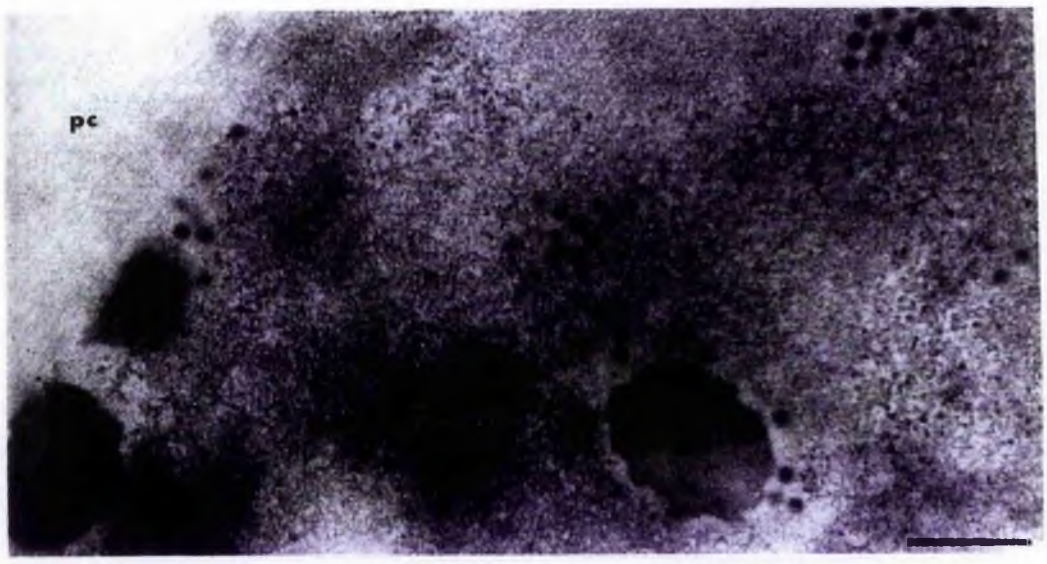

Figure 3.84: Localisation of protein IVa2 within Ad2 infected cells. Part of the nucleus of an Ad5 infected HeLa cell (17 h.p.i). Immunogold detection of protein IVa2 within glutaraldehyde fixed cells. IVa2 was localised to virus-induced electron dense amorphous inclusions (ai) often found close to protein crystals (pc) and the nucleolus. Bar 0.5μm. Reproduced from Lutz *et al* (1996).

This is of particular interest, as the proposed 40kd cleavage product of the 52/55kd protein has been implicated as the functional partner of IVa2 in the formation of the DEF-A complex (Gustin *et al.*, 1996). The DEF-A and DEF-B (which is comprised of a IVa2 homodimer) complexes have been proposed to be involved in the late-stage specific transactivation of major late promoter activity. If the viral protease is directly involved in DEF-A complex formation, then the enzyme must be active outwith the maturing virion, possibly within clear amorphous inclusions which are found to be associated with the electron dense bodies located at the nuclear periphery.

4 General Discussion.

4.1 The subcellular localisation of the Ad2 protease within lytically infected cells.

There is now strong evidence to suggest that the viral protease plays a critical role during the final stages of infection in which 'young' virions are matured into infectious particles. However, it is currently unknown what mechanism(s) are involved in the prevention of premature activation of the enzyme, and consequently, premature cleavage of precursor proteins. Likewise, the events and/or factors which facilitate cleavage of cytokeratins K18 and K7 are also unknown. Results presented within this thesis suggest that intranuclear viral protease could be regulated during the late-phase of productive infection by being sequestered to virus-induced clear amorphous inclusions.

4.1.1 Clear amorphous inclusions.

Puvion-Dutilleul *et al* (1995b) noted that clear amorphous inclusions which accumulate PML were present within infected nuclei as soon as virus-induced intranuclear changes became visible. At the later stage of nuclear transformation, when isolated and clustered viruses were more numerous, clear amorphous inclusions were located within the electron translucent area of the nuclear periphery (figure 4.1). The authors also observed that as infection progressed, these structures, which were initially small and irregularly shaped, became larger and more abundant. The authors speculated that sequestration of PML to these virus-induced inclusions might inactivate the protein, and facilitate the intranuclear development of progeny genomes and viruses.

It is believed that these structures are the same as those observed during the course of this study to contain the viral protease, protein pVIII, and possibly the L152/55kd protein. However, pVIII was not shown to colocalise with PML at 28 h.p.i, which suggested that PML might either be relocated from clear amorphous inclusions (and protein crystals) during the late-phase of nuclear transformation (between 18 and 28 h.p.i), or that structurally similar (but not identical) virus-induced inclusions have been identified.

It is thought unlikely that the viral protease is active within these inclusions during the late-phase of nuclear transformation as activity would presumably result in the premature cleavage

Figure 3.53: Part of the nucleus of an adenovirus-infected HeLa cell at 17 h.p.i. Immunogold labelling using anti-PML polyclonal antibody. Three juxtaposed clear amorphous inclusions (arrows) are localised at the border of the nucleus in an electron-translucent region (e) which also contains a large protein crystal (pc). Gold particles accumulate over the clear amorphous inclusions and are less numerous over the protein crystal. Peripheral replicative zone (p), ssDNA-accumulation sites (a), viral genome storage site (asterisk), and crystals of viruses (v), are almost entirely devoid of labelling. Bar 1μm. Reproduced from Puvion-Dutilleul *et al* (1995b).

of pVIII. Additionally, pVI was not detected within these structures during the late-phase of infection which also suggested that the viral protease may be inactive, as cleavage of pVIII *in vitro* required the addition of pVI-ct to the reaction mixture. However, it is noteworthy that the anti-pVIII polyclonal antiserum recognised protein VIII as well as pVIII. Therefore, it is unknown which form, if not both, was detected within the virus-induced inclusions. It is also noteworthy that the L1 52/55kd proteins were detected within the thread-like structures present within Ad2 and Ad2ts1 nuclei, yet Hasson *et al* (1992) have shown that neither of these proteins are cleaved within Ad2ts1 infected cells (at the non-permissive temperature).

Colocalisation of pVI and the 23kd protease (detected using Mab OA10b3) was detected, albeit infrequently, at sites that may be virus-induced inclusions. Unlike Mab OC11b11, OA10b3 did not immunoreact with viral protease present within assembly centres, but instead appeared to exclusively immunoreact with the enzyme present within punctate spots and thread-like structures which were later determined to be clear amorphous inclusions. Likewise, pVI was also infrequently observed to be within these inclusions, which were always small, regularly shaped and isolated from other virus-induced inclusions.

Although it is unclear whether these are the same sites where pVI/PML colocalisation was observed, it may be that these inclusions are an early to late-phase form of clear amorphous inclusion distinct from the irregularly shaped (early-phase) clear amorphous inclusion described by Puvion-Dutilleul *et al* (1995b). Similar irregularly shaped inclusions were detected during the course of this study within nuclei infected with Ad2ts1 (non-permissive temperature only). At 28 h.p.i these inclusions contained pVIII, the viral protease, and possibly the L1 52/55kd proteins.

Tentatively, it is thought possible that the viral protease might be active within intranuclear virus-induced inclusions during the early to late-phase of infection (18 to 22 h.p.i). This is not improbable as cytokeratin K18 cleavage (in the apparent absence of pVI) was detected as early as 20 to 22 h.p.i. This suggested that in addition to being directly involved in the maturation of 'young' virions, the viral protease also plays an active part in the degradation of the intermediate filament system (which is believed to facilitate the release of mature progeny virions), at least 12 hours prior to cell lysis. Likewise the protease might be involved in the inactivation of nuclear proteins such as PML, or other PML-body associated proteins, which are thought to play some part in the cellular defence mechanism against viral infections.

Alternatively, sequestration of the viral protease to clear amorphous inclusions may itself prevent the enzyme from being prematurely activated. During the late-phase of nuclear transformation, the inclusions could be thought of as loading centres from which the enzyme is packaged into assembled virions prior to virion release. This is consistent with the observation that there was a significantly greater degree of immunogold labelling of clear amorphous inclusions which were surrounded by crystalline arrays of virion particles in comparison with those which were generally surrounded by randomly distributed virions.

The observed localisation of the L1 52/55kd probable scaffold proteins to the punctate spots and thread-like structures also supports the hypothesis that clear amorphous inclusions may function as loading centres from which virion components are inserted into pre-assembled capsids. Hasson *et al* (1989 and 1992) have suggested that these probable scaffold proteins are critical for packaging of the viral genome within pre-assembled capsid structures. The proteins apparently remain associated with the particles until they are cleaved by the viral protease.

4.1.2 Distribution of the 23kd protease within Ad2ts1 infected nuclei.

The observed localisation of the viral protease within irregularly shaped clear amorphous inclusions, but not within crystalline arrays of assembled virion particles is consistent with results presented elsewhere (Rancourt et al., 1995). These authors demonstrated that the cause of the Ad2ts1 protease defect resided in a failure of enzyme activation and enzyme encapsidation at the non-permissive temperature. The temperature-sensitive protease was synthesised and transported to the nucleus in a manner similar to the wild type protease, but was not present within 'young' virions.

The suprising observation within this study was that virion particles did not appear to be in close proximity to the clear amorphous inclusions. It therefore seems likely that the ts1 defect may be, at least in part, due to specific interactions that occur within, or in close proximity to, the virus-induced clear amorphous inclusions. In that context, the unexpected finding presented by Rancourt *et al* (1995) that the *in vivo* and *in vitro* temperature sensitive phenotype could be rescued merely by provision of the activating peptide is particularly significant. The authors suggested that at 39°C the ts1 mutation causes a small but crucial structural change in the protein that prevents it from being in a position to be activated

through interaction with protein pVI, although the pVI-ct peptide itself can activate the enzyme both *in vivo* and *in vitro*.

Because the appearance of the virus-induced inclusions is altered within Ad2ts1 infected cells, it appears likely that the viral protease itself has some role in determining their structural integrity. As mentioned previously, it is thought possible that the viral protease may be active within these structures during the early to late stage (18 to 22 h.p.i) of nuclear transformation. Perhaps pVI mediated activation of the protease occurs during this period of infection and is required for the development of these virus-induced inclusions from the early small and irregularly shaped structures, into the larger and more regularly shaped inclusions detected during wild type infections at 28 h.p.i and ts1 infections (at the permissive temperature) at 48 h.p.i.

4.1.3 Does the viral protease localise to 'assemblons'?

The pathway for adenovirus assembly was first analysed using kinetic labelling experiments (reviewed by D'Halluin, 1995), however progress was hampered due to the large pool of structural proteins within infected cells, and the fact that only a fraction of structural proteins in infected cells were shown to be incorporated into virus particles. Another approach has involved the use of temperature defective mutants, usually in conjunction with pulse-chase experiments, and separation of assembly intermediates using CsCl gradients. Although much of the data presented using these techniques has been very informative, the various mechanisms involved in virion assembly and maturation are still poorly understood, as are the mechanisms by which the infected cell is lysed just prior to virion release.

In recent years there has been significant progress in determining the means by which adenovirus causes intranuclear rearrangements necessary for both replication and transcription. In contrast to studies which have primarily focused on events occurring during the late stage of infection, most of these studies have incorporated ultrastructural and cytochemical techniques to full effect.

Likewise, over the past few years there have been many advances in determining the events involved in the assembly of HSV-1 capsids within the nuclei of infected cells. Many of these studies have utilised both immunofluorescence and electron microscopy techniques as a general tool for the molecular dissection of many of the late events in HSV-1 biogenesis.

In cells infected with HSV-1, the viral proteins ICP5 (infected-cell protein 5)(the major capsid protein) and VP19c (the product of the U_L38 gene) are associated with mature capsids, whereas the same proteins, along with ICP35 (also referred to as VP22a), are components of immature capsids. All three proteins have been shown to coalesce at late times post-infection (Ward *et al.*, 1996) within structures located at the periphery of nuclei which the authors have termed assemblons. The fact that capsid proteins accumulated within assemblons suggested that HSV-1 assembly is facilitated by, and is dependant on, protein concentration. Furthermore, the presence of assemblon domains late in infection also raised questions regarding the mechanisms by which capsid proteins are sequestered to these structures, and segregated from proteins involved in DNA synthesis, and those forming the tegument.

Puvion-Dutilleul *et al* (1995c) have also noted that the cellular proteins PML, SP100, and P80-coilin are redistributed to electron translucent virus-induced structures which also contain HSV-1 capsid proteins. The functional significance of these structures, which are likely to be the assemblon structures observed using immunofluorescent microscopy, remains unknown. These authors proposed that the virus-structures have a potential role in the assembly of capsid proteins into capsid shells, and indeed, may be storage sites containing oversynthesised viral capsid proteins which may be assembled into non-functional or incomplete capsid shells. Additionally, it was thought possible that capsid proteins might interfere with sequestered PML and SP100, leading to their inactivation, and therefore, possibly contributing to the shutoff of host cell metabolism which occurs in HSV-1 infected cells.

Of interest is the fact that the HSV-1 protease (Pra) is involved in the assembly and maturation of viral capsids (Thomsen *et al.*, 1995; Robertson *et al.*, 1996). Pra is a 635 amino acid serine protease encoded by the U_L26 gene. The full length HSV-1 protease undergoes autoproteolytic processing at two sites (the release (R) and maturation (M) sites) generating N_O (the catalytic domain of the protease), N_b and a 25 amino acid C-terminal peptide. ICP35, a substrate of the HSV-1 protease, is encoded by the $U_L26.5$ gene. There is a family of ICP35 proteins designated *a* through to *f*, however, only ICP35*e*,*f* is present in B capsids (intermediates in assembly) and also found to be absent from mature virions. Since ICP35 overlaps, and is in frame with the C-terminal half of Pra, ICP35*c*,*d* can be *trans* cleaved at its C-terminus by the protease to generate ICP35*e*,*f* and a 25 amino-acid peptide.

It has been suggested that ICP35*e,f* has a possible scaffold protein role during capsid assembly and therefore may have functional roles similar to that of the Ad2 L1 52/55kd phosphoproteins.

The requirement for HSV-1 protease activity for capsid assembly and maturation has also been confirmed further using temperature defective mutants (Robertson *et al.*, 1996). Although capsid structures are observed in the absence of functional protease, the major capsid protein ICP5 (VP5) does not adopt the correct conformation and viral DNA is not encapsidated. It appears that the full length protease (Pra), the catalytic domain (N_O), and the R and M cleavage site mutant protease's are proteolytically active, however, the catalytic domain of the protease alone is insufficient to support viral growth, suggesting that N_a (N_b and the 25 amino-acid peptide) may be required to direct the catalytic domain to the site of capsid assembly. Likewise, it is thought likely that intranuclear interactions (possibly with the C-terminus of pVI) governing the localisation of the Ad2 protease to sites of capsid assembly are defective within Ad2ts1 infected cells. It is possible that the adenovirus-induced clear amorphous inclusions and HSV-induced asemblons/electron translucent patches have similar functional roles during the course of productive infections. In this context, it is of particular interest that both viral protease's are localised to these domains, and certainly in respect to HSV-1 infection, proteolytic activity has been shown to necessary for release of ICP35 from B capsids.

4.2 Ad2 protease activity: Possible regulation mechanisms.

The pVI-ct mediated activation of the Ad2 23kd protease has now been extensively studied, and has been shown to involve the formation of a stable complex. Likewise, modulation of Hepatitis C NS3 protease activity by the virus encoded NS4a polyprotein cleavage product also appears to involve complex formation, although the mechanism by which NS4A modulates proteinase activity is still not known (Bartenschlager *et al.*, 1995). Interaction between NS3 and NS4a may be required for localisation of NS3 to the endoplasmic reticulum membrane where most of the NS proteins are found. In this case, NS4a would increase the local NS3 protease concentration, thereby enhancing substrate cleavage. However, the NS3 protease has also been shown to be localised to the nucleus of infected hepatocytes, and

interestingly, this localisation is suppressed by NS4a cofactor but augmented by the cellular p53 protein (Muramatsu *et al.*, 1997). Whether pVI-ct exerts similar constraints on the subcellular localisation of the Ad2 protease is presently unclear, however, the observation that the Ad2ts1 protease was packaged within virions at the nonpermissive temperature after provision of pVI-ct to the medium (Rancourt *et al.*, 1995), might suggest that pVI-ct, or pVI itself, does play some part in intracellular trafficking of the viral protease. In that context, it is noteworthy that the viral protease does not appear to contain any known nuclear localisation signal, and therefore may be dependant on pVI, or pVI-ct, for nuclear/intranuclear localisation.

The HSV-1 (Schmidt and Darke, 1997), hCMV (Margosiak *et al*, 1996), EBV (Donaghy and Jupp, 1994) and HIV-1 (Davis *et al*, 1995) protease's appear to be regulated through the formation of homodimers. In the case of the protease's which belong to the Herpes virus family, the monomeric forms of these enzymes are inactive in all three cases. The *in vivo* dimerisation of hCMV protease is thought to have an important physiological role in the temporal regulation of processes that occur during virus assembly. It is known that during capsid maturation the critical proteolytic events are controlled by the oligomerisation or aggregation state of full length protease and its substrate. It has been proposed that the monomeric form produced in the cytoplasm remains inactive, and that hCMV protease becomes activated and performs maturation cleavages only when the local concentration of monomeric forms reaches a high enough concentration within immature capsids.

Although dimeric forms of the 23kd protease were not isolated from Ad2 infected HeLa cells, dimeric isoforms of the recombinant wild type, but not the ts1 mutant, enzyme were observed during the course of this study. The ability to form dimers *in vitro* was the only discernible difference between the two recombinant enzymes. After addition of pVI-ct, the recombinant ts1 protease was shown to be active regardless of the assay temperature. What relavence, if any, dimerisation has on regulation of both the wild type and ts1 enzymes *in vivo* is unclear, although Cys104 may be considered a likely candidate for inter-molecular disulphide bonds involved in the formation of homodimers. It is noteworthy that Keyvani-Amineh *et al* (1996) have shown that redox conditions other than the pVI-ct peptide were capable of activating the protease, although the relevance to virus infected cells was also questioned by these authors.

4.3 Suggestions for future work.

It is unclear why both pVIII and the 23kd protease colocalise within virus-induced nuclear inclusions and also within distinct cytoplasmic structures late in infection. It would be of particular interest to determine what other factors (both cellular and viral) are sequestered to these domains, and which, if any, are directly involved in the intranuclear localisation of pVIII and the viral protease. Additionally, further investigations might reveal what mechanism(s) are involved in regulating *in vivo* viral protease activity, and whether these events are in some way linked to other processes that occur during a typical lytic infection.

Investigating what protein-protein interactions occur, perhaps using the yeast two hybrid sytem, would potentially be usefull in determining further possible roles for pVIII and the viral protease late in infection. However, confirmation that pVIII and the viral protease are localised to the same virus-induced inclusions which have been shown to contain PML would be a prerequisite for any study that was a continuation of work presented within this thesis. Likewise, determining whether PML and P80-coilin are cleaved during a typical lytic infection, and at what times post-infection they are cleaved, would be of particular interest. In that context, an examination of both these cellular proteins and several viral proteins including hexon, fibre (which coalesce within protein crystals), pVI, pVIII and the 23 kd protease at different times post-infection using immunofluorescence and electron microscopy would be required.

Expression of the 23kd protease within virtually any animal cell using Semliki Forest Virus vectors, or other transfection vectors, might also be very informative. These systems could be utilised to determine whether pVI is required for cytokeratin K18 cleavage and/or nuclear localisation of the viral protease.

5 Bibliography

AKUSJÄRVI, G.; ALESTROM, P.; PETTERSSON, M.; LAGER, M.; JORNVALL, H. and PETTERSSON, U. (1984). The gene for the adenovirus type 2 hexon polypeptide. *The Journal of Biological Chemistry* **259**, 13976-13979.

AKUSJÄRVI, G. and PERSSON, H. (1981). Gene and mRNA for precursor polypeptide VI from adenovirus type 2. *Journal of Virology* **38**, 469-482.

AKUSJÄRVI, G.; PETTERSSON, U. and ROBERTS, R.J. (1986). Structure and function of the adeovirus-2 genome. In: *Adenovirus DNA: The viral genome and its expression.* Ed. by: W. Doerfler. Martin Nijhoff. Boston. pp 53-95.

ALESTROM, P.; AKUSJÄRVI, G.; LAGER, M.; YEH-KAI, L. and PETTERSSON, U. (1984). Genes encoding the core proteins of adenovirus type 2. *Journal of Biological Chemistry* **259**, 13980-13985.

ALESTROM, P.; AKUSJÄRVI, G.; PERRICAUDET, M.; MATHEWS, M.B.; KLESSIG, K.F. and PETTERSSON, U. (1980). The gene for polypeptide IX of adenovirus type 2 and its unspliced messenger RNA. *Cell* **19**, 671-681.

AMBERG, S.M.; NESTOROWICZ, D.W; McCOURT, D.W. and RICE, C.M. (1994). NS2B-3 proteinase-mediated processing in the yellow fever virus structural region: in vitro and in vivo studies. *Journal of Virology* **68**, 3794-3802.

ANDERSON, C.W. (1990). The proteinase polypeptide of adenovirus type 2 virions. *Virology* **177**, 259-272.

ANDERSON, C.W.; BAUM, P.R. and GESTELAND, R.F. (1973). Processing of adenovirus 2 induced proteins. *Journal of Virology* **12**, 241-252.

ANGELETTI, P.C. and ENGLER, J.E. (1996). Tyrosine kinase-dependant release of an adenovirus preterminal protein complex from the nuclear matrix. *Journal of Virology* **70**, 3060-3067.

ATHAPILLY, F.K.; MURALI, R.; RUX, J.J.; CAI, Z. and BURNETT, R.M. (1994). The refined crystal structure of hexon, the major coat protein of adenovirus type 2, at 2.9Å resolution. *Journal of Molecular Biology* **242**, 430-455.

BABISS, L.E.; GINSBERG, H.S. and DARNELL, J.R. (1985). Adenovirus E1B proteins are required for accumulation of late viral mRNA and for effects on cellular mRNA translation and transport. *Molecular and Cellular Biology* **5**, 2552-2558.

BAI, M.; HARFE, B. and FREIMUTH, P. (1993). Mutations thet alter the Arg-Gly-Asp (RGD) sequence in the adenovirus type 2 penton base protein abolish its cell rounding activity and delay virus reproduction in flat cells. *Journal of Virology* **67**, 5198-5205.

BARTENSCHLAGER, R.; LOHMANN, V.; WILKINSON, T. and KOCH, J.O. (1995). Complex formation between the NS3 serine-type proteinase of the hepatitis C virus and NS4A and its importance for polyprotein maturation. *Journal of Virology* **69**, 7519-7528.

BAUM, E.Z.; DING, W.D.; SIEGEL, M.M.; HULMES, J.; BEBERNITZ, G.A.; SRIDHARAN, L.; TAEI, K.; KRISHNAMURTHY, G.; CAROFIGLIO, T.; GROVES, J.T.; BLOOM, J.D.; DIGRANDI, M.; BRADLEY, M.; ELLESTAD, G.; SEDDON, A.P. and GLUZMAN, Y. (1996a). Flavins inhibit human cytomegalovirus UL80 protease via disulphide bond formation. *Biochemistry* **35**, 5847-5855.

BAUM, E.Z.; SIEGEL, M.M.; BEBERNITZ, G.A.; HULMES, J.; SRIDHARAN, L.; SUN, L.; TABEI, K.; JOHNSTON, S.H.; WILDEY, M.J.; NYGAARD, J.; JONES, T.R. and GLUZMAN, Y. (1996b). Inhibition of human cytomegalovirus UL80 protease by specific intramolecular disulphide bond formation. *Biochemistry* **35**, 5838-5846.

BELIN, M.T. and BOULANGER, P. (1987). Processing of vimentin occurs during the early stages of adenovirus infection. *Journal of Virology* **61**, 2559-2566.

BELIN, M.T and BOULANGER, P. (1993). Involvement of cellular adhesion sequences in the attachment of adenovirus to the HeLa cell surface. *Journal of General Virology* **74**, 1485-1497.

BESSE, S. and PUVION-DUTILLEUL, F. (1994). High resolution localisation of replicating viral genome in adenovirus-infected HeLa cells. *European Journal of Cell Biology* **63**, 269-279.

BESSE, S. and PUVION-DUTILLEUL, F. (1995). Anchorage of adenoviral RNAs to clusters of interchromatin granules. *Gene Expression* **5**, 79-92.

BHATTI, R.A. and WEBER, J.M. (1979). Protease of adenovirus type 2: Partial characterisation. *Virology* **96**, 478-485.

BLAIR, G.E. and RUSSELL, W.C. (1978). Identification of a protein kinase activity associated with human adenoviruses. *Virology* **86**, 157-166.

BOHMANN, K.; FERREIRA, J.A. and LAMOND, A.I. (1995). The mutational analysis of P80 coilin indicates a functional interaction between coiled bodies and the nucleolus. *Journal of Cell Biology* **131**, 817-831.

BONDESSON, M.; OHMAN, K.; MANNERVIK, M.; FAN, S. and AKUSJÄRVI, G. (1996). Adenovirus E4 open reading frame 4 protein autoregulates E4 transcription by inhibiting E1A transactivation of the E4 promoter. *Journal of Virology* **70**, 3844-3851.

BOOY, F.P.; TRUS, B.L.; NEWCOMB, W.W.; BROWN, J.C.; CONWAY, J.F. and STEVEN, A.C. (1994). Finding a needle in a haystack: detection of a small protein (the 12kd VP26) in a large complex (the 200md capsid of herpes simplex virus). *Proceedings of the National Acadamy of Sciences* (USA) **91**, 5652-5656.

BORDEN, K.L.B.; BODDY, M.N.; LALLY, J.; O'REILLY, N.J.O.; MARTIN, S.; HOWE, K.; SOLOMON, E. and FREEMONT, P.S. (1995). The solution structure of the RING finger domain from acute promyelocytic leukaemia proto-oncoprotein PML. *The EMBO Journal* **14**, 1532-1541.

BOSHER, J.; DAWSON, A. and HAY, R.T. (1992). Nuclear factor I is specifically targeted to discrete subnuclear sites in adenovirus type 2 infected cells. *Journal of Virology* **66**, 3140-3150.

BOUDIN, M.; MONCANY, M.; D'HALLUIN, J.C.; BOULANGER, P.A. (1979). Isolation and characterisation of adenovirus type 2 vertex capsomer (penton base). *Virology* **92**, 125-128.

BOUDIN, M.; D'HALLUIN, J.; COUSIN, C. and BOULANGER, P. (1980). Human adenovirus type 2 protein IIIa II: Maturation and encapsidation. *Virology* **101**, 144-156.

BOULANGER, P. and BLAIR, G.E. (1991). Expression and interactions of human adenovirus oncoproteins. *Biochemical Journal* **275**, 281-299.

BOULANGER, P.; LEMAY, P.; BLAIR, G.E. and RUSSELL, W.C. (1979). Characterisation of adenovirus protein IX. *Journal of General Virology* **44**, 783-800.

BRASCH, K. and OCHS, R.L. (1992). Nuclear bodies (NBs): A newly 'rediscovered' organelle. *Experimental Cell Research* **202**, 211-223.

BRIDGE, E.; CARMO-FONSECA, M.; LAMOND, A.I. and PETTERSSON, U. (1993). Nuclear Organisation of splicing small nuclear ribonucleoproteins in adenovirus-infected cells. (1993). *Journal of Virology* **67**, 5792-5802.

BRIDGE, E.; XIA, D.X.; CARMO-FONSECA, M.; CARDINALI, B.; LAMOND, A.I. and PETTERSSON, U. (1995). Dynamic organisation of splicing factors in adenovirus-infected cells. *Journal of Virology* **69**, 281-290.

BRIDGE, E. and PETTERSSON, U. (1995). Nuclear organisation of replication and gene expression. In: The Molecular Repertoire of Adenoviruses II. Ed. by: W. Doerfler and P. Bohm. Springer-Verlag. Hiedelberg. pp 101-117.

BROWN, D.T.; WESTPHAL, M.; BURLINGHAM, B.T.; WINTERHOFF, U. and DOERFLER, W. (1975). Structure and composition of the adenovirus type 2 core. *Journal of Virology* **16**, 366-387.

BUKRINSKY, M.I.; HAGGERTY, S.; DEMPSEY, M.P.; SHAROVA, N.; ADZHUBEL, A.; SPITZ, L.; LEWIS, P.; GOLDFARB, D.; EMERMAN, M. and STEVENSON, M. (1993). A nuclear localisation signal within HIV-1 matrix protein that governs infection of non-dividing cells. *Nature* **365**, 666-669.

BUTKIEWICZ, N.J.; WENDEL, M.; ZHANG, R.; JUBIN, R.; PICHARDO, J.; SMITH, E.B.; HART, A.M.; INGRAM, R.; DURKIN, J.; MUI, P.W.; MURRAY, M.G.; RAMANATHAN, L. and DASMAHAPATRA, B. (1996). Enhancement of hepatitis C NS3 proteinase activity by association with NS4A-specific synthetic peptides: identification of sequence and critical residues of NS4A for cofactor activity. *Virology* **225**, 328-338.

CABRITA, G.; IQBAL, M.; REDDY, H. and KEMP, G.D. (1997). Activation of the Adenovirus protease requires sequence elements from both ends of the activating peptide.*The Journal of Biological Chemistry* **272**, 5635-5639.

CARMO-FONSECA, M.; FERREIRA, J. and LAMOND, A.I. (1993). Assembly of snRNP-containing coiled bodies is regulated in interphase and mitosis-Evidence that the coiled body is a kinetic nuclear structure. *Journal of Cell Biology* **120**, 841-851.

CARREY, E.A. (1990). Peptide mapping. In: *Protein Structure: A Practical Approach.* Ed. by: T.E. Creighton. IRL Press. Oxford. pp117-143.

CARVALHO, T.; SEELER, J.S.; OHMAN, K.; JORDAN, P.; PETTERSSON, U.; AKUSJÄRVI, G.; CARMO-FONSECA, M. and DEJEAN, A. (1995). Targeting of adenovirus E1A and E4-ORF3 proteins to nuclear matrix-associated PML bodies. *Journal of Cell Biology* **131**, 45-56.

CASIGLIA, C.L. and FLINT, S.J. (1983). Effects of adenovirus infection on RNA synthesis and maturation in HeLa cells. *Molecular and Cellular Biology* **3**, 662-671.

CEPKO, C.L. and SHARP, P.A. (1983). Analysis of Ad5 hexon and 100k temperature sensitive mutants using conformation specific monoclonal antibodies. *Virology* **129**, 137-154.

CHALY, N. and CHEN, X. (1993). Assembly of adenovirus-specific inclusions in lytically infected HeLa cells: an ultrastructural and cytochemical study. *Journal of Biochemical and Cellular Biology* **71**, 475-487.

CHAN, E.K.L.; TAKANO, L.E.C.; ANDRADE, L.E.C.; HAMEL, J.C. and GREGORY, M.A. (1994). Structure, expression and chromosomal localisation of human P80-coilin gene. *Nucleic Acids Research* **22**, 4462-4469.

CHATERJEE, P.K.; VAYDA, M.E.; and FLINT, S.J. (1985). Interactions among the three adenovirus core proteins. *Journal of Virology* **55**, 379-386.

CHATTERJEE, P.K.; YANG, U.C. and FLINT, S.J. (1986). Comparisons of the interactions of the adenovirus type 2 major core protein and its precursor with DNA. *Nucleic Acids Research* **14**, 2721-2735.

CHEN, P.H; ORNELLES, D.A. and SHENK, T. (1993). The adenovirus L3 23kd proteinase cleaves the amino-terminal head domain from cytokeratin 18 and disrupts the cytokeratin network of HeLa cells. *Journal of Virology* **67**, 3507-3514.

CLEGHON, V.; PIDERIT, A.; BROUGH, D.E. and KLESSIG. (1993). Phosphorylation of the adenovirus DNA-binding protein and epitope mapping of monoclonal antibodies against it. *Virology* **197**, 564-575.

CLEVER, J. and KASAMATSU, H. (1991). Simian virus 4 VP2/3 small structural proteins harbor their own nuclear transport signal. *Virology* **181**, 78-90.

COLBY, W.W. and SHENK, T. (1981). Adenovirus type 5 virions can be assembled in vivo in the absence of detectable protein IX. *Journal of Virology* **39**, 977-980.

COTTEN, M. and WEBER, J.M. (1995). The adenovirus protease is required for virus entry into host cells. *Virology* **213**, 494-502.

CREIGHTON, T.E. (1990). Disulphide bonds between cysteine residues. In: *Protein Structure: A Practical Approach.* Ed. by: T.E. Creighton. IRL Press. Oxford. pp155-166.

CUILLEL, M.; CORTOLEZZIS, B.; CHROBOCZEK, J.; LANGOWSKI, J.; RUIGROK, R.W.H. and JACROT, B. (1990). Purification and characterisation of wild-type and ts112 mutant protein IIIa of human adenovirus 2 expressed in *E.coli*. *Virology* **175**, 222-231.

CUPO, J.F.; REZANKA, L.J. and HARPST, J.A. (1987). Column purification of adenovirus cores. *Analytical Biochemistry* **164**, 267-270.

DAVEY, J.; DIMMOCK, N.J. and COLMAN, A. (1985). Identification of the sequence responsible for the nuclear accumulation of the influenza virus nucleoprotein in Xenopus oocytes. *Cell* **40**, 667-675.

DAVIS, D.A.; DORSEY, P.T.; STAHL, S.J.; KAUFMAN, J.; FALES, H.M.; LEVINE. R.L. (1995). Regulation of HIV-1 protease activity through cysteine modification. *Biochemistry* **35**, 2482-2488.

DEFER, C.; BELIN, M.; CAILLET-BOUDIN, M. and BOULANGER, P. (1990). Human adenovirus-host cell interactions: comparitive study with members of subgroups B and C. *Journal of Virology* **64**, 3661-3673.

DEPPERT, W. and SCHIRMBECK, R. (1995). The nuclear matrix and virus function. *International Review of Cytology* **162.A**, 485-537.

DEVAUX, C.; ADRIAN, M.; BERTHET-COLOMINAS, C; CUSACK, S. and JACROT, B. (1987). Structure of adenovirus fibre I: Analysis of crystals of fibre from adenovirus seroypes 2 and 5 by electron microscopy and X-ray crystallography. *Journal of Molecular Biology* **215**, 567-588.

DEZAZZO, J.D.; FALCK-PEDERSON, E. and IMPERIALE, M.J. (1991). Sequences regulating temporal poly(A) site switching in the adenovirus major late transcription unit. *Molecular and Cellular Biology* **11**, 5977-5984.

D'HALLUIN, J.C. (1995). Virus Assembly. *The Molecular Repertoire of Adenoviruses* I. Ed. by: W. Doerfler and P. Böhm. Springer-Verlag. Heidelberg. pp47-61.

D'HALLUIN, J.C.; COUSIN, C.; BOULANGER, P.A. (1982). Physical mapping of adenovirus type 2 ts mutations by restriction nuclease analysis of interserotypic recombinants. *Journal of Virology* **41**, 410-413.

D'HALLUIN, J.C.; MILLEVILLE, P. BOULANGER, P.A. and MARTIN, G. (1978). Temperature sensitive mutant of adenovirus type 2 blocked in virion assembly: accumulation of light intermediate particles. *Journal of Virology* **26**, 344-356.

DING, J.; McGRATH, W.J.; SWEET, R.M. and MANGEL, W. (1996). Crystal structure of the human adenovirus proteinase with its 11 amino acid cofactor. *The EMBO Journal* **15**, 1778-1783.

DIOURI, M.; GIROUARD, G.S.; ALLEN, C.M.; SIRCAR, S.; VAN LIER, J.E. and WEBER, J.M. (1996). New stimulation ligand of the adenovirus 2 protease. *Virology* **224**, 510-516.

DONAGHY, G. and JUPP, R. (1995). Characterisation of the epstein-barr virus proteinase and comparison with the human cytomegalovirus proteinase. *Journal of Virology* **69**, 1265-1270.

DORFMAN, T.; BUKOVSKY, A.; OHAGEN, A.; HOGLUND, S.; GOTTLINGER, H.G. (1994). Functional domains of the capsid protein of human immunodeficiency virus type 1. *Journal of Virology* **68**, 8180-8187.

DOUCAS, V.; ISHOV, A.M.; ROMO, A.; JUGUILON, H.; WEITZMAN, M.D.; EVANS, R.M. and MAUL, G.G. (1996). Adenovirus replication is coupled with the dynamic properties of the PML nuclear structure. *Genes and Development* **10**, 196-207.

ECKHART, W. (1990). Polyomavirus and their replication. In. *Virology*. 2nd Edition. Ed. by: B.N. Fields and D.M. Knipe. Raven. New York. pp1593-1607.

EDVARDSSON, B.; EVERITT, E.; JORNVALL, H.; PRAGE, L. and PHILIPSON, L. (1976). Intermediates among adenovirus assembly. *Journal of Virology* **19**, 533-547.

EVERETT, R.D. and MAUL, G.G. (1994). HSV-1 IE protein Vmw 110 causes redistribution of PML. *The EMBO Journal* **13**, 5062-5069.

EVERETT, R.D.; MAUL, G.G.; ORR, A. and ELLIOT, M. (1995b). The cellular finger protein PML is not a functional counterpart of herpes simplex virus type 1 TING finger protein Vmw 110. *Journal of General Virology* **76**, 791-798.

EVERETT, R.D.; MEREDITH, M.; ORR, A.; CROSS, A.; KATHORIA, M; PARKINSON, J. (1997). A novel ubiquitin-specific protease is dynamically associated with PML nuclear domain and binds to a herpesvirus regulatory protein. *The EMBO Journal* **16**, 1519-1530.

EVERETT, R.D.; O'HARE, P.; O'ROURKE, D.; BARLOW, P. and ORR, A. (1995a). Point mutations in the herpes simplex virus type 1 Vmw 110 RING finger helix affect activation of gene expression, viral growth, and interaction with PML-containing nuclear structures. *Journal of Virology* **69**, 7339-7334.

EVERITT, E.; LUTTER, L. and PHILIPSON, L. (1975). Structural proteins of adenovirus. *Virology* **67**, 197-208.

FERREIRA, J.A.; CARMO-FONSECA, M. and LAMOND, A.I. (1994). Differential interaction of splicing snRNPs with coiled bodies and interchromatin granules during mitosis and assembly of daughter cell nuclei. *Journal of Cell Biology* **126**, 11-23.

FRANGIONI, J.V. and NEEL, B.G. (1993). Solubilisation and purification of enzymatically active glutathione S-transferase (pGEX) fusion proteins. *Analytical Biochemistry* **210**, 179-187.

FREDMAN, J.N. and ENGLER, J.A. (1993). Adenovirus precursor to terminal protein interacts with the nuclear matrix *in vivo* and *in vitro*. *Journal of Virology* **67**, 3384-3395.

FREIMUTH, P. and ANDERSON, C.W. (1992). Human adenovirus serotype 12 virion precursors pMu and pVI are cleaved at amino-terminal and carboxy-terminal sites that conform to the adenovirus 2 endoproteinase cleavage consensus sequence. *Virology* **193**, 348-355.

FLINT, J. and SHENK, T. (1989). Adenovirus E1A protein paradigm viral transactivator. *Annual Review of Genetics* **23**, 141-161.

FRIGUET, B.; DJAVADI-OHANIANCE, L. and GOLDBERG, M.E. (1990). Immunochemical analysis of protein conformation. In: *Protein Structure: A Practical Approach.* Ed. by: T.E. Creighton. IRL Press. Oxford. pp287-309.

FURCINITTI, P.S.; OOSTRUM, J. and BURNETT, R.M. (1989). Adenovirus polypeptide IX revealed as capsid cement by difference images from electron microscopy and crystallography. *The EMBO Journal* **8**, 3563-3570.

GAO, M.; MATUSICK-KUMAR, L.; HURLBURT, W.; DI TUSA, S.F.; NEWCOMB, W.W.; BROWN, J.C.; McCANN, P.J.; DECKMAN, I. and COLONNO, R.J. (1994). The protease of herpes simplex virus type 1 is essential for functional capsid formation and viral growth. *Journal of Virology* **68**, 3702-3712.

GARCIA-BUSTOS, J.; HEITMAN, J.; HALL, M.N. (1991). Nuclear Protein Localisation. *Biocimica et Biophysica Acta* **1071**, 83-101.

GARON, C.F.; BERRY, K.W.; HIERHOLZER, J.C. and ROSE, J.A. (1973). Mapping of base sequence heterologies between genomes from different adenovirus serotypes. *Virology* **54**, 414-426.

GEORGATOS, S.D.; MEIER, J. and SIMOS, G. (1994). Lamins and Lamin-associated proteins. *Current Opinions in Cell Biology* **6**, 347-353.

GOLDBERG, M.E. (1991). Investigating protein conformation, dynamics and folding with monoclonal antibodies. *TIBS* (october), 358-362.

GOLDMAN, R.D.; GOLDMAN, A.A.; GREEN, K.J.; JONES, J.C.R.; JONES, S.M. and YANG, H.Y. (1986). Intermediate filament networks: organisation and possible functions of a diverse group of cytoskeletal elements. *Journal of Cell Science*: Supplement **5**, 69-97.

GRAHAM, F.L. (1984). Transformation by and oncogenicity of human adenoviruses. In: *The Adenoviruses* pp339-398. Ed. by: H.S. Ginsberg. Plenum Press. New York.

GREBER, U.F.; WILLETTS, M.; WEBSTER, P. and HELENIUS, A. (1993). Srepwise dismantling of adenovirus type 2 during entry into cells. *Cell* **75**, 477-486.

GREBER, U.F.; WEBSTER, P.; WEBER, J.M. and HELENIUS, A. (1996). The role of the adenovirus protease in virus entry into cells. *The EMBO Journal* **15**, 1766-1777.

GREEN, M.; LOWENSTEIN, P.M.; PUSZTAIR, R. and SYMINGTON, J.S. (1988). An adenovirus E1a protein domain activates transcription *in vivo* and *in vitro* in the absence of protein synthesis. *Cell* **53**, 921-926.

GREEN, N.M; WRIGLEY, N.G.; RUSSELL, W.C.; MARTIN, S. and McLACHLAN, A.D. (1983). Evidence for a repeating cross-ß sheet structure in the adenovirus fibre. *The EMBO Journal* **2**, 1357-1365.

GRIERSON, A.W.; NICHOLSON, R.; TALBOT, P.; WEBSTER, A. and KEMP, G. (1994). The protease of adenovirus serotype 2 requires cysteine residues for both activation and catalysis. *Journal of General Virology* **75**, 2761-2764.

GRIFFITHS, G. (1993). *Fine Structure Immunocytochemistry*. Springer-Verlag. Hiedelberg.

GROTZINGER, T.; STERNSDORF, T.; JENSEN, K. and WILL, H. (1996). Interferon-modulated expression of genes encoding the nuclear-dot-associated proteins SP100 and PML. *European Journal of Biochemistry* **238**, 554-560.

GRUTTER, M. and FRANKLIN, R.M. (1974). Studies on the molecular weight of the adenovirus type 2 hexon and its subunit. *Journal of Molecular Biology* **89**, 163-171.

GUAN, K. and DIXON, J.E. (1991). Eukaryotic proteins expressed in *E.coli*: An improved thrombin cleavage and purification procedure of fusion proteins with glutathione S-transferase. *Analytical Biochemistry* **192**, 262-267.

GUSTIN, K.E.; LUTZ, P. and IMPERIALE, M.J. (1996). Interaction of the adenovirus L1 52/55-kilodalton protein with the IVa2 gene product during infection. *Journal of Virology* **70**, 6463-6467.

HAMMARSKJOLD, M.L. and WINBERG, G. (1980). Encapsidation of adenovirus 16 DNA is directed by small DNA sequences at the left end of the genome. *Cell* **20**, 787-795.

HANKE, T.; BOTTING, C.; GREEN, E.A.; SZAWLOWSKI, P.W.; RUD, E. and RANDALL, R.E. (1994). Expression and purification of nonglycosylated SIV proteins and their use in induction and detection of SIV-specific immune-responses. *Aids Research and Human Retroviruses* **10**, 665-674.

HASSAN, A.B. (1995). Functional organisation of human nuclei. *Clinical Science* **89**, 13-18.

HASSON, T.B.; SOLOWAY, P.D.; ORNELLES, D.A.; DOERFLER, W. and SHENK, T. (1989). Adenovirus L1 52- and 55kd proteins are required for assembly of virions. *Journal of Virology* **63**, 3612-3621.

HASSON, T.B.; ORNELLES, D.A. and SHENK, T. (1992). Adenovirus L1 52- and 55- kd proteins are present within assembling virions and colocalise with nuclear structures distinct from replication centres. *Journal of Virology* **66**, 6133-6142.

HAY, R.T.; FREEMAN, A.; LEITH, I.; MONAGHAN, A. and WEBSTER, A. (1995). Molecular interactions during adenovirus DNA replication. In. *The Molecular Repertoire of Adenoviruses* II. Ed. by: W.Doerfler and P. Bohm. Springer-Verlag. Hiedelberg. pp31-43.

HARLOW, E. and LANE, D. (1988). *Antibodies: A laboratory manual*. Cold Spring Harbour Publications. New York.

HELIN, K.; HARLOW, E. and FATTAEY A.R. (1993). Inhibition of E2F-1 transactivation by direct binding of the retinoblastoma protein. *Molecular and Cellular Biology* **13**, 6501-6508.

HELLEN, C.U.T.; KRÄUSSLICH, H-G. and WIMMER, E. (1989). Proteolytic processing of polyproteins in the replication of RNA viruses. *Biochemistry* **28**, 9881-9890.

HENDRIX, R.W. and GARCEA, R.L. (1994). Capsid assembly of dsDNA viruses. *Seminars in Virology* **5**, 15-26.

HÉRISSE, J.; RIGOLET, M.; DUPONT, S. and GALIBERT, F. (1981). Nucleotide sequence of adenovirus 2 DNA fragment encoding for the carboxilic region of the fibre protein and the entire E4 region. *Nucleic Acids Research* **9**, 4023-4042.

HONG, J.S. and ENGLER, J.A. (1991). The amino terminus of the fiber protein encodes the nuclear localisation signal. *Virology* **185**, 758-767.

HONG, S.S. and BOULANGER, P. (1995). Protein ligands of the human adenovirus type 2 outer capsid identified by biopanning of a phage-displayed peptide library on seperate domains of wild-type and mutant penton capsomers. *The EMBO Journal* **14**, 4714-4727.

HORWITZ, M.S. (1990a). Adenoviridae and their replication. In: *Fields of Virology Volume* 2. Second Edition pp1679-1722. Ed. by: B.N. Fields and D.M. Knipe. Raven Press. New York.

HORWITZ, M.S. (1990b). Adenoviruses. In: *Fields of Virology Volume* 2. Second Edition pp1723-1742. Ed. by: B.N. Fields and D.M. Knipe. Raven Press. New York.

HOSOKAWA, K. and SUNG, M.T. (1976). Isolation and characterisation of an extremely basic protein from adenovirus type 5. *Journal of Virology* **17**, 924-934.

HOUDE, A. and WEBER, J.M. (1990). Adenovirus type 2 precursor proteins are cleaved by proteinases of other adenoviruses. *Virology* **179**, 485-486.

HOUGHTON, M (1996). Hepatitis C viruses. In: *Fields Virology*. 3rd Edition. Ed. by: B.N. Fields, D.M. Knipe, and P.M. Howley. Raven Press. New York. pp1035-1058.

HOZAK, P.; HASSAN, B.A.; JACKSON, D.A. and COOK, P.R. (1993). Visualisation of replication factories attached to a nucleoskeleton. *Cell* **73**, 361-373.

HUANG, M.J.; ORENSTEIN, J.M.; MARTIN, M.A. and FREED, E.O. (1995). P6 (gag) is required for particle-production from full-length human-HIV-1 molecular clones expressing protease. *Journal of Virology* **69**, 6810-6818.

IMPERIALE, M.J.; AKUSJÄRVI, G. and LEPPARD, K.N. (1995). Post-transcriptional control of adenovirus gene expression. In: *The Molecular Repertoire of Adenoviruses* II. Ed. by: W. Doerfler and P. Böhm. Springer-Verlag. Heidelberg. pp139-166.

ISIBASHI, M. and YASUE, H. (1984). Adenoviruses of animals. In: *The Adenoviruses* pp497-592. Ed. by: H.S. Ginsgerg. Plenum Press. New York.

JACKSON, P. and BLYTHE, D. (1993). Immunolabelling techniques for light microscopy. Immunocytochemistry: A practical approach. Ed. by: J.E. Beesley. IRL Press. Oxford. pp15-41.

JOACHIMS, M.; HARRIS, K.S. and ETCHISON, D. (1995). Poliovirus protease 3C mediates cleavage of microtubule-associated protein 4.*Virology* **211**, 451-461.

JONES, S.J.; IQBAL, M.; GRIERSON, A.W. and KEMP, G. (1996). Activation of the protease from human adenovirus type 2 is accompanied by a conformational change that is dependant on cysteine-104. *Journal of General Virology* **77**, 1821-1824.

KARAYAN, L.; GAY, B.; GERFAUX, J. and BOULANGER, P. (1994). Oligomerisation of recombinant penton base of adenovirus type 2 and its assembly with fiber in baculovirus infected cells. *Virology* **202**, 782-795.

KAY, J. and DUNN, B.M. (1989). Viral proteinases: weakness in strength. *Biochemica et Biophysica Acta* **1048**, 1-18.

KAWAHARA, N.; YANG, X.Z.; SAKAGUCH, T.; KIYTANI, K.; NAGAI, Y. and TOSHIDA, T. (1992). Distribution and substrate specificity of intracellular proteolytic processing enzyme(s) for paramyxovirus fusion glycoproteins. *Journal of General Virology* **73**, 583-590.

KELLY, C.; VAN DRIEL, R. and WILKINSON, W.G. (1995). Disruption of PML-associated nuclear bodies during human cytomegalovirus infection. *Journal of General Virology* **76**, 2887-2893.

KEYVANI-AMINEH, H.; DIOURI, M.; GUILLEMETTE, J.G. and WEBER, J.M. (1995). Electrophoretic and spectral characterisation of wild type and mutan adenovirus protease. *The Journal of Biological Chemistry* **270**, 23250-23253.

KEYVANI-AMINEH, H.; DIOURI, M.; TIHANYI, K. and WEBER, J.M. (1996). Adenovirus type 2 endoproteinase: isoforms and redox effects. *Journal of General Virology* **77**, 2201-2207.

KIDD, A.H.; CHROBOCZEK, J.; CUSACK, S. and RUIGROK, R.W.H. (1993). Adenovirus type 40 virions contain two distinct fibers. *Virology* **192**, 73-84.

KOCK, J.O.; LOHMANN, V.; HERIAN, U. and BARTENSCHLAGER, R. (1996). In Vitro studies on the activation of the hepatitis C virus NS3 proteinase by the NS4A cofactor. *Virology* **221**, 54-66.

KOKEN, M.H.M.; PUVION-DUTILLEUL, F.; GUILLEMIN, M.C.; VIRON, A.; LINARES-CRUZ, G.; STUURMAN, N.; DE JONG, L.; SZOSTECKI, C.; CALVO, F.; CHOMIENNE, C.; DEGOS, L.; PUVION, E. and DE THÊ, H. (1994). The t(15;17) translocation alters a nuclear body in a retinoic acid-reversible fashion. *The EMBO Journal* **13**, 1073-1083.

KRÄUSSLICH, H-G.; FÄCKE, M.; HEUSER, A-M.; KONVALINKA, J. and ZENTGRAF, H. (1995). The spacer peptide between human immunodeficiency virus capsid and nucleocapsid proteins is essential for ordered assembly and viral infectivity. *Journal of Virology* **69**, 3407-3419.

KRÄUSSLICH, H-G. and WIMMER, E. (1988). Viral Proteinases. *Annual Review of Biochemistry* **57**, 701-754.

LARSSON, S.; SVENSSON, C. and AKUSJÄRVI, G. (1992). Control of adenovirus major late gene expression at multiple levels. *Journal of Molecular Biology* **225**, 287-298.

LEPPARD, K.N. (1993). Selective effects on adenovirus late gene expression of deleting the E1b 55k protein. *Journal of General Virology* 74, 575-582.

LEWIS, B.A.; TULLIS, G.; SETO, E.; HORIKOSHI, N.; WEINMANN, R. and SHENK, T. (1994). Adenovirus E1A proteins interact with the cellular YY1 transcription factor. *Journal of Virology* **69**, 1628-1636.

LIDDINTON, R.C.; YAN, Y., MOULAI, J.; SAHLI, R.; BENJAMIN, T.L. and HARRISON, S.C. (1991). Structure of simian virus 40 at 3.8-Â resolution. *Nature* **354**, 278-284.

LOUIS, N.; FENDER, P.; BARGE, A.; KITTS, P. and CHROBOCZEK, J. (1994). Cell binding domain of adenovirus type 2 fibre. *Journal of Virology* **68**, 4104-4106.

LOVE, R.A.; PARGE, H.E.; WICKERSHAM, J.A.; HOSTOMSKY, Z.; HABUKA, N.; MOOMAW, E.W.; ADACHI, T. and HOSTOMSKA, Z. (1996). The crystal structure of hepeatitis C virus Ns3 proteinase reveals a trypsin-like fold and a structural zinc binding site. *Cell* **87**, 331-342.

LUCAS, J.J. and GINSBERG, H.S. (1971). Synthesis of virus-specific RNA in KB cells infected with type 2 adenovirus. Journal of Virology **8**, 203-213.

LUI, G.; BABISS, L.E.; VOLKERT, F.C; YOUNG, C.S.H. and GINSBERG, H.S. (1985). A thermolabile mutant of adenovirus 5nresulting from a substitution in the protein VIII gene. *Journal of Virology* **53**, 920-925.

LUNT, R.; VAYDA, M.E.; YOUNG, M. and FLINT, S.J. (1988). Isolation and characterisation of monoclonal antibodies against the adenovirus core proteins. *Virology* **164**, 275-279.

LUTZ, P. and KEDINGER, C. (1996). Properties of the adenovirus IVa2 gene product, an effector of late-phase dependant activation of the major late promoter. *Journal of Virology* **70**, 1396-1405.

LUTZ, P.; PUVION-DUTILLEUL, F.; LUTZ, Y. and KEDINGER, C. (1996). Nucleoplasmic and nucleolar distribution of the adenovirus IVa2 gene product. *Journal of Virology* **70**, 3449-3460.

LYONS, R.H.; FERGUSON, B.Q. and ROSENBERG, M. (1987). Pentapeptide nuclear localisation signal in adenovirus E1a. *Molecular and Cellular Biology* **7**, 2451-2456.

MAIZEL, J.V.; WHITE, D.O. and SCHARFF, M.D. (1968a). The polypeptides of adenovirus I: Evidence for multiple protein components of the virion and a comparison of types 2, 7a, and 12. *Virology* **36**, 115-125.

MANGEL, W.F.; McGRATH, W.J.; TOLEDO, D. and ANDERSON, C.W. (1993). Viral DNA and a viral peptide are cofactors of adenovirus virion proteinase activity. *Nature* **361**, 274-275.

MARAMATSU, S.; ISHIDO, S.; FUJITA, T.; ITOH, M. and HOTTA, H. (1997). Nuclear localisation of Hepatitis C Virus and factors affecting the localisation. *Journal of Virology* **71**, 4954-4961.

MARGOSIAK, S.A.; VANDERPOOL, D.L.; SISSON, W.; PINKO, C. and KAN. C-C. (1996). Dimerisation of the human cytomegalovirus protease: Kinetic and biochemical characterisation of the catalytic homodimer. *Biochemistry* **35**, 5300-5307.

MARSTON, A.O. (1986). The purification of eukaryotic polypeptides synthesised in *E.coli*. *Biochemical Journal* **240**, 1-12.

MATHEWS, D.A. and RUSSELL, W.C. (1994). Adenovirus protein-protein interactions: hexon and protein VI. *Journal of General Virology* **75**, 3365-3374.

MATHEWS, D.A. and RUSSELL, W.C. (1995). Adenovirus protein-protein interactions: molecular parameters governing the binding of protein VI to hexon and the activation of the adenovirus 23kd protease. *Journal of General Virology* **76**, 1959-1969.

MATUSICK-KUMAR, L.; McCANN, P.J.; ROBERTSON, B.J.; NEWCOMB, W.W.; BROWN, J.C. and GAO, M. Release of the catalytic domain No from the herpes simplex virus type 1 protease is required for viral growth. *Journal of Virology* **69**, 7113-7121.

MAUL, G.G.; ISHOV, A.M. and EVERETT, R.D. (1995). Nuclear domain 10 as preexisting potential replication start sites of HSV-1. *Virology* **217**, 67-75.

McGRATH, W.J.; ABOLA, P.; TOLEDO, D.L.; BROWN, M.T., MANGEL, W.F. (1996). Characterisation of human adenovirus proteinase activity in disrupted virus particles. *Virology* 217, 131-138.

MEREDITH, M.; ORR, A.; ELLIOT, M. and EVERETT, R. (1995). Separation of sequence requirements for HSV-1 Vmw 110 multimerisation and interaction with a 135kd cellular protein. *Virology* **209**, 174-187.

MICHAEL, N.; SPECTOR, D. and MAVROMARA-NAZOS, P. (1988). The DNA binding properties of the major regulatory protein α4 of herpes simplex viruses. *Science* **239**, 1531-1534.

MIRZA, M.A. and WEBER, J.M. (1979). Uncoating of adenovirus type 2. *Journal of Virology* **30**, 462-471.

MONAGHAN, P. and ROBERTSON, D. (1993). Immunolabelling techniques for electron microscopy. In: *Immunocytochemistry: A Practical Approach*. Ed. by: J.E. Beesley. IRL Press. Oxford. pp43-75.

MORAN, E. and MATHEWS, M.B. (1987). Multiple functional domains in the adenovirus E1A gene. *Cell* **48**, 177-178.

MORIN, N. and BOULANGER, P. (1984). Morphogenesis of human adenovirus type 2: sequence of entry of proteins into previral and viral particles. *Virology* **136**, 153-167.

MORIN, N.; DELSERT, C.; KLESSIG, D.F. (1989). Nuclear localisation of the adenovirus DNA-binding protein: requirement for two signals and complementation during viral infection. *Molecular and Cellular Biology* **9**, 4372-4380.

NAKANO, H.; YAMAZAKI, T.; IKEDA, M.; MASAI, H.; MIYATAKE, S-I. and SAITO, T. (1993). Purification of glutathione S-transferase fusion proteins as a non-degraded form by using a protease negative *E.coli* strain, AD202. *Nucleic Acids Research* **22**, 543-544.

NEILL, S.D.; HEMSTROM, P.M.D.; VERTANEN, A. and NEVINS, J. (1990). An adenovirus E4 gene product trans-activates E2 transcription and stimulates stable E2F binding through a direct association with E2F. *Proceedings of the National Acadamy of Sciences* (USA) **87**, 2008-2012.

NERMUT, M.V. (1979). Structural elements in adenovirus cores. Evidence for a core shell and linear structures in 'relaxed cores'. *Archives of Virology* **64**, 175-196.

NEWCOMB, W.W.; BORING, J.W. and BROWN, J.C. (1984). Ion etching of human adenovirus 2: structure of the core. *Journal of Virology* **51**, 52-56.

NORDQVIST, K.; OHMAN, K. and AKUSJÄRVI, G. (1994). Human adenovirus encodes two proteins which have opposite effects on accumulation of alternatively spliced mRNAs. *Molecular and Cellular Biology* **14**, 437-445.

NORRBY, E.; BARTH, A.; BOULANGER, T.; DREIZEN, R.; GINSBERG, H.S.; KALTER, S.S.; KAWAMARU, H.; ROWE, W.P.; RUSSELL, W.C.; SCHLESINGER, W. and WIGAND, R. (1977). Adenoviridae. *Intervirology* **7**, pp117-125.

OHMAN, K.; NORDQVIST, K.; AKUSJÄRVI, G. (1993). Two adenovirus proteins with redundant activities in virus growth facilitate tripartite leader mRNA accumulation. *Virology* **194**, 50-58.

O'MALLEY, R.P.; DUNCAN, R.F.; HERSHEY, J.W.B.; MATHEWS, M.B. (1988). Modification of protein synthesis initiation factors and the shut-off of host protein synthesis in adenovirus-infected cells. *Virology* **168**, 112-118.

ORNELLES, D.A. and SHENK, T. (1991). Localisation of the adenovirus early region 1B 55k protein during lytic infection: Association with nuclear viral inclusions requires the early region 4 34k protein. *Journal of Virology* **62**, 424-439.

PACE, C.N.; SHIRLEY, B.A. and THOMSON, J.A. (1990). Measuring the conformational stability of a protein. In: *Protein Structure: A Practical Approach.* Ed. by: T.E. Creighton. IRL Press. Oxford. pp311-329.

PATEL, A.H. and MACLEAN, J.B. (1995). The product of the UL26 gene of herpes simplex virus type 1 is associated with virus capsids. *Virology* **206**, 465-478.

PATTERSON, S. and RUSSELL, W.C. (1983). Ultrastructural and immunofluorescence studiesof early events in adenovirus-HeLa cell interactions. *Journal of General Virology* **64**, 1091-1099.

PETTERSSON, U. (1984). Structural and nonstructural adenovirus proteins. In: The Adenoviruses. Ed. by: H.S. Ginsberg. Plenum Press. New York. pp205-270.

PHILIPSON, L. (1983). Structure and assembly of adenoviruses. *Current Topics in Microbiology and Immunology* **109**, 1-52.

PHILIPSON, L. (1995). Adenovirus- An eternal archetype. In: *The Molecular Repertoire of Adenoviruses* I. Ed. by: W. Doerfler and P. Böhm. Springer-Verlag. Heidelberg. pp1-19.

PHILIPSON, L.; LONGBERG-HOLM, K. and PETTERSSON, U. (1968). Virus-receptor interaction in an adenovirus system. Journal of Virology **2**, 1064-1075.

PIENIAZEK, N.; VELARDE, J.; PIENIAZAK, D. and LUFTIG, R.B. (1989). Nucleotide sequence of human enteric adenovirus type 41 hexon-associated precursor (pVIII) including the early region E3 promoter. *Nucleic Acids Research* **17**, 5398.

PILDER, S.; MOORE, M.; LOGAN, J. and SHENK, T. (1986). The adenovirus EiB-55k transforming polypeptide modulates transport or cytoplasmic stabilisation of viral and host cell mRNAs. *Molecular and Cellular Biology* **6**, 470-476.

POMBO, A. and CARMO-FONSECA, M. (1995). Interactions of adenovirus with the nucleus of the host cell. *Medical Virology* **5**, 213-218.

POMBO, A.; FERREIRA, J.; BRIDGE, E. and CARMO-FONSECA, M. (1994). Adenovirus replication and transcription sites are spatially seperated in the nucleus of infected cells. *The EMBO Journal* **13**, 5075-5085.

PRECIOUS, B. and RUSSELL, W.C. (1991). Growth, purification, and titration of adenoviruses. *Virology: A practical approach.* Ed. by: B.W.J. Mahy. IRL Press. Oxford. pp193-205.

PRESTON, V.G.; AL-KOBAISI, M.F.; McDOUGALL, I.M. and RIXON, F.J. (1994). The herpes simplex virus gene UL26 proteinase in the presence of the UL26.5 gene product promotes the formation of scaffold-like structures. *Journal of General Virology* **75**, 2356-2365.

PUVION-DUTILLEUL, F.; BACHELLERIE, J.P.; VISA, N. and PUVION, E. (1994). Rearrangements of intranuclear structures involved in RNA processing in response to adenovirus infection. *Journal of Cell Science* **107**, 1457-1468.

PUVION-DUTILLEUL, F.; BESSE, S.; CHAN, E.K.L.; TAN, E.M. and PUVION, E. (1995a). P80-coilin: a component of coiled bodies and interchromatin granule-associated zones. *Journal of Cell Science* **108**, 1143-1153.

PUVION-DUTILLEUL, F.; CHELBI-ALIX, M.K.; KOKEN, M.; QUIGNON, F.; PUVION, E. and DE THÊ, H. (1995b). Adenovirus infection induces rearrangements in the intranuclear distribution of the nuclear body-associated PML protein. Experimental Cell Reseacrch **218**, 9-16.

PUVION-DUTILLEUL, F. and CHRISTENSEN, M.E. (1993). Alterations of fibrillarin distribution and nucleolar ultrastructure induced by adenovirus infection. *European Journal of Cell Biology* **61**, 168-176.

PUVION-DUTILLEUL, F.; ROUSSEV, R. and PUVION, E. (1992). Distribution of viral RNA molecules during the adenovirus type 5 infectious cycle in HeLa cells. *Journal of Structural Biology* **108**, 209-220.

PUVION-DUTILLEUL, F. and PUVION, E. (1990). Replicatingsingle-stranded adenovirus type 5 DNA molecules accumulate withinn well-delimited intranuclear areas in lytically infected HeLa cells. *European Journal of Cellular Biology* **52**, 379-388.

PUVION-DUTILLEUL, F. and PUVION, E. (1995). Immunocytochemistry, autoradiography, in situ hybridisation, selective staining: Complementary tools for ultrastructural study of structure-function relationships in the nucleus. Applications to adenovirus-infected cells. *Microscopy Research and Technique* **31**, 22-43.

PUVION-DUTILLEUL, F.; VENTURINI, L.; GUILLEMIN, M-C.; DE THÊ, H. and PUVION, E. (1995c). Sequestration of PML and SP100 proteins in an intranuclear viral structure during herpes simplex virus type 1 infection. *Experimental Cell Research* **221**, 448-461.

QIU, X.; CULP, J.S.; DI LELLA, A.G.; HELLMIG, B.; HOOG, S.S.; JANSON, C.A.; SMITH, W.W.; ABDEL-MEGUID, S.S. (1996). Unique fold and active site in cytomegalovirus protease. *Nature* **383**, 275-279.

QUILLENT, C.; BORMAN, A.M.; PAULOUS, S.; DAUGUET, C. and CLAVEL, F. (1996). Extensive regions of Pol are required for efficient human immunodeficieny virus polyprotein processing and particle maturation. *Virology* **219**, 29-36.

RANCOURT, C.; KEYVANI-AMINEH, H.; SIRCAR, S.; LABRECQUE, P. and WEBER, J.M. (1995). Proline 137 is critical for adenovirus protease encapsidation and activation but not enzyme activity. *Virology* **209**, 167-173.

RANCOURT, C.; KEYVANI-AMINEH, H.; DIOURI, M. and WEBER, J.M. (1996). Mutagenesis of conserved residues of the adenovirus protease. *Virology* **224**, 561-563.

RANCOURT, C.; TIHANYI, K.; BOUBONNIERE, M. and WEBER, J.M. (1994). Identification of active-site residues of the adenovirus endopeptidase. *Proceedings of the National Acadamy of Sciences* (USA) **91**, 844-847.

REBELO, L.; ALMEIDA, F.; RAMOS, C.; BOHMANN, K.; LAMOND, A.I. and CARMO-FONSECA, M. (1996). The dynamics of coiled bodies in the nucleus of adenovirus infected cells. *Molecular Biology of the Cell* **7**, 1137-1151.

REKOSH, D.M.K.; RUSSELL, W.C.; BELLET, A.J.D. and ROBINSON, A.J. (1977). Identification of a protein linked to the ends of adenovirus DNA. *Cell* **11**, 283-295.

RICIGLIANO, J.W.; BROUGH, D.E. and KLESSIG, D.F. (1994). Identification of a high molecular weight complex containing the adenovirus DNA binding protein. *Virology* **202**, 715-723.

RILEY, D. and FLINT, S.J. (1993). RNA-binding properties of a translational activator, the adenovirus L4 100k protein. *Journal of Virology* **67**, 3586-3595.

ROBERTS, R.J.; O'NEIL, K.E. and YEN, C.T. (1984). DNA sequences from the Ad2 genome. *Journal of Biological Chemistry* **259**, 13968-13975.

ROBERTS, M.M.; WHITE, J.L.; GRUTTER, M.G. and BURNETT, R.M. (1986). The three dimensional structure of the adenovirus major coat protein hexon. *Science* **232**, 1148-1151.

ROBERTSON, B.J.; McCANN, B.J.; MATUSICK-KUMAR, L.; NEWCOMB, W.W.; BROWN, J.C.; COLONNO, R.J. and GAO, M. (1996). Seperate functional domains of the herpes simplex virus type 1 protease: evidence for cleavage inside capsids. *Journal of Virology* **70**, 4317-4328.

RODRIGUEZ, E. and EVERITT, E. (1996). Adenovirus uncoating and nuclear establishment are not affected by weak base amines. *Journal of Virology* **70**, 3470-3477.

ROIZMAN, B. and SEARS, A.E. (1990). Herpes simplex viruses and their replication. In.*Virology*. 2nd Edition. Ed.by B.N. Fields and D.M. Knipe. Raven. New York. pp 1795-1841.

ROOVERS, D.J.; YOUNG, C.S.H.; VOS, H.L. and SUSSENBACH, J.S. (1990). Physical mapping of two temperature sensitive adenovirus mutants affected in the DNA polymerase and DNA binding protein. *Virus Genes* **4**, 53-61.

ROSA, P.; WEISS, U.; PEPPERCOK, R.; ANSORGE, W. and HUTTNER, W.B. (1989). An antibody against secretogranin I (chromatogranin B) is packaged into secretory granules. *Journal of Cell Biology* **109**, 17-34.

ROSENBERG, A.H.; LADE, B.N.; CHUI, D-S.; LIN, S-W.; DUNN, J.J. and STUDIER, F.W. (1987). Vectors for selective expression of cloned DNAs by T7 RNA polymerase. *Gene* **56**, 125-135.

ROWE, W.P.; HUEBNER, R.J.; GILMORE, L.K.; PARROTT, R.H. and WARD, T.G. (1953). Isolation of the cytopathogenic agent from human adenoids undergoing spontaneous degeneration in tissue culture. *Proceedings of the Society for Experimental Biology and Medicine* **84**, 570-573.

RUSSELL, W.C.; WEBSTER, A.; LEITH, I.R.; KEMP, G.D. (1989). Phosphorylation of adenovirus DNA-binding protein. Journal of General Virology **70**, 3249-3259.

RUSSELL, W.C. and PRECIOUS, B. (1982). Nucleic acid binding properties of adenovirus structural polypeptides. *Journal of General Virology* **63**, 69-79.

RUSSELL, W.C. and KEMP, G.D. (1995). The role of adenovirus structural proteins in the regulation of adenovirus infection. In. *The Molecular Repertoire of Adenoviruses* I. Ed. by: W.Doerfler and P. Bohm. Springer-Verlag. Hiedelberg. pp81-98.

RUSSELL, W.C.; LAVER, W.G. and SANDERSON, P.J. (1968). Internal components of adenovirus. *Nature* **219**, 1127-1130.

SAIKI, R.K.; SCHARF, S.; FALOONA, F.; MULLIS, K.B.; HORN, G.T.; ERLICH, H.A. and ARNHEIM, N. (1985). Enzymatic amplification of ß-globulin genomic sequences and restriction site analysis for diagnosis of sickle cell anaemia. *Science* **230**, 1350-1354.

SALUNKE, D.M.; CASPER, L.D.; GARCEA, R.L. (1986). Self assembly of purified polyomavirus capsid protein VP. *Cell* **46**, 895-904.

SAMBROOK, J.; FRITSCH, E.F. and MANIATIS, T. (1989). *Molecular Cloning: A laboratory manual.* 2nd edition. Cold Spring Harbour Laboratory Publications. New York.

SASSENFIELD, H.M. (1990). Engineering proteins for purification. *TIBTECH* **8**, 88-93.

SCARIA, A. and WOLD, W.S.M. (1994). Mapping of sequences that suppress splicing in the E3 complex transcription unit of adenovirus. *Virology* **205**, 406-416.

SCHAAK, J. HO, W.Y.; FREIMUTH, P and SHENK, T. (1990). Adenovirus terminal protein mediates both nuclear matrix association and efficient transcription of adenovirus DNA. *Genes and Development* **4**, 1197-1208.

SCHMID, S.I. and HEARING, P. (1995). Selective encapsidation of adenovirus DNA. In: *The Molecular Repertoire of Adenoviruses.* Ed.by: W. Doerfler and P. Böhm. Springer-Verlag. Hiedelberg. pp67-80.

SCHMIDT, U. and DARKE, P.L. (1997). Dimerisation and activation of the Herpes Simplex Virus Type 1 protease. *The Journal of Biological Chemistry* **272**, 1265-1270.

SCHNEITER, R.; KADOWAKI, T. and TATAKOFF, A.M. (1995). mRNA transport in yeast: Time to reinvestigate the functions of the nucleolus. *Molecular Biology of the Cell* **6**, 357-370.

SCHUL, W.; GROENHOUT, B.; KOBERNA, K.; TAKAGAKI, Y.; JENNY, A.; MANDERS, E.M.M.; RASKA, I. VAN DRIEL, R. and DE JONG, L. (1996). The RNA 3' cleavage factors CstF 64kd and CPSF 100kd are concentrated in nuclear domains closely associated with coiled bodies and newly synthesised RNA. *The EMBO Journal* **15**, 2883-2892.

SHARP, P.A. (1984). Adenovirus transcription. In: *The Adenoviruses*. Ed. by: H.S. Ginsberg. Plenum Press. New York. pp173-204.

SHIEH, H.S.; KURUMBAIL, R.G.; STEVENS, A.M.; STEGEMAN, R.A.; STURMAN, E.J.; PAK, J.Y.; WITTWER, A.J.; PALMIER, M.O.; WIEGAND, R.C.; HOLWERDA, B.C. and STALLINGS, W.C. (1996). Three-dimensional structure of human cytomegalovirus protease. *Nature* **383**, 279-282.

SIGNAS, C.; AKUSJÄRVI, G. and PETTERSSON, U. (1985). Adenovirus 3 fibre polypeptide gene: implications for the structure of the fibre protein. *Journal of Virology* **53**, 672-678.

SILVERMAN, L. and KLESSIG, D.F. (1989). Characteisation of the translational defect to fiber synthesis in monkey cells abortively infected with human adenovirus: Role of ancillary leaders. *Journal of Virology* **63**, 4376-4385.

SKERN, T. and LIEBEG, H-D. (1994). Picornians 2A and 3C. *Methods in Enzymology* 244. Ed. by: A.J. Barrett. Academic Press. London.

SMART, J.E. and STILLMAN, B.W. (1982). Adenovirus terminal protein precursor. Partial amino acid sequence and the site of covalent linkage to virus DNA. *The Journal of Biological Chemistry* **257**, 13499-13506.

SMILEY, J.K.; YOUNG, M.A. and FLINT, S.J. (1990). Intranuclear location of the adenovirus type 5 E1B 55kd protein. *Journal of Virology* **64**, 4558-4564.

SMILEY, J.K.; YOUNG, M.A.; BRANSBACH, C.C. and FLINT, S.J. (1994). The metabolism of small cellular RNA species during productive subgroup C adenovirus infection. *Virology* **206**, 100-107.

SMITH, D.B. and JOHNSON, K.S. (1988). Single-step purification of polypeptides expressed en *E.coli* as fusions with glutathione S-transferase. *Gene* **67**, 31-40.

STAUFENBIEL, M.; EPPLE, P. and DEPPERT, W. (1986). Progressive reorganisation of the host cell cytoskeleton during adenovirus infection. *Journal of Virology* **60**, 1186-1191.

STEWART, P.L. and BURNETT, R.M. (1995). Adenovirus structure by X-Ray Crystallography and Electron Microscopy. In: *The Molecular Repertoire of Adenoviruses* I. Ed. by: W. Doerfler and P. Böhm. Springer-Verlag. Heidelberg. pp25-37.

STEWART, P.L.; BURNETT, R.M.; CYRKLAFF, M and FULLER, S.D. (1991). Image reconstruction reveals the complex molecular organisation of the adenovirus. *Cell* **67**, 145-154.

STEWART, P.L.; FULLER, S.D. and BURNETT, R.M. (1993). Difference imaging of adenovirus: bridging the resolution gap between X-ray crystallography and electron microscopy. T*he EMBO Journal* **12**, 2589-2599.

STOW, N.D. and HAY, R.T. (1993). Viral DNA replication. *Molecular Virology: A practical approach.* IRL Press. Oxford. pp75-107.

STUURMAN, N.; GRAAF, A.; FLOORE, A.; JOSSO, A.; HUMBEL, B.; DE JONG, L. and VAN DRIEL, R. (1992). A monoclonal antibody recognising nuclear matrix-associated nuclear bodies. *Journal of Cell Science* **101**, 773-784.

SUNG, M.T.; CAO, T.M.; COLEMAN, R.T. and BUDELIER, K.A. (1983). Gene and protein sequences of adenovirus protein VII, a hybrid basic chromosomal protein. *Proceedings of the National Acadamy of Sciences of the United States of America* **80**, 2902-2906.

SVENSSON, U. and PERSSON, R. (1984). Entry of adenovirus 2 into HeLa cells. *Journal of Virology* **51**, 687-694.

SZEKELY, L.; POKROVSKAJA, K.; JIANG, W-Q.; DE THÊ, H.; RINGERTZ, N. and KLEIN, G. (1996). The epstein-barr virus-encoded nuclear antigen EBNA-5 accumulates in PML-containing bodies. *Journal of Virology* **70**, 2562-2568.

TEODORO, J.G.; MARCELLUS, R.C.; QUERIDO, E. and BRANTON, P.E. (1995). Role of adenovirus type 5 E1A and E1B proteins in p53-dependant and p53-independant apoptosis. Lect.at: Adenovirus Workshop. Univ. of StAndrews. Abst.p 17.

THOMSEN, D.R.; NEWCOMB, W.W.; BROWN, J.C. and HOMA, F.L. (1995). Assembly of the herpes simplex virus capsid: requirement for the carboxyl-terminal twenty five amino acids of the proteins encoded by the UL26 and UL26.5 genes. *Journal of Virology* **69**, 3690-3703.

TIHANYI, K.; BOURBONNIERE, M.; HOUDE, A.; RANCOURT, C. and WEBER, J.M. (1993). Isolation and properties of adenovirus type 2 proteinase. *The Journal of Biological Chemistry* **268**, 1780-1785.

TOLLEFSON, A.E.; RYERSE, J.S.; SCARIA, A.; HERMISTON, T.W.; WOLD, W.S.M. (1996b). The E3-11.6k adenovirus death protein (ADP) is required for efficient cell death: characterisation of cells infected with adp mutants. *Virology* **220**, 152-162.

TOLLEFSON, A.E.; SCARIA, A.; HERMISTON, T.W.; RYERSE, J.S.; WOLD, L.J. and WOLD, W.S.M. (1996a). The adenovirus death protein (E3-11.6k) is required at very late stagesb of infection for efficient cell lysis and release of adenovirus from infected cells. *Journal of Virology* **70**, 2296-2306.

TOMASSELLI, A.G. and HEINRIKSON, R.L. (1994). Specificity of retroviral proteases: an analysis of viral and non-viral protein substrates. Methods in Enzymology 241. Ed.by: L.C. Kuo. and J.A. Shafer. Academic Press. London. pp279-301.

TONG, L.; QIAN, C.; MASSARIOL, M.J; BONNEAU, P.R., CORDINGLY, M.G. and LAGACE, L. (1996). A new serine-protease fold revealed by the crystal structure of human cytomegalovirus protease. *Nature* **383**, 272-275.

TOOGOOD, C.I.A.; MURALI, R.; BURNETT, R.M. and HAY, R.T. (1989). The adenovirus type 40 hexon: Sequence, predicted structure and relationship to other adenovirus hexons. *Journal of General Virology* **70**, 3202-3214.

TREMBLEY, M.L.; DERY, C.V.; TALBOT, B.G. and WEBER, J. (1983). *In vitro* cleavage specificity of the adenovirus type 2 protease. *Biochemica et biophysica acta* **743**, 239-245.

TRENTIN, J.J, YABE, Y., AND TAYLOR, G. (1962). The quest for human cancer viruses. *Science* **137**, 835-849.

TRIBOULEY, C.; LUTZ, P.; STAUB, A. and KEDINGER, C. (1994). The product of the adenovirus internediate gene IVa2 is a transcriptional activator of the major late promoter. *Journal of Virology* **68**, 4450-4457.

TSUZUKI, J. and LUFTIG, R.B. (1983). The adenovirus type 5 capsid protein IIIa is phosphorylated during an early stage of infection of HeLa cells. *Virology* **129**, 529-533.

VALENTINE, R.C. and PEREIRA, H.G. (1965). Antigens and structure of the adenovirus. *Journal of Molecular Biology* **13**, 13-20.

VAN DER VLEIT, P.C. (1995). Adenovirus DNA replication. In: The Molecular Repertoire of Adenoviruses II. Ed. by: W. Doerfler and P. Bohm. Springer-Verlag. Hiedelberg. pp1-24.

VAN DOORN, L.J. (1994). Molecular biology of the hepatitis C virus. *Journal of Medical Virology* **43**, 345-356.

VAN OOSTRUM, J. and BURNETT, R.M. (1985). Molecular composition of the adenovirus type 2 virion. *Journal of Virology* **56**, 439-448.

VAN OOSTRUM, J.; SMITH, P.R.; MOHRAZ, M. and BURNETT, R.M. (1987). The structure of the adenovirus capsid III. Hexon packing determined from electron micrographs of capsid fragments. *Journal of Molecular Biology* **198**, 73-89.

VAYDA, M.E. and FLINT, S.J. (1987). Isolation and characterisation of adenovirus core nucleoprotein subunits. *Journal of Virology* **61**, 3335-3339.

VERCHAT, J. and CARRINGTON, J.C. (1995). Evidence that the potyvirus P1 proteinase functions in *trans* as an accessory factor for genome amplification. *Journal of Virology* **69**, 3668-3674.

WARD, P.L.; OGLE, W.O. and ROIZMAN, B. (1996). Assemblons: Nuclear structures defined by aggregation of immature capsids and some tegument proteins of Herpes Simplex Virus 1. *Journal of Virology* **70**, 4623-4631.

WEBER, J.M. (1976). Genetic analysis of adenovirus type 2. III. Temperature sensitivity of processing of viral proteins. *Journal of Virology* **17**, 462-471.

WEBER, J.M. (1995). Adenovirus endopeptidase and its role in virus infection. In: *The Molecular Repertoire of Adenoviruses* I. Ed. by: W. Doerfler and P. Böhm. Springer-Verlag. Heidelberg. pp227-234.

WEBER, J.M. and ANDERSON, C.W. (1988). Identification of the gene coding for the precursor of adenovirus core protein X. *Journal of Virology* **62**, 1741-1745.

WEBER, J.M. and KHITOO, G. (1983). The role of phosphorylation and core protein V in adenovirus assembly. *Journal of General Virology* **64**, 2063-2068.

WEBER, J.M.; KHITOO, G. and BHATTI, A.R. (1983). Adenovirus core proteins. *Canadian Journal of Microbiology* **29**, 235-241.

WEBSTER, A. (1992). Characterisation of the adenovirus protease. *Phd thesis* (University of St.Andrews).

WEBSTER, A.; HAY, R.T. and KEMP, G. (1993). The adenovirus protease is activated by a virus-coded disulphide-linked peptide. *Cell* **72**, 97-104.

WEBSTER,A. and KEMP, G.D. (1993). The active adenovirus protease is the intact L3 23k protein. Journal of General Virology **74**, 1415-1420.

WEBSTER, A.; LEITH, I.R. and HAY, R.T. (1994). Activation of the adenovirus protease and processing of preterminal protein. *Journal of Virology* **68**, 7292-7300.

WEBSTER, A.; RUSSELL, S.; TALBOT, P.; RUSSELL, W.C. and KEMP, G.D. (1989a). Characterisation of the adenovirus proteinase: substrate specificity. *Journal of General Virology* **70**, 3225-3234.

WEBSTER, A.; RUSSELL, W.C. and KEMP, G.D. (1989b). Characterisation of the adenovirus proteinase: Development and use of a specific peptide assay. *Journal of General Virology* **70**, 3215-3223.

WELKER, R.; KOTTLER, H.; KALBITZER, H.R. and KRÄUSLICH, H-G. (1996). HIV-1 Nef protein is incorporated into virus particles and specifically cleaved by the viral protease. *Virology* **219**, 228-236.

WHITE, E. and CIPRIANI, R. (1989). Specific disruption of intermediate filaments and the nuclear lamina by the 19kd product of the adenovirus E1B oncogene. *Proceedings of the National Acadamy of Sciences* (USA) **86**, 9886-9890.

WHITE, E.; SABBATINI, P.; LAKSHMI, RAO.; JEONGHOON, H.; PEREZ, D.; MODHA, D. and CHIOU, S. (1995). Regulation of apoptosis by oncogenes and tumor suppressor genes. Lect. at: Adenovirus Workshop. Univ. of StAndrews. Abst. p23.

WHYTE, P.; BUCHKOVICH, K.J.; HOROWITZ, J.M.; FRIEND, S.H.; RAYBUCK, M.; WEINBERG, R.A. and HARLOW, E. (1988). Association between an oncogene and an anti-oncogene: The adenovirus E1A proteins bind to the retinoblastoma gene product. *Nature* **334**, 124-129.

WICKHAM, T.J.; MATHIAS, P.; CHERESH, D.A. and NEMEROW, G.R. (1993). Integrins $\alpha_v\beta_3$ and $\alpha_v\beta_5$ promote adenovirus internalisation but not virus attachment. *Cell* **73**, 309-319.

WILLS, E.J. and RUSSELL, W.C. (1973). Adenovirus-induced crystals: Studies with temperature sensitive mutants. *Journal of General Virology* **20**, 407-412.

WOLD, W.S.M. and GOODING, L.R. (1991). Region E3 of Adenovirus: Acassette of genes involved in host immunosueveillance and virus-cell interactions. *Virology* **184**, 1-8.

WOLD, W.S.M.; TOLLEFSON, A.E. and HERMISTON, T.W. (1995). E3 transcription unit of adenovirus. In. *The Molecular Repertoire of Adenoviruses* I. Ed. by: W.Doerfler and P. Bohm. Springer-Verlag. Hiedelberg. pp237-266.

WU,X.; CONWAY, J.A.; KIM, J. and KAPPES, J.C. (1994). Localisation of the Vpx packaging signal within the c-terminus of the HIV-2 gag precursor protein. *Journal of Virology* **68**, 6161-6169.

XIA, D.; HENRY, L.; GERARD, R.D. and DEISENHOFER, J. (1995). Structure of the receptor binding domain of adenovirus type 5 fiber protein. In: *The Molecular Repertoire of Adenovirusess* I. Ed. by: W. Doerfler and P.Bohm. Springer-Verlag. Hiedelberg. pp 39-46.

YANG, U.C.; HUANG, W. and FLINT, S.J. (1996). mRNA export corrolates with activation of transcription in human subgroup C adenovirus-infected cells. *Journal of Virology* **70**, 4071-4080.

YEH-KAI, L.; AKUSJÄRVI, G.; ALESTROM, P. PETTERSSON, U.; REMBLEY, M. and WEBER, J.M. (1983). Genetic identification of an endoproteinase encoded by the adenovirus genome. *Journal of Molecular Biology* 167, 217-222.

YU, X-F.; MATSUDA, Q-C.; YU, T-H.; ESSEX, M. (1995). Role of the c terminus Gag protein in human immunodeficiency virus type 1 virion assembly and maturation. *Journal of General Virology* **76**, 3171-3179.

YUAN, X.; YU, X.; LEE, T-H.; ESSEX, M. (1993). Mutations in the N-terminal region of human immunodeficiency virus type 1 matrix protein block intracellular transport of the gag precursor. *Journal of Virology* **67**, 6387-6394.

ZAMANIAN, M. and La THANGUE, N.B. (1992). Adenovirus E1a prevents the retinoblastoma gene product from repressing the activity of a cellular transcription factor. *The EMBO Journal* **11**, 2603-2610.

ZHANG, Y. and SCHNEIDER, R.J. (1993). Adenovirus inhibition of cellular protein synthesis and the specific translation of late viral mRNAs. *Seminars in Virology* **4**, 229-236.

ZHANG, Y. and SCHNEIDER, R.J. (1994). Adenovirus inhibition of cell translation facilitates release of virus particles and enhances degradation of the cytokeratin network. *Journal of Virology* **68**, 2544-2555.

ZHAO, L.J. and PADMANABHAN, R. (1988). Nuclear transport of adenovirus DNA polymerase is facilitated by interaction with preterminal protein. *Cell* **55**, 1005-1015.

ZHONGHE, Z.; NICKERSON, J.A.; KROCHMALNIC, G. and PENMAN, S. (1987). Alterations in nuclear matrix structure after adenovirus infection. *Journal of Virology* **61**, 1007-1018.

ZHOU, Z.H.; PRASAD, B.V.V.; JAKANA, J.; RIXON, F.J. and CHIU, W. (1994). Protein subunit structures in the herpes simplex virus A-capsid determined from 400kv spot-scan electron cryomicroscopy. *Journal of Molecular Biology* **242**, 456-469.